ISSN 0031-0301, Paleontological Journal, 2006, Vol. 40, Suppl. 2, pp. S91–S204. © Pleiades Publishing, Inc., 2006.

Abstract—This work is the first detailed description of the Late Pleistocene–Holocene and Recent Ostracoda of the Laptev Sea. A total of 45 species in 22 genera and 13 families have been identified. All these species are described monographically. Three different ecological assemblages of ostracodes corresponding to different combinations of environmental parameters have been established; they are restricted to three regions of the sea: western-central, eastern, and southern. The recent ostracode assemblages of the Laptev Sea have been compared with those from other Arctic areas and are most similar to those of the Beaufort and Kara seas. Data on recent Ostracoda are used for paleoenvironmental reconstructions on the eastern shelf and western continental slope of the Laptev Sea. For this purpose, ostracodes from five sections obtained from these parts of the sea have been examined. The oldest sediments, which are of Late Pleistocene age (15.8 cal. ka BP), have been recovered in a core from the western continental slope. These yielded five ostracode assemblages, which correspond to different paleoenvironments and replaced each other in the course of the rapid postglacial sea-level rise, thus showing variations in the Atlantic water inflow from the west and freshwater discharge from the subaerially exposed shelf. On the outer shelf of the eastern part of the sea, the rapid sea-level rise in the Early Holocene (lowermost dating 11.3 cal. ka BP) led to a rapid transition from assemblages of brackish-water nearshore environments to those of modernlike normal marine environments; modern environments were established about 8.2 cal. ka ago. Since the core sections from the inner shelf correspond to the time when the level of the sea had already reached its modern values, the changes in the taxonomic composition of ostracode assemblages primarily mirror variations in river runoff.

DOI: 10.1134/S0031030106080016

INTRODUCTION

The Laptev Sea belongs to the Central Arctic Ocean Basin and is located on the junction of the western and eastern sectors of the Arctic, which differ strongly both in their modern hydrologic conditions and in the history of their development in the Holocene. Scattered data on the structure and stratigraphy of the Quaternary deposits of the shelf and continental slope (Holmes and Creager, 1974) have recently been considerably supplemented by numerous new data obtained by Russian and foreign scientists who have studied this area intensively (Drachev et al., 1995, 1999; Kim and Verba, 1995; Bogdanov et al., 1998; Bauch et al., 1999, 2001a; Kim et al., 1999; Vinogradov and Drachev, 2000; Andreeva et al., 2001; Kosheleva et al., 2001; Rekant, 2002).

The investigations undertaken by Russian scientists on the Taimyr Peninsula, New Siberian Islands, and the Laptev Sea (Alekseev, 1961, 1978, 1989; Arkhipov, 1971; Isaeva et al., 1976, 1981; Troitskii, 1979; Andreeva, 1980; Bardeva and Isaeva, 1980; Andreeva et al., 1982; Isaeva, 1982a, 1982b, 1982c; Isaeva and Kind, 1982; Pavlidis et al., 1998; Rekant, 2002) and the results obtained by foreign scientists (Bauch et al., 1999, 2001b; Svendsen et al., 1999, 2004) have revealed that in the Late Pleistocene there were no ice sheets on the shelf of the Laptev Sea. During the Sartanian glaciation the climate became drier and colder. This led to the complete subaerial exposition of the shelf on which the periglacial zone was formed (Are, 1982; Alekseev, 1989). The Taimyr Peninsula became a transitional zone between western Eurasia, where the Late Pleistocene glaciation had a wide distribution, and eastern Eurasia, where no traces of glaciation have been found (Isaeva and Kind, 1982; Svendsen et al., 1999, 2004). The subsequent rapid sea-level rise resulted in the rapid inundation of the shelf during the Late Pleistocene–Holocene. According to the available data on the development of the Holocene transgression on the Laptev Sea shelf (Polyakova, 1997; Bauch et al., 2001b), the sea level reached 40–50 m below the modern level about 10–11 thousand calendar years ago. Since that time there has been marine sedimentation. The most significant change to the formation of present normal marine environments on the continental slope and outer shelf of the Laptev Sea occurred 9.5 thousand calendar years ago, which is supported by the increased abundance of $\delta^{13}C$ in sedimentary organic matter and by the increased concentrations of marine biomarkers (Mueller-Lupp et al., 2000; Stein and Fahl, 2000). The transgression was very uneven. The levels of 50, 43, and 31 m below the modern sea level have been shown to be inundated 11.1, 9.8, and 8.9 thousand calendar years ago, respectively (Bauch et al., 2001b). The rate of sea-level rise was 5.4, 13.3, and 7.9 mm/yr, respectively. On the outer shelf of the Laptev Sea, a decrease in the sedimentation rate was recorded about 9 thousand calendar years ago (Bauch et al., 2001b). Around six thousand calendar years ago, the sea-level continued to rise and nearly reached modern values; this was accompanied by a decrease in sedimentation rates on the outer and middle shelves (Bauch et al., 1999, 2001b). At that time, the coastal plains and river valleys were flooded, and the islands assumed their present outlines. Due to the slowing down of the sea-level rise and its gradual stabilization, the formation of the modern Lena Delta started (Andreeva et al., 1982; Romanovskii et al., 2000; Schwamborn et al., 2002). In the Late

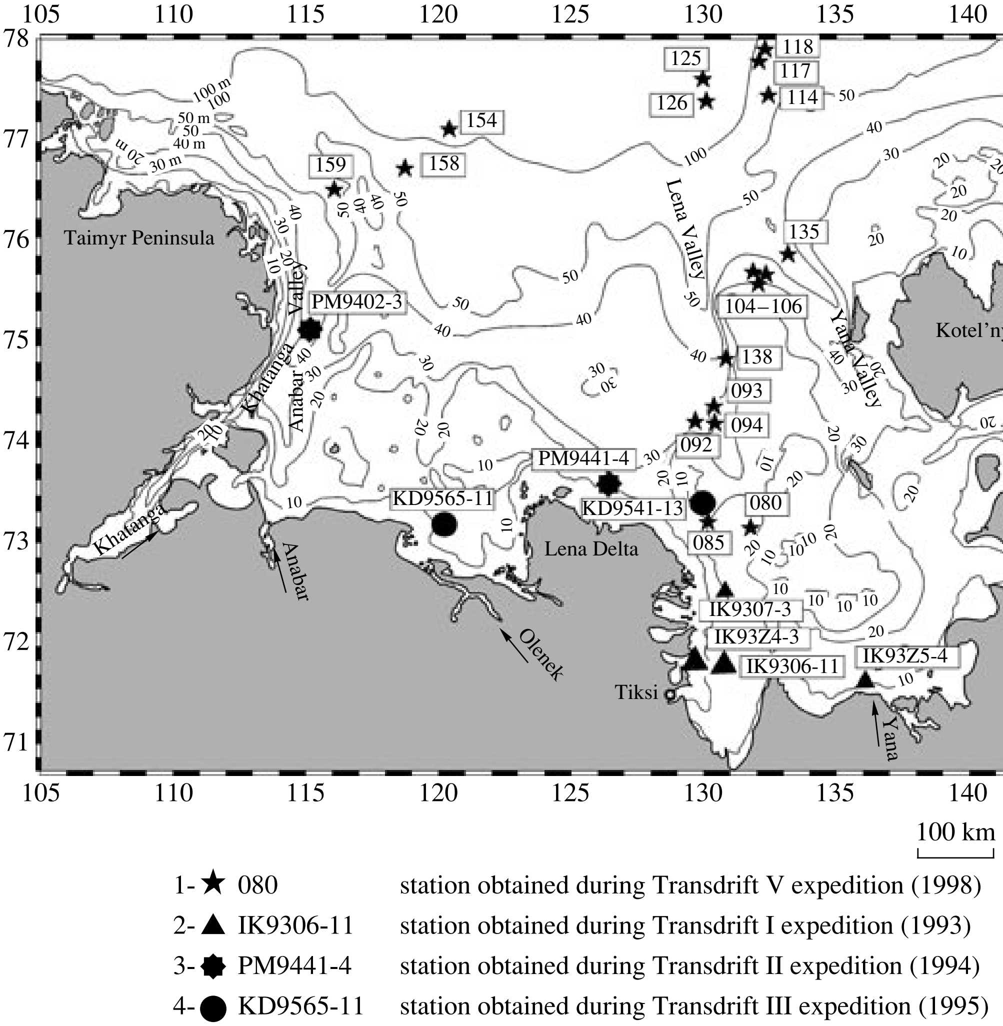

Fig. 1. Location of stations of the TRANSDRIFT I, II, III, and V expeditions to the Laptev Sea: (1) stations obtained during Transdrift V expedition (1998); (2) stations obtained during Transdrift I expedition (1993); (3) stations obtained during Transdrift II expedition (1994); (4) stations obtained during Transdrift III expedition (1995).

Holocene the sedimentation rates remained quite stable, varying from 1.2 mm/yr in the Lena River valley to 0.1 mm/yr in the Khatanga River valley (Bauch et al., 2001b).

In marine sediments, the changes caused by sea-level rise and variations in river discharge and water parameters are reflected in downcore variations of fossil benthic assemblages, such as ostracodes, mollusks, and foraminifers; among these, ostracodes are the most sensitive to environmental changes, water depth and salinity. Analysis of ostracode assemblages allows reconstructing paleoenvironments in great detail. Since this group is so important for paleoreconstructions, we have undertaken a comprehensive study of recent and fossil ostracodes from the Laptev Sea, data on which still remain quite scarce. This work is based on new materials obtained in the framework of the cooperative Russian-German projects "Laptev Sea System" and "Laptev Sea System-2000."

CHAPTER 1. MATERIALS AND METHODS

In this study we investigated samples obtained by Taldenkova and, partly, by the author from sediment core sections PS51/138-12(10), PS51/135-4, PS51/080-13(11), and PS51/92-12(11) from the eastern Laptev Sea shelf and a core section from the western continental slope PS51/154-11, as well as 44 coretop sediment samples collected from 26 stations from different parts of the shelf and upper continental slope (Fig. 1).

Surface samples and sediment cores were obtained during the Russian-German TRANSDRIFT V expedition in August 1998 in the Laptev Sea aboard the German research vessel *Polarstern*. An additional eight coretop samples were analyzed. They were collected from nearshore localities during TRANSDRIFT I, II, and III (1993, 1994, and 1995) expeditions aboard the Russian research vessels *Ivan Kireev* (samples with abbreviation IK), *Professor Mul'tanovskii* (samples with abbreviation PM), and *Kapitan Dranitsyn* (sam-

Table 1. Location of stations, water depth, temperature, bottom water salinity, lithology, and the percentage of ostracodes collected alive

Station	Dry bulk weight, g	Region	Depth, m	Coordinates		*t*, °C	Salinity, ‰	Lithology	Percentage of ostracodes collected alive, %
				latitude	longitude				
PS-51/158-8	28.9481	West	68	76°57′49″	118°35′37″	–1.481	33.488	Sandy silt	96
PS-51/159-8	13.1489	West	61.6	76°45′99″	116°01′86″	–1.617	33.687	Clayey silt	95
PS-51/154-9	21.5036	West	276.4	77°16′61″	120°36′03″	0.395	34.708	Sandy silt	97
PS-51/118-1	18.1008	Center	121	77°53′6″	132°12′57″	–0.7	No data	Sandy silt	80
PS-51/125-12	39.2087	Center	127	77°36′09″	130°00′07″	–1.54	No data	Silty sand	95
PS-51/114-13	29.3503	Center	66	77°35′52″	132°15′82″	–1.345	33.776	Sandy-silty clay	99
PS-51/117-3	39.4596	Center	76	77°49′8″	132°14′42″	–0.949	34.105	Sandy silt	92
PS-51/126-2	20.1833	Center	85	77°32′9″	130°07′9″	–1.54		Silty sand	90
PS-51/094-3	22.2406	South	31	74°33′36″	130°27′2″	–1.592	32.673	Silty sand	No data
PS-51/093-1	6.2587	South	33	74°56′74″	130°34′15″	–1.608	32.992	Sandy silt	100
PS-51/092-11	7.8209	South	34	74°35′5″	130°08′4″	–1.584	32.427	Sandy-silty clay	100
PS-51/085-2	No data	South	22	73°33′9″	131°16′3″	–1.086	27.896	Sandy-silty clay	98
PS-51/080-11	7.0	South	21	73°27′83″	131°39′0″	–1.062	23.407	Silty clay	85
PS-51/135-2	19.22	East	51	76°09′93″	133°14′78″	–1.6		Sandy silt	100
PS-51/104-14	37.9471	East	34	75°57′83″	132°09′06″	–1.565	32.638	Sandy silt	100
PS-51/106-1	No data	East	33	75°56′97″	132°04′39″	–1.5		Silty sand	90
PS-51/105-3	34.7664	East	33	75°57′2″	132°06′13″	–1.590	32.821	Sandy silt	94
PS-51/138-10	12.4038	East	41	75°09′18″	130°49′75″	–1.648	33.219	Sandy silt	100
IK9306-11	No data	South	17.5	72°00′63″	130°59′23″	–	No data	Clay	No data
IK9307-3	No data	South	20.7	72°32′97″	131°17′80″	–	No data	Mud	No data
IK93Z4-3	No data	South	14	72°01′90″	130°07′55″	–	No data	Silty clay	No data
IK93Z5-4	No data	South	11	71°41′41″	137°00′40″	–	No data	Mud	No data
PM9402-3	No data	West	47	75°29′44″	115°14′94″	–	No data	No data	No data
PM9441-4	No data	South	14	74°00′00″	125°59′29″	–	No data	No data	No data
KD9541-13	No data	South	22	73°22′80″	129°56′57″	–	No data	Clayey silt	No data
KD9565-11	No data	South	21	73°50′76″	120°19′00″	–	No data	Sandy silt	No data

ples with abbreviation KD) (Table 1). All surface samples from the TRANSDRIFT V expedition were collected with a giant box-corer, they are represented by approximately the upper 1 cm of undisturbed surface sediment, obtained with a frame that measures 10 × 10 cm. Samples form two sets, which were treated differently. The first set consists of 1-cm-deep samples of undisturbed surface sediment that were collected from an area of about 400 cm^2. These samples were washed over a 63-µm-mesh sieve onboard and stained with Rose Bengal, to be used later to estimate the percentage of ostracode specimens collected alive (Table 1). There is some disagreement about the accuracy of this method of distinguishing dead and living specimens (Brouwers et al., 2000). In this work we assume that both strongly and slightly colored valves and carapaces belong to living ostracodes. The slightly colored valves and carapaces were rare, while many of the strongly colored specimens had their chitinous soft-body parts preserved. The second set consists of 1-cm-deep samples of undisturbed surface sediment, which were collected from an area of about 100 cm^2, were freeze-dried, weighed, and also washed over a 63-µm-mesh sieve (Table 1). Although all the ostracodes were well preserved, there is certain difference between the two sets of samples. The samples that were initially freeze-dried and then washed (second set) contained mainly single valves, whereas those that were stained and washed onboard the ship during the expedition (first set) had considerable numbers of complete carapaces. The two sets also differ slightly in taxonomic diversity; this can most probably be attributed to the different sizes of the sediment samples: the samples of the first set are about four times as large as those of the second set.

The ostracodes picked from the surface sediment samples were identified and counted; the complete carapaces and valves were also counted. For quantitative analysis and calculations of percentages, it was

Table 2. Dry bulk weight of sediment samples in the sections

Sample	Depth, cm	Weight, g
PS51/138-12 (10)		
1	525–528	
2	511–514	185.72
3	505–508	179.02
4	487–490	142.91
5	481–484	178.81
6	475–478	171.68
7	451–454	174.85
8	439–442	151.58
9	427–430	183.34
10	400–403	159.12
11	397–400	175.57
12	391–394	189.89
13	367–370	176.46
14	355–358	215.71
15	349–352	197.71
16	329–332	194.09
17	311–314	217.85
18	287–290	209.02
19	351–254	205.69
20	239–242	210.3
21	193–196	186.47
22	169–172	227.58
23	151–154	170.11
24	129–132	171.22
25	105–108	154.33
26	87–90	189.31
27	54–57	169.28
28	51–54	169.61
29	33–36	107.28
PS51/92-12 (11)		
1	417–420	
2	370–373	
3	196–199	
4	39–41	131.73
5	35–37	148.12
6	31–33	122.93
7	25–27	106.2
8	23–25	120.54
9	17–19	127.09
10	11–13	116.58
11	9–11	107.83
12	7–9	137.22
13	3–5	121.21
PS51/080-11		
13	42–45	203.73
14	40–43	153.60
15	37–39	126.12
16	33–35	126.56
17	29–31	135.86
18	25–27	91.86
19	21–23	109.81
20	17–19	112.68
21	13–15	128.57
22	9–11	141.29
23	1–3	161.88
PS51/154-11		
1	573	84.62
2	555	95.51
3	550	95.63
4	545	89.58
5	543	98.62
6	521	122.38
7	518	116.91
8	513	83.65
9	507	101.21
10	493	92.70
11	467	108.75
12	443	110.46
13	439	146.75
14	421	107.08
15	417	105.94
16	413	113.11
17	411	91.67
18	408	149.88
19	403	126.10
20	395	109.67
21	393	124.24
22	391	105.67
23	388	142.91
24	387	131.92
25	383	132.80
26	381	120.05
27	379	93.91
28	377	109.02
29	375	113.03
30	373	88.54
31	371	100.59
32	369	124.96
33	367	90.92
34	365	81.97
35	363	120.28
36	361	79.47
37	359	102.77
38	357	109.66
39	353	97.41
40	351	117.95
41	349	111.49
42	347	153.28
43	343	90.05
44	341	81.73
45	339	98.15
46	337	119.10
47	335	120.31
48	333	91.06
49	331	129.05
50	329	116.87
51	327	93.65
52	325	117.13
53	323	120.01
54	321	118.50
55	319	108.78
56	317	101.72
57	315	80.82
58	313	83.81
59	311	101.65
60	309	83.01
61	307	117.19
62	305	89.34
63	303	113.88
64	301	108.97
65	299	92.19
66	297	85.45
67	295	76.76
68	293	71.85
69	290.5	62.55
70	289	84.83
71	285	128.57
72	283	110.06
73	280	102.25
74	278	101.84
75	277	79.76

Table 2. (Contd.)

Sample	Depth, cm	Weight, g	Sample	Depth, cm	Weight, g	Sample	Depth, cm	Weight, g
76	276	–	104	195	64.61	132	83	59.31
77	275	120.30	105	190	51.01	133	81	55.00
78	273	103.27	106	187	93.85	134	79	70.02
79	271	89.98	107	185	83.24	135	77	73.17
80	269	93.50	108	181	73.36	136	75	86.28
81	267	112.98	109	179	81.32	137	73	59.62
82	265	124.56	110	177	95.26	138	71	72.61
83	263	100.20	111	175	98.26	139	69	63.84
84	261	86.21	112	173	87.27	140	67	60.07
85	257	90.32	113	169	79.81	141	65	77.68
86	255	114.69	114	167	61.32	142	61	68.53
87	245	114.89	115	161	99.16	143	59	57.28
88	243	97.55	116	157	74.74	144	57	61.06
89	241	82.75	117	153	87.07	145	55	79.17
90	239	87.76	118	151	78.45	146	53	65.22
91	233	85.88	119	149	60.05	147	51	66.07
92	227	91.62	120	135	72.50	148	49	59.42
93	225	102.63	121	133	95.26	149	47	73.57
94	223	101.23	122	129	83.15	150	45	68.33
95	221	90.18	123	127	55.54	151	42	68.00
96	217	90.79	124	123	57.05	152	39	62.57
97	214	99.85	125	121	74.49	153	37	66.98
98	212	94.20	126	119	50.04	154	35	88.96
99	211	103.56	127	113	51.05	155	29	85.89
100	207	94.02	128	99	74.78	156	27	91.75
101	203	95.43	129	97	63.63	157	21	83.50
102	201	98.25	130	93	84.03	158	19	89.78
103	197	85.06	131	85	56.79	159	9	62.58

assumed that a complete carapace is equal to two valves. The abundance of ostracodes was calculated per 100 grams of dry bulk sediment weight. For each sample the percentages of marine, euryhaline, and brackish-water ecological groups were calculated.

For determination of environmental parameters characteristic of different species of ostracodes, we compared average frequencies (proportion of the most abundant species) with water depth and average summer surface salinity (according to the method applied by Polyak et al., 2002).

For cluster analysis, the percentages of 39 taxa from 24 samples (sample KD9541-13, containing only two specimens, was excluded) were processed by the Statistica 6.0 statistical software package. We used the expression 1 – r (where r is Pearson's correlation coefficient) as a measure of difference in the average linkage cluster method to attain the cluster dendrogram.

In order to compare the ostracode assemblages of the Laptev Sea with those of other Arctic seas, we used published data from other authors, the unpublished data of Schornikov, and our own data on the Kara Sea Ostracoda to calculate the value of Jaccard's index, which is equal to the total number of species that occur in both comparable areas ×100%/(total number of species in the first area + total number of species in the second area – total number of species that occur in both comparable areas) (Jaccard, 1912).

Sediment core sections were obtained with the use of gravity corers (PS-51/138-12) and giant box corers (PS51/135-4, PS51/080-13(11), PS51/92-12(11), and PS51/154-11). Samples from cores PS51/138-12(10), PS51/135-4, PS51/080-13(11), PS51/92-12(11), and PS51/154-11 were freeze-dried. Samples from cores PS51/138-12(10), PS51/80-11, PS51/92-12(11), and PS51/154-11 were weighed after freeze-drying (Table 2). The lithological description of the sediment was pre-

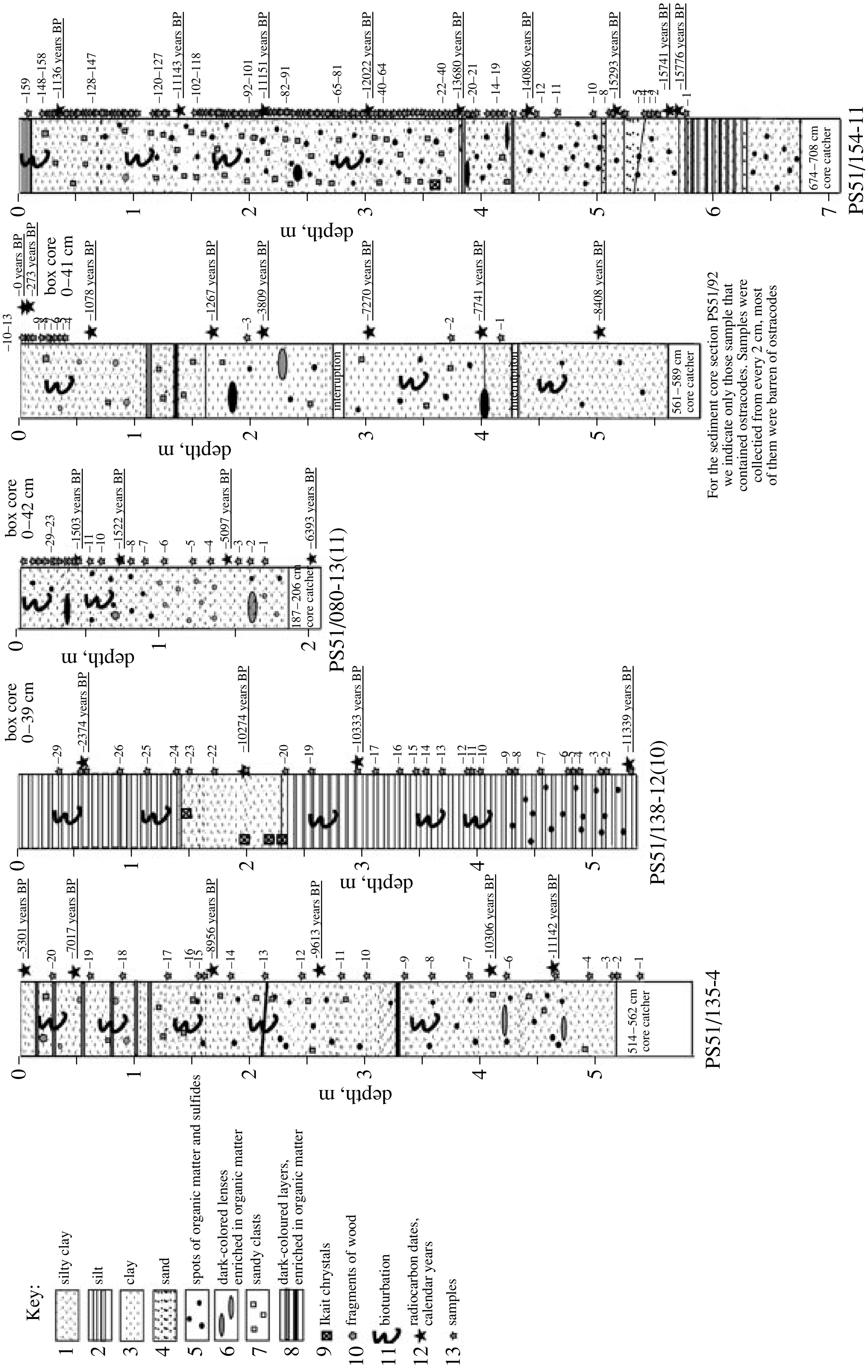

For the sediment core section PS51/92 we indicate only those sample that contained ostracodes. Samples were collected from every 2 cm, most of them were barren of ostracodes

Fig. 2. Lithological description of the sediment cores studied, location of samples, and radiocarbon dates converted into calendar years.

Table 3. Radiocarbon dates

Core	Depth, cm	No. of sample	Bivalves	AMS^{14}C dates	Dates, calendar years
135-4	562	KIA-6918	*Portlandia arctica*	10360 ± 55	11339
	456	KIA-6917	*Portlandia arctica*	10187 ± 60	11142
	403	KIA-6916	*Portlandia arctica*	9580 ± 45	10306
	266	KIA-6915	*Macoma calcarea*	8945 ± 55	9613
	143	KIA-6914	Foraminifers and ostracodes	8460 ± 70	8956
	80	KIA-6913	*Nuculana* sp.	7100 ± 55	7610
	40	KIA-6912	*Yoldia amygdalea hyperborea*	6480 ± 50	7017
	8	KIA-6911	*Macoma* cf. *calcarea*	4920 ± 40	5301
	4	KIA-6910	*Leionucula bellotii*		0
138-2(10)	520	KIA-11043	*Portlandia aestuariorum*	10260 ± 55	11168
	300	KIA-11042	*Portlandia arctica*	9685 ± 50	10333
	197	KIA-11041	*Portlandia arctica*	9440 ± 50	10274
	161	KIA-12930	*Leionucula bellotii*	7745 ± 50	8213
	141	KIA-12929	*Nuculana* sp.	7605 ± 50	8102
	53	KIA-11040	*Nuculana lamellosa lamellosa*	2905 ± 30	2374
080-13	202	KIA-6876	*Portlandia arctica*	5950 ± 35	6393
	142	KIA-6875	*Portlandia arctica*	4795 ± 30	5097
	71.5	KIA-6874	*Portlandia arctica*	1940 ± 25	1522
	41.5	KIA-6873	*Portlandia arctica*	1910 ± 25	1503
092-12	500	KIA-6882	*Macoma* sp.	7950 ± 55	8408
	402	KIA-6881	*Leionucula bellotii*	7280 ± 45	7754
	300	KIA-6880	*Macoma* sp.	6725 ± 40	7270
	160	KIA-6879	*Macoma moesta*	1680 ± 35	1267
	64	KIA-6878	*Leionucula bellotii*	1505 ± 35	1078
	2	KIA-6877	*Leionucula bellotii*	590 ± 25	273
151-11	569		No data	No data	15776
	567		No data	No data	15741
	518	KIA-6925	*Portlandia arctica*	13120 ± 60	15293
	440	KIA-6924	*Yoldiella intermedia*	12525 ± 55	14086
	375	KIA-6923	*Yoldiella lenticula*	12180 ± 60	13680
	300	KIA-6922	*Yoldiella intermedia*	10725 ± 50	12022
	204	KIA-6921	*Leionucula bellotii*	10235 ± 45	11151
	138	KIA-6920	*Macoma calcarea*	10120 ± 55	11143
	31	KIA-6919	*Yoldiella intermedia*	1540 ± 45	1136

pared by Bauch and Musatov during the expedition TRANSDRIFT V to the Laptev Sea in August 1998 on board the German research vessel *Polarstern* (Fig. 2).

Samples were washed over a 63-µm-mesh sieve. After the washed samples were dried, all ostracodes were picked, identified, and counted. The abundance of ostracodes was calculated per 100 g of dry bulk sediment weight. Among ostracodes three ecological groups were distinguished: brackish-water, euryhaline, and marine species; the percentage of each ecological group was estimated for all samples and the results were plotted on graphs. For cores PS51/135-4, PS51/080-13(11), and PS-51/138-12 percentages of juvenile valves were also calculated for each sample. We plotted data on the distribution of different species of ostracodes, mollusks, and foraminifers in sections of all cores studied; in order to do this, we used the additional data of Taldenkova and Dem'yankov on the distribution of mollusks and foraminifers in sediment samples (Taldenkova et al., 2005). We also plotted data on the percentage of valves of different ostracode species in samples. This work was carried out in the Research Center for marine geosciences (GEOMAR) in Kiel (Germany) and in the Russian-German Otto Schmidt Laboratory for Polar and Marine Research in the Arctic and Antarctic Research Institute (St. Petersburg).

The chronology of the cores is based on radiocarbon ages from marine biogenic calcite of bivalves determined by accelerator mass spectrometry (AMS) in the Leibniz Laboratory at Kiel University. All the AMS^{14}C dates were converted to calendar years BP using CALIB 4.3 software program (Stuvier et al., 1998) (Table 3).

For morphological analysis of the assemblages we subdivided all ostracodes into smooth and sculptured forms, and the latter into those with massive sculpture and mezo-sculptured forms. We calculated the proportions of all three morphological types of valves in each sample. In terms of carapace size, we distinguished three size groups: small (in which the length of the carapace is less than 0.4 mm), medium (0.4–0.6 mm), and large (more than 0.6 mm). We calculated the proportions of all three size groups in each sample.

Picking of ostracodes was carried out in the Lomonosov Moscow State University (MGU, Moscow), Paleontological Institute of the Russian Academy of Sciences (Moscow), and in the GEOMAR (Germany). We used a binocular microscope (MBS-9), a dissecting needle, and a brush. A total of 162 samples were analyzed from core sections and samples from 26 surface stations (most of the samples from core PS51/92-12 did not contain ostracodes and they are not taken into account here). Ostracodes were found in 150 samples from the core sections, whereas all surface samples contained ostracodes. A total of 4975 valves and 109 carapaces of ostracodes from core sections and 1287 valves and 583 carapaces from surface sediment samples were picked. The total number of valves and complete carapaces is 6262 and 692, respectively.

Ostracodes were photographed using a scanning electronic microscope (CamScan) in the Paleontological Institute of the Russian Academy of Sciences. A total of 45 species, belonging to 22 genera and 13 families, were identified; four taxa have remained unidentified. Chapter 5 contains descriptions of all the identified species (collection of ostracodes MGU, no. 292/1-292 is housed in the Department of Paleontology, MGU).

CHAPTER 2. MODERN ENVIRONMENTAL SETTING OF THE LAPTEV SEA

The Laptev Sea belongs to the Central Arctic Ocean Basin and is a wide-shelf sea. It is bounded by the Taimyr Peninsula on the west and the New Siberian Islands on the east (Fig. 1).

According to its geographical position and hydrologic conditions, this sea is considered to be a continental marginal sea. Within accepted boundaries the Laptev Sea has a surface area of 662 km^2, a water volume of 353 km^3, a mean depth of 533 m, and a maximum depth of 3385 m.

There are tens of islands in the Laptev Sea, most of them are located in the western part of the sea, some of them in groups, others separately. The Laptev Sea completely occupies the shelf (depths 80–100 m), continental slope, and a minor part of the ocean floor, that is why its bottom is a gently sloping plain, breaking off abruptly toward the north (Semenov and Shkatov, 1971; Zalogin and Dobrovol'skii, 1982). There are four distinct river paleovalleys on the shelf. Starting from the last global sea-level rise, these valleys were the main sedimentation centers (Bauch et al., 1999; Mueller-Lupp et al., 2000).

The high-latitudinal position and great distance from the Atlantic and Pacific oceans, as well as the proximity of the Asian mainland and the presence of the polar ice, make the Laptev Sea one of the most severe among the Arctic seas. Its climate may be classified as continental with prominent marine features. The continental climate is clearly apparent in the large range of air temperature variations, which are, in fact, smoothed in comparison to the variations on the mainland.

Most of the year the sea is ice-covered: from October until mid-July. In the shallow coastal zone fast ice has a thickness of 1.5–2 m. The northern boundary of the fast ice runs approximately along the 20–25 m depth contour, where an up-to-100-km-wide polynya can form in winter, separating the fast ice from the region with drift ice (Gukov, 1999).

The polynya is the source of salinization of marine waters, occurring during ice formation, since the formed ice is fresh, while salts concentrate in the water. River discharge plays an important role in the distribution of salinities in the water column, primarily it applies to the Lena River, the annual discharge of which exceeds that of all the other rivers and makes up 70%. During summer, waters are freshened and more strongly stratified due to considerable continental river run-off and ice melting. The thickness of the upper freshened layer decreases from the nearshore areas towards the outer edge of the fast ice, in the same direction reduces the vertical salinity gradient in the halocline. During autumn storms the waters of the shallow parts of the Laptev Sea mix intensively, thus equalizing parameters vertically (Gukov, 1999; Wegner, 2004). Most likely, salinity anomalies are caused by continental river run-off (Zalogin and Dobrovol'skii, 1982; Fig. 3).

On average, the salinity of both surface and bottom waters is lower in the eastern Laptev Sea (Dmitrenko et al., 2001a; Dmitrenko and Kirillov, unpublished). Following the distribution of riverine waters, the average salinity of summer surface waters ranges from about 5‰ in the southeast to 10–15‰ in the east and up to 30‰ in the west (Fig. 3a). In winter, the reduced river runoff and sea ice formation increase the average

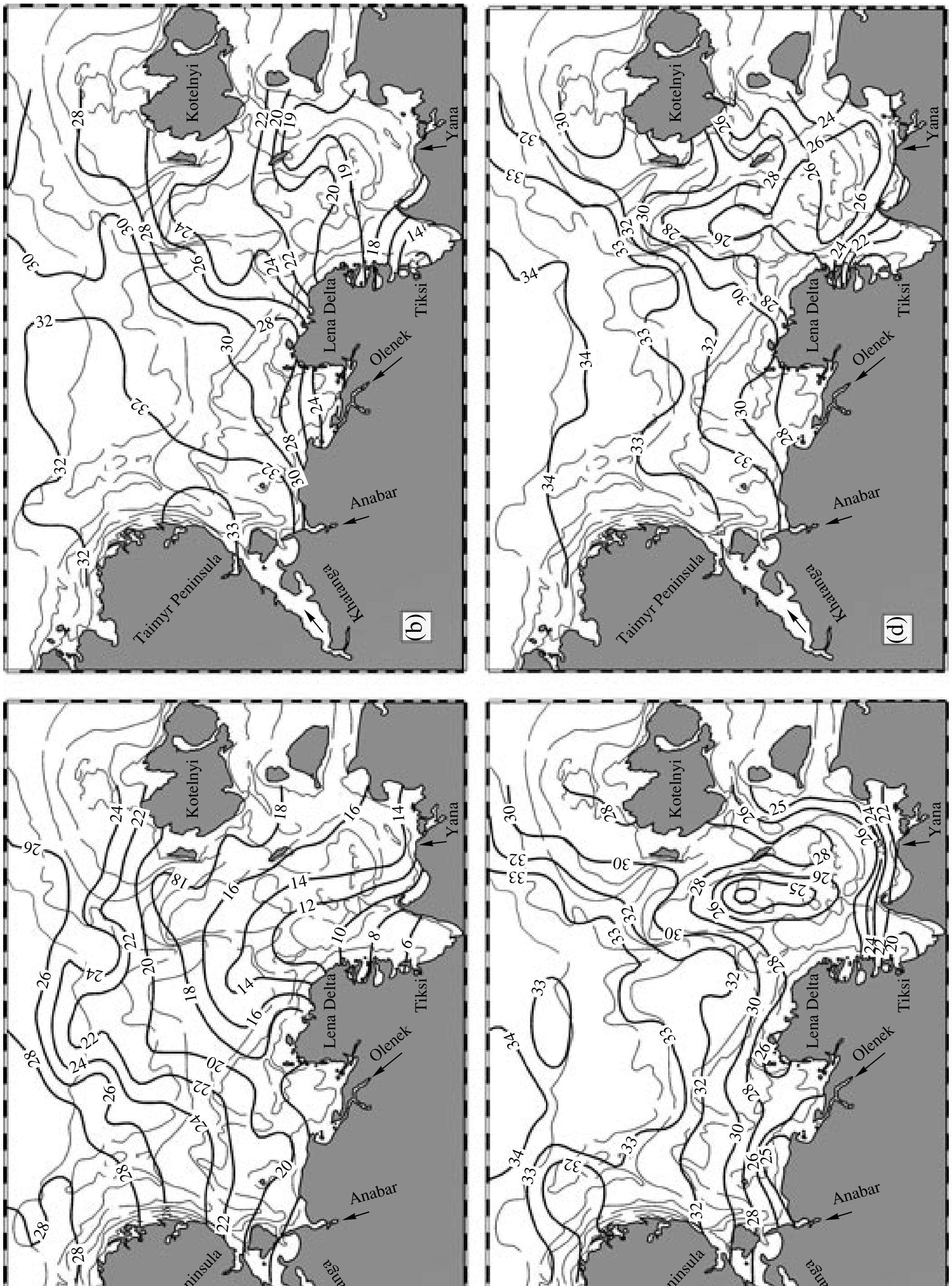

Fig. 3. Average salinity: (a) average surface salinity in summer; (b) average surface salinity in winter (Dmitrenko et al., 2001a); (c) average bottom salinity in summer; (d) average bottom salinity in winter (Dmitrenko and Kirillov, unpublished data).

surface salinity, which varies from 10–12‰ in the southeast to 33‰ in the west (Fig. 3b). The bottom salinity is less dependent upon river runoff. In both summer and winter, it varies from 18–20‰ in the shallow southeastern region to 30–34‰ at depths exceeding 30 m (Figs. 3c, 3d).

Bottom water temperature reflects the distribution of salinities. In the estuarine-arctic waters dominating the shallow parts of the Laptev Sea close to the Lena River mouth, the water temperature drops to –0.2°C in winter and rises locally up to +9°C in summer, but usually it varies from 0 to +4°C. Farther north, in deeper waters (40–60 m), the water temperature is constant; variations in surface water temperature are noticeable only in summer (Gukov, 1999).

The Atlantic waters are of crucial importance for the climate of the northern polar regions: they transfer heat and salts from temperate to polar latitudes. The Atlantic waters enter the Nansen Basin of the Central Arctic Ocean and then move along the continental slope of this basin as a deepwater current. These waters enter the northern parts of marginal seas through deepwater troughs. At depths exceeding 80–100 m, the water temperature rises up to 0.6–1°C under the influence of warm Atlantic waters. Recent oceanographic investigations (Dmitrenko et al., 2001b) have shown that sometimes the bottom countercurrents may be sufficiently strong to bring these relatively warm Atlantic waters along the paleovalleys as far as the shelf at depths of 20–40 m.

CHAPTER 3. RECENT OSTRACODA FROM THE LAPTEV SEA AND THEIR ENVIRONMENTAL ASSEMBLAGES

3.1.1. Previous Studies of Ostracoda in the Russian Arctic

Although ostracodes play an important role in paleoenvironmental reconstructions of high-latitudinal shallow shelves, data on the recent Ostracoda of the Russian Arctic are limited and fragmentary. Scott (1899) and, earlier, Brady and Norman (1889) described the ostracode faunas of the Barents Sea, Franz Josef Land, and Spitsbergen; the faunas of these regions were also studied by Müller (1931) and Klie (1942). Elofson (1941) mentioned several species recorded from the Kara Sea and the Matochkin Shar Strait region. Gorbunov (1946) listed 26 species from the shallow waters around the New Siberian Islands; from the same region Akatova (1946) described several ostracode species. In 1957 she published descriptions of five ostracode species from the Onega Bay of the White Sea (Akatova, 1957), and in 1962 Rudyakov described 20 species from the Kandalaksha Bay of the White Sea (Rudyakov, 1962). Schneider (1962) described two ostracode species from the Arctic Basin. One of the major works is that of Neale and Howe (1975); they listed species recorded from the Barents Sea and compared the ostracode fauna of the Russian Harbor (Novaya Zemlya) with those from other high-latitudinal areas.

Chavtur studies Arctic Myodocopa; he published a paper with detailed descriptions of carapaces and soft body parts of these ostracodes from the northern Hemisphere, including 34 new species (Chavtur, 1983). The distribution of 37 myodocopid species in the White, Barents, Kara, Laptev, East-Siberian, and Chukchi seas, as well as in the Central Arctic Basin was given by Chavtur in the list of free-living invertebrates of the Eurasian Arctic seas and adjacent regions (2001).

Information on the distribution of 97 species of Podocopida in the Chukchi, Kara, Barents, Laptev, and East-Siberian seas, as well as in the Central Arctic Ocean, is contained in the Arctic Podocopid Database (Cronin et al., 1991). Most of the stations were located at depths exceeding 70 m.

Schornikov has been studying Arctic Ostracoda for many years (Schornikov, 1980, 2001, 2004; Schornikov and Tsareva, 2002). At present, he has prepared for publication a paper on the ostracode fauna of the White Sea, where he lists 95 ostracode species. Earlier, he published a paper dealing with the genus *Jonesia* Brady from the White and Barents seas (Schornikov, 1980). The paper of Schornikov and Tsareva (2002) deals with changes in the surface sculpture of the White Sea members of *Hemicythere villosa* in ontogeny (Sars, 1866). The species list for the White, Barents, Kara, East-Siberian, and Chukchi seas, as well as for the Laptev Sea and the Central Arctic Ocean, was published by Schornikov in 2001. In 2004, he published a paper on the benthic ostracode fauna of the Laptev Sea, with a list of 63 ostracode species.

Aladin (1985) studied the Ostracoda of the White and Barents seas. In a paper devoted to the investigation of salinity adaptations of ostracodes, he listed 19 species from these seas. The most recent publication about ostracodes of the White Sea is by the present author (Stepanova, 2002). It contains illustrations of 13 ostracode species from bottom surface sediments from the Kandalaksha Bay of the White Sea.

A very important contribution to investigation of Neogene–Quaternary Ostracoda from the Russian Arctic was made by Lev (1970, 1972, and 1983): she studied fossil Ostracoda from coastal outcrops from the Arkhangel'sk region in the west to the Laptev Sea coast in the east. Lev's works contain detailed information about geological and geographical distribution and ecological preferences of most ostracode species, and she also described some of them. Despite the fact that the taxonomy of several species described by Lev was recently revised, her works have currently remained the most detailed sources of information on the taxonomy of the Ostracoda of the Russian Arctic.

In the work of Kupriyanova (1999) illustrations of 28 ostracode species and descriptions of different ecological assemblages are given for the Quaternary Ostracoda of the Pechora Sea.

Thus, the best studied among the Russian Arctic seas are the White and Barents seas (Brady and Norman, 1889; Scott, 1899; Müller, 1931; Klie, 1942; Neale and Howe, 1975; Schornikov, 1980, 2001; Aladin, 1985; Cronin et al., 1991; Schornikov and Tsareva, 2002; Stepanova, 2002), while the Kara, East-Siberian, and Chukchi seas are virtually not studied (Cronin et al., 1991; Schornikov, 2001). As for the Laptev Sea ostracodes, Stepanova et al. (2003, 2004) were the first to undertake their detailed investigation, in which not only species lists were given, but also illustrations and descriptions of species and fossil ostracode assemblages were used for paleoreconstructions (see the relevant chapters of the present paper).

3.1.2. Previous Studies of Ostracoda in the Laptev Sea

Only ten papers are currently available which mention recent ostracode species from the Laptev Sea (Akatova, 1946; Gorbunov, 1946; Cronin et al., 1991; Bauch et al., 1995; Erlenkeuser and von Grafenstein, 1999; Chavtur, 2001; Schornikov, 2001, 2004; Stepanova et al., 2003, 2004) (Table 4). Akatova (1946) gave a taxonomic description of seven ostracode species from the shallow waters around the New Siberian Islands (depths range from 14 to 68 m). Gorbunov (1946) provided a complete list of 26 Ostracoda species identified by Akatova from the same region. Neale and Howe (1975) used the data of Akatova (1946) in their review of high-latitude ostracode fauna in order to assess the relationship between ostracode faunas of different Arctic regions. In general, they regarded the ostracode fauna of the Arctic shelf waters as a single circumpolar province with minor differences between the eastern and western subprovinces. However, in their review the authors were mainly dealing with the data from the western Arctic. Sixteen ostracode species from five samples from different parts of the Laptev Sea collected during the voyage of the United States Coast Guard ship *Northwind*, 1963, were listed in the Modern Arctic Podocopid Database (Cronin et al., 1991). Three samples from the mid-depths of the western shelf (32–53 m) and two from the Lena paleovalley (22–33 m) exhibit a high taxonomic diversity (up to 15 species per sample) with predominance of *Paracyprideis pseudopunctillata, Heterocyprideis fascis*, and *Elofsonella neoconcinna.* In contrast, all samples from the eastern shallow-water Laptev Sea are rather poor in taxonomy—they contain only three species: *Sarsicytheridea bradii, Heterocyprideis sorbyana*, and *Paracyprideis pseudopunctillata*, the latter being the most abundant. Another two studies (Bauch et al., 1995; Erlenkeuser and von Grafenstein, 1999) merely presented lists of ostracode species found in coretop samples collected during two expeditions to the Laptev Sea in the early 1990s. In the work of Bauch et al. (1995) Cronin identified 17 ostracode species from samples located at water depths 16–46 m in the southern part of the Laptev Sea, a typical inner shelf Arctic assemblage dominated by *Paracyprideis pseudopunctillata, Sarsicytheridea* spp., *Heterocyprideis sorbyana*, and *Cluthia cluthae.* These authors concluded that a similar assemblage is also characteristic of the inner Alaskan and Canadian shelf (e.g., Cronin, 1989). In their paper on the isotopic composition of the ostracode calcareous carapaces, Erlenkeuser and von Grafenstein (1999) briefly review the distribution of 12 ostracode species in the surface sediment samples collected at depths 11–110 m from the southern and eastern regions of the Laptev Sea. Chavtur (2001) and Schornikov (2001), in a list of free-living invertebrates of the Eurasian Arctic seas, listed 22 species from the Laptev Sea collected at depths of 48–276 m, including those identified by Akatova (1946). Stepanova et al. (2003) identified 35 taxa to the species level, for the first time each of them was illustrated with photographs. We also established ecological ostracode assemblages corresponding to certain environmental parameters: depth and salinity (see the relevant chapters of the present paper). Later, I revised the genus *Cytheropteron* Sars, 1866; 16 species were described, one of which is new (Stepanova et al., 2004). Schornikov (2004) investigated the benthic ostracodes of the Laptev Sea. He listed 63 species, of which he identified 39. Three new species of *Sclerochilus* Sars, 1866 were described (Table 4).

3.2. Ecology of the Laptev Sea Ostracodes

Recent ostracodes have been studied in samples from 26 bottom stations collected at different depths from the shelf and continental slope of the Laptev Sea. Based on a quantitative analysis, three assemblages were established, the differences between them were defined by the environmental parameters, such as (water) depth, bottom water salinity, water mass circulation, and ice-rafting (Fig. 4).

Ecological characteristics of the species found in our samples are based on both our own data and the published evidence on their occurrences in other Arctic and high-latitudinal seas (Table 5; Neale and Howe, 1975; Cronin, 1977, 1981; Lev, 1983; McDougall et al., 1986; Nikolaeva et al., 1989; Brouwers, 1990, 1994; Cronin et al., 1991, 1994; Reimnitz et al., 1992; Jones et al., 1998; Brouwers et al., 2000). In order to demonstrate some possible environmental preferences of ostracodes, the average frequencies of the most abundant species were plotted versus water depth and average summer surface salinity (Fig. 5). In terms of water depth, four groups of ostracodes have been distinguished: those that prefer the shallow inner shelf (11–30 m), the middle and outer shelf (30–60 m), the upper continental slope (60–100 m), and depths exceeding 100 m (up to 276 m) (Fig. 5). We used the average summer surface (water) salinity to estimate the influence of river runoff on the ostracode community (Fig. 5). Pre-

Table 4. Species list of the Laptev Sea Ostracoda

Our data	Identification of other researchers	Gorbunov, 1946; Akatova, 1946	Cronin et al., 1991	Bauch et al., 1995	Erlenkeuser and von Grafenstein, 1999	Schornikov, 2001	Chavtur, 2001	Schornikov, 2004
11–276 m		14–68 m	22–53 m	16–46 m	11–110 m	48–276 m	–	–
Bythocythere constricta		+						+
Pseudocythere caudata								+
Sclerochilus sp. 1		+						+
Jonesia acuminata		+				+		
Cytheromorpha macchesneyi				+				
Cluthia cluthae			+	+				+
Cytheropteron arcuatum			+	+				+
C. biconvexa								+
C. champlainum					+			+
C. elaeni				+	+			
C. inflatum								+
C. montrosiense								+
C. nodosoalatum			+					+
C. porterae								+
C. tumefactum								+
C. sulense								+
C. suzdalskyi								+
C. pseudomontrosiense			+		+			
C. perlaria								
Semicytherura complanata			+	+	+			+
Palmenella limicola		+	+	+		+		
Acanthocythereis dunelmensis		+	+	+	+	+		+
Rabilimis septentrionalis		+		+		+		+
Heterocyprideis sorbyana		+		+	+	+		+
H. fascis			+					+
Sarsicytheridea bradii				+		+		+
S. punctillata		+		+		+		+
Paracyprideis pseudopunctillata			+	+	+	+		+
Krithe glacialis		+	+			+		+
Argilloecia cylindrica								+
Argilloecia sp.								+
Elofsonella concinna		+	+	+	+	+		
Eucythere argus								
Polycope bireticulata								+
Polycope orbicularis								+
Polycope punctata								+
Polycope sp. 1								+
	Paracyprideis fennica	+						
	Philomedes brenda	+					+	+
	Polycope sp. juv. Akatova, 1946	+					+	
	Cytheridea papillosa	+						
	Eucythere undulata	+				+		
	Hemicythere angulata	+						
	Hemicythere sp. Akatova, 1946	+						
	Rabilimis mirabilis	+				+		+
	Cythereis sp. Akatova, 1946	+						

Table 4. (Contd.)

Our data	Identification of other researchers	Gorbunov, 1946; Akatova, 1946	Cronin et al., 1991	Bauch et al., 1995	Erlenkeuser and von Grafenstein, 1999	Schornikov, 2001	Chavtur, 2001	Schornikov, 2004
11–276 m		14–68 m	22–53 m	16–46 m	11–110 m	48–276 m	–	–
	Cytherura sp. Akatova, 1946	+						
	Robertsonites tuberculatus	+	+			+		+
	Roundstonia globulifera	+	+			+		+
	Cytheropteron alatum	+				+		
	Cytheropteron spp.	+	+					
	Argilloecia spp.	+		+				
	Paracythereis sp. Akatova, 1946	+						
	Semicytherura affinis		+					
	S. concentrica		+					
	Krithe cf. *glacialis*				+			
	Cytheropteron paralatissimum				+			+
	Normanicythere leioderma				+			+
	Rabilimis paramirabilis				+			
	Boroecia maxima						+	
	B. borealis						+	
	Jonesia arctica					+		
	Finmarchinella barenzovensis					+		+
	Krithe minima					+		+
	Baffinicythere sp.			+				
	Polycope spp.			+				
	Sarsicytheridea macrolaminata			+				+
	Discoconchoecia elegans						+	
	Argilloecia sp. Schornikov, 2001							+
	Jonesia arctica							+
	Jonesia barentsovensis							+
	Sclerochilus (*Sclerochilus*) *jurasovi*							+
	Sclerochilus (*Sclerochilus*) *laptevensis*							+
	Sclerochilus (*Sclerochilus*) *laptevi*							+
	Microcytherura sp. Schornikov, 2001							+
	Palmenella dentomarginata							+
	Cluthia sp. Schornikov, 2004							+
	Eucythere sp. 1 Schornikov, 2004							+
	Eucythere sp. 2 Schornikov, 2004							+
	Pontocythere sp. Schornikov, 2004							+
	Acanthocythereis agapensis							+
	Cytheretta teshekpukensis							+
	Elofsonella neoconcinna							+
	E. pinegensis							+
	Pteroloxa venipuncta							+
	Cytherura sp. Schornikov, 2004							+
	Semicytherura sp. 1 Schornikov, 2001							+
	Semicytherura sp. 2 Schornikov, 2001							+
	Cytheropteron dimlingtonensis							+
	Cytheropteron sp. cf. *elaeni*							+
	Cytheropteron testudo							+
	Paracytherois sp. A Schornikov, 2004							+

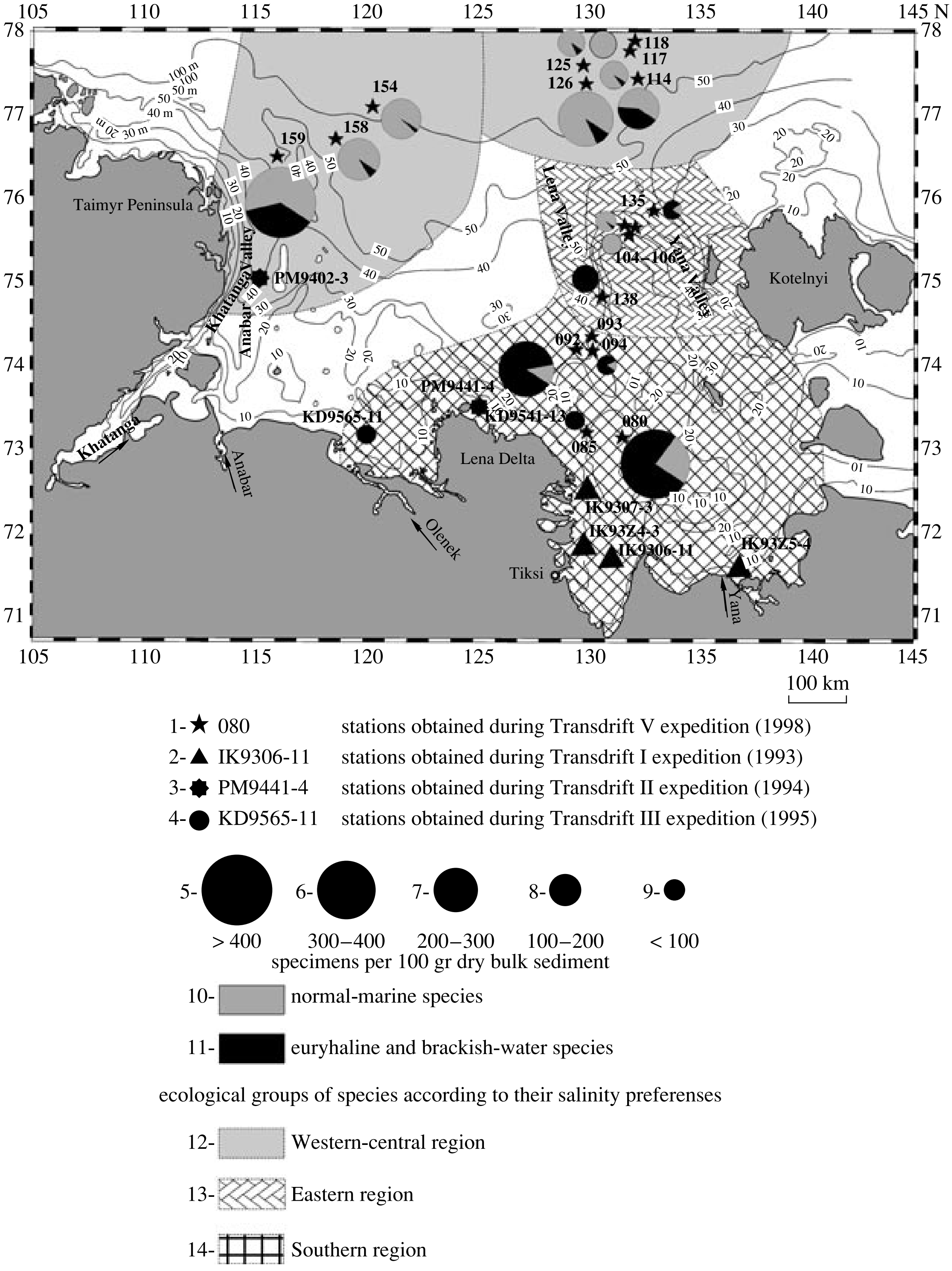

Fig. 4. Location of the stations studied and geographical distribution of the assemblages: (1) stations obtained during Transdrift V expedition (1998); (2) stations obtained during Transdrift I expedition (1993); (3) stations obtained during Transdrift II expedition (1994); (4) stations obtained during Transdrift III expedition (1995); (5–9) specimens per 100 g dry bulk sediment; (10–11) ecological groups of species according to their salinity preferences; (10) normal-marine species; (11) euryhaline and brackish-water species; (12–14) ecological groups of species according to their salinity preferences; (12) Western-central region; (13) Eastern region; (14) Southern region.

Table 5. Ecological characteristics of the species studied

Ostracode species identified from the Laptev Sea by the present author	Shallow-shelf	Middle-outer shelf	Continental slope	Marine	Euryhaline	Brackish-water
Bythocythere constricta			+	+		
Pseudocythere caudata			+	+		
Sclerochilus sp.			+	+		
Jonesia acuminata			+	+		
Cytheromorpha macchesneyi	+					+
Cluthia cluthae		+	+	+		
Cytheropteron arcuatum		+	+	+		
C. biconvexa			+	+		
C. champlainum			+	+		
C. elaeni	+	+		+		
C. inflatum			+	+		
C. montrosiense	+	+		+		
C. nodosoalatum		+	+	+		
C. porterae			+	+		
C. tumefactum			+	+		
C. sulense			+	+		
C. suzdalskyi	+	+		+		
C. pseudomontrosiense			+	+		
C. perlaria			+	+		
Semicytherura complanata	+	+	+	+		
Palmenella limicola	+	+	+	+		
Acanthocythereis dunelmensis	+	+	+	+		
Rabilimis septentrionalis	+		+	+		
Heterocyprideis sorbyana	+		+		+	
H. fascis			+		+	
Sarsicytheridea bradii		+	+	+		
S. punctillata			+	+		
Paracyprideis pseudopunctillata	+	+	+		+	
Krithe glacialis			+	+		
Argilloecia cylindrica			+	+		
Elofsonella concinna	+	+	+	+		
Eucythere argus			+	+		
Polycope bireticulata	+	+	+	+		
Polycope orbicularis	+	+	+	+		
Polycope punctata	+	+	+	+		

viously Polyak et al. (2002) used this method in their study of the benthic foraminiferal assemblages in the Kara Sea. These authors distinguished three types of assemblages: river-proximal (<15 m), river-intermediate (15–25 m), and river-distal (>25 m) (Table 5).

In addition, we calculated the total abundance per 100 g dry bulk sediment weight for most of the stations, as well as the percentage of ostracodes collected alive and the proportion of juvenile valves (Fig. 4).

In general, the ostracode abundance is high in the southern nearshore zone and in the Khatanga paleovalley: from 300 to 600 specimens per 100 g dry weight of sediment (Fig. 4). The abundance is also relatively high on the continental slope (160–350). Although samples from the eastern middle shelf contain considerably less valves (27–113), they have the highest abundance of living ostracodes (up to 100%; Table 1). These stations are restricted to those parts of submarine river valleys

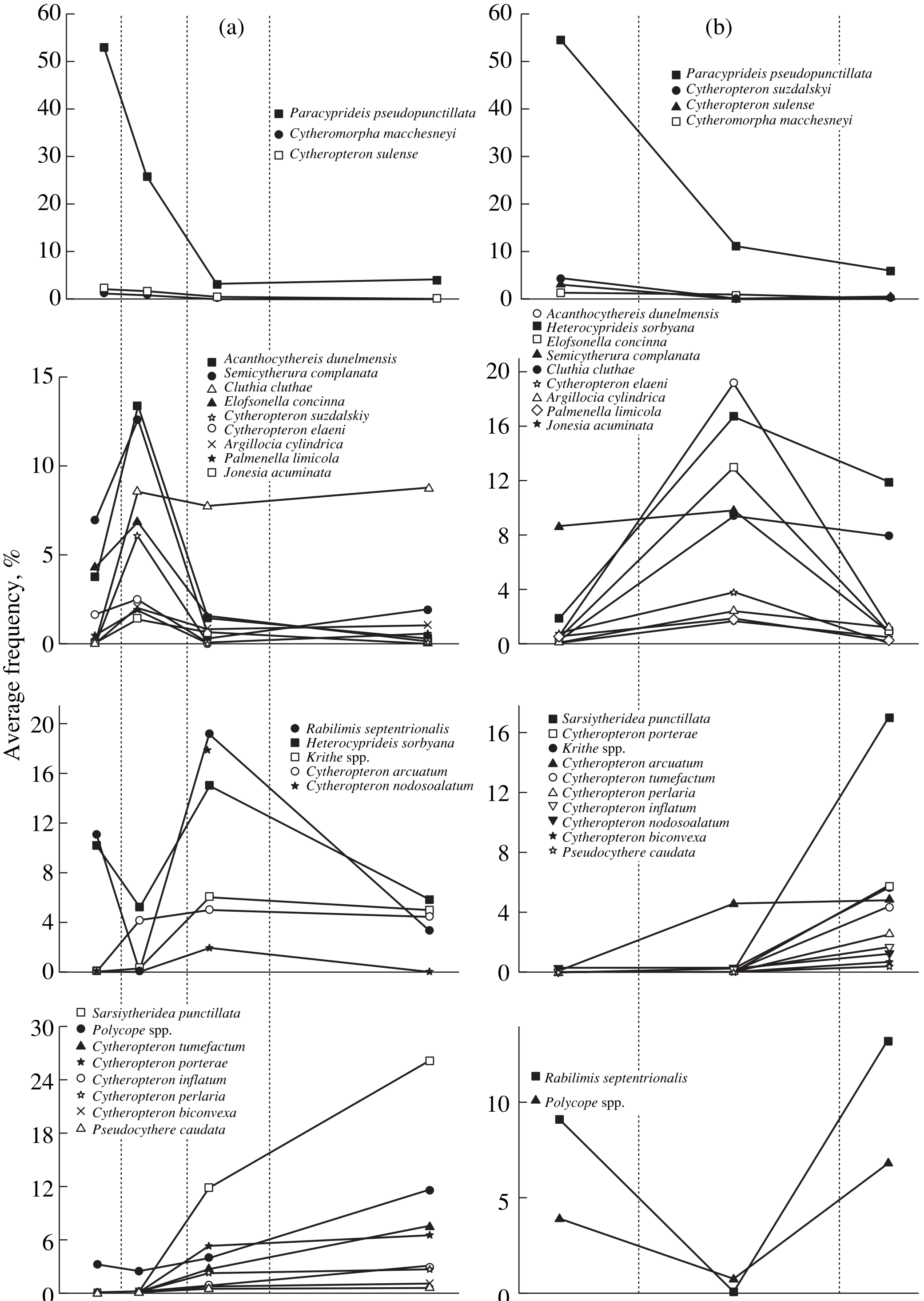

Fig. 5. Average frequencies of ostracode species abundance (average value of the share of valves of species in a sample in a certain range of depth and salinity) vs. (a) water depth; (b) salinity.

where the strongest bottom currents have been observed (Dmitrenko et al., 2001a). It is probable that these currents carry away dead valves from these sites. Such a situation is quite common in hydrodynamically active environments (Frenzel and Boomer, 2005). Also possibly for the same reasons no juvenile valves have been found in the samples from shallow-water areas and only a few juveniles were recognized in the deeper

Table 6. Distribution of ostracode species in the surface samples from the western Laptev Sea

Species/station	158-8		159-8		154-9		PM9402-3
	1	2	1	2	1	2	
Bythocythere constricta	4v 3c						
Pseudocythere caudata	2c				2c		
Sclerochilus sp.	1v 8c						
Jonesia acuminata	4v 2c						
Cluthia cluthae	1v 8c	3v	1v	9v	6c	10v	
Cytheropteron sulense	2c	2v					
C. arcuatum	2v 6c	1v	1v	3v	1v 2c		
C. porterae	2v 6c	15v	4v 2c		4v 1c	3v	
C. perlaria	2c	1v					
C. tumefactum	3v 5c			6v	5v 13c		
C. discoveria		2v					
C. biconvexa		2v					
C. inflatum		4v 1jc		1v			1v
C. nodosoalatum	1v 1c	4v					
C. cf. *nodosum*							1v
Semicytherura complanata			2c			5v	
Palmenella limicola						4v	
Acanthocythereis dunelmensis			2v			2v	
Rabilimis septentrionalis	1v 8c	5v 2jv	34v 13c	1v	2v 1c	11v 7jv	
Heterocyprideis sorbyana	2c	3v	16v 4c	2v	8v	7v	10v
H. fascis							16v
Heterocyprideis sp. juv.							4 jv
S. bradii				3v		6v	
S. punctillata	2v	2v		18v 1c 14jv	58v 16c		
Paracyprideis pseudopunctillata	1c	1v	23v 25c			22v	15v
K. glacialis	8v 2c	11v	1v		2v1c		1v
Argilloecia cylindrica	1c				1v 2c		
Elofsonella concinna			4v			1v	13v
Eucythere cf. *argus*		1v					
Polycope punctata		1c	1c				
Polycope spp.	2c				1v 9c		

Note: Here and forth: (v) single valves; (c) carapaces; (jv) juvenile valves; (jc) juvenile carapaces; and (1, 2) sets of samples: set 1 of samples was stained with Rose Bengal; set 2, unstained.

western and central regions (Tables 6, 7). On the other hand, it is not inconceivable that juvenile carapaces were rapidly dissolved in the extremely undersaturated Arctic waters.

Taxonomic diversity was found to decrease in an eastward direction, from 15 or 16 species per sample in the west to 5 to 7 species per sample in the east (Tables 6–9). The lowest diversity was recorded in the nearshore zone close to the Lena Delta and Yana estuary (Table 9) and in the samples obtained in the Sannikov Strait near the New Siberian Islands (Cronin et al., 1991).

The samples studied were obtained from the western-central, southern, and eastern parts of the sea (Fig. 4, Tables 6–9). Stations were grouped according to their geographical location. This geographical grouping is also supported by the results of cluster analysis. The dendrogram (Fig. 6) clearly shows two major clusters that generally correspond to the western-central and southeastern regions. Most stations in the western and central Laptev Sea are located on the upper continental slope (at depths 62–276 m). The southern and eastern stations are restricted to shallow-water shelf areas (11–55 m). Most samples from the western-cen-

Table 7. Distribution of ostracode species in the surface sediments of the central part of the Laptev Sea

Station	118-1		125-12		114-3		117-3		126-2	
Species/set	1	2	1	2	1	2	1	2	1	2
Bythocythere constricta	1v 2c						1v 1c			
Cluthia cluthae	8c		1c	4v		5v	12c	4v	5c	4v
Cytheropteron sulense			1v							
C. arcuatum	9v	4c	1v				6c	2v	2v 2c	12v
C. porterae	7v 1c	5v		5v 1c	1v		2v 2c	5v	3v	2v
C. perlaria	3v	4v	1v 1c				1v 3c	3v	4c	
C. tumefactum	7v 1c		2v 1c				2v 1c	1v	2v 1c	
C. biconvexa	2c								2c	1v
C. nodosoalatum										1v
C. champlainum							1v	2v		
C. inflatum		7v		4v						1v
Semicytherura complanata	2v	2v		1v						
Acanthocythereis dunelmensis					5v 2c		4c	1v		
Rabilimis septentrionalis			2v 1c		9v 16c	17, 1jv	1v 1c	1v	3v 5c	8v, >50jv
Heterocyprideis sorbyana	5v		5v 2c	3v	26v 47c	25v 1c	2v 1c	4v		5v 1c
Sarsicytheridea punctillata	6v 1c	2v	19v 5c	18v 3c	4v 1c	2v	8v 3c	11v 1c 28jv	4v	5v 1c
S. bradii				14v		1v				
Paracyprideis pseudopunctillata			3v	3v	8v	1v	3v 2c	1v		
Krithe glacialis	7v 1c	6v	2v		5v 4c	6v	1v	1v	10v 5c	5v
Argilloecia cylindrica	1c						3c		2v	1v
Argilloecia sp.						2v				
Elofsonella concinna					3v 3c	6v				
Eucythere cf. *argus*				4v						
Polycope spp.	10c		4v 6c				3v 13c		1c	
(*Polycope punctata, P. bireticulata, P. orbicularis*)										
Polycope sp.										

tral region represent a single assemblage (Fig. 6, cluster II). Cluster III includes stations of the southern region. Clusters I and IV include stations from the southern and eastern regions (Fig. 6).

3.3.1. Western-Central Region of the Laptev Sea

The ostracode assemblage of this region (water depths 62–276 m) exhibits the highest taxonomic diversity among the studied samples and consists of 35 species (Fig. 6, cluster II; Tables 6, 7). It is distinguished from the others by the presence of relatively deepwater species (Fig. 4) such as *Pseudocythere caudata* (about 2%), *Krithe glacialis* (1–14%), *Cytheropteron inflatum* (from <1 to 5%), *C. biconvexa* (1–3%), *C. nodosoalatum* (1–3%), *C. tumefactum* (3–7%), *C. porterae* (3–14%), *C. perlaria* (2–5%), and *Polycope* spp. (*P. punctata, P. orbicularis,* and *P. bireticulata;* 1–15%). All these species are typical of the Arctic seas and the North Atlantic (Joy and Clark, 1977; Cronin, 1989, 1996; Cronin et al., 1994, 1995; Jones et al., 1998, 1999; Whatley et al., 1998; Didié, 2001). However, their relative abundance in the samples and the total species composition change with depth (Fig. 6). Most samples combined into cluster II (water depth 62–276 m) are dominated by deepwater species: *C. porterae* and *C. arcuatum* and, at the greater depths, by *S. punctillata* and *Polycope* spp. (*P. punctata, P. orbicularis, P. bireticulata*, and *Polycope* sp.). Three samples PS51/159, PS51/126, PS51/114 (water depth 62–85 m) are dominated by shallow-water *R. septentrionalis* and *H. sorbyana* (up to 53%), but also include many of the abovementioned deepwater forms. The increased abundance

Table 8. Distribution of ostracode species in the surface sediments of the eastern Laptev Sea

Species/station	104-14		105-2		106-1		135-2		138-10	
Jonesia acuminata	1c		2v 3c		1v					
Cytheromorpha macchesneyi					1v				1c	
Cluthia cluthae		2v	4v 14c	3v	6c		10c			
Cytheropteron arcuatum			2c		4v 7c					
C. elaeni						2v	3v 7c	1v		
C. suzdalskyi					1v				1v 5c	3v 1c
C. nodosoalatum			1v	1v						1v
Semicytherura complanata		9v	4c	4v	5c		3v 11c		2c	6v 1c
Palmenella limicola		1c					4v 5c			
Acanthocythereis dunelmensis	1v 15c	14v	4v 8c	6v	4v 4c	3v	1v 7c	2v		
Sarsicytheridea bradii				3v						
Paracyprideis pseudopunctillata			2c	1c	4v 2c		1v 3c	11v	1v 1c	
Argilloecia cylindrica	1v 5c		1v				1v			
Elofsonella concinna	1v 2c	4v	4v 8c		1v 2c					
Polycope spp.	2v 1c									

Table 9. Distribution of ostracode species in the surface sediments of the southern Laptev Sea

Species	Stations														
	085-2		092-11		093-1		080-11		IK93	IK93	IK93	IK93	PM94	KD95	KD95
									06-11	07-3	Z4-3	Z5-4	41-4	41-13	65-11
	1	2	1	2	1	2	1	2							
Bythocythere constricta	1c														
Cutheromorpha macchesneyi		1v							1fr.		3v				
Cluthia cluthae					1c	1v									
Cytheropteron sulense	2v 3c	1v	1c		3v	7v			1v						
C. arcuatum					1c										
C. montrosiense	1v 3c	1v			2c	2v									
C. elaeni				1v			1c								1v
C. suzdalskyi															
Semicytherura complanata	10c			1v	2c					1v					1v
Palmenella limicola	2c			1v											
Rabilimis septentrionalis												22v 1c			
Acanthocythereis dunelmensis							1c								3v
Heterocyprideis sorbyana			1c		9v 2c	5v		1v					6v 1c		
Paracyprideis pseudopunctillata			3v 3c	21v	17v 17c	27v	6v 11c	2v 1c	23v	3v 1c	41v 10c			2v	2v
P. sf. *pseudopunctillata*													1v		
Elofsonella concinna								1v							2v 1c
Polycope punctata	7c				2v 9c				1v						
P. bireticulata															
P. orbicularis															
Polycope sp.															

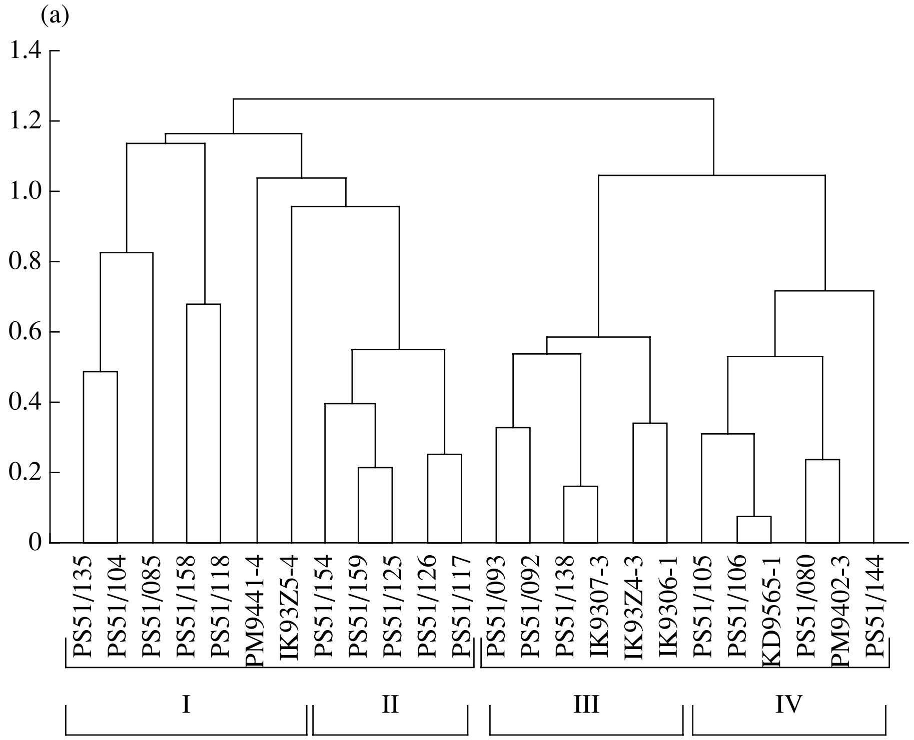

(b)

Cluster	Region	Depth, m	Dominant species
I	Southern and eastern (+2 samples from the western and central regions: PS51/158, PS51/118)	11-121	*Paracyprideis pseudopunctillata, Acanthocythereis dunelmensis, Semicytherura complanata, Heterocyprideis sorbyana*
II	Western and central	62-276	*Semicytherura punctillata, Rabilimis septentrionalis, Polycope* spp.
III	Southern regions (+1 sample from the eastern region, PS51/138)	14-41	*Paracyprideis pseudopunctillata*
IV	Southern and eastern (+2 samples from the western and central regions: PM9402-3 PS51/114)	21-66	*Cluthia cluthae, Acanthocythereis dunelmensis, Heterocyprideis sorbyana, Paracyprideis pseudopunctillata*

Fig. 6. Cluster analysis: (a) cluster analysis dendrogram of 24 samples based on the relative abundance of 39 ostracode species; (b) description of the clusters obtained (assemblages).

of shallow-water species that were found alive in these samples could result from ice-rafting, a well-known factor affecting the sedimentation in the Arctic (Cronin et al., 1994; Jones et al., 1998, 1999). As seen in Fig. 5, *R. septentrionalis* and *H. sorbyana* have in fact two peaks in abundance: in the shallow inner shelf zone and on the upper continental slope within a water depth range of 60–100 m.

3.3.2. Eastern Laptev Sea Region

Samples from the eastern part of the Laptev Sea (33–51 m) form a single, well-defined assemblage that contains 17 species (partly clusters I and IV, Fig. 6) and is dominated by normal marine neritic species (Table 8, Figs. 4, 5) such as *Acanthocythereis dunelmensis* (14–53%), *Semicytherura complanata* (10–36%), *Elofsonella concinna* (7–17%), and *Cluthia cluthae* (2–30%). Cluster I includes three samples from the central, western, and southern regions of the sea (PS51/118, PS51/158, and PS51/085) because they all contain *Bythocythere constricta.* Cluster IV also includes samples from the central and western regions of the sea (PS51/114 and PM9402-3) because these samples contain considerable amounts of *Elofsonella concinna,* which is also abundant in the eastern region of the sea (Fig. 6).

3.3.3. Southern Laptev Sea Region

The ostracode assemblage from the southern Laptev Sea (water depth 11–34 m, Fig. 6, cluster III) considerably differs from the assemblages of the other studied regions in the predominance of inner shelf euryhaline species (Table 9, Fig. 4). This assemblage is very low in diversity: 1 or 2 species per sample in the shallow near-shore area (st. IK9307, IK93Z5, and KD9541). Although these samples are so low in diversity, they have the highest abundance of valves (e.g., 600 specimens/100 g at st. 80). Taxonomic diversity increases northward, while abundance decreases (down to 27 at st. 94). Cluster III includes stations from the southern region of the sea, one sample from the eastern region (PS51/138) was also included because of the presence of the brackish-water species *Cytheromorpha macchesneyi. P. pseudopunctillata* predominates within most of the samples forming this cluster (Fig. 5), *H. sorbyana* and *Semicytherura complanata* are also very abundant. All three species are known to inhabit shallow inner shelf environments (McDougall et al., 1986; Brouwers et al., 1991; Reimnitz et al., 1993; Brouwers et al., 2000). *P. pseudopunctillata* and *Heterocyprideis sorbyana* are known to be tolerant of salinities as low as 5–10‰ (Neale and Howe, 1975; Cronin, 1977; Lev, 1983). Several valves of the brackish-water species *Cytheromorpha macchesneyi* (up to 5%) were also found in the southern region of the sea. This is the only assemblage in which the proportion of brackish-water and euryhaline species reaches 76–88%, thus considerably exceeding that of marine species (Fig. 4).

3.4. Results

Thus, our investigations show that the distribution of ostracode species in the surface sediment samples reflects varying environmental conditions. In terms of water depth, the most pronounced differences are found between the western-central assemblage of the upper continental slope (water depths >60 m) and assemblages from the eastern and southern shelf regions (water depths less than 60 m). We used the Jaccard index for comparison of these assemblages (Jaccard, 1912). Our calculations show that there is a strong similarity between the eastern and southern assemblages (60%), while the Jaccard index for the similarity between the western-central assemblage and the eastern and southern assemblages is considerably smaller: 37%. The main reason for this is the presence of relatively deep-water species, known from the North Atlantic and Central Arctic Ocean, in the western-central part of the sea. This fact is most probably related to the penetration of Atlantic waters from the west (Zalogin and Dobrovol'skii, 1982).

Salinity is also an important factor in the distribution of ostracodes, especially in regions strongly affected by river runoff. Taxonomic diversity usually decreases at lower salinities, while the total abundance of ostracode valves increases (Frenzel and Boomer, 2005). Compared to the assemblage from the western-central region with normal marine salinity and taxonomically diverse assemblage (34 species), the total number of species found in the eastern and southern assemblages is considerably smaller (20 species). However, the highest abundance of ostracode valves was recorded in the southern, most freshened, region of the sea (600 specimen/100 g, Fig. 5).

With increasing water depth and salinity (from southern to eastern region of the sea), shallow normal-marine species such as *Acanthocythereis dunelmensis, Semicytherura complanata, Cluthia cluthae*, and *Elofsonella concinna*, which together sometimes account for 100% of the assemblage (Fig. 5), become dominant. This assemblage is also characteristic of the area where a polynya forms during wintertime. A similar assemblage was found in sea-ice sediments sampled from an ice floe in the Beaufort Sea (Reimnitz et al., 1993). As shown by Reimnitz et al. (1992, 1993), the middle shelf (10 to 30–40 m water depth) is the main area where benthic organisms can be easily entrained into ice. Some shallow-water species (*Heterocyprideis sorbyana, S. complanata, C. cluthae*, and *Cytheromorpha macchesneyi*) have been reported even from central Arctic Ocean surface sediments as a part of the "ice-rafted assemblage" (Cronin et al., 1994; Jones et al., 1998, 1999). It might be therefore concluded that many of the shallow-water species found in our samples from the upper continental slope (*Rabilimis septentrionalis, H. sorbyana*, and *Paracyprideis pseudopunctillata*) were also ice-rafted. It is interesting in this respect that most ostracodes (90–95%, Table 1) were alive during sampling. Currently, it is unknown whether ostracodes can survive ice-rafting. However, it has been observed that some other crustaceans, for example, copepods can (E. Abramova, personal communication). It seems therefore conceivable that some shallow-water species are able to settle onto the seafloor after having been ice-rafted.

3.5. Comparison of Ostracode Assemblages of the Laptev Sea with Assemblages from Other Arctic Areas

One of the first attempts to review data on the geographical distribution of ostracodes in high latitudes was undertaken by Neale and Howe (1975). Their investigation showed that, in general, the shallow water fauna forms a circumpolar province, although the eastern and western subprovinces slightly differ in species composition. Comparison of our new data from the Laptev Sea with published materials from other Arctic regions reveals that ostracodes have similar distribution patterns. Table 10 contains a comprehensive species list of the Laptev Sea Ostracoda, where all species ever mentioned for this area are listed. This list is based on

Table 10. Occurrence of recent ostracodes from the Laptev Sea in other Arctic regions: (+) occurrence of the Laptev Sea ostracode species in other seas; our data are shaded

		Neale and Howe, 1975; Cronin et al., 1991												
Laptev Sea Ostracoda (only identifications to species level are included) (our data; Akatova, 1946; Cronin et al., 1991, Bauch et al., 1995; Erlenkeuser and von Grafenstein, 1999; Chavtur, 2001; Schornikov, 2001, 2004)	White Sea (Akatova, 1957; Rudyakov, 1962; Stepanova, 2002; unpublished data of Schornikov)	Russian Harbour	Matochkin Shar	Franz Josef Land	Spitsbergen fjords	Western-central Barents Sea	Norwegian-Barents Sea	Barents Sea (Chavtur, 2001; Schornikov, 2001)	Kara Sea (Cronin et al., 1991; Chavtur, 2001; Schornikov, 2001; our unpublished data)	East Siberian Sea (Cronin et al., 1991; Chavtur, 2001; Schornikov, 2001)	Chukchi Sea (Cronin et al., 1991; Chavtur, 2001; Schornikov, 2001)	Beaufort Sea (Neale and Howe, 1975; Cronin et al., 1991; Reimnitz et al., 1993)	Greenland Sea, Scoresby Sund fjord system (Whatley et al., 1996, 1998)	Western Canadian Arctic, eastern Greenland (Neale and Howe, 1975; Cronin et al., 1991)
Bythocythere constricta		+			+		+	+	+			+	+	
Pseudocythere caudata				+			+	+	+	+			+	+
Sclerochilus sp. 1	+	+		+			+		+		+	+		+
Jonesia acuminata	+							+	+	+				+
Cytheromorpha macchesneyi		+						+	+		+	+		
Cluhia cluthae	+		+	+	+				+		+	+	+	+
Cytheropteron arcuatum	+								+	+		+	+	+
C. biconvexa									+			+		
C. champlainum								+	+			+		
C. elaeni	+						+	+	+		+	+		+
C. inflatum	+							+	+			+	+	+
C. montrosiense	+				+			+	+	+		+	+	
C. nodosoalatum	+	+		+			+	+	+		+	+		
C. porterae									+				+	
C. timefactum	+								+			+	+	
C. sulense									+			+		
C. suzdalskyi	+							+	+		+	+		
C. perlaria							+		+				+	
Semicytherura complanata	+							+	+		+	+		
Palmenella limicola	+	+	+	+					+		+	+		+
Acanthocythereis dunelmensis	+	+	+	+	+			+	+	+	+	+		+
Rabilimis septentrionalis	+	+	+	+					+		+	+		+
Heterocyprideis sorbyana	+	+		+	+		+	+	+	+	+	+		+

Table 10. (Contd.)

		Neale and Howe, 1975; Cronin et al., 1991												
Laptev Sea Ostracoda (only identifications to species level are included) (our data; Akatova, 1946; Cronin et al., 1991, Bauch et al., 1995; Erlenkeuser and von Grafenstein, 1999; Chavtur, 2001; Schornikov, 2001, 2004)	White Sea (Akatova, 1957; Rudyakov, 1962; Stepanova, 2002; unpublished data of Schornikov)	Russian Harbour	Matochkin Shar	Franz Josef Land	Spitsbergen fjords	Western-central Barents Sea	Norwegian-Barents Sea	Barents Sea (Chavtur, 2001; Schornikov, 2001)	Kara Sea (Cronin et al., 1991; Chavtur, 2001; Schornikov, 2001; our unpublished data)	East Siberian Sea (Cronin et al., 1991; Chavtur, 2001; Schornikov, 2001)	Chukchi Sea (Cronin et al., 1991; Chavtur, 2001; Schornikov, 2001)	Beaufort Sea (Neale and Howe, 1975; Cronin et al., 1991; Reimnitz et al., 1993)	Greenland Sea, Scoresby Sund fjord system (Whatley et al., 1996, 1998)	Western Canadian Arctic, eastern Greenland (Neale and Howe, 1975; Cronin et al., 1991)
H. fascis							+	+	+			+		
Sarsicytheridea bradii	+	+	+	+		+	+		+	+	+	+		+
S. punctillata	+	+	+	+	+	+	+	+	+	+	+	+		+
Paracypideis pseudopunctillata	+							+	+	+	+	+		
Krithe glacialis	+							+	+	+		+	+	
Argilloecia cylindrica									+				+	
Elofsonella concinna	+				+		+	+	+	+	+	+		+
Eucythere argus	+								+			+		
Polycope bireticulata								+	+				+	
Polycope orbicularis				+					+				+	
Polycope punctata									+				+	
Roundstonia globulifera		+			+			+	+		+	+		
Semicytherura affinis		+					+	+	+			+	+	+
S. concentrica		+			+			+	+			+		+
Cetheropteron pseudomontrosiense										+				
Robertsonites tuberculatus		+	+	+	+	+		+				+		+
Paracyprideis fennica								+						
Cytheridea papillosa														
Hemicythere angulata	+	+						+				+	+	+
Rabilimis mirabilis	+						+	+	+	+	+	+	+	
Rabilimis paramirabilis														
Eucythere undulata														
Normanicythere leioderma		+				+	+	+	+	+	+	+		+

Table 10. (Contd.)

		Neale and Howe, 1975; Cronin et al., 1991												
Laptev Sea Ostracoda (only identifications to species level are included) (our data; Akatova, 1946; Cronin et al., 1991, Bauch et al., 1995; Erlenkeuser and von Grafenstein, 1999; Chavtur, 2001; Schornikov, 2001, 2004)	White Sea (Akatova, 1957; Rudyakov, 1962; Stepanova, 2002; unpublished data of Schornikov)	Russian Harbour	Matochkin Shar	Franz Josef Land	Spitsbergen fjords	Western-central Barents Sea	Norwegian-Barents Sea	Barents Sea (Chavtur, 2001; Schornikov, 2001)	Kara Sea (Cronin et al., 1991; Chavtur, 2001; Schornikov, 2001; our unpublished data)	East Siberian Sea (Cronin et al., 1991; Chavtur, 2001; Schornikov, 2001)	Chukchi Sea (Cronin et al., 1991; Chavtur, 2001; Schornikov, 2001)	Beaufort Sea (Neale and Howe, 1975; Cronin et al., 1991; Reimnitz et al., 1993)	Greenland Sea, Scoresby Sund fjord system (Whatley et al., 1996, 1998)	Western Canadian Arctic, eastern Greenland (Neale and Howe, 1975; Cronin et al., 1991)
Finmarrchinella barenzovensis	+	+				+		+	+	+	+	+	+	+
Krithe minima													+	
Sarsicytheridea macrolaminata	+	+	+				+	+	+		+	+		
Jonesia arctica								+			+			
Jonesia barentsovensis								+						
Sclerochilus (*S*) *jurasovi*														
Sclerochilus (*S*) *laptevensis*														
Sclerochilus (*S*) *laptevi*														
Palmenella dentomarginata														
Acanthocythereis agapensis	+							+			+			
Cytheretta teshekpukensis								+			+	+		
Elofsonella neoconcinna											+	+		+
E. pinegensis	+													
Pteroloxa venipuncta											+			
Cytheropteron alatum	+						+		+	+		+		
Cytheropteron paralatissimum		+		+					+			+		
Cytheropteron dimilingtonensis								+						
Cytheropteron testudo							+	+					+	
Philomedes brenda	+				+			+	+	+	+			
Boroecia maxima								+	+	+				
B. borealis									+					
Discoconchoecia elegans								+	+					

Table 11. Comparison of the ostracode association of the Laptev Sea with associations of other Arctic regions

		Neale and Howe, 1975; Cronin et al., 1991						
	Laptev Sea Ostracoda (only identifications to species level are included) (our data; Akatova, 1946; Cronin et al., 1991, Bauch et al., 1995; Erlenkeuser and von Grafenstein, 1999; Chavtur, 2001; Schornikov, 2001, 2004)	White Sea (Akatova, 1957; Rudyakov, 1962; Stepanova, 2002; unpublished data of Schornikov)	Russian Harbour	Matochkin Shar	Franz Josef Land	Spitsbergen fjords	Western-central Barents Sea	Norwegian-Barents Sea
Total number of species identified	67	95	45	9	31	46	6	59
Number of shared species		29	19	8	13	11	5	17
Depth range		0–79	15	18–28	3–55	0–1000	100–200	192–264
Jaccard index, %		22	20	12	15	11	7	16

	Barents Sea (Chavtur, 2001; Schornikov, 2001)	Kara Sea (Cronin et al., 1991; Chavtur, 2001; Schornikov, 2001; our unpublished data)	East Siberian Sea (Cronin et al., 1991; Chavtur, 2001; Schornikov, 2001)	Chukchi Sea (Cronin et al., 1991; Chavtur, 2001; Schornikov, 2001)	Beaufort Sea (Neale and Howe, 1975; Cronin et al., 1991; Reimnitz et al., 1993)	Greenland Sea, Scoresby Sund fjord system (Whatley et al., 1996, 1998)	Western Canadian Arctic, eastern Greenland (Neale and Howe, 1975; Cronin et al., 1991)
Total number of species identified	134	83	21	72	78	61	46
Number of shared species	38	47	17	26	39	20	21
Depth range	–	5–500	21–276	41–55–?	1–1000	274–3355	2–3065
Jaccard index, %	23	46	24	23	37	19	23

our own data and on that of Akatova (1946); Modern Arctic Podocopid Database (Cronin et al., 1991), Bauch et al. (1995), and Erlenkeuser and von Grafenstein (1999), as well as the data of Chavtur (2001) and Schornikov (2001, 2004) and data on occurrences of these species in other Arctic seas (White, Barents, Kara, East Siberian, Chukchi, Beaufort, and Greenland seas and eastern Canadian Arctic) according to different publications; unpublished data of Schornikov, which he kindly put at our disposal; and our own data on the Kara Sea Ostracoda.

A total of 95 ostracode species have been reported to date from the White Sea (Akatova, 1957; Rudyakov, 1962; Stepanova, 2002; Schornikov, unpublished data), 29 of these species were also found in the Laptev Sea (Tables 10, 11), both in the southern shallow nearshore area and in the western deep-sea area.

Recent ostracode assemblages from water near Novaya Zemlya in the Barents Sea were described in detail by Neale and Howe (1975), who also summarized data from Matochkin Shar Strait (Novaya Zemlya), waters near Franz Josef Land, Spitsbergen, the eastern-central Barents Sea, and the Norwegian-Barents Sea area. Additional data are available from the Modern Arctic Podocopid Database (Cronin et al., 1991). The number of species that occur both in the Barents and Laptev seas ranges between 5 and 19, depending on the area (Tables 10, 11). Schornikov (2001) identified 134 species of ostracodes for the Barents Sea, 38 of which were also found in the Laptev Sea. Most of the common species inhabit shallow-water near-shore areas of the Laptev Sea. As a whole, the Barents Sea ostracode fauna is considerably more diverse than the Laptev Sea fauna. This may be due to more favorable environmental conditions in the Barents Sea, which has a stronger influence of Atlantic waters.

According to data from the Modern Arctic Podocopid Database (Cronin et al., 1991), data of Schornikov and Chavtur (2001), and our unpublished data, 83 ostracode species inhabit the Kara Sea, 47 of which occur also in the Laptev Sea; thus, the assemblages of these areas have much in common.

Data on the East Siberian Sea ostracodes are given only in the Modern Arctic Podocopid Database (Cronin et al., 1991) and in the species list compiled by Schornikov and Chavtur (2001). A total of 21 ostracode species has been reported for this area, 17 of them are also known to occur in the Laptev Sea. The data on ostracodes given in the Modern Arctic Podocopid Database are nonrepresentative, because most of the samples contain only two or three valves, and only two samples contained more than 30 valves (Cronin et al., 1991).

Of five samples recovered in the Chukchi Sea, Cronin et al. (1991) identified 24 species, while Schornikov and Chavtur (2001) identified 72 species for this area. A total of 26 species also occur in the Laptev Sea, this shows a rather great dissimilarity between the ostracode assemblages of these areas.

Whatley et al. (1996, 1998) listed 61 species from the Greenland Sea and Scoresby Sund fjord system. Twenty of these species occur in samples from the deep western part of the Laptev Sea, influenced by the Atlantic water inflow.

Neale and Howe (1975) and Cronin et al. (1991) listed recent ostracodes collected in fjords from the Western Greenland coast and Eastern Canadian Arctic. This fairly diverse fauna has little in common with the assemblages from the Laptev Sea (Tables 10, 11).

Ostracodes of the Beaufort Sea have been studied in great detail. Neale and Howe (1975) described ostracodes from the Colville River delta. This assemblage includes shallow-water and euryhaline species (Tables 10, 11) typical of the Arctic shallow waters and very similar to the inner-shelf assemblage of the Laptev Sea (31 species in common). Reimnitz et al. (1993) listed 13 species of ostracodes entrained by sea ice found in the Beaufort Sea, water depth 150 m. According to the taxonomy of the identified species, the ice-floe was formed in the shallow-water middle-shelf area of the Beaufort Sea. Nine of these species were identified in the Laptev Sea. The most detailed data on the Ostracoda from the Beaufort Sea are cited in the Modern Arctic Podocopid Database (Cronin et al., 1991). It contains information on the species composition from more than 300 samples, which were obtained from water depths ranging from 1 to more than 1000 m. A total of 78 species has been identified of which 39 also occur in the Laptev Sea. Nearly all species identified in the surface sediment samples of the Laptev Sea (in total 67) were also found in the Beaufort Sea, except for some rare deepwater species, predominantly of North Atlantic origin (*P. caudata, C. perlaria*, and *C. porterae*). However, the taxonomic diversity of the Beaufort Sea ostracode fauna is almost twice as great as that of the Laptev Sea, this in many respects appears to be attributable to the more detailed investigation of this area.

Based on the above analysis of data on the distribution of ostracodes in different Arctic areas, we believe that in most cases the degree of similarity of ostracode assemblages from different areas depends on how much the Ostracoda of these areas have been studied. At present, the least studied faunas in terms of ostracodes are the Chukchi and East Siberian seas, and the best studied are ostracode assemblages of the Beaufort and Barents seas. Data on the Ostracoda from the Kara and White seas (our data and Schornikov's unpublished data) are also quite abundant. The closest similarity was revealed between the ostracode associations of the Kara and Laptev seas. Comparison of ostracode associations of these areas using the Jaccard index yielded the highest values of 46%, which is due to the geographical proximity of these areas and similar environmental conditions: vast shelf with depths less than 100 m (most of samples were obtained from depths less than 100 m), considerable influence of river runoff, and the presence of sea-ice cover and polynya during winter. The ostracode association of the Beaufort Sea also proved to be quite similar to that of the Laptev Sea (Jaccard index 37%), this also is due to similar environmental conditions.

Many of the species identified for the Laptev Sea occur throughout all the Arctic seas; however, based on their abundance, taxonomy, and the presence of indicator species, two geographically different assemblages may be distinguished: the western-central and southeastern parts of the Laptev Sea. The most characteristic feature of the western-central Laptev Sea is the presence of relatively deepwater species that are known in the North Atlantic and Arctic oceans. The ostracode assemblages from the southeastern Laptev Sea have many species in common with the shelf assemblages of the Kara and Beaufort seas due to similar environmental conditions (considerable river discharge, ice coverage, and the existence of a polynya).

3.6. Morphological Characteristics of Ostracode Assemblages

Many scientists studied the relationship between the carapace morphology of ostracodes and their ecology (Schornikov, 1981; Nikolaeva, 1989b; Puckett, 1996; etc.). Diverse and sometimes contradictory data were obtained. The most common objects of study have been correlations between the size, salinity, and temperature and the relationships between the carapace sculpture, type of substratum, water depth, and environmental conditions. One of our goals was to evaluate the possible correlation between the carapace morphology of ostracodes and the environments they inhabit and to determine, using our material, the correlation between the morphology of the assemblage and its environmental parameters. Theoretically, the morphology of the carapace is supposed to reflect the specific character of their ecological preferences. It is known that most of the freshwater ostracodes have a smooth carapace, while most of the marine ostracodes have sculptured carapaces. However, each specific case of carapace morphology may be determined by specific agents. We tried to reveal the possible correlation between cara-

Table 12. Groups of ostracodes from the Laptev Sea according to their surface sculpture development and carapace size

Species	Sculpture			Size		
	smooth	mesosculp-tured	macrosculp-tured	<0.4	0.4–0.6	>0.6
				small	medium	large
Bythocythere constricta		+				+
Pseudocythere caudata	+				+	
Sclerochilus sp.	+				+	
Jonesia acuminata	+					+
Cytheromorpha macchesneyi		+			+	
Cluthia cluthae		+		+		
Cytheropteron arcuatum		+				
C. discoveria		+			+	
C. biconvexa		+		+		
C. champlainum		+			+	
C. elaeni		+		+		
C. inflatum		+			+	
C. montrosiense		+			+	
C. nodosoalatum		+			+	
C. porterae		+			+	
C. tumefactum		+			+	
C. sulense		+			+	
C. suzdalskyi		+			+	
C. pseudomontrosiense		+		+		
C. perlaria		+		+		
Semicytherura complanata		+		+		
Palmenella limicola			+		+	
Acanthocythereis dunelmensis			+			+
Rabilimis septentrionalis			+			+
Heterocyprideis sorbyana			+			+
H. fascis			+			+
Sarsicytheridea bradii	+				+	
S. punctillata		+				+
Paracyprideis pseudopunctillata	+					+
Krithe glacialis	+					+
Argilloecia cylindrica	+			+		
Argilloecia sp.	+			+		
Elofsonella concinna			+			+
Eucythere argus		+		+		
Polycope bireticulata		+		+		
Polycope orbicularis		+		+		
Polycope punctata		+		+		

pace size, surface sculpture, and the salinity and water depth (bottom water temperature in the Laptev Sea is stable during the whole year; bottom grounds on the studied sites were represented by uniform muddy-clayey sediments).

In order to characterize assemblages in terms of predominant carapace morphology, all species were divided into those with smooth and those with sculptured carapaces, the latter we subdivided into heavily ornamented and mezosculptured forms. In terms of sizes, three size groups were distinguished: with small carapace (maximum length less than 0.4 mm), medium carapace (maximum length 0.4–0.6 mm), and large carapace (maximum length more than 0.6 mm). We calculated the proportions of all the above-mentioned morphological groups for all samples (Tables 12, 13). Cor-

Table 13. Relative abundance of ostracode valves with different surface sculpture and carapace size in recent assemblages of the Laptev Sea

Assemblages	Sculpture			Size		
	smooth	mesosculptured	macrosculptured	<0.4 small	0.4–0.6 medium	>0.6 large
	valves, %	valves, %	valves, %	valves, %	valves, %	valves, %
Western-Central	18	48	34	18	25	57
Eastern	14	50	36	25	32	43
Southern	54	30	16	18	22	60

relation between carapace surface sculpture and ostracode ecology is still under discussion. For example, Elofson (1941) calculated that the proportion of smooth forms increases with depth, while Benson (1975) came to the opposite conclusion, in particular, he showed that the proportion of forms with spines increases with depth and the number of these spines also increases.

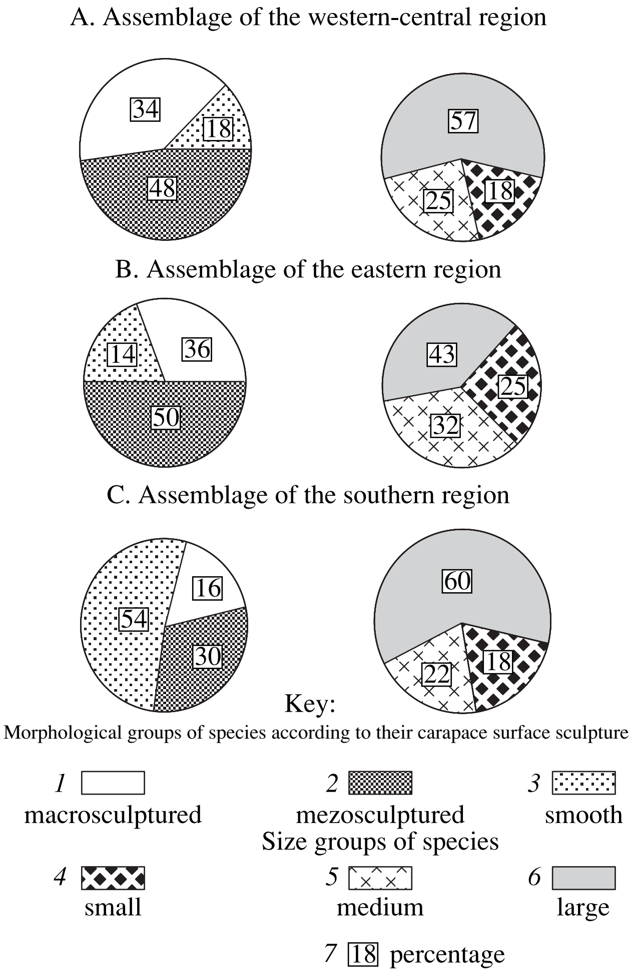

Fig. 7. Share of valves of different morphological groups of species.

In the Laptev Sea the proportion of smooth forms is nearly equal both in the assemblages of the western-central part of the sea at water depths 60–270 m and in the eastern part of the sea at water depths 30–60 m (Table 13, Fig. 7), while the proportion of smooth forms in the assemblage of the freshened southern part of the sea is more than two times greater than the respective proportions in the other two assemblages because of the predominance of one euryhaline species, *Paracyprideis pseudopunctillata*, with a smooth carapace. This species is present in all three assemblages, but dominates the first assemblage. The proportion of mezosculptured forms varies from 48–50% in the western and eastern parts of the sea to 30% in the southern part of the sea. The proportion of macrosculptured forms varies from 34–36% in the western and eastern parts of the sea to 16% in the southern part of the sea. Consequently, there is only one correlation: a considerable increase of the proportion of ostracodes with smooth and nearly smooth carapaces in regions with the lowermost salinity.

Macrosculpture on ostracode carapaces can have different functions: protective, locomotive, and that of reinforcement of the carapace (Schornikov, 1981). Usually, macrosculptured forms inhabit sandy substrata (Nikolaeva, 1989b). The fact that the proportion of macrosculptured forms decreases with decreasing depths may, in our opinion, reflect a more uniform distribution of coarse sand fraction caused by ice-rafting.

In terms of carapace size, ostracodes are distributed quite evenly in all three established assemblages: in the assemblages of the western-central and southern regions the proportions of all three size groups are virtually the same, and only in the eastern part of the sea the proportion of large forms (43%) is slightly less than in the other two assemblages (57–60%). Thus, the size of the carapace does not reflect differences in habitats occupied by ostracodes (Tables 12, 13, Fig. 7).

Morphologically, the western-central assemblage is characterized predominantly by species of the genus *Cytheropteron* with an alate extension in the ventral

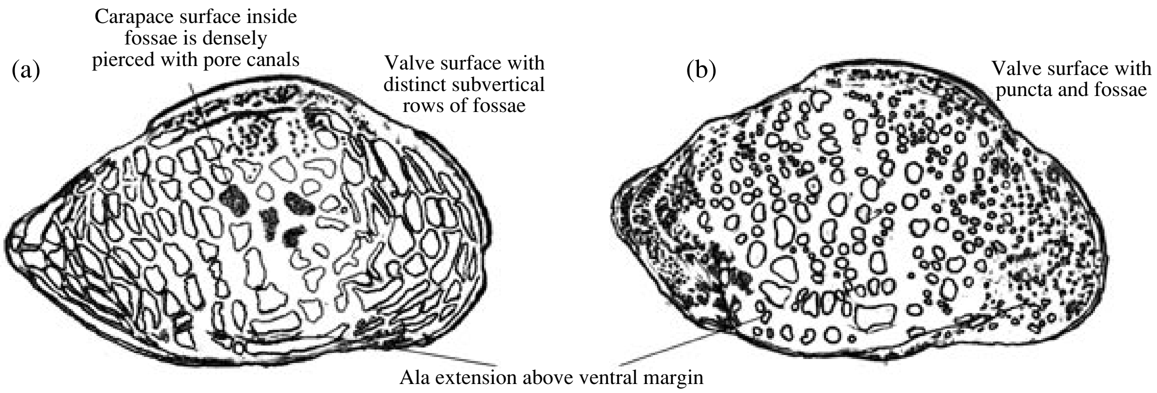

Fig. 8. Carapace morphology of the members of *Cytheropteron*: (a) *C. dimlingtonensis* and (b) *C. champlainum.*

part of the carapace (Fig. 8). According to Schornikov (1981), this morphological feature provides no information about the ecology of the species, since forms with an alate extension live on both soft and hard substrates. In our case the sediment is clayey silt; thus, the alate extension is, most probably, used for improving the stability of the carapace during locomotion on the substrate. Typical species of this assemblage have smooth carapaces: *Krithe glacialis, Argilloecia conoidea*, and *Pseudocythere caudata.* Species of the genus *Krithe* were studied by many scientists. Moyes and Peypouquet hypothesized (1977) that the width of the vestibule of the carapaces reflects the oxygen dissolved in water. Whatley and Zhau (1993) disputed this view and showed that carapaces with vestibules of different sizes often occur together. Although we have not yet studied *Krithe glacialis* in detail, its strongly pronounced sexual dimorphism allowed us to established the presence of both male and female specimens in the Laptev Sea. According to Carbonel (2004, personal communication), this is evidence that these organisms lived in favorable conditions.

The assemblage of the middle and outer shelf of the eastern Laptev Sea is characterized by two macrosculptured species with a large carapace and two mezosculptured species with a small carapace. The spiny sculpture of *Acanthocythereis dunelmensis* is probably protective in function. According to Schornikov (1981), spines may also serve for disguise when the entire carapace surface between spines is covered with mud, or spines form an obstacle preventing the ostracode from sinking into the sediment.

The assemblage of the inner shelf of the southern part of the Laptev Sea is characterized by two macrosculptured forms with large carapaces, one smooth form with a large carapace, and two mezosculptured forms of medium and small size.

Analysis of the carapace morphology of the established assemblages has revealed no direct correlation between the morphology of the assemblage and the ecology of species. In the Laptev Sea only one correlation has been revealed: a considerable increase in the proportion of smooth and nearly smooth forms in the regions with the lowest salinity values. The size of the carapace does not reflect differences in habitats occupied by ostracodes. Among modern marine ostracodes two major groups are distinguished: shallow-water neritic species and those inhabiting bathyal zone and greater depths (Nikolaeva, 1989b). Except for several relatively deepwater species of the western-central assemblage, all species identified in the Laptev Sea area are shallow-water neritic dwellers, which is why no distinctive morphological features pointing to their ecology were found. Almost all taxa (except for deepwater forms) occur in different proportions in all three assemblages. We subscribe to the opinion of Schornikov (1981) that in many cases carapace sculpture reflects soft body anatomy, i.e., it results from the tension of muscles fixed to the valves and has no direct correlation with environments. Thus, it is more expedient to analyze the environmental dependence of the morphology of each individual species rather than that of the entire assemblage.

CHAPTER 4. QUANTITATIVE ANALYSIS OF THE LATE QUATERNARY OSTRACODE ASSEMBLAGES OF THE LAPTEV SEA, AND ENVIRONMENTAL CHANGES DURING THE POSTGLACIAL AND HOLOCENE

The above discussion of the distribution of recent ostracodes in the Laptev Sea shows that the distribution of assemblages depends primarily on water depth and salinity. Based on the comparison of recent and fossil ostracode assemblages from the sediment core sections obtained from different parts of the sea and corresponding to different intervals of the Postglacial and Holocene, we reconstruct changes in marine paleoenvironments caused by variations in sea water depth, river runoff influence, temperature-salinity characteristics, and bottom hydrodynamics.

4.1. Holocene Ostracode Assemblages of the Central Part of the Eastern Laptev Sea Shelf

We studied the distribution of ostracodes in two sediment cores from the central eastern Laptev Sea shelf, Lena paleovalley (water depth 45 m), and Yana paleovalley (water depth 51 m) (Figs. 1, 2; Tables 9, 10, 11). In parallel with the ostracode study, foraminifers and mollusks from the same samples were studied (Taldenkova et al., 2005). The changes in the fossil assemblages of mollusks and ostracodes occurred simultaneously, while in the distribution of foraminifers no distinct boundaries have been distinguished; only the early stage of inundation was marked by minor variations in the species composition.

Sediment core PS-51/138-12 mainly consists of dark-gray silt, often bioturbated (Fig. 9). Below 200 cm depth in the core, sediments are enriched in plant debris. Above this level the amount of plant debris decreases and is very low in the upper 50 cm. Sand content is low: 3–4% in the lower two-thirds of the sedimentary sequence (Fig. 9). At 150–170 cm core depth, sand content increases up to 10–12%. The sedimentary sequence of core PS-51/135-4 consists of gray to dark gray silt, enriched in organic matter and often bioturbated (Fig. 10).

Both cores were AMS^{14}C-dated back to 11.2–11.3 cal. ka (Figs. 2, 9, 10). According to the distribution of dates, the sediment accumulation was extremely uneven. In the Lena paleovalley, most of the core sequence (530–197 cm) was accumulated very rapidly, over less than one thousand years, between 11.2 and 10.3 cal. ka. Subsequently, an abrupt reduction in sedimentation rates occurred, and later sedimentation went on much more slowly and without any evident changes. A similar pattern existed in the Yana paleovalley, but there sedimentation almost stopped about 5 cal. ka BP. A date of 5301 cal. yr. BP was obtained at a core depth of 8 cm; this may be attributed to strong bottom currents, typical of this area, eroding the bottom surface (Dmitrenko et al., 2001b; Wegner, 2002) (Figs. 9, 10).

Fossil ostracodes, mollusks, and foraminifers were found throughout the whole sediment sequence in both cores studied (Figs. 9, 10; Tables 14, 15). The material is in a good state of preservation, and practically no traces of dissolution have been observed.

Assemblages of core section PS-51/138-12

Ostracodes. The total abundance of ostracodes varies along the core section, ranging from 80 specimens per 100 g in the interval 400–350 cm core depth to single valves in its lower and middle parts. This is a rather low abundance compared to that in the coretop sediments (Tables 6–9, 14, 15). The higher percentage of juvenile valves and carapaces in the lower part of the core is evidence for a rapid burial of these fragile valves most probably because of high sedimentation rates (Fig. 11).

In the lower unit (interval 530–410 cm, 11.2–10.8 cal. ka), the first brackish-water assemblage, including ten species, was distinguished. This assemblage is dominated by the inner neritic euryhaline species *Heterocyprideis sorbyana* (up to 100%), *Paracyprideis pseudopunctillata* (20–60%), and *Pteroloxa cumuloidea* (less than 18%), tolerating freshened conditions, and contains the brackish-water species *Cytheromorpha macchesneyi* (up to 10%) and *Loxoconcha venepidermoidea* (up to 5%). The proportion of euryhaline and brackish-water species reaches 100% at the core base and gradually decreases upwards (Fig. 11).

The second, transitional assemblage (interval 410–160 cm, 10.8–8.2 cal. ka) comprises 12 ostracode species belonging to different ecological groups. This assemblage is dominated by the brackish-water *Cytheromorpha macchesneyi* (20–80%), the euryhaline *P. pseudopunctillata* (20–60%), and the normal marine *Rabilimis septentrionalis* (20–65%) and *R. mirabilis* (20–90%). In the upper part of this interval, some normal marine species appear for the first time: *Acanthocythereis dunelmensis* (up to 5%), *Semicytherura complanata (*up to 5%), and *Palmenella limicola* (up to 10%).

These normal marine species became the dominant group in the third assemblage, which comprises 12 species (interval 160–0 cm, 8.2 cal. ka to Recent), along with the normal marine species *Cluthia cluthae* (less than 10%), *Jonesia acuminata* (up to 10%), *Cytheropteron nodosoalatum* (up to 10%), *C. elaeni* (10–90%), and *Sclerochilus* sp. 1 (up to 5%), which have not been found in the underlying sediments. This uppermost assemblage of core PS-51/138 resembles a modern assemblage, with *Acanthocythereis dunelmensis* that we have described from the central part of the eastern Laptev Sea shelf (Fig. 11).

Mollusks. According to Taldenkova et al. (2005), a total of 15 bivalve and 6 gastropod species were identified in the core section. Their taxonomic diversity gradually increases upcore. In the lower unit (530–410 cm), only *Portlandia arctica* (Gray), *P. aestuariorum* (Mossewitsch), and *Cyrtodaria kurriana* Dunker were recognized. The latter two species are typical representatives of shallow-water and estuarine environments dwelling at depths not exceeding 10–15 m (Gukov, 2001).

Of the seven species identified in the overlying unit (410–160 cm), *Portlandia arctica* predominates and forms an almost monospecific assemblage, accompanied by numerous *Cylichna* sp. (a small predatory gastropod).

The uppermost unit (160–0 cm) shows a sharp increase in taxonomic diversity from 7 to 13 species. Although *P. arctica* is still present, but rare. The dominant species in this assemblage are *Leionucula bellotii* (Adams)*, Macoma calcarea* (Gmelin), and *Nuculana lamellosa lamellosa* (Leche) along with other species typical of the modern macrozoobenthic assemblage of this area.

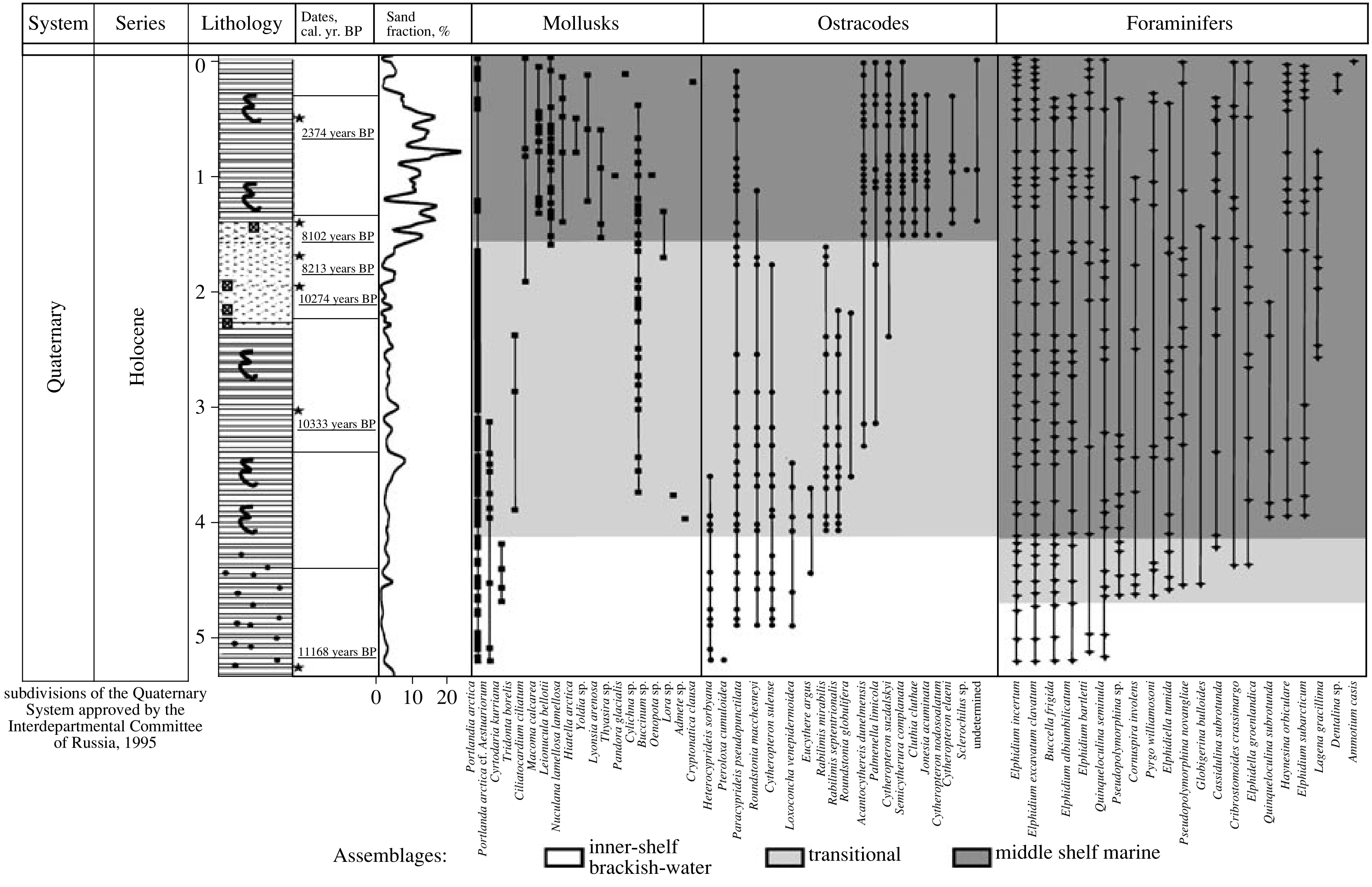

Fig. 9. Distribution of ostracodes, mollusks, and foraminifers in core section PS51/138, obtained in the Lena valley; for lithology see Fig. 2.

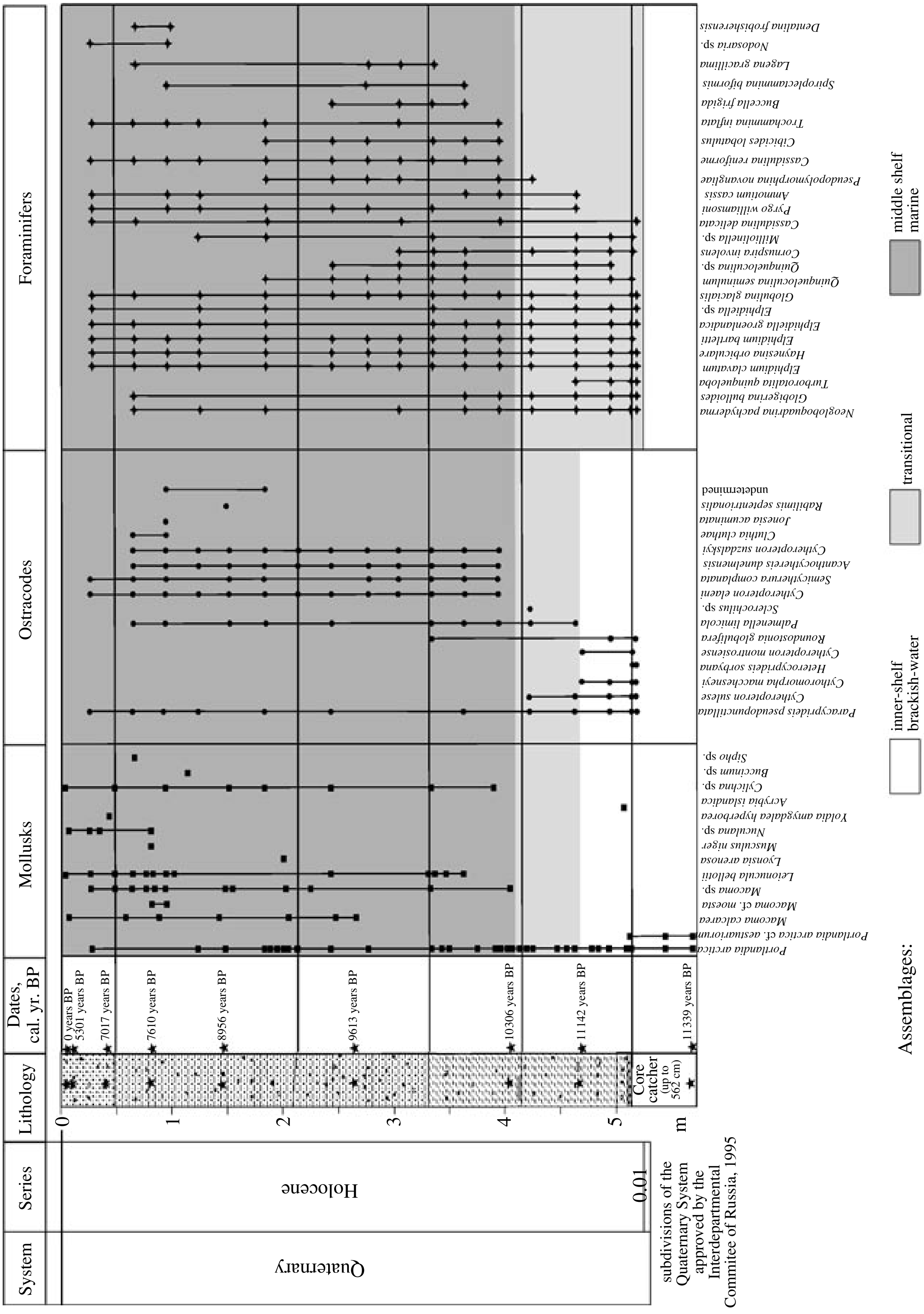

Fig. 10. Distribution of ostracodes, mollusks, and foraminifers in core section PS51/135, obtained in the Yana valley; for lithology see Fig. 2.

Table 14. Distribution of ostracode species in core section PS51-138: (v) valves; (c) carapaces; and (jv) juvenile

Samples	1	2	3	4	5	6	7	8	9	10	11	12	13	14
Depth of sampling, cm	525–528	511–514	505–508	487–490	481–484	475–478	451–454	439–442	427–430	400–403	397–400	391–394	367–370	355–358
Heterocyprideis sorbyana		9v	10v	6v	15v	14v	9v	14v		7v	24v	16v	1v	2v
Pteroloxa cumuloidea		2v												
Paracyprideis pseudopunctillata				2c	15v	13v	3v + 1j	17v 1j	2v	4v	12v 1c	38v 2c	37v	108v 6jv 7c
Cytheromorpha macchesneyi				2v + 1jv			1v	8v				5v		58v
Cytheropteron sulense				4v	2v	1v	1v	7v	3v		1v	2v	4v	13v
Loxoconcha venepidermoidea					1v			1v			6v		1v	1v
Rabilimis mirabilis										3v	33v	49v 1c	14v	14v
Rabilimis septentrionalis										7v	10v 9jv 4c	52v 13j 1c	9v 6jv	
Eucythere argus								3v			2v		3v	6v
Roundstonia globulifera														2v
Acanthocythereis dunelmensis														
Palmenella limicola														
Cytheropteron suzdalskyi														
Semicytherura complanata														
Cluthia cluthae														
Jonesia acuminata														
Cytheropteron nodosoalatum														
Cytheropteron elaeni														

Table 14. (Contd.)

Samples	15	16	17	18	19	20	21	22	23	24	25	26	27	28	29
Depth of sampling, cm	349–352	329–332	311–314	287–290	251–254	239–242	193–196	169–172	151–154	129–132	105–108	87–90	54–57	51–54	33–36
Heterocyprideis sorbyana															
Pteroloxa cumuloidea															
Paracyprideis pseudopunctillata	2v	8v	1v	6v	1v			1v 1c	1v	9v		1v 1jv		1v	
Cytheromorpha macchesneyi	1v		12v	10v	4v			5v							
Cytheropteron sulense		2v 2jv 1c	1v	4v											
Loxoconcha venepidermoidea		1v							4v	18v	6v	2v		2v	
Rabilimis mirabilis	4v	22v 1c	9v	2v	3v	3v		2v							
Rabilimis septentrionalis		4v 4jv	4v 19jv	4v	2v 1jc 9jv	2jv									
Eucythere argus															
Roundstonia globulifera															
Acanthocythereis dunelmensis		1jv	1jv						14v 9jv	18v 7jv	7v 2jv	6jv 7v	4v 1jv	2v	2v 2jv
Palmenella limicola			1v							3v			2v		1v
Cytheropteron suzdalskyi						2v			3v	35v	8v	6v	6v	1c	13v
Semicytherura complanata									5v	14v	2v	9v	5v	1v	13v
Cluthia cluthae									5v	7v	2v	2v	2v		3v
Jonesia acuminata									2v	4v	2v	3v			
Cytheropteron nodosoalatum									1v						
Cytheropteron elaeni										7v		11v			

Table 15. Distribution of ostracode species in core section PS51-135: (v) valves; (c) carapaces; (j) juvenile; and (n) numerous

Samples	1	2	3	4	5	6	7	8	9	10
Depth of sampling, cm	525	514–516	512–514	490–493	460–463	420–423	390–393	360–363	330–333	300–303
Paracyprideis pseudopunctillata		5v	9v	7v 2c	6v 2c	2v 3c		1j		
Cytheropteron sulense		3v	7v	24v 14c	1v	1v				
Cytheromorpha macchesneyi		2c	1v	5v 2c	1v					
Heterocyprideis sorbyana		1v	2v							
Roundstonia globulifera		2v		3v					1v	
Cytheropteron montrosiense			1v		1v					
Sclerochilus sp. 1						2v				
Cytheropteron elaeni							2v	11v 1j	26v(n.j.) 1c	21v(n.j.)
Semicytherura complanata							1v	6v	31v(n.j.) 2c	6v
Acanthocythereis dunelmensis							3c 1jc	13v 8jv	30v(n.j.) 17c	11v 13jv
Cytheropteron suzdalskyi							2v	4v	5v 1jv	4v
Cluthia cluthae										
Jonesia acuminata										
Palmenella limicola					2v	1v	1v	1v	4v	
Cytheropteron sp.										
Rabilimis septentrionalis										

Samples	11	12	13	14	15	16	17	18	19	20
Depth of sampling, cm	275–278	240–243	210–213	180–183	150	147	120–123	90–93	60–63	25–28
Paracyprideis pseudopunctillata				1jc			3v	14v	36v	45v 1jv
Cytheropteron sulense										
Cytheromorpha macchesneyi										
Heterocyprideis sorbyana										
Roundstonia globulifera										
Cytheropteron montrosiense										
Sclerochilus sp. 1										
Cytheropteron elaeni	5v	10v 1jc	2v	11v 3c	2v	2v	1v	13v 2c	15v 2c	3v
Semicytherura complanata	1v			1v	1v			14v 3c	26v 6c	1v
Acanthocythereis dunelmensis	4v 3jv	6v 8jv 1c	1v	5v 6jv 2c	3v	4v	2v	6v 7jv 1c	8v 6jv	
Cytheropteron suzdalskyi	10v	7v	1v	1v 1c	2v	5v	1v	1v	1v	
Cluthia cluthae								3v	1v	
Jonesia acuminata								3v		
Palmenella limicola		1v		1v	2v			2v 2c	3v	
Cytheropteron sp.					1v					
Rabilimis septentrionalis						2v				

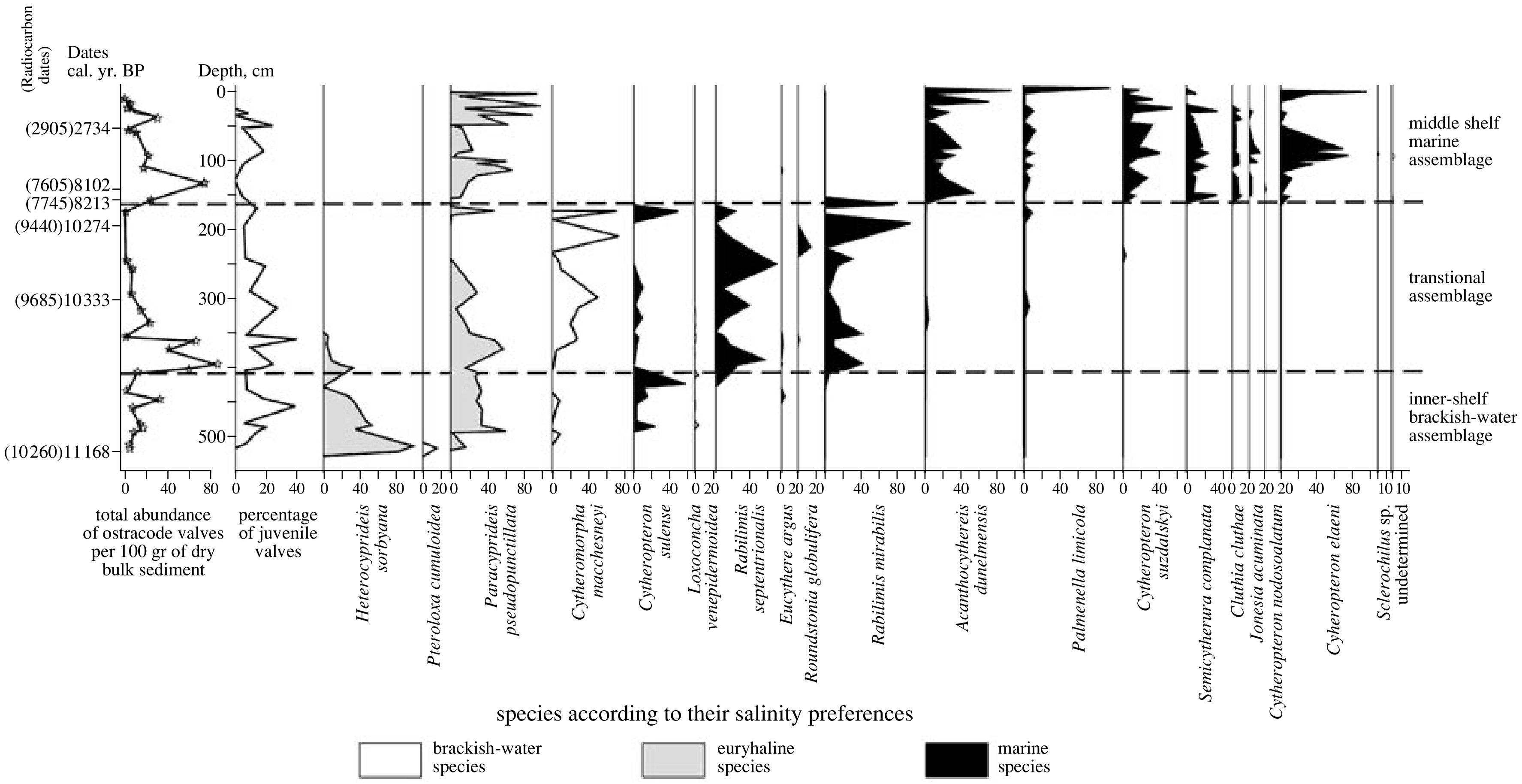

Fig. 11. Distribution of ostracode species in core section PS-51/138-12, obtained in the Lena valley.

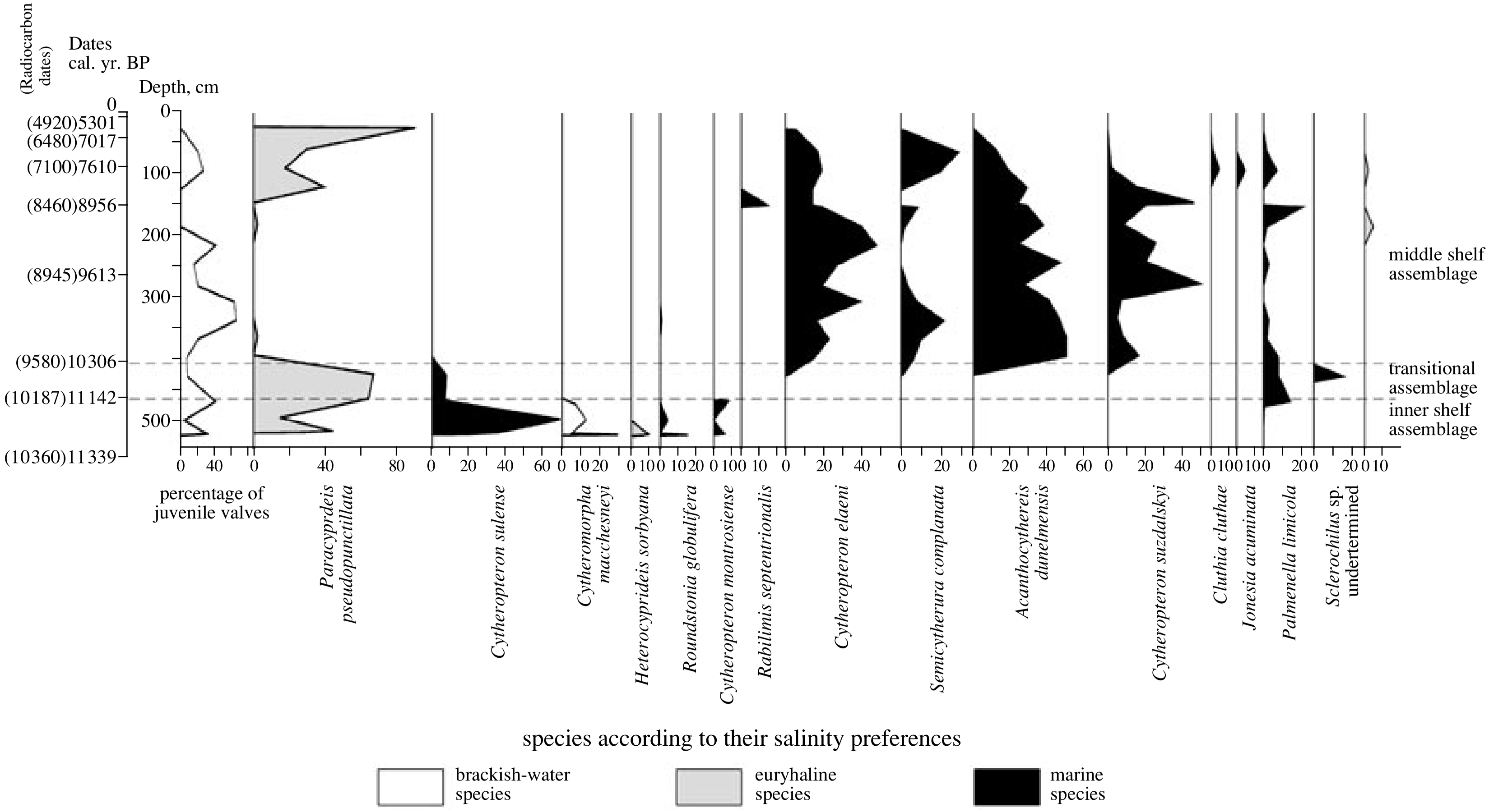

Fig. 12. Distribution of ostracode species in core section PS-51/135-4, obtained in the Yana valley.

Foraminifers. In contrast to mollusks and ostracodes, no boundaries or trends have been revealed in the distribution of foraminifers (Taldenkova et al., 2005). The whole sequence is dominated by different members of the Elphidiidae. Most of these species are characteristic of "river-proximal" environments, typical of estuarine near-shore environments; they can survive strong seasonal variations in environmental conditions (Polyak et al., 2002). As in mollusks and ostracodes, the taxonomic diversity of foraminifers increases upcore, but gradually, and most species are present throughout the core section (Fig. 9).

Assemblages of the core section PS-51/135-4

Ostracodes. The oldest assemblage (514–460 cm, 11.3–11.1 cal. ka) comprises six species, almost all of which are inner neritic species characteristic of near-shore estuarine environments: *Heterocyprideis sorbyana* (up to 10%), *Paracyprideis pseudopunctillata* (40–60%), *Cytheromorpha macchesneyi* (10–30%), and *Roundstonia globulifera* (up to 18%). In the overlying transitional assemblage, which comprises 8 species (460–120 cm, 11.1–10.3 cal. ka), the latter species are replaced by normal marine species, such as *Semicytherura complanata* (up to 10%), *Cytheropteron elaeni* (up to 20%), *Acanthocythereis dunelmensis* (up to 40%), and *Palmenella limicola* (up to 12%). The proportion of juvenile valves and carapaces is high (up to 60%), which may be attributed to relatively calm depositional environments and high sedimentation rates. The uppermost assemblage (120–0 cm, 10.3 cal. ka) is the most taxonomically diverse (11 species) and includes some more typical marine species that have not been found in the underlying layers: *Cluthia cluthae* (up to 10%) and *Jonesia acuminata* (up to 10%) (Figs. 10, 12).

Mollusks. As in core PS-51/138-12, the succession of the mollusk assemblages is similar to that of ostracodes (Taldenkova et al., 2005). The lowermost mollusk assemblage (562–460 cm) is taxonomically poor and consists of *P. arctica* and *P. aestuariorum,* with a single specimen of the gastropod species *Acrybia islandica.* The latter presently inhabits the nearshore freshened zone down to a water depth of 10 m. Upward in the core (460–120 cm), a transitional assemblage occurs with *Portlandia arctica, Leionucula bellotii*, and *Macoma* sp. The uppermost assemblage (120–0 cm) is most taxonomically diverse. It is dominated by *L. bellotii* and different species of *Macoma* (Fig. 10).

Foraminifers. Like in core PS-51/138, foraminiferal assemblages are dominated by different elphidiids and show only minor changes in species composition between the basal part (lowermost 50 cm) and the rest of the core (Taldenkova et al., 2005).

It is noteworthy that the sediments of core sequence PS-51/135, which accumulated earlier than 10 cal. ka BP, also include abundant planktonic foraminifers (up to 50% of the total), while in overlying layers they are very rare. Tamanova (1971) recorded numerous planktonic foraminifers from recent sediments of the nearshore zone located northwest of the Lena delta. She assumed that these finds represent a thanatocenosis formed in a place where Atlantic waters met riverine waters. Possibly, the presence of planktonic foraminifers in the lower unit is due to reworking of older marine beds (Bauch, 1999), but the very good preservation of material allows us to assume that they were introduced with Atlantic waters during early stages of shelf inundation.

Development of the Eastern Laptev Sea Shelf during the Holocene

In both core sections studied, the successions of ostracode and mollusk assemblages are similar. In both, three assemblages were established: the lowermost assemblage of the inner shelf (brackish-water), transitional assemblage, and the assemblage of the middle shelf (marine) (Fig. 13). They replace each other upcore, reflecting the gradual inundation of the shelf during the Holocene transgression. Boundaries of ostracod and mollusk assemblages are isochronous.

A similar tendency toward changes in the composition of ostracodes, mollusks, and foraminifers from brackish-water to marine during the postglacial flooding was also observed in other Arctic and high-latitudinal areas (Cronin, 1977, 1981, 1989; Syvitski et al., 1989; Dyke et al., 1996; Schoning and Wastegård, 1999; Polyak et al., 2000; Duplessy et al., 2001; Gordillo and Aitken, 2001).

Our data on the downcore distribution of ostracodes, mollusks, and foraminifers allow the conclusions that follow and that considerably supplement the data on the chronology of the Holocene transgression in this region (Mueller-Lupp et al., 2000; Bauch et al., 2001a, 2001b).

In sediment core sections from present water depths of 45–51 m, the Lower Holocene (11.3–8.2 cal. ka) has the highest thickness and temporal resolution. Shortly after the present 50 m depth contour was inundated, both paleovalleys became inhabited by a taxonomically poor benthic assemblage, which was composed of species tolerant to both reduced salinity and considerable amount of terrigenous material supplied by river runoff and coastal erosion. At that time both paleovalleys were inhabited by brackish-water and euryhaline species. Only such species were able to survive in the estuarine-like parts of paleovalleys with depths about 5–10 m, or even less. Bottom salinity supposedly was about 18–20‰. According to composition of diatom associations from core PS-51/135, surface salinity was less than 7–9‰ (Polyakova et al., in press). Due to a rapid sea-level rise, sedimentation rates were extremely high, up to 500 cm/kyr in the Yana paleovalley. The inner shelf brackish-water assemblages of ostracodes and mollusks

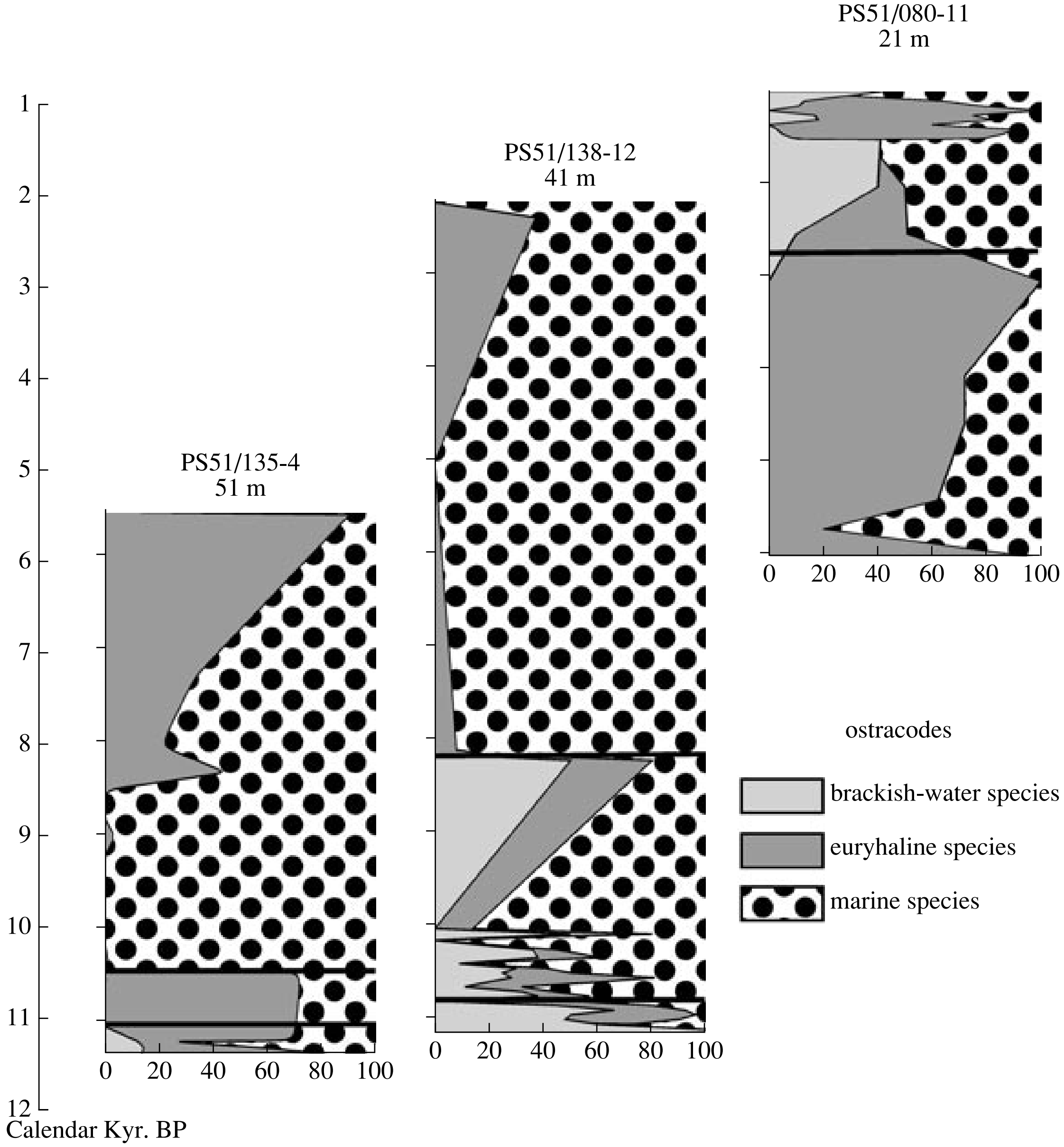

Fig. 13. Changes in the proportions of different ecological groups of ostracode species during the Late Pleistocene and Holocene in different parts of the Laptev Sea.

existed during very short time intervals: between 11.3 and 11.1 cal. ka BP in the Yana paleovalley, and between 11.2 and 10.8 cal. ka BP in the Lena paleovalley.

Upcore several shallow-water normal marine species appear and brackish-water forms gradually disappear, thus indicating that the shelf was gradually inundated and water depths and salinity increased. The transitional ostracode assemblage with a predominance of euryhaline and brackish-water species is similar to the recent inner-shelf assemblage of this region of the sea. It is interesting to note that the transition to a more taxonomically diverse assemblage in the Lena paleovalley around 10.5–10.9 cal. ka BP was marked by distinct peaks in the total abundance of ostracodes and foraminifers (Fig. 9). In the Yana paleovalley, an "avalanche-like precipitation" of freshwater diatoms was recorded for a rather short time span: 11.1–10.7 cal. ka BP (Novichkova et al., 2002; Polyakova et al., in press). Therefore, these peaks in abundance of microfossils probably indicate that the surface productivity was high due to a rich supply of nutrients and that the inflow of sediments was lower than in the initial period of transgression. Between 10.8 and 8.2 cal. ka BP, sedimentation rates in the Lena paleovalley remained relatively high: about 100 cm/kyr, which is comparable to sedimentation rates in the modern depocenter of the Lena River, located at water depths of 20–25 m (Kuptsov and Lisitzin, 1996). In this zone most of the suspended sediment particles

Table 16. Distribution of ostracode species in core section PS51-080: (v) valves; (c) carapaces; (j) juvenile; and (f) fragments

Samples	1	2	3	4	5	6	7	8	9	10	11
Depth of sampling, cm	170–173	160–163	150–153	130–133	120–123	110–113	100–103	90–93	80–83	70–73	60–63
Paracyprideis pseudopunctillata	10v 22jv	2jc	32v 13jv	15v 16jv 1jc f	64v 3jv 2c	20v 15jv f	9v 9jc 1jp 1c	15v 21jv f	2v 4jv	23v 7jv	15v
Heterocyprideis sorbyana								2v 2jv	3v 1jv	26v 1c	6v 1jv
Semicytherura complanata		2v	19v	8v	1v			6v 2c		3v	13v 1c
Bythocythere constricta											
Rabilimis mirabilis											
Polycope punctata											
P. bireticulata					1v	1v		6v		1v	
P. orbicularis								5v			
Cytheromorpha macchesneyi					1v			4v	1v	7v	4v 11jv
Roundstonia globulifera										4v	
C. sulense			2v	1v	1v f	3v		4v		8v	5v
C. elaeni	1v	2v	3v 1jv	3v				f			1v
C. montrosiense									1v	1v	4v 7jv
C. inflatum								f		1v	
Cluthia cluthae		4v	2v 1jv	1v		3v		3v			2v
Cl. ex gr. *cluthae*											

Table 16. (Contd.)

Samples	12	13	14	15	16	17	18	19	20	21	22	23
Depth of sampling, cm	50–53	42–45	40–43	37–39	33–35	29–31	25–27	21–23	17–19	13–15	9–11	1–3
Paracyprideis pseudopunctillata	25v 2c 41jv f	19v	22v 27jv	13v 5jv	26v 2jv	3v + frs	2v + 7jv	9v	4v	7v	20v	42v 28jv
Heterocyprideis sorbyana	3v 3jv f		1jv	1v							2v	3v
Semicytherura complanata	18v		2v		2v	1v					2v	6v
Bythocythere constricta	1jv											
Rabilimis mirabilis	1v											
Polycope punctata												3v
P. bireticulata	1v		2v									
P. orbicularis												
Cytheromorpha macchesneyi	3v	3v	4v		1v			2v		1v	2v	9v
Roundstonia globulifera			1v				2v					
C. sulense	7v	2v	1v			1v					2v	5v
C. elaeni	1v		1v 1jv	1v + f								
C. montrosiense	1v	1v						1v		1v	1v	
C. inflatum												
Cluthia cluthae	3v										2v	
Cl. ex gr. *cluthae*												2v

Table 17. Distribution of ostracode species in core section PS51-92: (v) valves; (c) carapaces; and (f) fragments

Samples	1	2	3	4	5	6	7	8	9	10	11	12	13
Depth of sampling, cm	417–420	370–373	196–199	39–41	35–37	31–33	25–27	23–25	17–19	11–13	9–11	7–9	3–5
Paracyprideis pseudopunctillata	1v		1v	f	6v + f	3v + 1f	5v + f	3v 3f	3v 2f	11v	5v	6v	12v 2c
Heterocyprideis sorbyana										1v			1v
Semicytherura complanata							3v			2v		1v	4v
Krithe sp.													1v
Sarsicytheridea bradii										8v			
Elofsonella concinna										1v			
Acanthocythereis dunelmensis	2v	1v			1f		6v + f	1v 1f					
Cytheropteron elaeni						1f							

are of silt size, and these particles accumulate, together with those of clay size, in the depocenter during the mixing of riverine and marine waters in the flocculation zone, where colloidal particles precipitate. The extremely high sedimentation rates characteristic of the early stage of the transgression were due to rapid sea-level rise and active thermal abrasion of coasts and sea bottom. The considerable influence of freshwater runoff upon water masses of the middle Laptev Sea shelf (eastern part) during this time is also supported by the isotopic composition of organic carbon (Mueller-Lupp et al., 2000) and by the fact that the supply of terrigenous organic matter to the continental slope was at a maximum from 10 to 9.6 cal. ka BP (Stein and Fahl, 2000). By approximately 9.5–8 cal. ka BP modern marine conditions were established on the Laptev Sea continental margin (Boucsein et al., 2000). It seems likely that before 9.8 cal. ka BP, the site in the Lena paleovalley was located in a river estuary, because in a nearby small topographic depression (thermokarst lakes) on the water divide a sudden change to the marine environment occurred at that time (Bauch et al., 2001b; Romanovskii et al., 2004). The composition of benthic assemblages, which have their analogues in the recent assemblage of the inner shelf in the southeastern Laptev Sea, suggests that water depths at the sites studied had gradually reached 20–25 m by 10.3 cal. ka BP in the Yana paleovalley and by 8.2. cal. ka BP in the Lena paleovalley, and the average bottom salinity had risen to 26–28‰. The observed difference in the time of the onset of this environment is likely to be due to a 6-m difference of water depths between the core sites.

The composition of mollusk and ostracode assemblages, which mainly consist of shallow-water normal marine species, suggests that about 10.3 cal. ka BP in the Yana paleovalley and 8.2 cal. ka BP in the Lena paleovalley, an abrupt transition to modern-like environments occurred. Further south, inland migration of the coastline resulted in a decrease in sedimentation rates down to approximately 15 cm/kyr. The high taxonomic diversity of all groups studied and the disappearance of all brackish-water and most euryhaline taxa indicate that bottom salinity attained its modern level of 30–32‰. At the beginning of this stage, high abundances of ostracodes were accompanied by the complete absence of juvenile valves, thus reflecting the changes to more active near-bottom hydrodynamic conditions and a decrease in sedimentation rates (Fig. 13). At the same level, a sharp increase in sand content occurred, from 3–4% to 10–12% on average (Fig. 9). This change might have been caused by active erosion of former islands, now submarine tops, located on both sides of the valleys. Currently, these parts of submarine valleys are affected by strong bottom countercurrents (Dmitrenko et al., 2001; Wegner, 2002). Thus, the sharp increase in sand content can be related to these currents and the establishment of modern-like environments.

Conclusions. As a result of the investigation of fossil ostracodes, mollusks, and foraminifers, three phases in paleoenvironmental changes were recognized:

(1) 11.3–11.1 cal. ka BP in the Yana paleovalley and 11.2–10.8 cal. ka BP in the Lena paleovalley, nearshore freshened environments existed, with depths less than 10 m, reduced and seasonally variable salinity (on average 18–20‰), high sedimentation rates (up to 500 cm/kyr in the Yana paleovalley), and an active

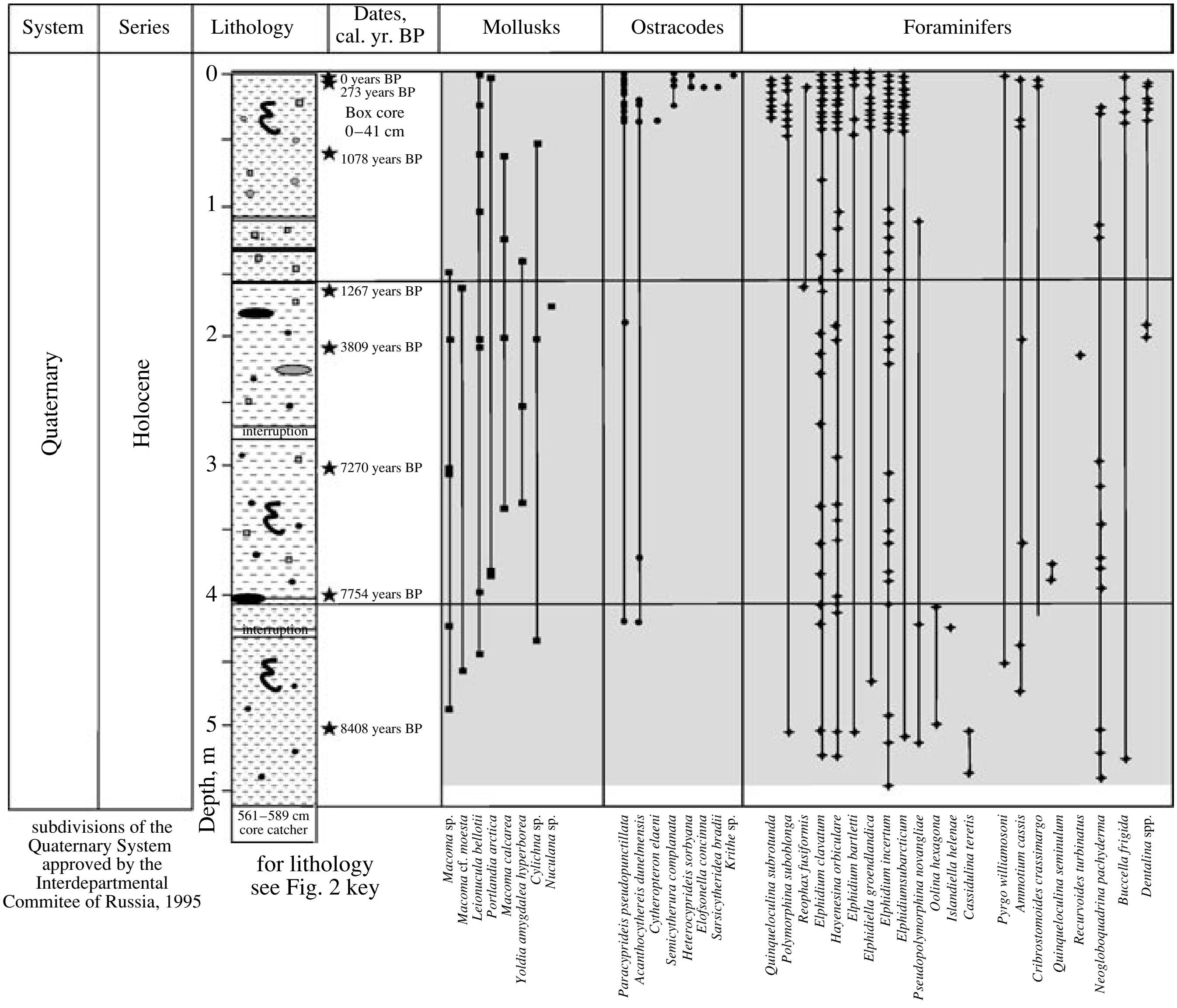

Fig. 14. Distribution of ostracodes, mollusks, and foraminifers in core section PS51/92, obtained in the Lena valley.

input of terrestrial plant debris caused by intensive shelf-coastal erosion and fluvial runoff;

(2) 11.1–10.3 cal. ka BP in the Yana paleovalley and 10.8–8.2 cal. ka BP in the Lena paleovalley, shallow-water environments established, with considerable fluvial runoff influence, water depths about 20–25 m, bottom water salinity about 26–28‰, and high sedimentation rates that decreased progressively (about 100 cm/kyr).

(3) 10.3 cal. ka BP in the Yana paleovalley and 8.2 cal. ka BP in the Lena paleovalley, environmental conditions analogous to those of modern marine environments have established, with a bottom water salinity of about 30–32‰, low sedimentation rates of about 15 cm/kyr (in the Yana paleovalley very low sedimentation rates have established since 5 cal. ka BP), and strong bottom currents.

4.2. Holocene Ostracode Assemblages of the Eastern Inner Shelf of the Laptev Sea

We carried out a quantitative analysis of ostracode assemblages from two sediment core sections: PS-51/092 (water depth 34 m) and PS-51/080 (water depth 21 m) (Figs. 1, 2; Tables 16, 17). These core sections date back to 6.4 and 8.4 cal. ka, respectively. Changes in the fossil assemblages from these sections are not very distinct. In general, taxonomic diversity increases upcore, but no analogies to the assemblages established on the middle shelf have been found. In core PS-51/092 assemblages have not been distinguished at all due to the fact that samples were almost barren of ostracodes (Fig. 14). We suppose that this may be due to the dissolution of carapaces in the sediments while the core was in storage. It was kept for three years in humid conditions in the cool store in GEOMAR, long enough for ostracode carapaces to dissolve. This hypothesis is also supported by the fact that box core samples (upper 40 cm) from the same site, which were dried immediately after collection, contained numerous microfossils.

Nevertheless, foraminifers in this core section are quite abundant, this is most likely due to different from ostracodes construction of their test mura (ostracode carapaces contain a great amount of organic inclusions, foraminifer tests do not). In samples from the lower unit of core PS-51/092, which date back to 8.4 cal. ka BP, numerous planktonic foraminifers were found (the same phenomenon was recorded in the lower part of core PS51/135), their proportion here reaches 100% (Fig. 14). Two more peaks in the abundance of foraminifers were observed at levels dated back to 7.7–6 and 1.1–0.3 cal. ka BP. The basal part of this core section contains benthic foraminifers of the species *Cassidulina teretis,* which is known as an indicator of Atlantic waters (Lubinski et al., 2001). In the surface coretop sediment samples, planktonic foraminifers and *C. teretis* were only recorded in samples from the continental slope. The presence of abundant planktonic foraminifers in shallow-water environments on the early stage of inundation possibly reflects advection of Atlantic waters. It is known that at present Atlantic waters lie below 80–100 m water depth, but the latest oceanographic research has revealed that bottom countercurrents bring these waters along paleovalleys to depths of 20–40 m (Dmitrenko et al., 2001; Wegner, 2002).

Two assemblages were established in sediment core section PS-51/080, obtained from the inner-shelf area. The lowermost assemblage is taxonomically poor and is dominated by euryhaline *Paracyprideis pseudopunctillata* (20–100%). In about 2.7 cal. ka BP this assemblage was replaced by the other taxonomically more diverse assemblage, which includes, quite unexpectedly, numerous specimens of the euryhaline *Heterocyprideis sorbyana* and brackish-water *Cytheromorpha macchesneyi*, both species have not been found in the underlying layers (Fig. 15).

It was only possible to calculate the total abundance of ostracodes for the upper part of the core section, for the samples obtained from the box core, interval 2–40 cm. The total abundance of ostracodes here varies between 3 and 30 specimens per 100 g dry bulk sediment weight, which is quite low in comparison to the coretop samples (Tables 6–9). The fact that the proportion of juvenile valves and complete carapaces remains high throughout the core section suggests relatively rapid burial (Fig. 16). Taxonomic diversity increases upward, in a manner resembling core sections from the middle shelf (Fig. 15).

The oldest ostracode assemblage, established in the lower part of the core (170–90 cm; 6.4–2.7 cal. ka), is characterized by the neritic, normal marine species *Cluthia cluthae* (5–40%), *Semicytherura complanata* (up to 25%), and *Cytheropteron elaeni* (5–18%) and the euryhaline species *P. pseudopunctillata*, which predominates in this assemblage, comprising on average 60% of all valves (Figs. 15, 16).

The younger assemblage (90–0 cm, sediments younger than 2.7 cal. ka) is represented by different ecological groups of ostracodes. Predominant species are the brackish-water *C. macchesneyi* (5–30%), the euryhaline *P. pseudopunctillata* (20–100%) and *H. sorbyana* (5–35%), and the normal marine *Semicytherura complanata* (15–25%), *Cytheropteron sulense* (5–20%), and *C. montrosiense* (up 20%) (Fig. 16). The taxonomic diversity of this assemblage is almost twice as high as that of the older assemblage.

Conclusions. On the inner-shelf of the southeastern part of the sea, at least as early as 6.4 cal. ka BP, nearshore shallow-water environments with relatively low sedimentation rates (30 cm/kyr) existed (Fig. 13). Around 2.7 cal. ka BP these environments were replaced by modern-like environments. The high taxonomic diversity of ostracodes and the appearance of brackish-water and euryhaline species are evidence of drastic changes in bottom water parameters. The species composition of the ostracode assemblage suggests that the fresh-water influence increased, probably due to a change in the direction and/or volume of river flow. The sharp increase in sedimentation rates about 1.5 cal. ka BP also supports this supposition.

4.3. Late Pleistocene–Holocene Ostracode Assemblages of the Western Continental Slope of the Laptev Sea

Core PS-51/154 was recovered from the western region of the Laptev Sea, from a water depth of 276 m (Figs. 1, 2, 17; Table 18), which corresponds to the upper part of the continental slope. This section is unique for paleoreconstructions, since it is located close to the Olenek paleodelta (Kleiber and Niessen, 2000) and has extremely good chronological resolution (Bauch et al., 2001b). The oldest record dates back to 13.6 ^{14}C ka BP (15.8 cal. ka BP) and was obtained from a level of 570 cm (Fig. 17). The extrapolated age of the base of the core is about one thousand years older. Thus, the core section documents most of the postglacial transitional epoch and the entire Holocene, representing the longest chronological record of the events that took place in the Laptev Sea. The core is 708 cm thick. The interval of the core section from its base (708 cm) up to 574 cm is practically barren of any fossils: only a few foraminifer tests were taken from the core catcher (probably, they accidentally fell there during sampling). However, these sediments are rich in small plant debris, vivianite, and mica. As a whole, this evidences the proximity of the paleocoast to the slope break prior to 15.8 cal. ka BP and active input of terrigenous material with the continental river runoff.

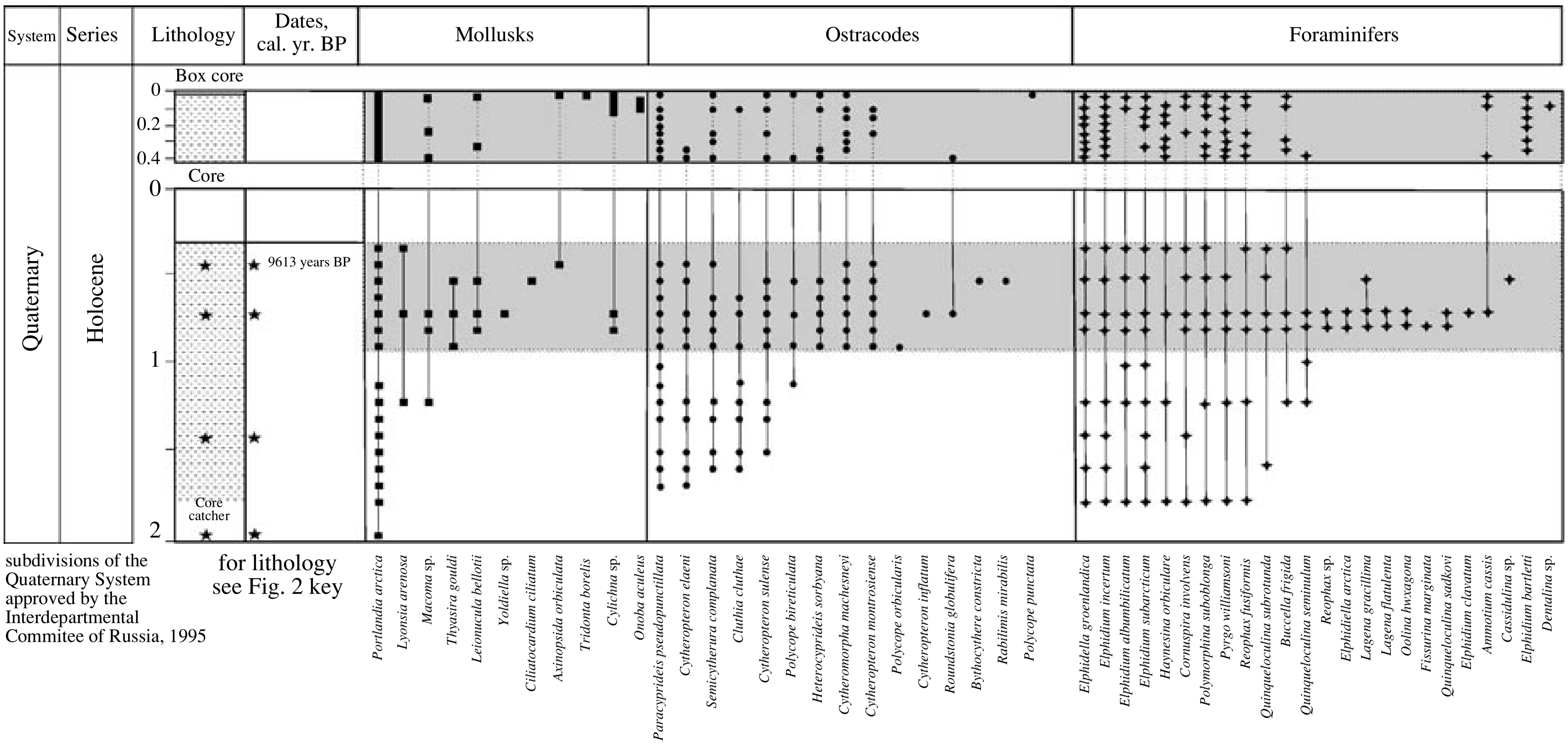

Fig. 15. Distribution of ostracodes, mollusks, and foraminifers in core section PS51/80.

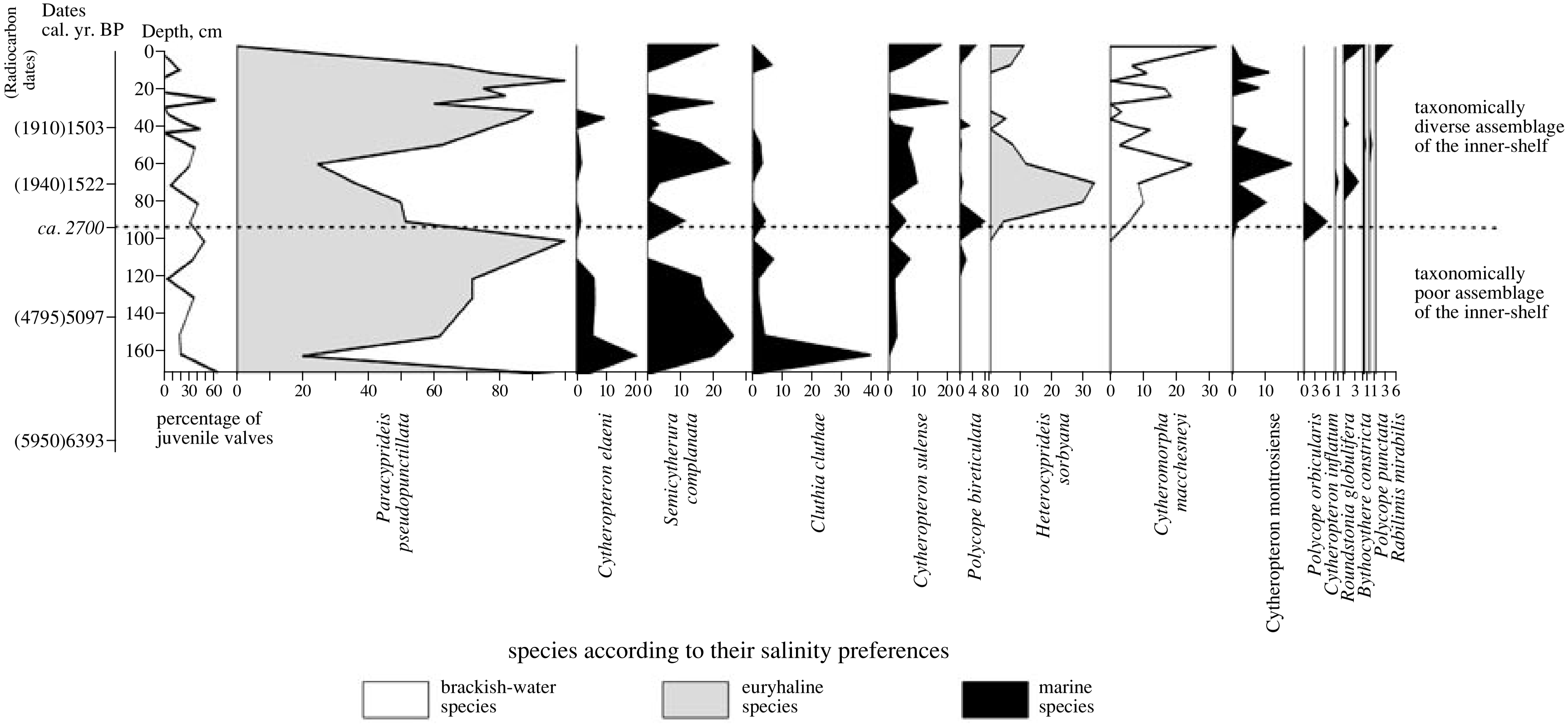

Fig. 16. Distribution of ostracode species in core section PS-51/080-13, obtained in the Lena paleovalley.

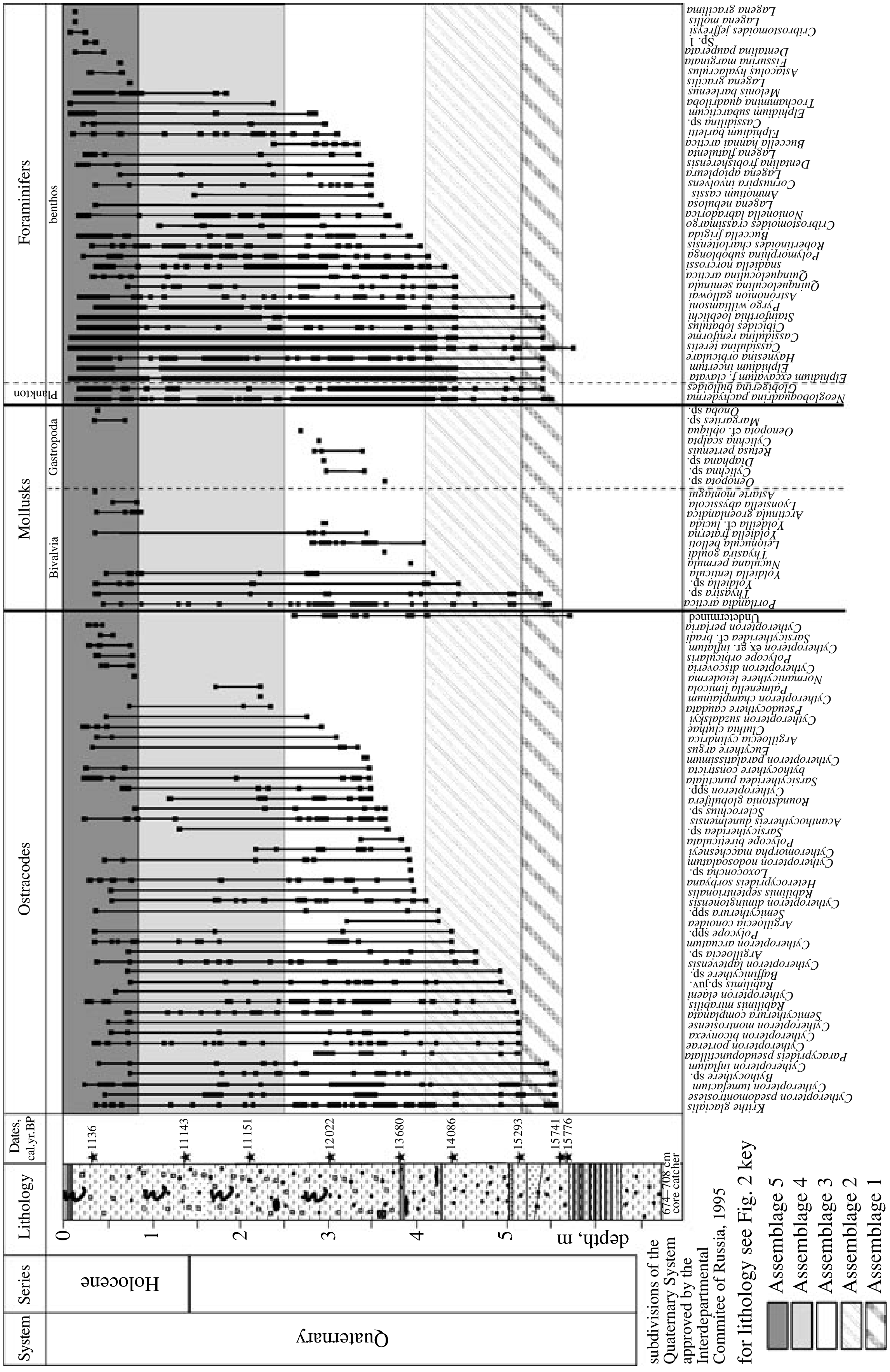

Fig. 17. Distribution of ostracodes, mollusks, and foraminifers in core section PS51/154.

Table 18. Distribution of ostracode species in core section PS51/154: (v) valves; (c) carapaces; (j) juvenile; and (fr) fragments

Samples	Sampling depth, cm	*C. inflatum*	*C.* ex gr. *inflatum*	*Krithe glacialis*	*Cytheropteron pseudomontrosiense*	*Paracyprideis pseudopunctillata*	*Semicytherura complanata*	*Cytheropteron tumefactum*	*Rabilimis mirabilis*	*Cytheropteron elaeni*	*Argilloecia conoidea*	*Cytheropteron porterae*	*Bythocythere* sp. 1	*Cytheropteron dimlingtonensis*	*Cytheropteron champlainum*	*Acanthocythereis dunelmensis*	*Sclerochilus* sp. 1	*Cytheropteron laptevensis*	*Heterocyprideis sorbyana*	*Cytheromorpha macchesneyi*	*Sarsicytheridea punctillata*	*Eucythere argus*	*Cytheropteron arcuatum*	*Argilloecia cylindrica*	*Cytheropteron biconvexa*	*Roundstonia globulifera*	*Cytheropteron suzdalskyi*	*Cytheropteron nodosoalatum*	*Pseudocythere caudata*	*Palmenella limicola*	*Cytheropteron discoveria*	*Bythocythere constricta*	*Rabilimis septentrionalis*	*Cytheropteron montrosiense*	*Cluthia cluthae*	*Cytheropteron perlaria*	*Sarsicytheridea* sp.	*Loxoconcha* sp.	*Semicytherura* spp.	*Baffinicythere* sp.	*Argilloecia* sp.	*Sarsicytheridea* cf. *bradii*	*Cytheropteron* spp.	*Normanicythere* sp.	*Polycope* spp. (*P. bireticulata, P. orbicularis*)	Undetermined
1	573																																													fr
2	555			20 jv																																										
3	550			5jv	1v			fr?					1v																																	
4	545	1v		2v fr				2v																																						
5	543	1fr		4v 2jv																																										
6	521				4v																																									
7	518				17 v 10 jv	fr		4v 1jv				11 v fr													1v									1v												
8	513				1fr	5v fr	2v	1v																																						
9	507							1v 2jv	1v 1jv	1jv																																				
10	493			5jv	5v	1v		8v	17 jv			frs																												1v						
11	467								3v 11 jv			frs						1v																							1jv					
12	443			12 jv	1 jv fr		1v		2v 4jv									3v																												
13	439			2v 3jv	1jv													1jv					1jv																		1jv				2jv	
14	421			2v					1jv		1v	2v 2jv																											1v fr							
15	417			7v		1c		2v	2v 3jv																																					
16	413			10 v					1v 7jv																																					
17	411			2v					2jv					1v																																fr

Table 18. (Contd.)

Samples	Sampling depth, cm	*C. inflatum*	*C.* ex gr. *inflatum*	*Krithe glacialis*	*Cytheropteron pseudomontrosiense*	*Paracyprideis pseudopunctillata*	*Semicytherura complanata*	*Cytheropteron tumefactum*	*Rabilimis mirabilis*	*Cytheropteron elaeni*	*Argilloecia conoidea*	*Cytheropteron porterae*	*Bythocythere* sp. 1	*Cytheropteron dimlingtonensis*	*Cytheropteron champlainum*	*Acanthocythereis dunelmensis*	*Sclerochilus* sp. 1	*Cytheropteron laptevensis*	*Heterocyprideis sorbyana*	*Cytheromorpha macchesneyi*	*Sarsicytheridea punctillata*	*Eucythere argus*	*Cytheropteron arcuatum*	*Argilloecia cylindrica*	*Cytheropteron biconvexa*	*Roundstonia globulifera*	*Cytheropteron suzdalskyi*	*Cytheropteron nodosoalatum*	*Pseudocythere caudata*	*Palmenella limicola*	*Cytheropteron discoveria*	*Bythocythere constricta*	*Rabilimis septentrionalis*	*Cytheropteron montrosiense*	*Cluthia cluthae*	*Cytheropteron perlaria*	*Sarsicytheridea* sp.	*Loxoconcha* sp.	*Semicytherura* spp.	*Baffinicythere* sp.	*Argilloecia* sp.	*Sarsicytheridea* cf. *bradii*	*Cytheropteron* spp.	*Normanicythere* sp.	*Polycope* spp. (*P. bireticulata*, *P. orbicularis*)	Undetermined
18	408			2v				1v	4v 1jv																																					
19	403			18 v 5jv					3v 3jv			1v																																		
20	395			4v 2jv										1v																			2v								1jv					fr
21	393			3v 7jv									1v					3v																							1jv					
22	391			1v 2jv														1v	1jv																			1v	1jv							
23	388			6v 1jv									1v												1v			1v																		
24	387					1jv														1jv																										fr
25	383																	1v																												
26	381												1v																																2v	
27	379												1v	1jv																																
28	377			5jv																																										
29	375			2jv									2v																																	
30	373			1v														1v																												
31	371			1c														2v																												
32	369			4 jv 1jc								1v																									1jv									
33	367								3jv																																					
34	365			1jv									1v																																	
35	363			1v					2v			1v 1jv	3v			2jv	1v																													
36	361			6v					5jv			1v	4v			2jv		2v																												
37	359			1jv					2v 2jv				1v																																	
38	357			4jv				2v	6v			1v	1v			1jv																														
39	353			3v 2jv				2v 1jv	3v 3jv				1v				1jv		1v																											

Table 18. (Contd.)

Samples	Sampling depth, cm	*C. inflatum*	*C.* ex gr. *inflatum*	*Krithe glacialis*	*Cytheropteron pseudomontrosiense*	*Paracyprideis pseudopunctillata*	*Semicytherura complanata*	*Cytheropteron tumefactum*	*Rabilimis mirabilis*	*Cytheropteron elaeni*	*Argilloecia conoidea*	*Cytheropteron porterae*	*Bythocythere* sp. 1	*Cytheropteron dimlingtonensis*	*Cytheropteron champlainum*	*Acanthocythereis dunelmensis*	*Sclerochilus* sp. 1	*Cytheropteron laptevensis*	*Heterocyprideis sorbyana*	*Cytheromorpha macchesneyi*	*Sarsicytheridea punctillata*	*Eucythere argus*	*Cytheropteron arcuatum*	*Argilloecia cylindrica*	*Cytheropteron biconvexa*	*Roundstonia globulifera*	*Cytheropteron suzdalskyi*	*Cytheropteron nodosoalatum*	*Pseudocythere caudata*	*Palmenella limicola*	*Cytheropteron discoveria*	*Bythocythere constricta*	*Rabilimis septentrionalis*	*Cytheropteron montrosiense*	*Cluthia cluthae*	*Cytheropteron perlaria*	*Sarsicytheridea* sp.	*Loxoconcha* sp.	*Semicytherura* spp.	*Baffinicythere* sp.	*Argilloecia* sp.	*Sarsicytheridea* cf. *bradii*	*Cytheropteron* spp.	*Normanicythere* sp.	*Polycope* spp. (*P. bireticulata*, *P. orbicularis*)	Undetermined
40	351			1v 4jv	3v			6v	2v 12 jv				1v						1v																											
41	349			4jv	9v 1jv	1jv	1v		1v 6jv			1v		2v		8v 2 jv fr										2v															1jv		2v			
42	347				22 v 7jv	3v 6jv	6v	7v 1jv	15 v 1 jvv			3v 1jv	6v	2v 1jv		22 v 50 jv frs				2v	1jv				3v	1v 1jv						1v									1v					
43	343				2v	9jv	1v	1v	5v 12 jv			4v				2v 2jv									1v	2v 2c																				
44	341			1v 1 jv fr	3v	18 v 8jv	12 v	1v fr	5v 11 jv					1jv		4v 5jv										3v																	7v			
45	339			3v	2jv	6v 5jv	12 v	4v 1jv	5v 13 jv			2v fr		1v		8v 1 jv frs				5v					3v fr	10 v fr																	3v			fr
46	337			1v	18 v	2v 8jv		7v	4v 24 jv					2v		7v 23 jv				10 v	1v 1jv				fr	5v																	3v			
47	335			2v 2jv	24 v 6 jv 2c	11 v 10 jv	8v	2v	2v 9jv			5v		3v		7v 11 jv	4v			2v	1v 3jv																								2v	
48	333			3v	12 v	1v 1jv	1v	6v	2v 5jv			1v				4v				2v	2v 6jv		fr		1v																					
49	331			3v	6v	3 jv fr		1v	3v 1jv							4v					6jv					1v																				

Table 18. (Contd.)

Samples	Sampling depth, cm	*C. inflatum*	*C.* ex gr. *inflatum*	*Krithe glacialis*	*Cytheropteron pseudomontrosiense*	*Paracyprideis pseudopunctillata*	*Semicytherura complanata*	*Cytheropteron tumefactum*	*Rabilimis mirabilis*	*Cytheropteron elaeni*	*Argilloecia conoidea*	*Cytheropteron porterae*	*Bythocythere* sp. 1	*Cytheropteron dimlingtonensis*	*Cytheropteron champlainum*	*Acanthocythereis dunelmensis*	*Sclerochilus* sp. 1	*Cytheropteron laptevensis*	*Heterocyprideis sorbyana*	*Cytheromorpha macchesneyi*	*Sarsicytheridea punctillata*	*Eucythere argus*	*Cytheropteron arcuatum*	*Argilloecia cylindrica*	*Cytheropteron biconvexa*	*Roundstonia globulifera*	*Cytheropteron suzdalskyi*	*Cytheropteron nodosoalatum*	*Pseudocythere caudata*	*Palmenella limicola*	*Cytheropteron discoveria*	*Bythocythere constricta*	*Rabilimis septentrionalis*	*Cytheropteron montrosiense*	*Cluthia cluthae*	*Cytheropteron perlaria*	*Sarsicytheridea* sp.	*Loxoconcha* sp.	*Semicytherura* spp.	*Baffinicythere* sp.	*Argilloecia* sp.	*Sarsicytheridea* cf. *bradii*	*Cytheropteron* spp.	*Normanicythere* sp.	*Polycope* spp. (*P. bireticulata, P. orbicularis*)	Undetermined
50	329								5v 10 jv																								2v													
51	327			2jv	1v			4v	2jv				1fr										1v																							1v
52	325			13 v				4v	1v 1jv			1v	5v			2v			1v			1v	1v																							
53	323			2v 3jv				5v	2v							1v			6v 2jv		2jv		1v		2v																					fr
54	321			3v 4jv				13 v			1v								1v 1jv		2v 1jv		3v		1v	2v																				
55	319			3v				2v	1jv										1v				5v																							
56	317			1v				2v 3jv	2jv													1v	2v																						2v	
57	315								1v														1v																							
58	313			1v				5v	1v													2jv	2v 2jv																							
59	311							3v	1jv														1v																							
60	309			1jv		1jv		3v															3v	1v																						
61	307																																													fr
62	305			1v 1jv			1v	8v 3jv										2v	1v				5v 1c																							
63	303			3v 3jv				4v	1v 1jv									2v fr	1jv				11 v																							fr
64	301			5v		1v		5v	4v 2jv														9v 2jv		1fr																					1v
65	299			2jv		1jv	2v		2v 16 jv			1v		1v		2jv		1v	1v 1jv				10 v		1v																					
66	297					2v 7jv	4v fr		2v 23 jv							4v 6jv			6v	1v fr			8v fr																							1v
67	295					2v 2jv	frs		2v 7jv							2v 4 jv fr			1v																											

Table 18. (Contd.)

Samples	Sampling depth, cm	*C. inflatum*	*C.* ex gr. *inflatum*	*Krithe glacialis*	*Cytheropteron pseudomontrosiense*	*Paracyprideis pseudopunctillata*	*Semicytherura complanata*	*Cytheropteron tumefactum*	*Rabilimis mirabilis*	*Cytheropteron elaeni*	*Argilloecia conoidea*	*Cytheropteron porterae*	*Bythocythere* sp. 1	*Cytheropteron dimlingtonensis*	*Cytheropteron champlainum*	*Acanthocythereis dunelmensis*	*Sclerochilus* sp. 1	*Cytheropteron laptevensis*	*Heterocyprideis sorbyana*	*Cytheromorpha macchesneyi*	*Sarsicytheridea punctillata*	*Eucythere argus*	*Cytheropteron arcuatum*	*Argilloecia cylindrica*	*Cytheropteron biconvexa*	*Roundstonia globulifera*	*Cytheropteron suzdalskyi*	*Cytheropteron nodosoalatum*	*Pseudocythere caudata*	*Palmenella limicola*	*Cytheropteron discoveria*	*Bythocythere constricta*	*Rabilimis septentrionalis*	*Cytheropteron montrosiense*	*Cluthia cluthae*	*Cytheropteron perlaria*	*Sarsicytheridea* sp.	*Loxoconcha* sp.	*Semicytherura* spp.	*Baffinicythere* sp.	*Argilloecia* sp.	*Sarsicytheridea* cf. *bradii*	*Cytheropteron* spp.	*Normanicythere* sp.	*Polycope* spp. (*P. bireticulata*, *P. orbicularis*)	Undetermined
68	293					5v 4jv	2v		3v							18 v 3jv				5v						1v																				
69	291					7v 1jv	1v		1jv							1jv				fr																										
70	289			2v		4v 5jv	5v		3v					2v		5v				3v						1v									3v											fr
71	285					9v 15 jv	4v							fr		1v 1jv				1v						2v																				
72	283			1v		1v																																								
73	280						3v							3v 1 jv fr		3v 2jv				3v						2v fr		2v																		
74	278																									1v																				
75	277					1jv																																								
76	276																											1v																		
77	275			2v			6v		1fr				fr	2v		5v 1jv																							1jv							
78	273			4v 2jv					1jv																		1fr																			
79	271																											1v																		
80	269			3v 1jv			1v		1jv				4v	2v		1v		1v	4v																											
81	267								2v 2jv										5v																											
82	265	2v		3v	fr				6jv					1v		1v 1jv		1v	3v																								fr			
83	263								1v								2v																													
84	261			3v					1v					6v																																
85	257								1jv									1v																												fr
86	255								1v										1v																											

Table 18. (Contd.)

Samples	Sampling depth, cm	*C. inflatum*	*C.* ex gr. *inflatum*	*Krithe glacialis*	*Cytheropteron pseudomontrosiense*	*Paracyprideis pseudopunctillata*	*Semicytherura complanata*	*Cytheropteron tumefactum*	*Rabilimis mirabilis*	*Cytheropteron elaeni*	*Argilloecia conoidea*	*Cytheropteron porterae*	*Bythocythere* sp. 1	*Cytheropteron dimlingtonensis*	*Cytheropteron champlainum*	*Acanthocythereis dunelmensis*	*Sclerochilus* sp. 1	*Cytheropteron laptevensis*	*Heterocyprideis sorbyana*	*Cytheromorpha macchesneyi*	*Sarsicytheridea punctillata*	*Eucythere argus*	*Cytheropteron arcuatum*	*Argilloecia cylindrica*	*Cytheropteron biconvexa*	*Roundstonia globulifera*	*Cytheropteron suzdalskyi*	*Cytheropteron nodosoalatum*	*Pseudocythere caudata*	*Palmenella limicola*	*Cytheropteron discoveria*	*Bythocythere constricta*	*Rabilimis septentrionalis*	*Cytheropteron montrosiense*	*Cluthia cluthae*	*Cytheropteron perlaria*	*Sarsicytheridea* sp.	*Loxoconcha* sp.	*Semicytherura* spp.	*Baffinicythere* sp.	*Argilloecia* sp.	*Sarsicytheridea* cf. *bradii*	*Cytheropteron* spp.	*Normanicythere* sp.	*Polycope* spp. (*P. bireticulata*, *P. orbicularis*)	Undetermined
87	245																																													
88	243												3v																																	
89	241						1fr						1v																																	
90	239	3v					3v		1jv																																					
91	233												3v fr				1v fr	1v		1v									1v														fr			
92	227	1v												3v												1v																				
93	225	1v					1v					1v																																		
94	223				1v			1v fr						3v	1v											1v				fr													2v fr			
95	221							2v																		1v																				
96	217			1v			2v						1v							1v								1v																		
97	214							2v	1jv					2v																																
98	212				1v				1v 1jv																																					
99	211						2v																																							
100	207			1jv																																										
101	203											3v 1jv	1v																1v																	
102	201																																													
103	197											1v									2jv																									
104	195						1fr							1v																																
105	190																																													
106	187																	1v																												
107	185							2v	1v																																					
108	181							2v	1jv																																					
109	179			2v 3jv	1v			5v	1v			1v	1v					1v 2jv																												
110	177							2v				2v		1v				1v	2v				2v fr		1v																					
111	175				5v 1jv									1v 1jv																																

Table 18. (Contd.)

Samples	Sampling depth, cm	*C. inflatum*	*C.* ex gr. *inflatum*	*Krithe glacialis*	*Cytheropteron pseudomontrosiense*	*Paracyprideis pseudopunctillata*	*Semicytherura complanata*	*Cytheropteron tumefactum*	*Rabilimis mirabilis*	*Cytheropteron elaeni*	*Argilloecia conoidea*	*Cytheropteron porterae*	*Bythocythere* sp. 1	*Cytheropteron dimlingtonensis*	*Cytheropteron champlainum*	*Acanthocythereis dunelmensis*	*Sclerochilus* sp. 1	*Cytheropteron laptevensis*	*Heterocyprideis sorbyana*	*Cytheromorpha macchesneyi*	*Sarsicytheridea punctillata*	*Eucythere argus*	*Cytheropteron arcuatum*	*Argilloecia cylindrica*	*Cytheropteron biconvexa*	*Roundstonia globulifera*	*Cytheropteron suzdalskyi*	*Cytheropteron nodosoalatum*	*Pseudocythere caudata*	*Palmenella limicola*	*Cytheropteron discoveria*	*Bythocythere constricta*	*Rabilimis septentrionalis*	*Cytheropteron montrosiense*	*Cluthia cluthae*	*Cytheropteron perlaria*	*Sarsicytheridea* sp.	*Loxoconcha* sp.	*Semicytherura* spp.	*Baffinicythere* sp.	*Argilloecia* sp.	*Sarsicytheridea* cf. *bradii*	*Cytheropteron* spp.	*Normanicythere* sp.	*Polycope* spp. (*P. bireticulata*, *P. orbicularis*)	Undetermined
112	173	1v			5v		1v					2v		1v																1v															1fr	
113	169																																													
114	167				1v																																									
115	161				1v							2v						2v																												
116	157				1jv		3v																1v																							
117	153																						1v																							
118	151																																													
119	149			1v																																										
120	135						2v fr																																							
121	133						1v																																							
122	129																	3v																												
123	127																						2v														1v									
124	123															1jv																														
125	121			1v								1v																																		
126	119			2v			1v																			2v																				
127	113											1v																																		
128	99																																													
129	97																																													
130	93																																													
131	85															1jv																														
132	83																																													
133	81							2v																																						
134	79																																	1v												
135	77																		2v				2v																					1jv		
136	75	1v					1v	2v				3v					1c	2v					3v						1v		10v	5v 2jv											3v		2v	
137	73							3v	2jv			3v 3jv	1v			2v	3v	6v					1v								3v	2v 1jv		1v												
138	71		1jv				1v fr																2v		fr																1jv		1v			

Table 18. (Contd.)

Samples	Sampling depth, cm	*C. inflatum*	*C.* ex gr. *inflatum*	*Krithe glacialis*	*Cytheropteron pseudomontrosiense*	*Paracyprideis pseudopunctillata*	*Semicytherura complanata*	*Cytheropteron tumefactum*	*Rabilimis mirabilis*	*Cytheropteron elaeni*	*Argilloecia conoidea*	*Cytheropteron porterae*	*Bythocythere* sp. 1	*Cytheropteron dimlingtonensis*	*Cytheropteron champlainum*	*Acanthocythereis dunelmensis*	*Sclerochilus* sp. 1	*Cytheropteron laptevensis*	*Heterocyprideis sorbyana*	*Cytheromorpha macchesneyi*	*Sarsicytheridea punctillata*	*Eucythere argus*	*Cytheropteron arcuatum*	*Argilloecia cylindrica*	*Cytheropteron biconvexa*	*Roundstonia globulifera*	*Cytheropteron suzdalskyi*	*Cytheropteron nodosoalatum*	*Pseudocythere caudata*	*Palmenella limicola*	*Cytheropteron discoveria*	*Bythocythere constricta*	*Rabilimis septentrionalis*	*Cytheropteron montrosiense*	*Cluthia cluthae*	*Cytheropteron perlaria*	*Sarsicytheridea* sp.	*Loxoconcha* sp.	*Semicytherura* spp.	*Baffinicythere* sp.	*Argilloecia* sp.	*Sarsicytheridea* cf. *bradii*	*Cytheropteron* spp.	*Normanicythere* sp.	*Polycope* spp. (*P. bireticulata*, *P. orbicularis*)	Undetermined
139	69			1v				1v 1jv								2jv									1v			1v																		
140	67						1v	2v																																						
141	65																																										fr			
142	61																						1v																							
143	59																		1v																											
144	57			fr				1v		fr																																				
145	55																																1v 2jv													
146	53			2jv					2jv												1jv		1v																			fr				
147	51			2v				1v				1v fr		2jv					1jv				1v		2v																					
148	49				2jv			1v	2v 1jv			1v												1v							1v			2v	2v											
149	47																											1v																		
150	45			1v				2v	1v 1jv																		1v									1v										
151	42			2v																																										
152	39	0/1v	1jv					5v				5v						7v	2v		4v		2v 1jv								1v					1v										
153	37			4v				1v	1v 1jv			1v							5v		3v			1v															2v			fr				
154	35	1v		9v 1jv				5v	1v 2jv										5v		3v 3jv	2v	2v												2v										2v	
155	29								1jv			1jv									2jv											1v													4v	
156	27		1v					1v	4v 4jv							1jv			6v		1v														1v	1v										
157	21							2v											2v		6v 2jv														1v											
158	19																				2v 2jv																									
159	9																																													

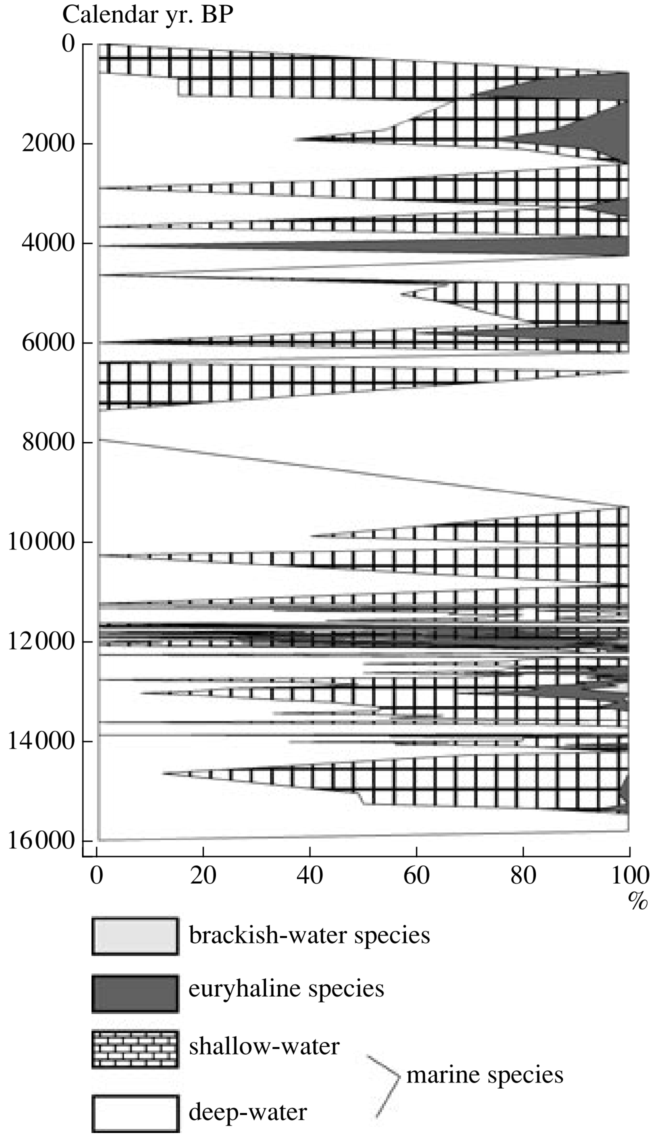

Fig. 18. Changes in the proportions of different ecological groups of species in core section PS51/154.

In 15.8 cal. ka BP, water depth at the core site PS-51/154 was about 150–170 m, in other words, this site was located on the continental slope, but 100–120 m higher than now. In the surface samples that were previously studied from this part of the sea, we identified numerous deepwater species that are typical of the North Atlantic and the Central Arctic Ocean. The surface samples from the western and central parts of the Laptev Sea were grouped into a single assemblage, typical of normal marine waters at depths greater than 60 m. Thus, the difference between the present and paleowater depths at the core site was unlikely to affect the taxonomic composition of the ostracode assemblage. When investigating fossil ostracodes from this section we agreed to divide normal marine species into shallow-water neritic species and deep-water species of North Atlantic origin, inhabiting the continental slope (Fig. 18).

As a result, five ostracode assemblages were established.

(1) The oldest assemblage existed during a very short time period, from 15.8 to 15.1 cal. ka BP (interval 570–510 cm in the section) (Figs. 17, 18). This assemblage has the poorest taxonomic diversity: five species. The ostracodes are dominated by a few relatively deepwater species. The high percentage of *Krithe glacialis* (up to 60%) is indicative of cold bottom environments and low nutrient content (Cronin et al., 1995). According to Taldenkova's data, *Portlandia arctica* is dominant among the mollusks. This species is able to survive in harsh arctic environments with high sedimentation rates and a high input of plant debris (Syvitski et al., 1989; Aitken and Gilbert, 1996). According to Dem'yankov, two ecological groups dominate the foraminifers: the opportunistic species *Elphidium excavatum* f. *clavata*, surviving under harsh conditions (Polyak et al., 2002), and the relatively deepwater *Cassidulina teretis* and *C. reniforme.* The presence of *C. teretis* is especially remarkable, since its occurrence in the Arctic Ocean is clearly associated with the subsurface Atlantic-derived waters (Lubinski et al., 2001). Thus, already in 15.8 cal. ka BP the Atlantic waters were inflowing to the western Laptev Sea continental slope, where the bottom environment was characterized by cold, low nutrient bottom waters, high sedimentation rates, and abundant plant debris. The existence of quite thick ice cover is probable. Planktonic foraminifers were very abundant, among them such typical Arctic Ocean species as *Neogloboquadrina pachyderma* sin. and *Globigerina bulloides.* Probably, this find indicates a local situation, which is totally unusual for the present environment, when close location of paleocoast resulted in formation of a polynya, where conditions were favorable for planktonic foraminifers due to the abundance of food at the pack ice edge.

(2) The second established assemblage (510–390 cm, 15.1–13.8 cal. ka BP) is similar to the previous assemblage, but it is more taxonomically diverse (19 species). The predominant species are *Krithe glacialis* (up to 60%), *Rabilimis mirabilis* (up to 20%), *Cytheropteron tumefactum* (up to 20%), and *C. pseudo-montrosiense* (up to 25%). The other species are of minor importance. An increase in taxonomic diversity was also recorded among mollusks and foraminifers (according to Taldenkova and Dem'yankov).

(3) The third assemblage (390–250 cm, 13.8–11.6 cal. ka BP) differs significantly from the previous assemblages in having a considerably increased taxonomic diversity: 36 species. This period is characterized by the increase in abundance and taxonomic diversity not only of ostracodes, but also of mollusks and foraminifers. The abundance of ostracodes and foraminifers reached a maximum around 13.0 cal. ka BP (according to Taldenkova and Dem'yankov). It is note-

worthy that this assemblage is represented by all three groups of ostracodes differing from each other in their tolerance to salinity: brackish-water, euryhaline, and normal marine. The latter group contains both deepwater and shallow-water species. Euryhaline and brackish-water species are very few: *Paracyprideis pseudopunctillata, Cytheromorpha macchesneyi, Heterocyprideis sorbyana*, and *Loxoconcha* sp. Their proportion in the samples does not exceed 5–20%. Their presence in minor quantities could be indicative of especially high freshwater discharge and active sea-ice transportation of these species from shallow depths to the continental slope. The high abundance of *E. excavatum* f. *clavata* in the layers formed at 13.8–13.0 cal. ka BP probably corresponds to the strongest meltwater event, this can be additionally supported by the diminished proportions of planktonic foraminifers and *C. teretis* (according to Taldenkova and Dem'yankov).

(4) The fourth assemblage (250–85 cm; 11.6–6.5 cal. ka BP) shows one more decrease in taxonomic diversity, to 26 species. This is mainly due to poor preservation of the material, which, in turn, may be caused by a sharp reduction in sedimentation rates at the site at about 11.1 cal. ka BP, which coincides with the flooding of the Laptev Sea outer shelf approximately 11.1–11.3 cal. ka BP (Bauch et al., 2001b, Taldenkova et al., 2005). This assemblage is characterized solely by marine deepwater species with clear North Atlantic affinities: *Cytheropteron tumefactum* (up to 30%), *C. pseudomontrosiense* (up to 90%), *C. laptevensis* (up to 20%), *C. arcuatum* (up to 10%), and *Bythocythere* sp. 1 (up to 80%) (Figs. 17, 18), thus suggesting an increase in the influence of the Atlantic waters at that time. According to Dem'yankov, the constant presence of *C. teretis* and planktonic foraminifers in all samples also supports this assumption.

(5) The fifth assemblage, the youngest, documents the last 6.5 thousand calendar years (85–0 cm). Its taxonomic composition is similar to that of the recent assemblage of the western-central part of the sea, amounting to 38 species. The assemblage is mainly represented by marine neritic species. Deepwater taxa also occur, but their proportion does not exceed 40%. The most abundant are *C. tumefactum* (up to 20%), *R. mirabilis* (up to 50%), *Sarsicytheridea punctillata (*up to 50%), and *Polycope* spp. (up to 50%). The increase in the proportion of shallow-water taxa is most likely due to ice-rafting, which may indicate that during the Late Holocene the Laptev Sea ice coverage was more extensive than in the previous warmer period of the Early–Middle Holocene. According to Dem'yankov, numerous tests of *C. teretis* and planktonic foraminifers were found among foraminifers in the samples.

Conclusions. On the western continental slope, the environment in the Late Pleistocene was most probably characterized by cold bottom waters with low nutrient content, high sedimentation rates, and a high supply of plant debris. Numerous records of the foraminifer *Cassidulina teretis* show that the Atlantic waters reached the western Laptev Sea continental slope already at 15.8 cal. ka BP. In 15.8–13.8 cal. ka BP, a polynya was probably formed at the core site because of the close proximity of paleocoast and winds from the continent. This assumption is additionally supported by the presence of abundant planktonic foraminifers in the samples. The sediments accumulated during a time period of 13.8–11.6 cal. ka BP contain species of different ecological preferences, including shallow- and brackish-water species, which indicate a considerable freshwater influence and ice-rafting. Around 11.1 cal. ka BP a sharp decrease in sedimentation rates occurred that was due to the onset of shelf flooding. Sediments that date back to 11.1–6.5 cal. ka BP (assemblage 4) contain only marine species, which are dominated by North Atlantic species. This most likely reflects an increase in the inflow of Atlantic waters at this time. Since 6.5 cal. ka BP modernlike environments have established, the assemblage is dominated by shallow-water taxa. This fact may be attributed to active ice-rafting and probably reflects an increase in ice coverage of the Laptev Sea during this time period.

CHAPTER 5. SYSTEMATIC PALEONTOLOGY

We follow the supragenetic taxonomy and the morphological terminology provided by Nikolaeva (Nikolaeva, 1989a; Nikolaeva et al., 1989) and Athersuch (1989). In descriptions the following size groups are used: small (0.3–0.4 mm), medium (0.4–0.6 mm), and large (more than 0.6 mm). The geographical distribution of fossil and modern ostracodes are considered separately here. By modern ostracodes we mean all ostracodes found in surface sediments, not necessarily living ones.

CLASS OSTRACODA LATREILLE, 1806

SUBCLASS PODOCOPA G.O. SARS, 1866

Order Podocopida G.O. Sars, 1866

Family Bythocytheridae G.O. Sars, 1926

Subfamily Bythocytherinae G.O. Sars, 1926

Genus *Pseudocythere* G.O. Sars, 1866

Pseudocythere: G.O. Sars, 1866, p. 88; Brady, 1868b, p. 453; Brady et al., 1874, p. 209; Brady, 1880, p. 144; G.O. Sars, 1928, p. 238; Wagner, 1957, p. 35; Kashevarova et al., 1960, p. 408; Sylvester-Bradley and Kesling, 1961, p. 268; Schornikov, 1981, p. 106; Athersuch et al., 1989, p. 254; Nikolaeva et al., 1989, p. 121.

Type species. *P. caudata* G.O. Sars, 1866; Recent; nearshore waters of Norway; by monotypy.

Diagnosis. Carapace small, ovate-triangular or ovate-rectangular, strongly beveled in posteroventral region, possesses caudal process that extends dorsal margin. Valves unequal, right valve overlaps left valve in anterior third. Surface smooth, in posteroventral region it commonly bears spine. Eye tubercule absent. Five ovate elongated muscle scars in anteroventral part of valve form row that is gently curved and parallel to

Plate 1

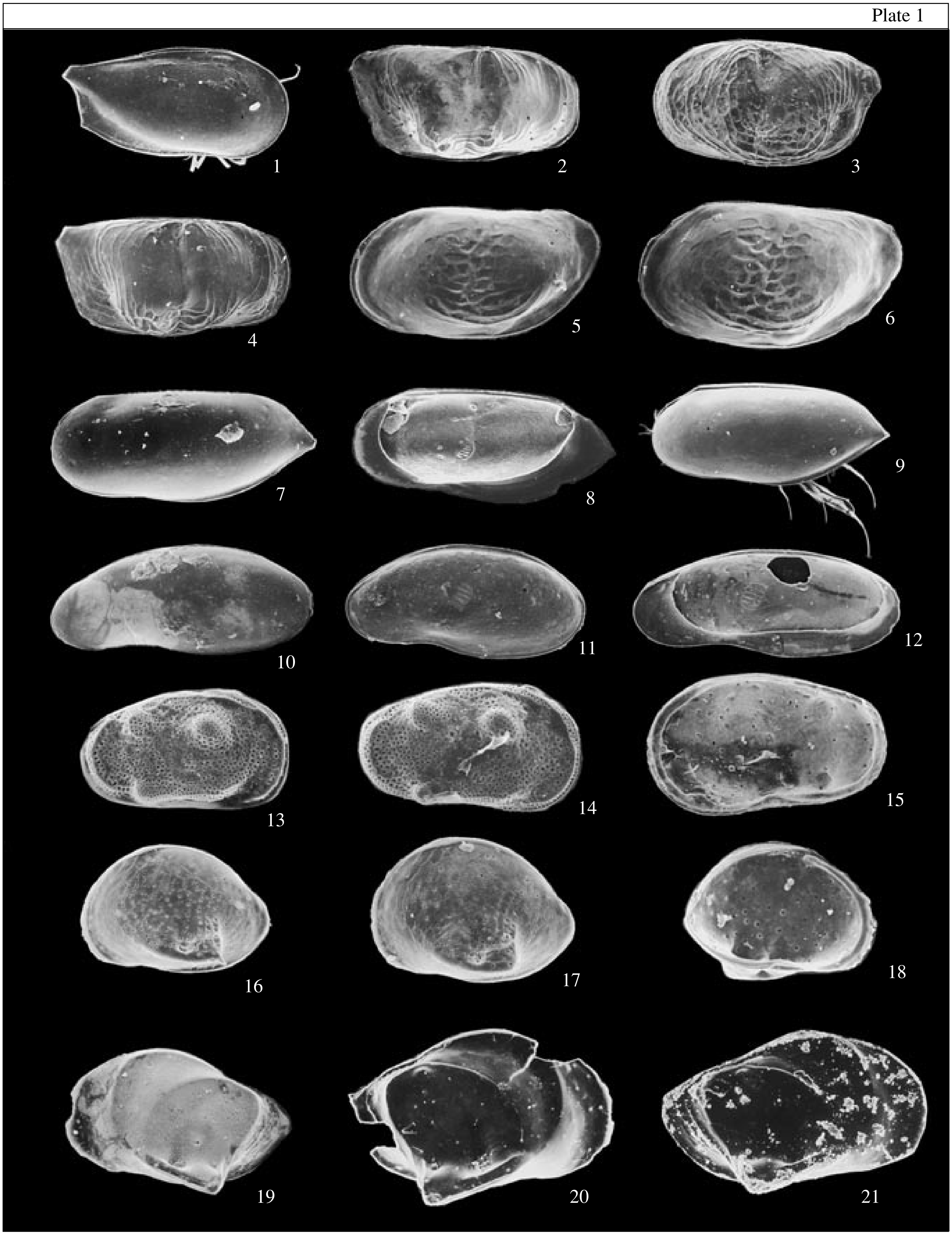

anterior margin. Hinge adont: in left valve, tapering rim; in right valve, narrow groove.

Taxonomic composition. About 30 species.

Comparison. The genus differs from *Loxocauda* Schornikov, 1969 (Miocene–Recent), which is similar in carapace lateral outline and size, in the absence of a slight concavity on the dorsal margin in front of the caudal process. Muscle scars are also different: carapaces of *Loxocauda* bear smaller muscle scars, and the row they form is oblique and subparallel to the posterodorsal margin and consists of four (not five) scars.

Remarks. According to Schornikov (1981), there are only five modern species belonging to this genus, since the rest should be attributed to other genera. Schornikov also supposed that there are many as yet undescribed species of this worldwide genus. He noted that very low morphological variability of carapaces of this genus makes their paleontological identification to species level almost impossible.

Stratigraphical range. Maastrichtian–Recent; marine deposits worldwide.

Pseudocythere caudata G.O. Sars, 1866

Plate 1, fig. 1

Pseudocythere caudata: G.O. Sars, 1866, p. 88; Brady, 1868b, p. 453, pl. 34, figs. 49–52, pl. 41, fig. 6; G.O. Sars, 1928, p. 239, pl. 109, fig. 2; Elofson, 1941, p. 336; 1969, p. 110; Wagner, 1957, p. 35, pl. 12; Kashevarova et al., 1960, p. 408, text-fig. 1218; Sylvester-Bradley and Kesling, 1961, fig. 195, 5; Neale, 1967, fig. 5(e, f, g, h, i); Joy and Clark, 1977, p. 137, pl. 1, figs. 1–3; Lev, 1983, pl. 18, fig. 16; Hao, 1988, pl. 42, figs. 4, 5; Athersuch et al., 1989, p. 255, fig. 108; Nikolaeva et al., 1989, p. 121, text-figs. 149, 150; Whatley et al., 1996, pl. 1, figs. 10, 12; Whatley et al., 1998, pl. 1, figs. 8, 9; Didié and Bauch, 2001, pl. 1, fig. 20; Stepanova et al., 2003, pl. 1, fig. 4.

Type material. G.O. Sars (1866) described this species from recent bottom surface sediments of nearshore waters of Norway. The current location of the type material is unknown. This species has not been revised; holotype and lectotype have not been designated.

Description. The carapace is small, ovate-rectangular in lateral view, with flattened dorsal, ventral, anterior, and posterior margins. The dorsal margin is nearly straight and short. It gradually passes into an evenly rounded anterior margin. The ventral margin is slightly concave in the anterior third, with a spine on the junction with the posterior margin. The anterior margin is evenly and arcuately rounded. The posterior margin is caudate. The caudal process lengthens the dorsal margin, is tubiform and subvertically cut off. The zone of marginal pore canals is relatively narrow. The greatest length is situated at the level of the caudal process extremity, and the greatest height is at the anterior hinge edge.

Dimensions in mm:

Specimen, no.	L	H
292/177	0.49	0.22

from here on the maximum length and maximum height are denoted by L and H, respectively.

Comparison. *P. caudata* differs from *P. britannica* Horne, 1986, which inhabits waters off Great Britain and is of similar size and with similar lateral carapace outline (Athersuch et al., 1989, p. 256, fig. 109), in possessing a longer carapace and narrower zone of marginal pore canals.

Variability. Carapaces may differ slightly in their height.

Remarks. This species was previously considered to be cosmopolitan (Sars, 1928). Neale (1967) accomplished a thorough study of this species from different localities, and discovered that there are at least two species, one of which is distributed in the northern Hemisphere, and the other in Antarctic waters. He noted that paleontological identification of these species is impossible. We believe that this species needs revision with additional study of soft parts.

Fossil distribution. Pliocene of the Yenisei River basin (Turukhan district); Quaternary of the Okinawa

---

Explanation of Plate 1

Fig. 1. *Pseudocythere caudata* Sars, 1866: carapace, lateral view, no. 292/177, ×83, recent surface sediments of the western Laptev Sea.

Figs. 2–4. *Bythocythere constricta* Sars, 1926: (2) right valve, external view, no. 292/169, ×74; (3) left valve, external view, no. 292/190, ×55; (4) right valve, external view, no. 292/181, ×55; recent surface sediments of the western Laptev Sea.

Figs. 5 and 6. *Bythocythere* sp. 1: (5) left valve, external view, no. 292/233, ×120; (6) carapace, lateral view, no. 292/232, ×130, Late Pleistocene of the western Laptev Sea.

Figs. 7–9. *Jonesia acuminata* (Sars, 1866): (7) left valve, external view, no. 292/51, ×40; (8) right valve, internal view, no. 292/52, ×40; (9) carapace, lateral view, no. 292/163, ×40; Holocene and recent surface sediments of the Laptev Sea.

Figs. 10–12. *Sclerochilus* sp. 1: (10) left valve, external view, no. 292/18, ×70; (11) right valve, internal view, no. 292/19, ×75; (12) right valve, internal view, no. 292/188, ×65; Holocene and recent surface sediments of the Laptev Sea.

Figs. 13–15. *Cluthia cluthae* (Brady, Crosskey et Robertson, 1874): (13) right valve, external view, no. 292/41, ×112; (14) right valve, external view, no. 292/42, ×120; (15) right valve, internal view, no. 292/74, ×100; Holocene and recent surface sediments of the Laptev Sea.

Figs. 16–18. *Cytheropteron arcuatum* Brady, Crosskey et Robertson, 1874: (16) left valve, external view, no. 292/77, ×140; (17) left valve, external view, no. 292/78, ×97; (18) right valve, internal view, no. 292/79, ×115; recent surface sediments of the western Laptev Sea.

Figs. 19–21. *Cytheropteron biconvexa* Whatley et Masson, 1979: (19) left valve, external view, no. 292/76, ×100; (20) right valve, external view, no. 292/262, ×130; (21) right valve, external view, no. 292/265, ×130; recent surface sediments of the western Laptev Sea.

Trough; Pleistocene of Scotland and Ireland; and Holocene of northwestern Europe.

Modern distribution. North Atlantic: waters off Great Britain, Ireland, Greenland, Franz Josef Land, Norway, and the Bay of Biscay; the Barents, Kara, Laptev, and East Siberian seas; the straits of the Canadian Arctic Archipelago, the Gulf of Alaska, Beaufort Sea, Frobisher Bay, and Hudson Bay; and the Mediterranean Sea, waters surrounding the Island of Capri.

Material. Four carapaces and three valves of good preservation from the Holocene and recent surface sediments of the western Laptev Sea.

Genus *Bythocythere* G.O. Sars, 1866

Bythocythere: G.O. Sars, 1866, p. 82; Brady, 1868b, p. 450; Brady et al., 1874, p. 207; Brady, 1880, p. 141; G.O. Sars, 1928, p. 233; Kashevarova et al., 1960, p. 409; Sylvester-Bradley and Kesling, 1961, p. 268; Swain, 1963, p. 828; Athersuch et al., 1983, p. 71; Athersuch et al., 1989, p. 241; Nikolaeva et al., 1989, p. 120.

Type species. *B. turgida* G.O. Sars, 1866; Recent; Norway; designated by Brady and Norman (1889).

Diagnosis. Carapace medium to large, ovate-rectangular in lateral view, with flattened posteroventral margin and obtuse caudal process. Valves equal. Surface smooth, punctate, wrinkled, or with fossae. Alate extension or lateral inflation usually occurs just above ventral margin. Eye tubercule absent. Five elongated adductor muscle scars form subvertical or slightly posteriorly inclined row. One more muscle scar located separately just above row, two more scars occur in front of adductor scars. Hinge lophodont: in left valve, bar with small sockets on its edges; right valve, complementary.

Taxonomic composition. More than 200 species.

Comparison. The genus differs from *Bythoceratina* Hornibrook, 1952 (Upper Cretaceous–Recent), which is similar in lateral outline, sculpture, and size, in the hinge construction: the hinge of *Bythoceratina* has dentate median elements and that of *Bythocythere* has smooth ones.

Stratigraphical range. Oligocene–Recent; marine deposits worldwide.

Bythocythere constricta G.O. Sars, 1866

Plate 1, figs. 2–4

Bythocythere constricta: G.O. Sars, 1866, p. 85; Brady et al., 1874, p. 208, pl. 16, figs. 9, 10; G.O. Sars, 1928, p. 235, pl. 108, fig. 1; Elofson, 1941, p. 335; Caralp et al., 1967, pl. 13, fig. 4; Elofson, 1969, p. 108; Neale and Howe, 1975, pl. 4, fig. 4; Lord, 1980, pl. 2, figs. 17–19; Lev, 1983, pl. 18, fig. 15; Stepanova et al., 2003, pl. 1, figs. 1–3.

Bythocythere montrosiense: Akatova, 1946, p. 229, text-fig. 8.

Bythocythere sp. aff. *constricta*: Athersuch et al., 1983, p. 78, pl. 2, figs. 12–14.

Bythocythere bicristata: Kupriyanova, 1999, pl. 1, fig. 8.

Type material. G.O. Sars (1866) described this species from recent bottom surface sediments of Oslo fjord, Norway. The location of the type material is currently unknown. This species has not been revised, and holotype and lectotype have not been designated.

Description. The carapace is medium to large, ovate-rectangular in lateral view. The dorsal margin is straight. It passes into the anterior margin through an obtuse (smoothed) cardinal angle. The ventral margin is almost straight, subparallel to the dorsal margin, and slightly concave in the anterior third. The anterior margin is flattened and evenly arcuately rounded. The posterior margin is also flattened, caudate. The caudal process extends the dorsal margin and has an obtuse-angled shape, gently beveled ventrally, where it is broadly evenly rounded. Dorsally, the caudal process is slightly concave. The greatest length is situated at the level of the base of the caudal process; and the greatest height, at the anterior hinge termination. The central part of the valve is strongly inflated, y-shaped, with a broad subvertical sulcus. The lower part of the swelling slightly overhangs the ventral margin. There are fine ribs along the valve margins and a y-shaped swelling contours them. The ribs fuse to form fossae. The central part of the valve and termination of the caudal process are smooth.

Dimensions in mm:

Specimen, no.	L	H
292/181	0.61	0.27
292/185	0.7	0.31
292/189	0.72	0.29

Comparison. This species differs from *B. bicristata* Brady et Norman, 1889 (p. 222, pl. 19, figs. 15, 16), inhabiting waters off Scotland, and of similar size and surface sculpture, in the shape of the posteroventral margin: in *B. bicristata* it is gently beveled and forms a continuous arch with ventral margin, while in *B. constricta* the ventral margin passes into the posterior through an obtuse angle.

Variability. Reticulation may vary in its degree: sometimes fossae are not developed on the caudal process and in the central part of the valve.

Remarks. Illustrations of *B. constricta* given in Brady (1868b, p. 451, pl. 35, figs. 47–52) do not correspond to its description. Illustrated specimens have smooth, not sculptured surface and a more smoothed lateral carapace outline.

Kupriyanova (1999, pl. 1, fig. 8) illustrated a specimen which she referred to *Bythocythere bicristata* Brady et Norman, 1889. In our opinion, it should be referred to as *B. constricta*, since its posterodorsal margin has an obtuse-angled outline typical of *B. constricta.*

Whatley et al. (1996, pl. 1, figs. 8, 9, 11), on the contrary, illustrated specimens from waters of Greenland that were identified as *B. constricta*, which needs to be referred to *B. bicristata.*

Fossil distribution. Quaternary of the North Sea; Pliocene–Pleistocene deposits of the Pechora Sea, southwestern part of the Pai-Khoi (tributary of the Karataikha River); Pleistocene of Norway; and Holocene of the Bay of Biscay and the Kara and western Laptev seas.

Modern distribution. The Bay of Biscay; Oslo Fjord; waters off Norway; Greenland; Barents Sea; waters off Novaya Zemlya; and the Kara, Laptev, and Beaufort seas.

Material. Fifteen adult valves, four juvenile valves, and five carapaces of good preservation from the Holocene and recent bottom surface sediments of the western Laptev Sea.

Bythocythere sp. 1

Plate 1, figs. 5, 6

Description. The carapace is small, thin-shelled, and ovate-rectangular in lateral view. The dorsal margin is straight. It passes into the anterior margin through an obtuse smoothed cardinal angle. The ventral margin is almost straight and subparallel to the dorsal margin. The anterior margin is flattened and evenly arcuately rounded. The posterior margin is also flattened, caudate, gently beveled ventrally, and broadly evenly rounded in its lower part. The caudal process extends the dorsal margin and has an obtuse subtriangular-rounded form. The greatest length is situated at the level of the caudal process extremity; and the greatest height, in the center of valve. The central part of the valve is strongly inflated, biconvex, y-shaped, and with a subvertical sulcus. Rare fine ribs are parallel to valve margins. They partly join and form fossae. The central part of the valve bears fossae of irregular shape with more solid muri. Above the ventral margin these muri join and form several short ribs. They outline a y-shaped swelling.

Dimensions in mm:

Specimen, no.	L	H
292/232	0.32	0.19

Comparison. This species is distinguished from *B. constricta*, which resembles *Bythocythere* sp. 1 in carapace lateral outline, by its considerably smaller size and less developed surface ornamentation.

Remarks. This form is most likely a new species. However, for its description more representative material is needed. It is also possible that the specimens we attributed to this form are juveniles. However, they differ considerably from juvenile valves of *B. constricta.*

Fossil distribution. Upper Pleistocene–Holocene of the western Laptev Sea.

Modern distribution. Kara Sea.

Material. Forty-six valves of good preservation, Pleistocene–Holocene deposits of the western Laptev Sea.

Genus *Jonesia* Brady, 1866

Jonesia: Brady, 1866, p. 363; Kashevarova et al., 1960, p. 408; Sylvester-Bradley and Kesling, 1961, p. 268; Schornikov, 1980, p. 1124; 1981, p. 99; Athersuch et al., 1989, p. 251.

Macrocythere: G.O. Sars, 1928, p. 240.

Type species. *Cythere simplex* Norman, 1865; Recent; waters off Great Britain; designated by Van den Bold (1946).

Diagnosis. Carapace large, ovate-elongated in lateral view, caudate. Caudal process acuminate. Valves equal. Surface smooth. Eye tubercule absent. Five elongated adductor muscle scars form subvertical or slightly posteriorly inclined row. Another muscle scar is located separately just above the row, two more scars occur in front of adductor scars. Hinge lophodont, weakly developed, with reduced terminal elements. Median bar of left valve more prominent on its edges than in central part.

Taxonomic composition. About 15 species.

Comparison. From *Kurilocythere* Schornikov, 1981 (Recent, Kuriles), which is similar in lateral outline and size, the genus differs in the posterior margin shape: it is caudate in *Jonesia* and broadly evenly rounded in *Kurilocythere.*

Stratigraphical range. Paleogene–Recent; northern Hemisphere.

Jonesia acuminata (G.O. Sars, 1866)

Plate 1, figs. 7–9

Cythere simplex: Norman, 1865b, p. 17, pl. 5, figs. 1–4.

Bythocythere acuminata: G.O. Sars, 1866, p. 86.

Bythocythere simplex: Brady, 1868b, p. 450, pl. 33, figs. 23–27, pl. 40, fig. 8; Brady et al., 1874, p. 208, pl. 7, figs. 20, 21; Brady and Norman, 1889, p. 224, pl. 23, fig. 9.

Macrocythere simplex: G.O. Sars, 1928, p. 241, pl. 110; Elofson, 1969, p. 111.

Jonesia simplex: Kashevarova et al., 1960, text-fig. 1220; Rosenfeld, 1977, p. 38, pl. 10, figs. 125, 126; Lord, 1980, pl. 3, figs. 12, 13; Schornikov, 1980, p. 1125, text-figs. 1, 1–6, figs. 2, 1, 5–8; Cronin, 1981, p. 408, pl. 3, fig. 10.

Jonesia acuminata: Sylvester-Bradley and Kesling, 1961, fig. 196, 1; Athersuch et al., 1989, p. 252, fig. 107; Stepanova et al., 2003, pl. 1, fig. 6.

Type material. In the collection of G.O. Sars type material was not preserved, it originated from Norway, Lofoten Islands.

Description. The carapace is large and ovate-elongated in lateral view. The dorsal margin is straight. It gradually passes into the anterior and posterior margins through obtuse cardinal angles. The ventral margin is convex: more convex in the posterior part of valve, slightly concave in the anterior third, and gradually passes into the anterior and posterior margins. The anterior margin is evenly arcuately rounded, slightly beveled from the dorsal side. The posterior margin bears an acuminate caudal process at mid-height, which is gently beveled in the posteroventral part. The greatest length is situated at the level of the caudal process extremity; and the greatest height, in the posterior third of valve. The surface is smooth.

Dimensions in mm:

Specimen, no.	L	H
292/51	1.1	0.5
292/52	1.15	0.5

Comparison. From *J. marecorallinensis* Correge, 1992, inhabiting the Coral Sea (Australia) (Correge, 1992, pp. 103–106), similar in carapace size and outline, this species differs in having less prominent ventral margin outline in its posterior part. Caudal process of *J. acuminata* is located at mid-height of the posterior margin, while in *J. marecorallinensis* it extends the dorsal margin.

Variability. Carapaces may slightly vary in height in the posterior half of the valve, these variations are most likely due to sexual dimorphism.

Remarks. Norman (1865) described *Cythere simplex.* Later, G.O. Sars (1866) described the same form as *Bythocythere acuminata.* The name given by Norman was shown to be preoccupied, since it had been previously given to another species: *Cythere auriculata* var. *simplex* Cornuel 1848, hence the precedence of the name *Bythocythere acuminata.* Norman's Type material is preserved in his collection. The collection of Sars does not contain type material of this species.

Fossil distribution. Pleistocene of Scotland, Ireland, Norway, and northeastern North America (St. Lawrence Lowlands and the Champlain Sea); Holocene of the eastern Laptev Sea.

Modern distribution. Waters off Great Britain, Hebrides, Shetland Islands, Faroes, Norway, Western Greenland; the North, White, Baltic, Barents, Laptev, East Siberian, Beaufort, Baffin, and Bering seas; Norton Sound; and the straits of the Canadian Arctic Archipelago.

Material. Seven valves and six carapaces of good preservation from recent surface sediments of the Laptev Sea.

Subfamily Pseudocytherinae Schneider, 1960

Genus *Sclerochilus* G.O. Sars, 1866

Sclerochilus: G.O. Sars, 1866, p. 89; Brady, 1868b, p. 455; Brady et al., 1874, p. 211; G.O. Sars, 1928, p. 246; Wagner, 1957, p. 100; Kashevarova et al., 1960, p. 407; Sylvester-Bradley and Howe, 1961, p. 315; Rosenfeld, 1977, p. 38; Schornikov, 1981, p. 111; Athersuch et al., 1989, p. 258; Nikolaeva et al., 1989, p. 121; Schornikov, 2004, p. 60.

Type species. *Cythere contorta* Norman 1862; Recent; waters off Great Britain; by monotypy.

Diagnosis. Carapace small to large, thin-shelled, ovate-nodular in lateral outline, valves unequal: left valve slightly larger than right valve. Surface smooth. Eye tubercule absent. Five elongated muscle scars form subvertical or slightly oblique row. Hinge adont: in left valve it has tapering rim, right valve has groove.

Taxonomic composition. About 100 species.

Comparison. *Oviferochilus* Schornikov, 1981 (Recent, Kuriles), similar in carapace lateral outline and size, is distinguished from *Sclerochilus* by the more elongated and fragile carapace.

Remarks. Schornikov (1981, 2004) erected three subgenera of the genus *Sclerochilus* and described 61 new species (taking into consideration soft anatomy and carapace morphology), he supposed that there are still many undescribed species. Athersuch et al. (1989) described nine species inhabiting waters off Great Britain (taking into consideration soft anatomy and carapace morphology). Twenty-six species were described earlier by different researchers (Schornikov, 1981). As for *Pseudocythere,* specific identification of members of genus *Sclerochilus* is complicated due to the great morphological similarity of their carapaces.

Stratigraphical range. Miocene–Recent; marine sediments worldwide.

Sclerochilus sp. 1

Plate 1, figs. 10–12

Sclerochilus contortus: Stepanova et al., 2003, pl. I, fig. 5.

Description. The carapace is of medium size, ovate-nodular in lateral outline. The dorsal margin is evenly arcuately rounded, gently beveled towards the anterior and posterior margins. The ventral margin is convex, slightly concave in the anterior third. The anterior margin is evenly arcuately rounded. The posterior margin is higher than the anterior margin and evenly arcuately rounded. The greatest length is at mid-height, and the greatest height is at the valve center. The surface is smooth.

Dimensions in mm:

Specimen, no.	L	H
292/18	0.65	0.28
292/19	0.57	0.26

Comparison. From *S. oshoroensis* Hiruta, 1976, inhabiting waters of the Sea of Japan and similar in carapace lateral outline, this species differs in its larger size and less prominent dorsal margin.

Remarks. The form described above does not differ from *S. contortus* Norman in its carapace morphology. This latter species was identified from high-latitude seas by many scientists (Brady, 1868b, p. 455, pl. 34, figs. 5–10, pl. 41, fig. 7; G.O. Sars, 1928, p. 247, pl. 112; Sylvester-Bradley and Kesling, 1961, fig. 244, 4; Neale and Howe, 1975, pl. 3, fig. 7; Cronin, 1977, pl. 3, figs. 21, 22; 1981, p. 410, pl. 1, figs. 7, 8; Rosenfeld, 1977, p. 38, pl. 10, fig. 124; Cronin and Ikeya, 1987, p. 86, pl. 3, fig. 19; Athersuch et al., 1989, p. 260, fig. 110; Nikolaeva et al., 1989, p. 121, text-figs. 151, 152; Kupriyanova, 1999, pl. 2, fig. 15; Stepanova et al., 2003, pl. 1, fig. 5). However, scrutiny of the soft anatomy revealed (Schornikov, 1981, 2004; Athersuch et al., 1989) that this species is heterogeneous and cannot be identified solely according to its carapace morphology, which is why we identified this taxon only to generic level.

Stratigraphical range. Pleistocene–Holocene and recent surface sediments of the western Laptev Sea.

Material. Thirteen valves and nine carapaces of good preservation from Pleistocene–Holocene and recent surface sediments of the western Laptev Sea.

Family Leptocytheridae Hanai, 1957

Genus *Cluthia* Neale, 1973

Cluthia: Neale, 1973b, p. 683; Brouwers, 1990, p. 30.

Type species. *Cythere cluthae* Brady, Crosskey et Robertson, 1874; Recent; North Atlantic; by monotypy.

Diagnosis. Carapace small, smoothed-trapezoidal, elongated, and with marginal rim. Valves equal. Surface punctate, puncta small. Lateral surface sculptured with nodes and massive ribs. Eye tubercule absent. Four muscle scars in the mid-length of valve form subvertical row. Two central scars are bifid, and lowermost and uppermost scars have elongated ovate shape. In front of them another very large nodular scar occurs. Hinge of left valve has two terminal pits and central narrow groove, which is bounded from below with densely dentate ridge, formed by inner layer of valve itself. Right valve complementary.

Taxonomic composition. Less than 10 species.

Comparison. From *Leptocythere* G.O. Sars 1928, similar in carapace outline and size, the genus differs in the surface ornamentation pattern: carapace lateral surface of members of *Cluthia* bears massive sculpture elements (nodes and ribs), while carapaces of *Leptocythere* usually lack such sculpture. Carapace outline is also slightly different: carapaces of *Cluthia* have a trapezoidal lateral outline and a posterior margin that is considerably lower than the anterior margin, while carapaces of *Leptocythere* have a smoothed rectangular outline and the posterior and anterior margins of similar height.

Stratigraphical range. Pleistocene–Recent; northern Hemisphere, high latitudes.

Cluthia cluthae (Brady, Crosskey et Robertson, 1874)

Plate 1, figs. 13–15

Cythere cluthae: Brady et al., 1874, p. 153, pl. 13, figs. 16, 17; Brady and Norman, 1889, p. 145, pl. 14, figs. 25–27, pl. 17, figs. 35, 36.

Leptocythere cluthae: Caralp et al., 1967, pl. 13, fig. 6.

Cluthia cluthae: Neale, 1973b, p. 684, pl. 1, figs. 1–11, text-fig. 1; Lord, 1980, pl. 3, figs. 18, 19; Benson et al., 1983, pl. 1, figs. 3, 4; Lev, 1983, p. 121, pl. 9, fig. 13; Cronin, 1989, pl. 2, fig. 4; Brouwers, 1990, p. 30, pl. 7, fig. 15, pl. 10, figs. 3–10, pl. 11, fig. 1; Lord et al., 1993, pl. 3, fig. 8; Whatley et al., 1996, pl. 3, figs. 17, 18; Ingram, 1998, pl. 1, fig. 13; Whatley et al., 1998, pl. 3, figs. 7, 8; Kupriyanova, 1999, pl. 2, fig. 14; Brouwers et al., 2000, p. 128, figs. 1, 2, 12 (C, D); Stepanova et al., 2003, pl. 1, figs. 9, 10.

Type material. The description of this species by G.S. Brady et al. (1874) was based on material from the Pleistocene deposits of Errol, Scotland. However, Brady's collection at the Hancock Museum in Newcastle (United Kingdom) contains only specimens from other locations: slide 1.08.34, cape Frazer (Arctic), depth 92 m; slide 1.08.35, Loch Fyne, depth 37 m (L. Jessop, personal communication, 2005).

Description. The carapace is small, smoothed-trapezoidal in lateral view, with a flattened anterior margin. The dorsal margin is straight or slightly convex. It passes into the anterior and posterior margins through obtuse cardinal angles. The ventral margin is concave in the central part. The anterior margin is arcuately rounded and slightly beveled from the dorsal side. The posterior margin is lower than the anterior margin and arcuately rounded. The greatest length is situated at mid-height; the greatest height, at the anterior hinge edge. A well-developed massive rib runs parallel to the ventral margin: it starts close to the anterior margin of the valve, gradually becomes more convex, and ends short of the posterior margin. The dorsal part of the valve contains two massive nodes; they are developed just above terminations of the ventral rib. The anterior node is larger and is located slightly lower than the posterior node, which is closer to the dorsal margin and can slightly project beyond the valve outline. One fine rib runs parallel to the dorsal margin; it starts in the posterior third of the valve and reaches the upper third of the anterior margin. The whole surface is evenly densely punctate.

Dimensions in mm:

Specimen, no.	L	H
292/42	0.33	0.18
292/41	0.33	0.17
292/40	0.34	0.18

Comparison. *C. cluthae* resembles *C. foresteri* Brouwers, 1990 (p. 31, pl. 10, figs. 11–15, pl. 11, fig. 2) from the Pleistocene deposits of Honshu Island and Pleistocene–Holocene deposits of the Gulf of Alaska in carapace outline and size, but differs in having a massive ventral rib, nodes on the dorsal side, and a densely punctate rather than finely reticulate surface of the carapace.

Variability. Specimens shown by Neale (1973b) have several fine ribs under the ventral rib. On the posterior margin they split into two or three ribs and stretch subvertically upwards to reach the dorsal margin of the valve. One of these ribs joins the posterior termination of the ventral rib and the posterior node on the dorsal side. Despite the doubtless affiliation to the same species, our specimens do not bear these ribs.

Fossil distribution. Upper Pliocene of Alaska; Pliocene–Lower Pleistocene of the lower Ob, lower Pechora, and lower Yenisei rivers; Pliocene–Holocene of Japan and the eastern part of the Gulf of Alaska; Quaternary of Scotland and the Pechora Sea; Pleistocene of Great Britain, North Sea, northern Germany, Denmark, Norway, Novaya Zemlya, Agapa, Franz Josef Land, Spitsbergen, and Greenland; Pleistocene–Holocene of the North Atlantic, Bering Sea, Cook Inlet, Kodiak shelf, Gulf of Alaska, northeastern North America (Goldthwait Sea, Quebec); and Holocene of the Bay of Biscay and the eastern Kara and Laptev seas.

Modern distribution. North Atlantic, waters surrounding Nova Scotia, English channel, Bay of Biscay, waters surrounding Finland, Greenland, Great Britain, Ireland, Franz Josef Land, Spitsbergen, Novaya Zemlya, and Norway; the Norwegian, Barents, Kara, Bering, Beaufort, and Laptev seas; waters surrounding Alaska, Cook Inlet (Alaska), Gulf of Maine, Hudson Bay, Norton Sound, Labrador Sea, and waters off Newfoundland.

Material. Ninety-one valves and 67 carapaces of good preservation from the Pleistocene and recent surface sediments of the Laptev Sea.

Family Cytheruridae G. Müller, 1894

Genus *Cytheropteron* G.O. Sars, 1866

Cytheropteron: G.O. Sars, 1866, p. 79; Brady, 1868b, p. 447; Brady et al., 1874, p. 201; Brady, 1880, p. 135; G.O. Sars, 1928, p. 223; Elofson, 1941, p. 313; Wagner, 1957, p. 89; Kashevarova et al., 1960, p. 404; Reyment et al., 1961, p. 292; Swain, 1963, p. 816; Whatley and Masson, 1979, pp. 224, 225; Lev, 1983, p. 116; Athersuch et al., 1989, p. 221; Nikolaeva et al., 1989, p. 133; Stepanova et al., 2003, p. 84.

Type species. *Cythere latissima* Norman, 1865; Recent, North Atlantic, designated by Brady and Norman (1889).

Diagnosis. Carapace small to medium, ovate-subrhomboidal or triangular in lateral view. Commonly, it possesses caudal process upturned towards dorsal margin and winglike lateral process, variable in size and shape. Valves are unequal, right valve overlaps left valve dorsally. Surface smooth, punctate, reticulate, it may bear weak ribs, tubercules or be wrinkled. Alate extension may terminate in spine. Eye tubercule absent. Usually, four elongated ovate muscle scars form subvertical row at midlength of valve, just above ventral margin. Hinge antimerodont, tripartite, consists of different elements, and has bar in left valve, in right valve with two terminal dentate hinge bars and median crenulate groove, left valve complementary.

Taxonomic composition. More than 200 species.

Comparison. From *Konarocythere* Krutak, 1961 (Upper Paleocene–Miocene of Eurasia and North America), which is similar in outline and size, the genus differs in the presence of a lateral winglike process and hinge construction: members of *Cytheropteron* have an antimerodont hinge, with a bar in the left valve, on the contrary, members of *Konarocythere* have a holomerodont hinge with a bar in the right valve.

Stratigraphical range. Lower Jurassic–Recent, marine deposits worldwide.

Cytheropteron arcuatum Brady, Crosskey et Robertson, 1874

Plate 1, figs. 16–18

Cytheropteron arcuatum: Brady et al., 1874, p. 203, pl. 8, figs. 16–18; pl. 14, fig. 19–22; Brady and Norman, 1889, p. 213, pl. 20, figs. 28–30; Whatley and Masson, 1979, p. 229, pl. 1, figs. 1–5; Lord, 1980, pl. 2, figs. 13–15; Cronin, 1981, p. 402, pl. 7, fig. 1; Lev, 1983, p. 117, pl. 11, fig. 6; Cronin, 1989, pl. 5, fig. 12; Whatley et al., 1996, pl. 1, fig. 16; Kupriyanova, 1999, pl. 2, fig. 10; Didié and Bauch, 2001, pl. 2, figs. 7, 8; Stepanova et al., 2003, pl. 2, figs. 13, 14; Stepanova et al., 2004, pl. 1, figs. 1, 2.

Type material. Collection of G.S. Brady at the Hancock Museum in Newcastle, slide 1.03.30, Scotland, Errol; Pleistocene.

Description. The carapace is small, subtriangular in lateral view, with flattened anterior and posterior margins. The dorsal margin is strongly convex, gradually passing into the anterior margin through an obtuse cardinal angle, and into the posterior margin through a slight concavity. The ventral margin is straight, slightly concave in the anterior third. The anterior margin is arcuately rounded. The posterior margin is lower than the anterior, caudate, and upturned towards the dorsal margin. The greatest length is situated at mid-height, and the greatest height is at the center of the valve. A well-developed winglike process with a rounded anterior edge and a subvertical posterior edge is located above the ventral margin. The alate extremity terminates in a spine; a round punctum occurs in the central part of the alate extension. The surface is pierced by pore canals aligned in subvertical rows forming a streamlike pattern. Fine ribs form weakly developed fossae on the anterior and posterior margins.

Dimensions in mm:

Specimen, no.	L	H
292/77	0.29	0.20
292/78	0.35	0.21
292/79	0.28	0.18

Comparison. *C. arcuatum* differs from *C. foresteri* Brouwers, 1994 from the Pleistocene–Holocene deposits of the Gulf of Alaska (Brouwers, 1994, pl. 24, pl. 17, figs. 13–18, pl. 18, figs. 2, 3, 6, pl. 19, figs. 1–4, pl. 20, figs. 10, 11, 22, 23) in the more convex dorsal margin, the absence of two nodes on the dorsal side, and in the smaller pore puncta that form a streamlike pattern.

Variability is insignificant. Carapaces may differ in height. Weak ornamentation of the margins varies from fine ribs to nearly smooth surface.

Fossil distribution. Neogene–Quaternary marine sediments of the lower Severnaya Dvina, lower Yenisei, lower Ob, and lower Pechora rivers, and Novaya Zemlya; Pleistocene of Scotland, Ireland, Norway, North and Laptev seas, northeastern North America (St. Lawrence Lowlands, Champlain Sea, coastal Maine, Boston "blue clay," and western Goldthwait Sea of Quebec); and Holocene of the eastern Kara and Laptev seas.

Modern distribution. Waters off Norway, Greenland, and the Barents, Kara, Laptev, East Siberian, Beaufort, and Baffin seas; and the Gulf of Alaska and Frobisher Bay.

Material. One hundred and thirty-four valves and 32 carapaces of good preservation, Pleistocene–Holocene and recent surface sediments of the Laptev Sea.

Cytheropteron biconvexa Whatley et Masson, 1979

Plate 1, figs. 19–21

Cytheropteron biconvexa: Whatley and Masson, 1979, p. 229, pl. 3, figs. 5, 10, 14–16, 18–20; Cronin, 1989, pl. 5, figs. 5, 6; Lord et al., 1993, pl. 3, fig. 4; Kupriyanova, 1999, pl. 2, fig. 5; Stepanova et al., 2003, pl. 2, figs. 7, 8; Stepanova et al., 2004, p. 86, pl. 1, figs. 3, 4.

Cytheropteron sp. A: Lord, 1980, pl. 2, figs. 20–22.

Holotype. Natural History Museum, London, OS 10800, adult left valve, borehole, Forties Field, North Sea, Lat. 57°43′54.5″ N, Long. 00°58′25.5″ W, type level 5 m depth in borehole; Pleistocene.

Description. The carapace is small and fragile, subtriangular in lateral view. The dorsal margin is slightly arched, gently beveled towards the anterior and posterior margins. The ventral margin is straight, slightly concave in the anterior third. The anterior margin is flattened, arcuate and evenly rounded. The posterior margin is also flattened, caudate, upturned towards the dorsal margin. The caudal process is convex in the posterodorsal part and straight or slightly concave in the posteroventral part. The greatest length is situated at mid-height; the greatest height, in the center of valve. The alate process with a rounded anterior edge and a subvertical posterior edge is located above the ventral margin. Two round puncta occur at the base of the alate extension close to its edges. The lateral valve surface bears two fine looplike ribs. The first rib stretches in a broad arc from the mid-dorsal point through the lateral surface and ends at the base of the anterior edge of the ala. The second rib forms an upward convex loop; its ends reach the anterior and posterior edges of the ala. This rib nearly touches the dorsal margin. A distinct fine rib runs along the anterior edge of the ala; the second fine rib, less distinct, extends along its posterior edge. The lateral valve surface between the ribs is smooth. Several weak subvertical streamlike ribs occur on the posterior margin.

Dimensions in mm:

Specimen, no.	L	H
292/76	0.40	0.23
292/262	0.36	0.22

Comparison. *C. biconvexa* differs from *C. inornatum* Brady and Robertson, 1872, which is similar in outline, in the number of fine ribs on the lateral surface (two instead of three) and their pattern.

Variability. Carapaces differ slightly in height in the center due to variations in convexity of the dorsal margin. In addition, the height of the posterior margin varies slightly.

Remarks. Specimens of this species from the Quaternary deposits of the western Russian Arctic are housed in VNIIOkeangeologia (St. Petersburg), collection of Lev. She did not identify them to species level.

Fossil distribution. Pleistocene of the North Sea, Northern Ireland, Norway, northeastern North America (Goldthwait Sea in Quebec); Pleistocene–Holocene of the Pechora and Laptev seas; and the Holocene of the eastern Kara Sea.

Modern distribution. Waters off northeastern Greenland, the western Laptev and Beaufort seas, the straits of the Canadian Arctic Archipelago, the Gulf of Alaska, and Frobisher Bay.

Material. Twenty-one valves and 4 carapaces of good preservation, Pleistocene–Holocene and recent surface sediments of the Laptev Sea.

Cytheropteron champlainum Cronin, 1981

Plate 2, figs. 1, 2

Cytheropteron champlainum: Cronin, 1981, p. 404, pl. 8, figs. 7, 8; 1989, pl. 4, fig. 7; Brouwers, 1994, p. 17, pl. 17, figs. 1–6; Stepanova et al., 2003, pl. 2, fig. 2; Stepanova et al., 2004, p. 87, pl. 1, figs. 5, 6.

Cytheropteron tarrensis: Brouwers, 1994, p. 36, pl. 21, fig. 1; pl. 22, figs. 4–10, 25.

Holotype. US National Museum (USNM), Department of Paleobiology, USNM311142, female right valve; Canada, Ontario, 5.6 km N of Kars, west side of road, north end of gravel pit; Pleistocene.

Description. The carapace is of medium size, trapezoidal in lateral view. The dorsal margin is arcuately convex, gently beveled towards the anterior and posterior margins. The ventral margin is straight, slightly concave in the anterior third. The anterior margin is arcuate and evenly rounded. The posterior margin is lower than the anterior, caudate, flattened, upturned towards the dorsal margin. The greatest length is situated at mid-height; the greatest height, in the center of the valve. A broad winglike process with a rounded edge overhangs the ventral margin. The ala is subdivided by a depression of a slightly variable size. The valve surface bears subvertical rows of puncta and fossae, or only fossae. A fine rib extends along the ala edge from the lower section of the anterior part of the valve and merges with fossae muri at the posterior part of the valve. A fine rib equal in length to the dorsal margin runs slightly below and parallel to it. Below the alate process, several fine ribs parallel to the ventral margin stretch from the anterior part of valve and eventually merge with fossae muri at the posterior part of valve. The whole valve surface, besides fossae muri, is pierced by pore canals.

Sexual dimorphism. In the original description, Cronin (1981) pointed to strong sexual dimorphism, our specimens demonstrate a similar pattern. The male carapace is higher and shorter, has a less convex dorsal

Plate 2

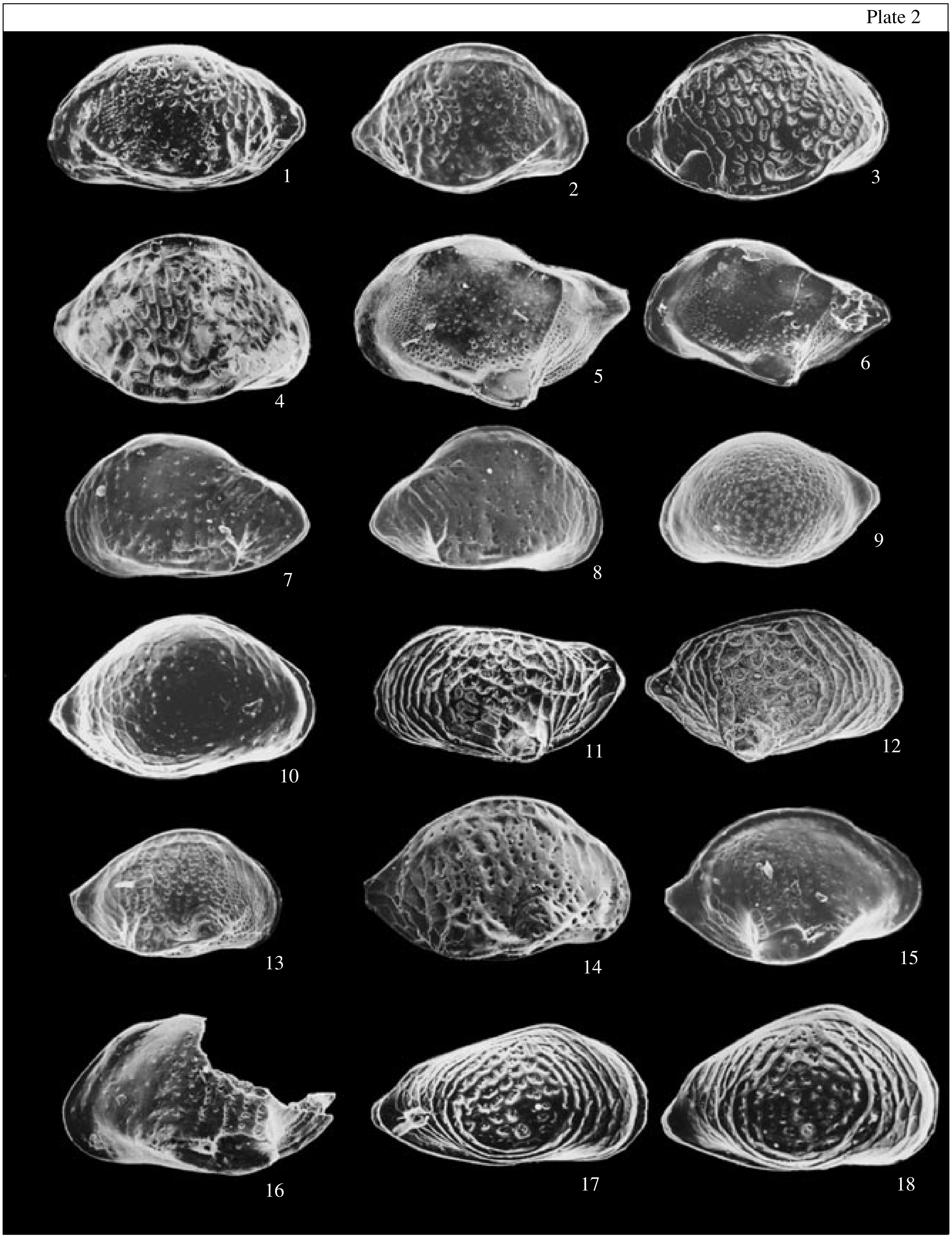

margin. Caudal process in the posterodorsal part is straight on male carapaces and slightly concave on female carapaces.

Dimensions in mm:

Specimen, no.	L	H
292/59	0.53	0.3
292/260	0.41	0.23
292/263	0.57	0.31

Variability. The degree of ornamentation development is strongly variable: from small puncta to fossae.

Comparison. *C. champlainum* Cronin, 1981 differs from *C. dimlingtonensis* Neale et Howe, 1973 in having less developed fossae and in the absence of pore puncta in fossae.

Remarks. Close examination of the published illustrations of *C. dimlingtonensis* Neale and Howe, 1973, *C. champlainum* Cronin, 1981, and *C. tarrensis* Brouwers, 1994 allowed us to include them in one group of species, since they have nearly identical shape and dimensions. Surface ornamentation within this group varies markedly, from small puncta to fossae. *Cytheropteron tarrensis* has the smoothest surface with puncta grading into elongated fossae in the posterior margin; size of puncta increases towards the posterior part of valve. We consider this species to be a synonym of *C. champlainum*, which has a similar but slightly more distinct ornament. *C. dimlingtonensis* has solely reticulate surface sculpture (Fig. 8).

Fossil distribution. Pleistocene of the Gulf of Alaska and northeastern North America (St. Lawrence Lowlands, Champlain Sea, Goldthwait Sea of Quebec, western Newfoundland, coastal Maine, Massachusetts, and Nova Scotia).

Modern distribution. Waters off Greenland, the Barents and western Laptev Sea, the straits of the Canadian Arctic Archipelago, and the Beaufort Sea.

Material. Twelve valves of good preservation, Pleistocene–Holocene deposits and recent surface sediments of the Laptev Sea.

Cytheropteron dimlingtonensis Neale et Howe, 1973

Plate 2, figs. 3, 4

Cytheropteron cf. *pyramidale*: Swain, 1961, fig. 2, N 28.

Cytheropteron pyramidale: Swain, 1963, p. 816, pl. 97, fig. 19, pl. 98, fig. 9.

Cytheropteron dimlingtonensis: Neale and Howe, 1973, p. 242, pl. 1, figs. 3, 5; Robinson, 1978, pl. 2, fig. 4; Whatley and Masson, 1979, p. 232, pl. 6, figs. 11, 13–16; Stepanova et al., 2004, p. 90, pl. 1, figs. 7, 8.

Cytheropteron champlainum: Kupriyanova, 1999, pl. 2, fig. 2.

Holotype. University of Hull; HU.50.Q.1.9, left valve; England, Yorkshire, Dimlington; Pleistocene.

Description. The carapace is of medium size, trapezoidal in lateral view. The dorsal margin is arcuately convex, gently beveled towards the anterior and posterior margins. The ventral margin is straight, slightly concave in the anterior third. The anterior margin is arcuate and evenly rounded. The posterior margin is lower than the anterior, caudate, flattened, upturned towards the dorsal margin. The greatest length is situated at mid-height; the greatest height, in the center of the valve. A broad winglike process with a rounded edge overhangs the ventral margin. The ala is subdivided by a rounded depression (about 0.03–0.02 mm). The valve surface bears distinct subvertical rows of fossae. A fine rib runs along the ala edge, extends from the lower section of the anterior part of the valve, and merges with the fossae muri at the posterior part of the valve. Another fine rib is equal in length to the dorsal margin and runs slightly below and parallel to it. Below the alate process, several fine ribs parallel to the ventral margin stretch from the anterior part of the valve and eventually merge with fossae muri at the posterior part of the valve. The whole valve surface, besides fossae muri, is densely punctate.

◄

Explanation of Plate 2

Figs. 1 and 2. *Cytheropteron champlainum* Cronin, 1981: (1) left valve, external view, no. 292/263, ×80, (2) right valve, external view, no. 292/59, ×86; recent surface sediments of the western Laptev Sea.

Figs. 3 and 4. *Cytheropteron dimlingtonensis* Neale et Howe, 1973: (3) right valve, external view, no. 292/279, ×80; (4) right valve, external view, no. 292/277, ×90; Late Pleistocene of the western Laptev Sea.

Figs. 5 and 6. *Cytheropteron discoveria* Brouwers, 1994: (5) left valve, external view, no. 292/271, ×115; (6) left valve, external view, no. 292/270, ×100; Holocene of the western Laptev Sea.

Figs. 7 and 8. *Cytheropteron elaeni* Cronin, 1989: (7) left valve, external view, no. 292/47, ×102; (8) right valve, external view, no. 292/282, ×102; Holocene of the eastern Laptev Sea shelf.

Figs. 9 and 10. *Cytheropteron inflatum* Brady, Crosskey et Robertson, 1874: (9) left valve, external view, no. 292/71, ×70; (10) left valve, external view, no. 292/281, ×130; recent surface sediments of the western Laptev Sea.

Figs. 11 and 12. *Cytheropteron montrosiense* Brady, Crosskey et Robertson, 1874: (11) left valve, external view, no. 292/266, ×90; (12) right valve, external view, no. 292/180, ×94; recent surface sediments of the southeastern Laptev Sea.

Figs. 13 and 14. *Cytheropteron nodosoalatum* Neale et Howe, 1975: (13) right valve, external view, no. 292/81, ×87; (14) right valve, external view, no. 292/213, ×87; recent surface sediments of the Laptev Sea.

Figs. 15 and 16. *Cytheropteron porterae* Whatley et Coles, 1987: (15) right valve, external view, no. 292/61, ×87; (16) left valve, external view, no. 292/89, ×90; recent surface sediments of the western Laptev Sea.

Figs. 17 and 18. *Cytheropteron pseudomontrosiense* Whatley et Masson, 1979: (17) right valve, external view, no. 292/285, ×135; (18) right valve, external view, no. 292/286, ×155; Late Pleistocene of the western Laptev Sea.

Dimensions in mm:

Specimen, no.	L	H
292/229	0.40	0.21
292/235	0.44	0.25
292/277	0.51	0.34
292/279	0.58	0.37

Variability. The degree of reticulation and the shape of fossae are slightly variable, the fossae vary in shape from elongated to more rounded. Carapace lateral outlines may vary: some of them are higher and shorter with a more convex dorsal margin, possibly due to sexual dimorphism (published photomicrographs are not separated into sexes).

Comparison. From the most similar in carapace outline and surface sculpture *C. champlainum* Cronin, 1981, this species differs in the presence of solely fossae and densely punctate valve surface within fossae, a feature not typical of *C. champlainum* (Fig. 8). *C. dimlingtonensis* differs from *C. latissimum* (Norman, 1864) from the Pleistocene deposits of the North Sea (Whatley and Masson, 1979, p. 225, pl. 6, figs. 7, 9, 12) similar in surface sculpture, in having more distinct subvertical rows of fossae, a more convex dorsal margin, and a more evenly rounded ala edge.

Remarks. Lev (1983, pl. 16, figs. 1, 2) identified as *C. subcircinatum* Sars 1866 ostracodes that could be probably referred to as *C. dimlingtonensis.* However, since descriptions of these specimens are not given, we can not be absolutely sure that these species are synonyms. Therefore, we did not include *C. subcircinatum* (*sensu* Lev, 1983) in the list of synonyms. Kupriyanova (1999, pl. 2, fig. 2) attributed several specimens to *C. champlainum* that we would rather refer to *C. dimlingtonensis,* since these specimens bear only reticulate ornament.

Fossil distribution. Pliocene–Pleistocene of Alaska (Gubik Formation); Pleistocene of Great Britain, Denmark, and the Laptev Sea; probably, Pleistocene–Holocene of the lower Severnaya Dvina and Mezen' rivers and the Kola Peninsula; and Holocene of the eastern Kara Sea.

Modern distribution. Laptev and Kara seas and waters off Spitsbergen.

Material. Forty-seven valves of good preservation, Pleistocene–Holocene deposits and recent surface sediments of the western Laptev Sea.

Cytheropteron discoveria Brouwers, 1994

Plate 2, figs. 5, 6

Cytheropteron discoveria: Brouwers, 1994, p. 20, pl. 11, fig. 5, pl. 13, figs. 1–6, 9; Stepanova et al., 2004, p. 91, pl. 1, figs. 9, 10.

Cytheropteron inornatum: Stepanova et al., 2003, pl. II, fig. 9.

Holotype. US National Museum (USNM); USNM 408516, left valve, Gulf of Alaska, locality DC2-80-EG-195; Pleistocene–Holocene (information about age is not precise).

Description. The carapace is small, thin-shelled, and subtriangular in lateral view. The dorsal margin is arcuately convex, gently beveled towards the anterior margin, and passes into the posterior margin through a slight concavity. The ventral margin is straight, slightly concave in the anterior third. The anterior margin is flattened and evenly arcuately rounded. The posterior margin is also flattened, subtriangular, with a caudal process upturned towards the dorsal margin. The caudal process is convex in posterodorsal part and slightly concave in the posteroventral part. The greatest length is situated at mid-height; and the greatest height, in the center of the valve. Just above the ventral margin there is an ala with the straight anterior edge and subvertical posterior edge. The protruding part of the ala is densely punctate with very small puncta; the largest puncta occur rarely at its base and on the lateral valve surface above it. Parts of the ala with small puncta and with larger puncta are divided by a biconvex rib. Very small puncta occur on the posterior and anterior parts of the valve. The lateral surface bears four fine ribs. One short rib extends parallel to the posterodorsal margin just below its concavity. Another short rib occurs below the anterior hinge edge subparallel to the dorsal margin. The third rib extends upwards from the ala extremity with a minor inclination towards the posterior margin and meets the first rib. The fourth rib extends from the ala extremity along the leading ala edge towards the anterior margin and ends just short of the anterior margin. Several fine ribs occur on the posterior part of the valve parallel to the posteroventral margin. They originate at the posterior side of the ala and disappear short of the caudal process extremity. These ribs partly merge to form elongated fossae. The carapace in the posterior and anterior parts is densely punctate.

Dimensions in mm:

Specimen, no.	L	H
292/270	0.44	0.22
292/271	0.42	0.19
292/84	0.4	0.22

Variability. Some carapaces are considerably less punctate than others (Stepanova et al., 2003, pl. 2, fig. 9).

Comparison. *Cytheropteron discoveria* Brouwers, 1994 differs from *C. inornatum* Brady and Robertson, 1872 from recent sediments from waters around Scotland (Whatley and Masson, 1979, p. 238, pl. 3, figs. 1–3, 5–7), similar in carapace outline, in having punctate surface and different number (four against three) and arrangement of fine ribs on the lateral surface.

Remarks. Previously (Stepanova et al., 2003), the valve of *C. discoveria* was mistakenly referred to as *C. inornatum* due to the poor material (two valves) of this species from the western Laptev Sea. Later we obtained more specimens from the Holocene deposits.

Fossil distribution. Pleistocene–Holocene of the Gulf of Alaska, Cook Inlet, Kodiak shelf, Pribylof Islands, and the western Laptev Sea.

Modern distribution. Gulf of Alaska and the western Laptev Sea.

Material. Seventeen valves of good preservation, Pleistocene–Holocene and recent surface sediments of the western Laptev Sea.

Cytheropteron elaeni Cronin, 1989

Plate 2, figs. 7, 8

Cytheropteron sp. nov.?: Neale and Howe, 1975, pl. 6, fig. 5.

Cytheropteron paralatissimum: Lev, 1983, p. 120, pl. 16, fig. 15; Kupriyanova, 1999, pl. 2, fig. 9.

Cytheropteron nealei: Cronin, 1981, p. 406, pl. 7, fig. 7.

Cytheropteron elaeni: Cronin, 1989, pl. 5, fig. 8; Brouwers, 1994, p. 23, pl. 22, figs. 11–13; Stepanova et al., 2003, pl. 1, fig. 14; Stepanova et al., 2004, p. 93, pl. 1, figs. 11, 12.

Cytheropteron bronwynae: Didié et al., 1998, pl. 1, fig. 14.

Holotype. US National Museum (USNM), Department of Paleobiology, USNM311151, female right valve?; Canada, Quebec, exposures on east side of Quebec Route 221, 7.2 km S of St. Remi; Pleistocene.

Description. The carapace is small, subtriangular in lateral view, with flattened anterior and posterior margins. The dorsal margin is arcuate, strongly convex, passes into the anterior margin through a slight ledge, slightly concave in front of the posterior margin. The ventral margin is straight, slightly concave in the anterior third. The anterior margin is arcuately rounded. The posterior margin is lower than the anterior margin and subtriangular. The greatest length is situated at the lower third; the greatest height, in the front third of the valve. A well-developed alate process is located above the ventral margin, it has a straight anterior edge and a subvertical posterior. Along the ala base a row of four fossae occurs, each contains a punctum. In the anterior part of the valve there are fine ribs parallel to the anterior margin. Close to the posterior margin there are three fine short subvertical ribs that reach the base of the ala. At hinge edges some ribs merge to form two elongated nodes. Valves are pierced with pore canals; pore puncta are arranged in subvertical rows.

Dimensions in mm:

Specimen, no.	L	H
292/268	0.36	0.22
292/282	0.39	0.25
292/47	0.41	0.22

Variability. The ornamentation is highly variable. Compared to our specimens, specimens shown in the majority of published micrographs possess more pronounced ribs on the anterior part of the valve and near the posterior margin. Therefore, when these ribs merge, the nodes they form on dorsal side are considerably larger.

Comparison. The species differs from *C. nodosum* Brady, 1868 from surface sediments of the seas around Great Britain and Ireland (Brady, 1868a, p. 448, 449, pl. 34, figs. 31–34), similar in outline and ornamentation, in the absence of pronounced reticulation and in the presence of smaller nodes on the dorsal side.

Remarks. Cronin (1981) described species *C. nealei.* Later, this name was shown to be preoccupied, having been used twice earlier by other authors (*"C." nealei* Jarn, 1975 and *C.*? *nealei* Joy and Clark, 1977). Consequently, Cronin (1989) gave this species a new name *C. elaeni* Cronin, 1989. Didié et al. (1998) illustrated a specimen from the Iceland Sea (pl. 1, fig. 14) and assigned it to *C. bronwynae.* We would refer it to as *C. elaeni.*

Fossil distribution. Neogene–Quaternary deposits of the Novaya Zemlya; Pleistocene of the lower Severnaya Dvina River, Kola Peninsula, Taimyr Peninsula, Pechora, Bering, and Beaufort seas, northeastern North America (St. Lawrence Lowlands, Champlain Sea, and Goldthwait Sea of Quebec); Pleistocene–Holocene of the Gulf of Alaska; and Holocene of the Laptev and eastern Kara seas.

Modern distribution. Norwegian Sea, waters of eastern Greenland, Iceland; the White, Barents, Kara seas, eastern Laptev, Chukchi, and Beaufort seas; the straits of the Canadian Arctic Archipelago, the Labrador Sea, Hudson Bay, Frobisher Bay, and Norton Sound.

Material. One hundred and thirty-seven valves, 20 carapaces, and 25 juvenile valves of good preservation, Holocene and recent surface sediments of the Laptev Sea.

Cytheropteron inflatum Brady, Crosskey et Robertson, 1874

Plate 2, figs. 9, 10

Cytheropteron inflatum: Brady, 1868a, pl. 5, figs. 8–10 (nomen nudum); Brady et al., 1874, p. 204, pl. 8, figs. 24–27, pl. 14, figs. 26–29; Brady and Norman, 1889, p. 209, pl. 20, figs. 19–21; G.O. Sars, 1928, p. 231, pl. 106, fig. 2; Whatley and Masson, 1979, p. 237, pl. 8, figs. 8, 13–16; Cronin, 1981, p. 404, pl. 2, figs. 3, 4; Lev, 1983, p. 118, pl. 15, figs. 7, 8; Cronin, 1989, pl. 5, fig. 11; Whatley et al., 1996, pl. 2, figs. 1, 2; Whatley et al., 1998, pl. 1, figs. 20, 21; Stepanova et al., 2003, pl. 2, fig. 1; Stepanova et al., 2004, p. 94, pl. 1, figs. 13, 14.

Cytheropteron testudo: Woszidlo, 1962, pl. 5, fig. 15.

Type material. For description of this species Brady et al. (1874) originally used material from the Pleistocene deposits of Errol and Drylers (Scotland). The current location of the type material is unknown. Revision of this species has never been undertaken; holotype and lectotype have not been designated.

Description. The carapace is of medium size, subtriangular in lateral view, inflated laterally, with flattened anterior and posterior margins. The dorsal margin is arcuately convex, gently beveled towards anterior and posterior margins. The ventral margin is straight, slightly concave in the anterior third. The anterior margin is arcuately rounded. The posterior margin is lower than the anterior, subtriangular. The greatest length is

Plate 3

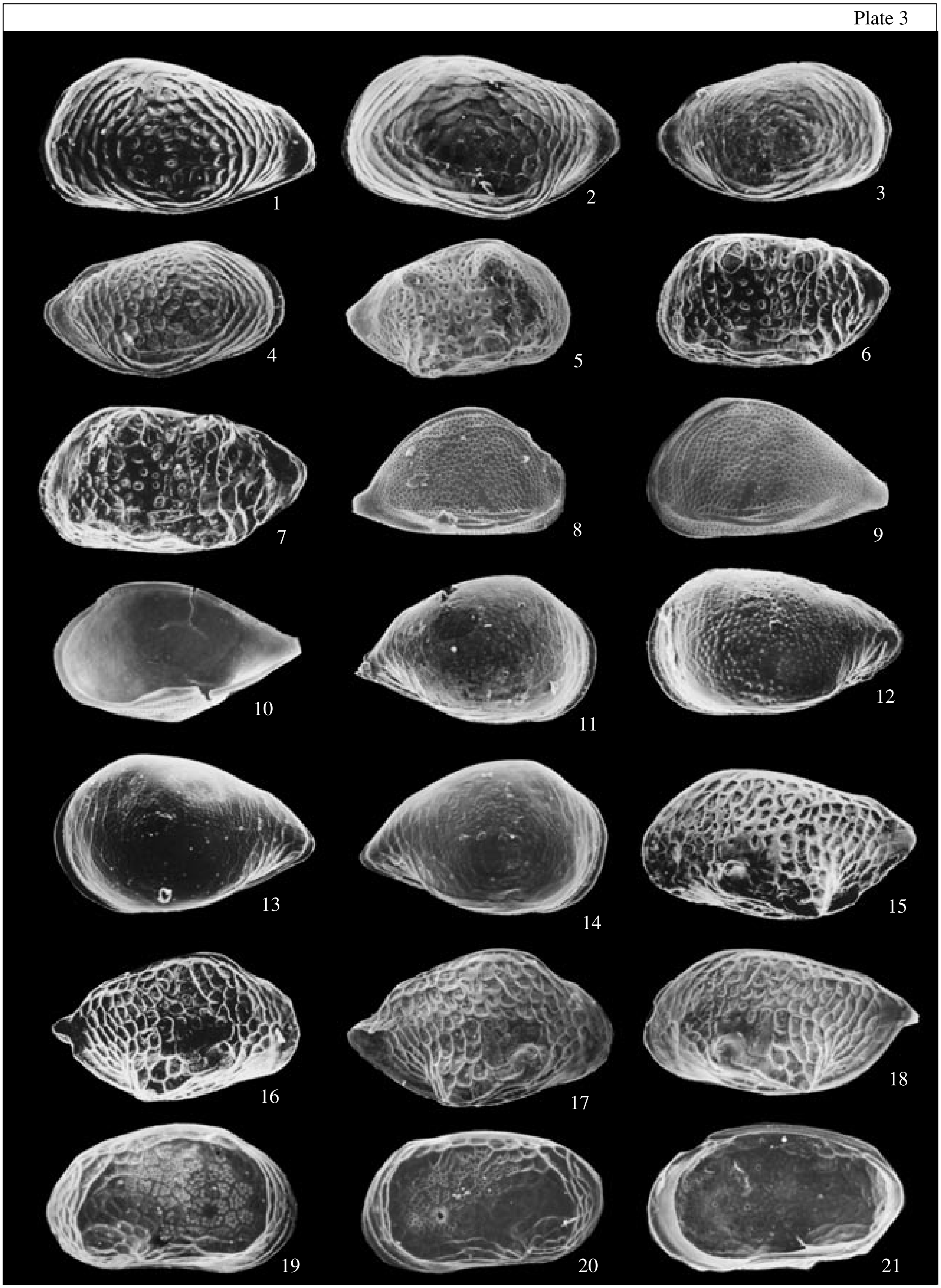

situated at mid-height; the greatest height, in the center of the valve. A strongly inflated lateral expansion is located above the ventral margin. Several fine ribs follow its outline and form weakly developed fossae on the posterior margin of the valve. The valve surface bears numerous sporadically distributed puncta with pore canals.

Dimensions in mm:

Specimen, no.	L	H
292/71	0.55	0.25
292/119	0.36	0.21
292/73	0.37	0.18
292/281	0.33	0.22

Variability. Ornamentation is slightly variable. Some specimens of *C. inflatum g*iven in publications differ from our specimens in the occurrence of fine ribs not only on the ventral, anterior, and posterior margins, but on the whole valve surface where they form weakly developed fossae.

Comparison. *C. inflatum* differs from *C. walli* Whatley and Masson, 1979 from Pleistocene–Recent sediments of Great Britain (Whatley and Masson, 1979, p. 256, pl. 8, figs. 1, 3–6), similar in outline, in the absence of distinct reticulation, more inflated carapace, and less defined lateral expansion. Compared to *C. testudo* G.O. Sars, 1869 (Sars, 1928, p. 230, pl. 56, fig. 1), *C. inflatum* has a more laterally inflated carapace and no winglike process.

Remarks. Brady (1868a) illustrated *C. inflatum*, but only in Brady et al. (1874) was the description of this species given. In the publication devoted to the Pleistocene ostracodes of Germany, Woszidlo (1962) identified species *C. testudo* (pl. 5, fig. 15), which we consider to be *C. inflatum.*

Fossil distribution. Quaternary deposits of the lower Pechora River, Cheshskaya Bay coast, lower Yenisei and lower Severnaya Dvina rivers, Taimyr Peninsula, Novaya Zemlya, North Sea; Pleistocene of Scotland, Northern Germany (Schleswig-Holstein), Denmark, northeastern North America (St. Lawrence Lowlands, Champlain Sea, Goldthwait Sea (Quebec), and Montreal); and Holocene of the Laptev Sea.

Modern distribution. North Atlantic; the Greenland, Irish, and Norwegian seas; waters surrounding Spitsbergen; waters surrounding Great Britain; the Barents, Kara, western Laptev, Baffin, and Beaufort seas; Hudson Bay, Frobisher Bay, and the straits of the Canadian Arctic Archipelago.

Material. Thirty-one valves of good preservation, Pleistocene–Holocene and recent surface sediments of the Laptev Sea.

Cytheropteron laptevensis Stepanova, 2004

Plate 3, figs. 15–18

Cytheropteron ? *sedovi*: Whatley and Masson, 1979, p. 251, pl. 7, figs. 15–19.

Cytheropteron ex gr. *sedovi*: Lev, 1983, p. 121, pl. 15, figs. 10–12.

Cytheropteron sedovi: Penney, 1990, pl. 1, fig. 1.

Cytheropteron laptevensis: Stepanova et al., 2004, p. 105, pl. 2, figs. 38–41.

Holotype. Department of Paleontology of Lomonosov Moscow State University, no. 292/280; adult left valve, western Laptev Sea; core PS51-154, Lat. 77°16′61″ N, Long. 120°36′03″ E, core depth 128–130 cm; Holocene.

Description. The carapace is of medium size, subrhomboidal in lateral view, with flattened anterior and posterior margins. The dorsal margin is almost straight, with obtuse cardinal angles, gently beveled towards the anterior and posterior margins, and bent towards the posterior margin. The ventral margin is slightly convex in the posterior half and slightly concave in the anterior third. The anterior margin is evenly arcuately rounded.

◄

Explanation of Plate 3

Fig. 1. *Cytheropteron pseudomontrosiense* Whatley et Masson, 1979: left valve, external view, no. 292/287, ×120, Late Pleistocene of the western Laptev Sea.

Figs. 2–4. *Cytheropteron sulense* Lev, 1972: (2) left valve, external view, collection of Lev housed at NIIGA, no. 1183-68, ×100; (3) right valve, external view, collection of Lev housed at NIIGA, no. 1183-69, ×100; Late Pliocene–Pleistocene of Malozemel'skaya tundra; (4) right valve, external view, no. 292/179, ×65, Pleistocene–Holocene of the Laptev Sea.

Figs. 5–7. *Cytheropteron suzdalskyi* Lev, 1972; (5) right valve, external view, no. 292/32, ×75; (6) left valve, external view, no. 292/49, ×75; (7) left valve external view, no. 292/267, ×85; Holocene and recent surface sediments of the eastern Laptev Sea.

Figs. 8–10. *Cytheropteron perlaria* Hao, 1988; (8) right valve, external view, no. 292/69, ×96; (9) left valve, external view, no. 292/71, ×120; (10) right valve, internal view, no. 292/70, ×135; recent surface sediments of the western Laptev Sea.

Figs. 11–14. *Cytheropteron tumefactum* Lev 1972: (11) right valve, external view collection of Lev housed at NIIGA, specimen from sample 2302, ×105; (12) left valve, external view, Lev's collection housed in NIIGA, specimen from sample 2302 (identified by Lev as *Cytheropteron punctatum*), ×105; (11–12) Late Pliocene–Eopleistocene of the Arkhangelsk region; (13) left valve, external view, no. 292/264, ×115, (14) right valve, external view, no. 292/60, ×96; (13–14) recent surface sediments of the western Laptev Sea.

Figs. 15–18. *Cytheropteron laptevensis* Stepanova 2004: (15) left valve, external view, holotype, no. 292/280, ×135; (16) right valve, external view, no. 292/278, ×110; (17) right valve, external view, no. 292/234, ×110; (18) left valve, external view, no. 292/201, ×130; Pleistocene–Holocene of the western Laptev Sea.

Figs. 19–21. *Semicytherura complanata* (Brady, Crosskey et Robertson, 1874): (19) right valve, external view, no. 292/194, ×70; (20) left valve, external view, no. 292/43, ×70; (21) right valve, external view, no. 292/44, ×70; Holocene of the eastern Laptev Sea shelf.

The posterior margin is caudate, slightly upturned towards the dorsal margin. On the left valve the posterior margin is slightly lower than the anterior, on the right valve they are nearly equal. The left valves have more smoothed cardinal angles, and the right valves have prominent cardinal angles and a more convex dorsal margin. The caudal process in the posterodorsal part in the left valve is straight or slightly convex, in the right valve concave. The greatest length is situated at mid-height; the greatest height, at the anterior hinge edge. Above the anterior margin there is a winglike process, with a straight anterior edge and a subvertical posterior. The anterior part of the ala has a rounded swelling, and a subvertically elongated socket behind it (0.02 × 0.015 mm). The surface is reticulate: fossae are large and irregularly shaped, mostly subvertically elongated. The solum of fossae is punctate.

Dimensions in mm:

Specimen, no.	L	H
292/220	0.36	0.19
292/234	0.41	0.25
292/253	0.38	0.23
292/278	0.4	0.22
292/280	0.36	0.18

Variability. Reticulation slightly varies in its degree.

Comparison. This species differs from *C. sedovi* from recent sediments of the Central Arctic Ocean (Schneider, 1962, p. 104, pl. 12, fig. 1) in having subrhomboidal instead of subtriangular outline, in lacking ribs, and in the presence of fossae. *C. sedovi* bears distinct parallel subvertical ribs on the posterior margin. Its lateral valve surface is nearly completely covered with subvertical rows of puncta. Ala morphology is also different: *C. sedovi* has rounded anterior edge of ala and subvertical posterior, and it bears a subvertical row of four puncta, while ala of *C. laptevensis* has a straight anterior edge and a swelling at its anterior base, behind which there is a socket.

Remarks. Whatley and Masson (1979) questionably attributed several specimens to *C.*? *sedovi* Schneider, 1962 and pointed out that they failed to find the original description of Schneider. We studied illustrations given in Schneider (1962) and came to the conclusion that specimens from our samples and those in publications of Whatley and Masson (1979) and Penny (1990) belong to different taxa and, therefore, it was necessary to establish a new species *C. laptevensis.*

Fossil distribution. Pleistocene of Ireland; North Sea; and the lower Yenisei, lower Ob, and Pechora rivers; and Pleistocene–Holocene of the western Laptev Sea.

Material. Forty-six adult and 3 juvenile valves, Late Pleistocene–Holocene deposits of the western Laptev Sea.

Cytheropteron montrosiense Brady, Crosskey et Robertson, 1874

Plate 2, figs. 11, 12

Cytheropteron montrosiense: Brady, 1868a, pl. 5, figs. 1–3 (only) (nomen nudum); Brady et al., 1874, p. 205, pl. 8, figs. 28–32 (only); Woszidlo, 1962, pl. 5, fig. 13; Lev, 1972, pl. 1, figs. 18, 19; Robinson, 1978, pl. 6, fig. 5a (only); Whatley and Masson, 1979, p. 240, pl. 2, figs. 1–4, 6; Lev, 1983, p. 117, pl. 15, figs. 4, 16, text-figs. 8, 9; McDougall et al., 1986, pl. 12, figs. 3, 5 (only); Cronin, 1989, pl. 5, fig. 2; Lord et al., 1993, pl. 3, figs. 1, 2; Whatley et al., 1996, pl. 2, figs. 3, 4; Kupriyanova, 1999, pl. 2, fig. 3; Stepanova et al., 2003, pl. 1, fig. 15; Stepanova et al., 2004, p. 95, pl. 1, figs. 15, 16.

Type material. Collection of Brady at the Hancock Museum in Newcastle, slide 1.30.37; Scotland, Drylers, Montrose; Pleistocene (L. Jessop, personal communication, 2005).

Description. The carapace is of medium size, subrhomboidal in lateral view, with flattened anterior and posterior margins. The dorsal margin is straight with a concavity in the anterior third, gently beveled towards the anterior margin and steeply beveled towards the posterior margin. The ventral margin is straight, slightly concave in the anterior third. The anterior margin is arcuately rounded. The posterior margin is lower than the anterior margin, caudate, slightly upturned towards the dorsal margin. The greatest length is situated at mid-height; and the greatest height, in the center of the valve. Valves differ in outline: the right valves are higher and shorter and have a more convex dorsal margin. The caudal process is slightly convex in the posterodorsal part in the left valve and concave in the right valve. A laterally inflated expansion is located above the ventral margin, its extremity is shaped as a massive spine and is located in the posterior third of the valve. The valve surface is reticulate, fossae are large: subvertically elongated fossae are found at the anterior and posterior margins (0.025 × 0.01 mm), and rounded fossae in the central part (diameter 0.02–0.03 mm).

Dimensions in mm:

Specimen, no.	L	H
292/130	0.34	0.18
292/180	0.51	0.25
292/266	0.47	0.24

Variability. Carapaces of this species slightly vary in the degree of development of reticulation, possibly due to preservation and partial dissolution.

Comparison. *C. montrosiense* differs from *C. sulense* Lev, 1972, which is similar in outline and ornamentation, in the presence of a massive spine.

Remarks. In Brady (1868a), only illustrations of *C. montrosiense* are given without a description, making it a nomen nudum. The first description of this species was published in 1874 (Brady et al., 1874).

Fossil distribution. Neogene–Quaternary deposits of the lower Yenisei, lower Ob, lower Pechora, lower Izhma, and lower Severnaya Dvina rivers, Vaigach Island, and Novaya Zemlya; Quaternary of the North and Pechora seas; Pleistocene of Ireland, Scotland, northern Germany (Schleswig-Holstein), Great Britain, and northwestern North America (Boston "blue clay" in Massachusetts); Late Pleistocene–Holocene of the Beaufort Sea; and Holocene of the Laptev and eastern Kara seas.

Modern distribution. North Atlantic; waters off Norway, Greenland, and Great Britain; the White, Barents, Kara, East Siberian, Beaufort, Baffin, eastern Laptev seas; and waters off northern Alaska.

Material. Thirty valves and 5 carapaces of good preservation, Pleistocene–Holocene deposits and recent surface sediments of the Laptev Sea.

Cytheropteron nodosoalatum **Neale et H. Howe, 1973**

Plate 2, figs. 13, 14

Cytheropteron nodosoalatum: Neale and Howe, 1973, p. 240, pl. 1, figs. 6, 7a, b; Neale and Howe, 1975, pl. 6, figs. 8, 10, pl. 7, figs. 2, 4, 10, 11; Whatley and Masson, 1979, p. 242, pl. 6, figs. 3, 5, 6, 10; Lord, 1980, pl. 2, fig. 16; Cronin, 1989, pl. 4, figs. 1–4; Stepanova et al., 2003, pl. 2, figs. 3, 4; Stepanova et al., 2004, p. 95, pl. 1, figs. 15, 16.

Holotype. University of Hull, HVH 9787; left valve; Dimlington of Yorkshire, (England); Pleistocene.

Description. The carapace is of medium size, subrhomboidal in lateral view, with flattened anterior and posterior margins. The dorsal margin is almost straight, slightly convex, gently beveled towards the anterior and posterior margins, and slightly concave passing into them. The ventral margin is straight, slightly concave in the anterior third. The anterior margin is arcuately rounded and bent ventrally. The posterior margin is lower than the anterior margin, caudate, slightly upturned towards the dorsal margin. The greatest length is situated at mid-height; the greatest height, in the center of the valve. The valves differ in outline: the right valve is shorter and higher with a more convex dorsal margin. The caudal process is straight or slightly convex in the posterodorsal part in the left valve and slightly concave in the right valve. A broad lateral winglike expansion, subdivided by a depression in its central part, overlaps the ventral margin. On the ala edges massive nodes flank this depression and give it a bipartite appearance. The surface is reticulate and punctate, fossae and puncta are arranged in subvertical rows, fossae are predominantly restricted to the posterior part of the valve, and puncta are distributed over the entire surface. In the central part round puncta prevail, on the anterior and posterior parts of the valve they are considerably smaller and occur more densely. Elongated subvertical fossae with low muri occur above the posterior node of the ala. A fine rib stretches from the lower part of the anterior margin of the valve, runs along the ala edge, and ends at its posterior edge. Here it splits into two or three upward branches; at mid-height point of the valve they merge with fossae muri. A fine rib equal in length to the dorsal margin runs slightly below and parallel to it. Several fine ribs parallel to the ventral margin, below the alate extension, run from the lower anterior part of the valve and merge with fossae muri on the posterior part. Threadlike ribs forming fossae with puncta inside occur on the posterior third of the valve and the anterior margin.

Dimensions in mm:

Specimen, no.	L	H
292/39	0.55	0.29
292/81	0.43	0.23
292/213	0.56	0.34

Variability. Degree of development of fossae and puncta varies from densely punctate surface to well-developed fossae with puncta within them.

Comparison. *C. nodosoalatum* differs from *C. champlainum* Cronin, 1981, which is similar in outline and sculpture, in having massive nodes on the alate extension.

Fossil distribution. Pleistocene of Great Britain, southeastern Virginia, North Sea, and northeastern North America (Goldthwait Sea in Quebec and the Presumpscot Formation in Maine); and Holocene of the Laptev Sea.

Modern distribution. Waters off Greenland, Franz Josef Land, and Novaya Zemlya; the Irish, Norwegian, White, Barents, Kara, Chukchi, Laptev, Beaufort, and Labrador seas; Davis Strait; Gulf of Alaska; Frobisher Bay; Norton Sound; Ungava Bay; and the straits of the Canadian Arctic Archipelago.

Material. Seventeen valves and 1 carapace of good preservation, Holocene deposits and recent surface sediments of the Laptev Sea.

Cytheropteron perlaria **Hao, 1988**

Plate 3, figs. 8–10

Cytheropteron testudo: Whatley and Coles, 1987, pl. 3, fig. 1; Whatley and Ayress, 1988, pl. 1, figs. 7, 8; Stepanova et al., 2003, pl. 2, figs. 5, 6.

Cytheropteron carolae: Brouwers, 1994, p. 17, pl. 8, figs. 12–14.

Cytheropteron perlaria: Hao, 1988, p. 280, pl. 47, figs. 4–9; Swanson and Ayress, 1999, pl. 1, figs. 7–13; pl. 2, figs. 1–3; Stepanova et al., 2004, p. 98, pl. 2, figs. 32, 33.

Cytheropteron sp. aff. *perlaria:* Swanson and Ayress, pl. 7, figs. 1–6; pl. 8, fig. 1.

Holotype. Chinese University of Geosciences in Beijing; N 40212, left valve; Okinawa Trough, station 919, 865; Upper Pleistocene.

Description. The carapace is small, subtriangular in lateral view, with flattened anterior and posterior margins. The dorsal margin is slightly convex, more convex in the right valve, strongly bent towards the posterior margin, so that it almost touches the ventral margin. The ventral margin is straight, not parallel to the dorsal margin, slightly concave in the anterior third. The anterior margin is arcuately rounded, bent ventrally. The posterior margin is considerably lower than the anterior margin, it is triangular, caudate. The caudal process in the posterodorsal part is straight or slightly convex in the left valves and slightly concave in the right valves. The greatest length is situated just above the ventral margin; the greatest height, at the anterior hinge edge. A winglike expansion with a rounded edge is located above the ventral margin. It is flat, peaklike, and subvertical to the valve surface. The rib runs along the ala edge. There are two fine ribs just above the alate extension. At the anterior margin there is one or several (maximum three) very fine, threadlike ribs. They stretch from the ala base parallel to the anterior margin, reach the dorsal margin, where they turn towards the posterior margin and extend further parallel to the dorsal margin. These ribs do not reach the posterior part of valve. The whole valve surface is evenly densely punctate. The puncta are small and round.

Dimensions in mm:

Specimen, no.	L	H
292/69	0.37	0.21
292/70	0.34	0.18
292/71	0.36	0.2

Variability. The number of fine ribs parallel to the anterior and dorsal margins varies from one to three.

Comparison. This species differs from *C. testudo* Sars, 1869, similar in outline and surface sculpture, in having a considerably smaller size, not exceeding 0.5 mm, while adult carapace length of *C. testudo* is more than 0.55 mm. Besides, *C. perlaria* has a less developed alate process and subtriangular lateral outline; while *C. testudo* has a well-developed alate process and subrhomboidal lateral outline.

Remarks. Swanson and Ayress (1999) included *Cytheropteron perlaria* into the "species group" *Cytheropteron testudo*, which also includes *C. delphinium* Swanson et Ayress, 1999; *C. bikurangiensis* Swanson et Ayress, 1999; *C. sarsi* Swanson et Ayress, 1999; *C. taciturnum* Swanson et Ayress, 1999; and *C. wellmani* Hornibrook, 1952. All these species have a subtriangular or rhomboidal lateral carapace outline, peaklike alate process just above the ventral margin, and densely evenly punctate valve surface. Some of them are cosmopolites and inhabit marine waters worldwide. *C. perlaria* and *C. testudo* were found to inhabit the northern Hemisphere, both were reported from the Arctic and North Atlantic. Morphologically, they are very similar and the only obvious difference is the carapace size. For a long time we have been mistakenly attributing our specimens from the Laptev Sea to *C. testudo* Sars, 1869, but according to Swanson and Ayress (1999), they should be referred to *C. perlaria* Hao, 1988, since none of them exceed 0.5 mm.

Swanson and Ayress (1999) consider distribution of *C. perlaria* Hao, 1988 to be subordinated by that of *C. testudo* Sars, 1869; therefore, we suppose that numerous finds of *C. testudo* might also contain specimens of *C. perlaria.*

We consider *C. carolae* Brouwers (1994, p. 17, pl. 8, figs. 12–14) from Pleistocene–Holocene deposits of the Gulf of Alaska to be a synonym of *C. perlaria.* In original description of *C. carolae* there is no comparison with *C. testudo* and *C. perlaria*, and, therefore, we conceive it to be expedient to attribute specimens shown by Brouwers to *C. perlaria,* since the carapace size and morphology of *C. carolae* does not differ from that of *C. perlaria.*

Fossil distribution. Paleogene–Neogene of southwestern Pacific, Indian, and North Atlantic oceans; Upper Eocene of New Zeeland; Miocene–Pleistocene of the New Caledonia basin, Lord Howe Rise, and Challenger Plato; Pleistocene–Holocene of the North Atlantic, Gulf of Alaska, Cook Inlet, Pribylof Islands, South Australian and East Australian continental slopes, Tasman Sea, and Okinawa Trough; and Holocene of the Queensland Plateau, western Laptev Sea, and Denmark Strait.

Modern distribution. North Atlantic, western Laptev and China seas, waters surrounding Australia (New Caledonia basin, Lord Howe Rise, Challenger Plato, East Australian and South Australian continental slopes), Okinawa Trough, Queensland Plateau, Kuergelen Plateau (Indian Ocean), and Prydz Bay (Antarctica).

Material. Fourteen valves and 10 carapaces of good preservation, Holocene deposits and recent surface sediments of the Laptev Sea.

Cytheropteron porterae Whatley et Coles, 1987

Plate 2, figs. 15, 16

Cytheropteron porterae: Whatley and Coles, 1987, p. 64, pl. 2, figs. 21–23; Whatley et al., 1996, pl. 2, figs. 7, 9; Whatley et al., 1998, pl. 2, figs. 1, 2; Didié and Bauch, 2001, pl. 2, figs. 19–21; Stepanova et al., 2003, pl. 2, figs. 10, 11; Stepanova et al., 2004, p. 99, pl. 1, figs. 19–21.

Holotype. Natural History Museum, London, OS 12536, adult right valve, North Atlantic, DSDP site 607, Lat. 41°00′07″ N, Long. 32°54′44″ W, water depth 3427 m; Late Pliocene.

Description. The carapace is of medium size, subrhomboidal in lateral view, with flattened anterior and posterior margins. The dorsal margin is arcuately convex, in the right valve stronger than in the left, gently beveled towards the anterior and posterior margins. The ventral margin is straight, slightly concave in the anterior third. The anterior margin is arcuately rounded and bent ventrally. The posterior margin is lower than the anterior margin, strongly caudate, slightly upturned towards the dorsal margin. The greatest length is situated at mid-height; the greatest height, at mid-length. A well-developed alate process is located above the ventral margin with a gently rounded anterior edge and a subvertical posterior edge. At the ala base there is a row of several (four to six) subvertically elongated fossae punctate within. The fossa nearest to the anterior margin contains a large pit (0.02 × 0.02 mm). Above the row of fossae, the ala surface is smooth. The central part of the valve bears subvertical rows of puncta. On the posterior and, rarely, anterior margins, threadlike ribs run parallel to them forming weakly developed fossae.

Dimensions in mm:

Specimen, no.	L	H
292/61	0.59	0.28
292/74	0.52	0.23
292/89	0.40	0.17

Variability. Reticulation varies in its degree on the anterior and posterior margins. On the anterior margin it is often not developed.

Comparison. *C. porterae* is distinguished from *C. paralatissimum* Swain, 1963 from the Gubik Formation (Pliocene–Pleistocene of Alaska; Swain, 1963, p. 817, pl. 95, fig. 12; text-fig. 8b) by the absence of a streamlike pattern formed by threadlike ribs on the whole valve surface.

Fossil distribution. Questionable fossil finds from the Miocene deposits of the Indian Ocean (Whatley and Coles, 1987); Pliocene of the North Atlantic; Quaternary of the North Atlantic; Pleistocene–Holocene of the western Laptev Sea; and Holocene of the eastern Kara Sea.

Modern distribution. North Atlantic; the Greenland, Kara, and western Laptev seas; and waters off Newfoundland.

Material. One hundred and thirty valves and 13 carapaces of good preservation, Pleistocene–Holocene deposits and recent surface sediments of the western Laptev Sea.

Cytheropteron pseudomontrosiense Whatley et Masson, 1979

Plate 2, figs. 17, 18; Plate 3, fig. 1

Cytheropteron montrosiense: Brady et al., 1874, p. 205, pl. 8, figs. 33–36 (only); Brady and Norman, 1889, p. 216, pl. 19, figs. 26, 27; Swain, 1963, p. 817, pl. 95, fig. 14 (only); Cronin, 1977, pl. 3, fig. 19; Robinson, 1978, pl. 6, fig. 5b (only); Lord, 1980, pl. 2, figs. 1–6.

Cytheropteron pseudomontrosiense: Whatley and Masson, 1979, p. 247, pl. 2, figs. 5, 7–10, 13, 14; Cronin, 1989, pl. 5, fig. 4; Brouwers et al., 1991, pl. 3, fig. 2; Cronin, 1981, p. 404, pl. 6, figs. 5, 7; Kupriyanova, 1999, pl. 2, fig. 8; Stepanova et al., 2004, p. 102, pl. 2, figs. 22–25.

Holotype. Natural History Museum, London, OS 10830, adult left valve; North Sea, Forties Field borehole, DB 13, Lat. 57°43′54.5″ N, Long. 00°58′25.5″ W, depth in core 5 m, upper part of the Quaternary succession.

Description. The carapace is of medium size, subtriangular in lateral view, with flattened anterior and posterior margins. The dorsal margin is almost straight, slightly concave in the posterior part, gently beveled towards the anterior and posterior margins. The dorsal margin passes into anterior margin through a concavity. The ventral margin is straight, slightly concave in the anterior third. The anterior margin is arcuately rounded. The posterior margin is lower than the anterior margin, it is triangular. The greatest length is situated at the lower third; the greatest height, at the anterior hinge edge. The valves differ in outline: the right valves have more convex (distinct) cardinal angles, and the left valves have gradually sloping cardinal angles. The caudal process in the posterodorsal part is straight or slightly convex on the left valves and slightly concave on the right valves. A rounded laterally inflated expansion is located above the ventral margin. The whole valve surface is reticulate, fossae are large and are arranged concentrically; in the central part of the valve fossae are rounded, on the margins elongated. Above the ventral margin fossae muri merge into ribs contouring the lateral expansion.

Dimensions in mm:

Specimen, no.	L	H
From sample N18, Belush’e (collection of Lev, NIIGA)	0.41	0.24
292/285	0.37	0.19
292/286	0.32	0.19
292/287	0.39	0.21

Variability. The degree of reticulation is variable. Usually fossae are well developed.

Comparison. *C. pseudomontrosiense* differs from *C. sulense* Lev, 1972 (Lev, 1972, p. 18, pl. 1, figs. 14–17) from the Late Pliocene–Early Pleistocene deposits of the Arkhangel’sk Region in having solely subtriangular lateral valve outline, while *C. sulense* is ovate or trapezoidal in lateral view.

Remarks. We consider *C. pseudomontrosiense* and *C. sulense* to be two distinct species. The most interesting fact is that in the original descriptions of both species, their authors (Lev, 1972, Whatley and Masson, 1979) put in the synonym list the same illustrations from Brady et al. (1874, p. 205, pl. 8, figs. 33–36). In the original description of *C. pseudomontrosiense* published micrographs demonstrate a solely subtriangular outline, although some of them are nearly trapezoidal. In the collection of Lev, who described *C. sulense*, specimens of both morphotypes are present, although they are predominantly trapezoidal. Thus, it is likely that Lev considered only trapezoidal carapaces as adults, while subtriangular ones she thought to be late molt stages. In studied samples from the Holocene of the eastern Laptev Sea and from the surface sediment samples, specimens of *C. sulense* were identified, but the Late Pleistocene–Holocene deposits of the western Laptev Sea contained *C. pseudomontrosiense*. At the same time, specimens of another morphotype are always present in small numbers. Usually, both morphotypes in publications are named *C. pseudomontrosiense* or *C. montrosiense*, since the works of Lev are not well known abroad. We consider them as separate species (as well as Whatley, personal communication, 2003 and Briggs, personal communication, 2003).

Therefore, subtriangular specimens are referred to as *C. pseudomontrosiense*; and subovate and trapezoidal specimens, as *C. sulense.*

Fossil distribution. Pliocene of Greenland; Quaternary of the North and Pechora seas; Pleistocene of Great Britain, Norway, northeastern North America (St. Lawrence Lowlands and Champlain Sea); and Pleistocene–Holocene of the North, Norwegian, Pechora, and Laptev seas.

Modern distribution. East Siberian, Beaufort, and Baffin seas and waters off Spitsbergen.

Material. One hundred and seventy-six valves and 2 carapaces of good preservation, Pleistocene–Holocene deposits of the western Laptev Sea.

***Cytheropteron sulense* Lev, 1972**

Plate 3, figs. 2–4

Cytheropteron montrosiense: Brady, 1868a, pl. 5, figs. 4, 5, (only); Swain, 1963, p. 817, pl. 97, fig. 21 (only); McDougall et al., 1986, pl. 12, figs. 1, 2, 4, 6 (only); Siddiqui, 1988, pl. 2, fig. 4; Schoning and Wastegård, 1999, pl. 1, fig. 4.

Cytheropteron sulense: Lev, 1972, p. 18, pl. 1, figs. 14–17; Lev, 1983, pl. 16, figs. 12, 13; Stepanova et al., 2003, pl. 1, figs. 12, 13; Stepanova et al., 2004, p. 103, pl. 2, figs. 26–29.

Cytheropteron cf. *C. montrosiense*: Brouwers et al., 1991, pl. 2, fig. 5.

?*Cytheropteron* sp. 3: Brouwers et al., 1991, pl. 2, fig. 7.

Holotype. VNIIOkeangeologiya, N1183-66; adult right valve; Russia, Arkhangel'sk Region, Malozemel'skaya tundra, Sula River, village of Kotkino, Late Pliocene–Early Pleistocene, layers with *Cytheropteron sulense.*

Description. The carapace is of medium size, trapezoidal to ovate in lateral view, with flattened anterior and posterior margins. The dorsal margin is almost straight, slightly concave in the posterior part, gently beveled towards the anterior and posterior margins. The dorsal margin passes into the anterior margin through a slight concavity. The ventral margin is straight, slightly concave in the anterior third. The anterior margin is arcuately rounded. The posterior margin is lower than the anterior margin, it is triangular. The greatest length is situated slightly higher of mid-height; the greatest height, at the anterior hinge edge. The valves differ in outline: the right valves have more convex (distinct) cardinal angles, and the left valves have gradually sloping cardinal angles. The caudal process in the posteroventral part is slightly convex in the left valve and slightly concave in the right valve. A rounded laterally inflated expansion is located above the ventral margin. The surface is reticulate, fossae are large and arranged concentrically; in the central part of the valve fossae are rounded; on the margins, elongated. Above the ventral margin fossae muri merge into ribs contouring the lateral expansion.

Dimensions in mm:

Specimen, no.	L	H
1183-68 (collection of Lev, NIIGA)	0.51	0.3
1183-69 (collection of Lev, NIIGA)	0.42	0.23
292/135	0.44	0.27
292/179	0.47	0.23

Variability. The degree of reticulation is variable. As a rule, fossae are well developed.

Comparison. For comparison with morphologically similar species see description of *C. montrosiense.*

Remarks. As previously mentioned, carapaces of *C. sulense* were often confused with both *C. montrosiense* and *C. pseudomontrosiense.* Here we consider the specimens given in McDougall et al. (1986, pl. 13, figs. 1, 2, 4, 6) from the Late Pleistocene–Holocene deposits of the Beaufort Sea shelf as *C. sulense*, because all these specimens demonstrate solely trapezoidal-ovate lateral outline.

Fossil distribution. Pliocene of Greenland; Late Pliocene–Pleistocene of Malozemel'skaya tundra; Late Pleistocene–Holocene of the Baltic and Beaufort seas; and Holocene of the eastern shelf of the Laptev Sea.

Modern distribution. The Kara, Laptev, and Beaufort seas and waters off northern Alaska.

Material. One hundred and twenty-five valves and 18 carapaces, Holocene and recent surface sediments of the Laptev Sea.

***Cytheropteron suzdalskyi* Lev, 1972**

Plate 3, figs. 5–7

Cytheropteron suzdalskyi: Lev, 1972, p. 19, pl. 1, figs. 1–5; 1983, pl. 15, figs. 13, 14; Brouwers, 1994, p. 35, pl. 18, figs. 4, 5; pl. 20, figs. 1–9, 34; Kupriyanova, 1999, pl. 2, fig. 4; Stepanova et al., 2003, pl. 1, fig. 11; Stepanova et al., 2004, p. 104, pl. 2, figs. 30, 31.

Cytheropteron cf. *nodosum*: Neale and Howe, 1975, pl. 7, fig. 5.

Cytheropteron cf. *suzdalskyi*: Cronin, 1989, pl. 4, fig. 8.

Holotype. NIIGA, no. 1183-87; adult right valve, Russia, Arkhangel'sk Region, lower Severnaya Dvina River, Ust'-Pinega; Late Pleistocene.

Description. The carapace is of medium size, trapezoidal in lateral view, with flattened posterior margin. The dorsal margin is slightly convex, almost straight, gently beveled towards the margins. The ventral margin is straight, parallel to the dorsal margin. The anterior margin is arcuately rounded and bent ventrally. The posterior margin is lower than the anterior margin, it is triangular, caudate, slightly upturned towards the dorsal margin. The greatest length is situated at the upper third of the valve; the greatest height, at the anterior hinge edge. The right valve is higher and shorter and has a more convex dorsal margin. The caudal process in the posteroventral part is straight on the left valve and slightly concave on the right valve. A broad lateral bipartite winglike expansion is located above the ventral margin, it is subdivided by a depression into two massive nodes. Two other massive nodes in the dorsal part are restricted to hinge margins, they are slightly larger than the ala nodes. The valve surface, except for the posterior part of the valve, is reticulate. Fossae are arranged in rows. Fossae are subvertically elongated at the anterior and posterior margins and rounded in the central part of the valve. Within the fossae the surface of the valve is punctate. On the ventral margin high fossae muri form several ribs parallel to it and contouring the ala outline.

Dimensions in mm:

Specimen, no.	L	H
292/49	0.54	0.32
292/267	0.55	0.30
292/143	0.53	0.30

Variability. Reticulation may vary in its degree; sometimes fossae are not developed, but puncta are always present (Pl. 3, fig. 5).

Comparison. *C. suzdalskyi* differs from *C. nodosum* Brady, 1868 from recent marine sediments around Great Britain and Ireland (Brady, 1868b, p. 448, pl. 34, figs. 31–34) in having more pronounced reticulation and considerably more massive nodes on the dorsal side of valve.

Fossil distribution. Quaternary deposits of the Kola Peninsula, lower Severnaya Dvina River, Cheshskaya Bay coast, lower Pechora River, Taimyr Peninsula; Pleistocene of the northeastern North America (St. Lawrence Lowlands and Champlain Sea); and Holocene of the eastern Kara and Laptev seas.

Modern distribution. Waters off Ireland, Greenland, and Novaya Zemlya; the Kara, eastern Laptev, Chukchi, and Beaufort seas; the straits of the Canadian Arctic Archipelago; and Hudson Bay.

Material. One hundred and twenty-six valves and 9 carapaces of good preservation, Holocene and recent surface sediments of the Laptev Sea.

Cytheropteron tumefactum **Lev, 1972**

Plate 3, figs. 11–14

Cytheropteron montrosiense: Brady et al., 1874, p. 205, pl. 14, figs. 13–16 (only); Cronin, 1977, pl. 3, fig. 17.

Cytheropteron tumefactum: Lev, 1972, p. 17, pl. 1, figs. 12, 13; Lev, 1983, p. 118, pl. 15, fig. 9, pl. 16, fig. 14; Kupriyanova, 1999, pl. 2, fig. 6; Stepanova et al., 2004, p. 104, pl. 2, figs. 34–37.

Cytheropteron montrosiense juv.: Lord, 1980, pl. 2, figs. 7, 8.

Cytheropteron punctatum: Lev, 1983, pp. 120, 121, pl. 16, figs. 6, 7; Kupriyanova, 1999, pl. 2, fig. 7.

Cytheropteron simplex: Whatley and Masson, 1979, p. 252, pl. 2, figs. 11, 12, 19–21; Cronin, 1981, p. 406, pl. 6, figs. 6, 8; Cronin, 1989, pl. 5, fig. 1; Brouwers et al., 1991, pl. 2, fig. 3; Lord et al., 1993, pl. 3, fig. 3; Whatley et al., 1996, pl. 3, fig. 4; Stepanova et al., 2003, pl. 2, fig. 12.

Holotype. NIIGA, no. 1183-74; adult right valve, Russia, Arkhangel'sk Region, Pechora River Basin, village of Khongurei; Late Pliocene–Early Pleistocene (Kolvinskaya Formation).

Description. The carapace is of medium size, rounded-triangular, strongly inflated, with flattened anterior and posterior margins. The dorsal margin is slightly convex, almost straight, bent towards the posterior margin. The ventral margin is straight, slightly concave in the anterior third. The anterior margin is arcuately rounded. The posterior margin is lower than the anterior margin, it is rounded triangular, caudate, slightly downturned ventrally. The greatest length is situated at the lower third; the greatest height, at the anterior hinge edge. A lateral winglike inflation is located above the ventral margin. Several fine ribs extend along the inflation and contour it. Their extension on the anterior and posterior margins form weakly developed elongated fossae. The whole valve surface is unevenly punctate; the puncta are very small.

Dimensions in mm:

Specimen, no.	L	H
From sample N2302, lower Severnaya Dvina River, *C. punctatum* (collection of Lev, NIIGA)	0.43	0.24
From sample N2302, lower Severnaya Dvina River, *C. tumefactum* (collection of Lev, NIIGA)	0.43	0.27
292/60	0.41	0.27
292/68	0.45	0.28

Variability. The number of puncta is variable; central parts of some specimens are virtually devoid of them. In addition, smoother specimens are larger and more rounded, while more punctate specimens are lower and nearly triangular.

Remarks. Diverse intraspecific morphological variability allowed Lev (1983) to attribute more punctate forms to *C. punctatum.* We studied Lev's collection and came to the conclusion that her specimens do not fit Brady's description (Brady, 1868b, p. 449, pl. 34, figs. 45–48). The "smooth" specimens were described by her as a new species, *C. tumefactum.* Whatley and Masson (1979) included both (punctate and smooth) morphotypes into a single new species that they described and named *C. simplex*, which is consequently a synonym of *C. tumefactum*, described earlier. Whatley and Masson (1979) mentioned strong intraspecific variability and supposed that these morphotypes are most likely to be two distinct species, but since they always occur together, their identification is too difficult. Based on the analysis of our own data we came to the conclusion that these morphotypes are to be attributed to a single highly variable species and further taxonomic subdivision is not necessary.

Previously, we identified this form as *C. simplex*, since we were not familiar with the collection of Lev (Stepanova et al., 2003).

Comparison. *C. tumefactum* differs from *C. montrosiense* in having a caudal process downturned towards the ventral (not dorsal) margin. The valve surface of *C. tumefactum* bears puncta and weakly developed fossae at the posterior, ventral, and anterior margins, while *C. montrosiense* is strongly reticulate.

Fossil distribution. Pliocene of Greenland; Quaternary of the North Sea, Scotland, Norway, lower Yenisei River, Arkhangel'sk region (lower Severnaya Dvina River, Cheshskaya Bay coast, and lower Pechora River), northeastern North America (St. Lawrence Lowlands, Champlain Sea, and Goldthwait Sea (Quebec)); Pleistocene–Holocene of western Laptev Sea; and Holocene of the Gulf of Alaska and the eastern Kara Sea.

Modern distribution. Waters off Great Britain and Greenland and the Norway, Kara, western Laptev, and Beaufort seas.

Material. Two hundred and one valves and 22 carapaces of good preservation, Late Pleistocene–Holocene and recent surface sediments of the Laptev Sea.

Genus *Semicytherura* Wagner, 1957

Semicytherura: Wagner, 1957, p. 80; Reyment et al., 1961, p. 299; Athersuch et al., 1989, p. 207.

Type species. *Cythere nigrescens* Baird, 1838; Recent; North Sea; original designation (Wagner, 1957).

Diagnosis. Carapace small, ovate-rectangular in lateral view, often with caudal process. Valves unequal, right valve slightly overlaps left valve dorsally. Surface smooth, or distinctly punctate, or reticulate. Eye tubercule absent. Four ovate-elongated muscle scars form subvertical row in anterior part of valve, in front of them three more scars are grouped, below another single scar occurs. Hinge merodont-entomodont, tripartite, with bar in left valve. In left valve hinge with two denticulated terminal pits and median notched bar, which is smooth in center and becomes narrower towards edges. Right valve complementary.

Taxonomic composition. About 50 species.

Comparison. From *Eucytherura* G. Müller (Cretaceous–Recent, worldwide), similar in carapace outline and size, the genus differs in the absence of marginal spines and right-, not left-overlapping carapace.

Stratigraphical range. Cretaceous–Recent; marine deposits worldwide.

Semicytherura complanata (Brady, Crosskey et Robertson, 1874)

Plate 3, figs. 19–21

Cytherura complanata: Brady et al., 1874, p. 194, pl. 11, figs. 19, 20; Swain, 1963, pl. 97, fig. 10.

Cluthia complanatoformis: Lev, 1983, p. 122, pl. 9, figs. 10–12.

Cytherura sp. D: McDougall et al., 1986, pl. 10, fig. 4.

Cluthia aff. *cluthae*: McDougall et al., 1986, pl. 10, fig. 6.

Semicytherura complanata: Cronin and Ikeya, 1987, p. 85, pl. 3, fig. 17; Cronin, 1989, pl. 3, figs. 7–9; Brouwers et al., 1991, pl. 3, fig. 3; Lord et al., 1993, pl. 3, fig. 10; Kupriyanova, 1999, pl. 2, fig. 11; Brouwers et al., 2000, p. 137, figs. 10–12 (G, H); Stepanova et al., 2003, pl. 2, fig. 15, pl. 3, fig. 1.

Type material. For the description of this species Brady et al. (1874) originally used material from the Pleistocene deposits of Scotland and Ireland. The current location of the type material is unknown. This species has not been revised; holotype and lectotype have not been designated.

Description. The carapace is small, rounded-rectangular in lateral view, flattened laterally. The dorsal margin is slightly convex, almost straight, slightly bent towards the posterior margin. The ventral margin is straight, slightly convex in the center. The anterior margin is evenly arcuately rounded. The posterior margin is slightly lower than the anterior margin, arcuately rounded, slightly beveled in its dorsal and ventral parts. The greatest length is situated at mid-height; the greatest height, at the anterior hinge edge. Above the ventral margin there is a spine-like swelling with an extremity directed posteroventrally. A fine circular rib runs along the valve margins, it bounds the flattened central part of the valve and outlines a spinelike swelling. The valve surface between the rib and valve margins is convex, it bears several fine ribs, running parallel to the margins. They partly merge, forming elongated fossae. The central part of the valve is punctate, more distinctly on the anterior part of the carapace, and reticulate, fossae are polygonal, isometric.

Dimensions in mm:

Specimen, no.	L	H
292/194	0.32	0.18
292/44	0.34	0.19
292/43	0.32	0.19

Variability. The degree of the development of ribs parallel to valve margins varies. Some carapaces have more smoothed surface, the spinelike swelling is also less pronounced on such specimens.

Comparison. This species differs from *Semicytherura nigrescens* (Baird, 1838), which is similar in carapace outline and ornamentation, in the absence of a caudal process and the presence of spinelike swelling in the posteroventral part of valve.

Remarks. Lev (1983, p. 122, pl. 9, figs. 10–12) described a new species, *Cluthia complanatoformis*, which in our opinion cannot be distinguished from *S. complanata* and, therefore, these species are synonyms.

McDougall et al. (1986), studied Late Quaternary deposits of the Prudhoe Bay (Alaska) and identified *Cytherura* sp. D (McDougall et al., 1986, pl. 10, fig. 4) and *Cluthia* aff. *cluthae* (McDougall et al., 1986, pl. 10, fig. 6). We believe that these forms should be attributed to *S. complanata.*

Fossil distribution. Neogene–Quaternary deposits of the lower Yenisei and lower Pechora rivers, southwestern Taimyr (lower Agapa River), Cheshskaya Bay coast, New Siberian Islands nearshore waters; Pliocene of Greenland; Pliocene–Pleistocene of Japan and Alaska; Quaternary of Sweden; Pleistocene of Scotland, northeastern North America (St. Lawrence Lowlands, Goldthwait Sea in Quebec, Presumpscot Formation in Maine, De Geer Sea, and New Brunswick), northern Germany, and Denmark; Pleistocene–Holocene of the Laptev and Pechora seas; and Holocene of the eastern Kara Sea.

Modern distribution. Waters off Greenland; Ireland; the White, Barents, Norwegian, Kara, Laptev, East Siberian, Chukchi, Bering, Beaufort, and Labrador seas; Ungava, Frobisher, and Hudson bays; and the straits of the Canadian Arctic Archipelago.

Material. Three hundred and five valves and 36 carapaces of good preservation, Late Pleistocene–Holocene and recent surface sediments of the Laptev Sea.

Family Schizocytheridae Mandelstam, 1960

Genus *Palmenella* Hirschmann, 1916

Palmenella: Hirschmann, 1916, p. 580; Triebel, 1957, p. 291; Kashevarova et al., 1960, p. 388; Howe et al., 1961a, p. 331; Swain, 1963, p. 830; Athersuch et al., 1989, p. 82; Nikolaeva, 1989, p. 137.

Kyphocythere: G.O. Sars, 1928, p. 180.

Type species. *Cythereis limicola* Norman, 1865; Recent; waters off Great Britain; by monotypy.

Diagnosis. Carapace small, rounded rectangular in lateral view, with hinge ears on the left valve. Valves are almost equal, left valve slightly larger than right valve. Lateral surface bears two massive ribs: ridge-like rib runs along ventral margin parallel to it, and bow-shaped rib is located in anterior upper third of valve, behind it large ovate muscle scar occurs. Surface reticulate: fossae large, fossae muri thin. Eye tubercule absent. Four adductor muscle scars form subvertical row, two more rounded scars occur in front of them. Hinge schizodont. In left valve in anterior part hinge represents pit with basal incision. Behind it, conical tooth with outlining bifurcation in upper part. Tooth passes into notched narrow bar of the median hinge section. Posterior section has semilunar pit. Right valve complementary.

Taxonomic composition. Three species.

Comparison. From *Schizocythere* Triebel 1950 (Paleocene–Miocene, worldwide), which is similar in carapace outline, size, and hinge construction, the genus differs in the absence of eye tubercule and in the presence of massive ridges on the lateral valve surface.

Stratigraphical range. Miocene–Recent, North Atlantic region and sediments of Arctic seas.

Palmenella limicola (Norman, 1865)

Plate 4, figs. 1–3

Cythere limicola: Norman, 1865, p. 20, pl. 6, figs. 1–4; Brady et al., 1874, p. 154, pl. 10, figs. 1–4.

Palmenella limicola: Hirschmann, 1916, p. 580, figs. 8–27; Elofson, 1941, p. 277; Triebel, 1949, p. 189, pl. 2, figs. 5, 6; Kashevarova et al., 1960, p. 388, text-figs. 1119, 1120; Howe et al., 1961a, figs. 256, 7; Elofson, 1969, p. 54; Neale and Howe, 1975, pl. 5, fig. 8; Cronin, 1977, pl. 3, fig. 7; 1981, p. 412, pl. 11, figs. 1, 2, 4; Rosenfeld, 1977, pl. 1, figs. 3–6; Lord, 1980, pl. 3, fig. 6; Lev, 1983, p. 143, pl. 14, fig. 4; McDougall et al., 1986, pl. 13, fig. 8; Athersuch et al., 1989, p. 82, fig. 28, pl. 1, fig. 2; Nikolaeva, 1989, p. 137, text-figs. 200–202; Brouwers, 1990, p. 19, pl. 1, fig. 15, pl. 4, figs. 9, 12, 17, pl. 6, fig. 1; Brouwers et al., 1991, pl. 1, fig. 7; Cronin, 1991, fig. 7.11; Hartmann, 1993, p. 241, pl. 1, figs. 2–4; Kupriyanova, 1999, pl. 1, fig. 11; Stepanova et al., 2003, pl. 3, figs. 2, 3.

Kyphocythere limicola: G.O. Sars, 1928, p. 181, pl. 82.

Palmenella limicola (Norman) var. *dentomarginata*: Akatova, 1946, p. 226, fig. 4.

Syntypes. Natural History Museum, London, collection of Norman, slide N1911.11.8 M3248, several valves; North Sea; Recent (Athersuch et al., 1989).

Description. The carapace is small, rounded-rectangular in lateral view, with flattened anterior and posterior margins. The dorsal margin is straight, on the left valve it passes into the anterior and posterior margins through acuminate hinge ears, on the right valve they are smoothed. The ventral margin is straight or slightly convex and slightly concave in the anterior third. The anterior margin is evenly arcuately rounded, slightly bent ventrally. The posterior margin has a small smoothed ledge at mid-height, and is arcuately rounded in the lower part and slightly concave in the upper part. The greatest length is situated just above the ventral margin; the greatest height, at the anterior hinge edge. A massive ridge runs along the ventral margin parallel to it, it starts in the posterodorsal part of the valve to stop short of its anterior margin. A massive rib that is convex towards the anterior margin is located in the anterior upper third of the valve, it stretches from the anterior hinge edge and, bending parallel to the anterior margin, ends at the mid-height of the valve. Behind the rib there is a massive ovate muscle scar node. Another ridge-like rib runs obliquely in the posterior part of the valve. It starts behind the muscle scar and, becoming more convex, ends in the posterior third of the dorsal margin, and goes far beyond the valve outline. Along the ventral margin there are several fine ribs parallel to it, they partly merge and form fossae. The whole valve surface is reticulate and punctate. The puncta are small. The fossae are large. The fossae on the anterior margin form a rim. The inner lamella has a semilunar outline.

Dimensions in mm:

Specimen, no.	L	H
292/153	0.46	0.24
292/47	0.35	0.25
292/193	0.47	0.27

Comparison. *P. californica* Triebel, 1957 from Pleistocene deposits of California (Triebel, 1957, p. 292, pl. 1, figs. 1–5) and *P. limicola* are similar in size and surface sculpture, but the former species has two (not one as in *P. limicola*) nodes in the posterodorsal part of the valve. The outline of the inner lamella is also different: semilunar in *P. limicola* and subtriangular in *P. californica.*

Remarks. Athersuch (1989) lists as syntypes for this species specimens from Brady's collection (Hancock Museum, slide N1.28.20); however, we consider this questionable, since Brady is not a coauthor of this species.

Plate 4

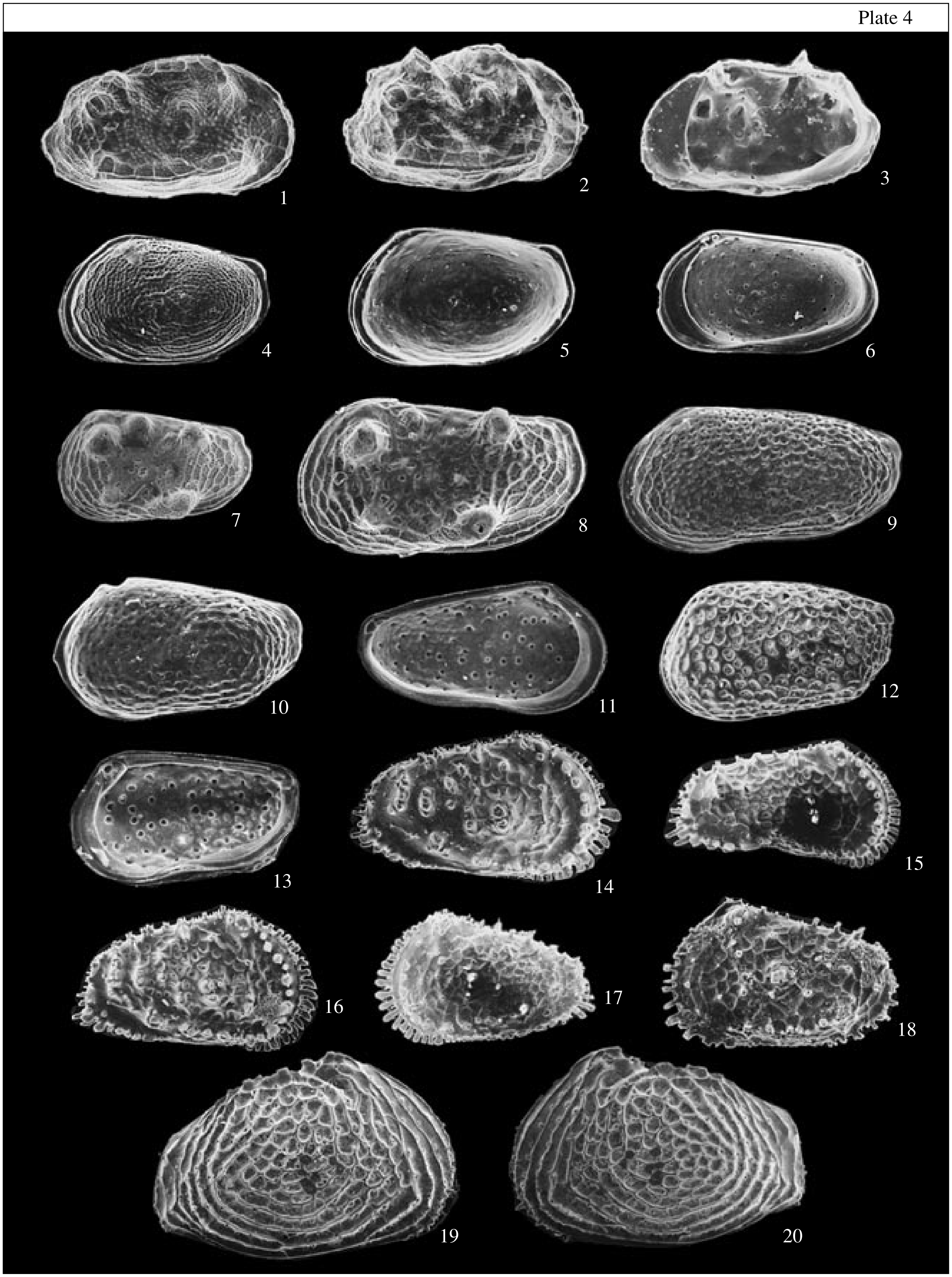

Variability. Carapaces may vary considerably in the length-to-height ratio (0.46/0.24–0.35/0.25), most likely due to sexual dimorphism. The degree of development of ribs and fossae may vary slightly.

Fossil distribution. Neogene–Quaternary deposits of the lower Yenisei and lower Pechora rivers; Pliocene of Iceland, Greenland, and Japan; Pleistocene of Scotland, Ireland, and Norway; of the lower Severnaya, lower Izhma, and lower Telza rivers; Cheshskaya Bay coast; Canada; and northeastern North America (St. Lawrence Lowlands, Champlain Sea, and the eastern Goldthwait Sea (western Newfoundland)); Pleistocene–Holocene of the North Atlantic, Pechora Sea, Severnaya Zemlya, Novaya Zemlya, Barents–Kara sea shelves, nearshore waters of the New Siberian Islands, Chukchi Sea, Japan, Gulf of Alaska, Cook Inlet, Pribylof Islands, Norton Sound, and Beaufort Sea; and Holocene of the Kola Peninsula, Spitsbergen, and the Kara and Laptev seas.

Modern distribution. Waters off Great Britain, Ireland, Franz Josef Land, Spitsbergen, Greenland, and Norway; the White, Baltic, Barents, Kara, and Laptev seas; nearshore waters of New Siberian Islands; Chukchi Sea; Gulf of Alaska; Kodiak shelf; Bering and Beaufort seas; straits of the Canadian Arctic Archipelago; Hudson Bay; Norton Sound; Atlantic coast of North America; and Labrador Sea.

Material. Thirty-five valves and 9 carapaces of good preservation, Holocene and recent surface sediments of the Laptev Sea.

Family Loxoconchidae G.O. Sars, 1925

Genus *Loxoconcha* G.O. Sars, 1866

Loxoconcha: G.O. Sars, 1866, p. 61; Brady, 1868b, p. 432; Brady et al., 1874, p. 185; Brady, 1880, p. 116; Brady and Norman, 1889, p. 183; G.O. Sars, 1928, p. 217; Klie, 1929, p. 290; Wagner, 1957, p. 64; Kashevarova et al., 1960, p. 394; Howe and Reyment, 1961, p. 313; Swain, 1963, p. 819; Naidina, 1968, p. 205; Athersuch et al., 1989, p. 173; Nikolaeva et al., 1989, p. 139; Brouwers, 1993, p. 28.

Type species. *Cythere rhomboidea* Fischer, 1855; Recent, Norway; designated by Brady and Norman (1889).

Diagnosis. Carapace medium, subrhomboidal to ovate in lateral view, often with flattened posteroventral margin. Valves almost equal, left valve slightly larger than right valve. Caudal process or lateral winglike expansion may be present. Lateral surface smoothed or punctate, puncta small. Eye spot present. Four adductor muscle scars form vertical row at mid-length of valve; uppermost scar of central two scars is larger than others. One or two scars may be slightly split. Large frontal curved scar occurs in front of them. Hinge gongylodont, in right valve it is represented by two terminal teeth and indented central groove. Frontal tooth is fringed from the ventral side with two furrows, and posterior tooth has horseshoe form. Left valve complementary.

Taxonomic composition. More than 600 species.

Comparison. From genus *Cytheromorpha* Hirschmann, 1909, similar in carapace size and surface sculpture, *Loxoconcha* differs in the morphology of the adductor muscle scars, which may be split on valves, while on those of *Cytheromorph*a they may not. In addition, carapaces of *Loxoconcha* have subrhomboidal or ovate lateral outline, while carapaces of *Cytheromorpha* have subrectangular lateral outline.

Stratigraphical range. Upper Cretaceous–Recent, brackish-water basins worldwide.

Loxoconcha venepidermoidea **Swain, 1963**

Plate 4, figs. 4–6

Loxoconcha sp.: Swain, 1961, fig. 2/22.

Loxoconcha venepidermoidea: Swain, 1963, p. 819, pl. 95, fig. 20; pl. 97, fig. 5; pl. 98, figs. 3a, 3b; text-figs. 13c, 13d; McDougall et al., 1986, pl. 7, figs. 2, 4; Brouwers et al., 1991, pl. 3, fig. 5.

Kuperiana venepidermoidea: Penney, 1990, pl. 1, figs. 4–6.

Holotype. US National Museum (USNM), Department of Microbiology, specimen's number not specified, right valve; Alaska, Lake Teshekpuk, party 47, line 30–48, shot point 16, type level 40–50 feet; Pliocene–Pleistocene, Gubik Formation.

Explanation of Plate 4

Figs. 1–3. *Palmenella limicola* (Norman, 1865): (1) right valve, external view, no. 292/96, ×100; (2) right valve, external view, no. 292/139, ×80; (3) right valve, internal view, no. 292/193, ×84; Holocene of the eastern Laptev Sea shelf.

Figs. 4–6. *Loxoconcha venepidermoidea* Swain, 1963: (4) left valve, external view, no. 292/21, ×75; (5) left valve, external view, no. 292/11, ×65; (5) right valve, internal view, no. 292/22, ×70; Holocene of the eastern Laptev Sea shelf.

Figs. 7 and 8. *Roundstonia globulifera* (Brady, 1868): (7) left valve, external view, no. 292/121, ×80; (8) left valve, external view, no. 292/218, ×130; Late Pleistocene–Holocene of the Laptev Sea.

Figs. 9–11. *Cytheromorpha macchesneyi* (Brady et Crosskey, 1871): (9) left valve, external view, no. 292/239, ×110; (10) left valve, external view, no. 292/13, ×82; (11) left valve, internal view, no. 292/14, ×80; Holocene of the Laptev Sea.

Figs. 12 and 13. *Pteroloxa cumuloidea* Swain, 1963: (12) left valve, external view, no. 292/1, ×85; (13) right valve, internal view, no. 292/2, ×85; Holocene of the eastern Laptev Sea shelf.

Figs. 14–18. *Acanthocythereis dunelmensis* (Norman, 1865): (14) right valve, external view, no. 292/148, ×53; (15) right valve, external view, no. 292/150, ×43; (16) right valve, external view, no. 292/102, ×50; (17) juvenile left valve, external view, no. 292/109, ×40; (18) juvenile left valve, external view, no. 292/103, ×88; Holocene and recent surface sediments of the Laptev Sea.

Figs. 19 and 20. *Rabilimis mirabilis* (Brady, 1868): (19) right valve, external view, no. 292/291, ×53; (20) left valve, external view, no. 292/292, ×53; Late Pleistocene–Holocene of the western Laptev Sea.

Description. The carapace is of medium size, ovate to subrhomboidal in lateral view. The anterior, posterior, anteroventral and posteroventral margins are flattened and form a rim. The dorsal margin is straight. It passes into the anterior and posterior margins through obtuse cardinal angles. The ventral margin is slightly concave in the anterior third. The anterior margin is evenly arcuately rounded, slightly bent ventrally. The posterior margin is slightly lower than anterior, arcuately rounded. The greatest length is situated at mid-height; the greatest height, at the anterior hinge edge. The lateral valve surface, except for its central part, bears numerous threadlike ribs, they run along the valve margins and form a streamlike pattern. The whole valve surface is evenly densely punctate; in the anterior upper third of the carapace, larger puncta form a semicircle.

Dimensions in mm:

Specimen, no.	L	H
292/21	0.43	0.26
292/11	0.46	0.30

Comparison. From *L. rhomboidea* (Fischer, 1855) (Athersuch et al., 1989, p. 174, fig. 69), inhabiting shallow waters of most of the British Isles and similar in size, this species differs in the rhomboidal lateral outline and in the presence of fine ribs.

Variability. Despite strong morphological stability of this species, some specimens are almost devoid of threadlike ribs and the valve surface is smoothed, probably due to partial dissolution of carapaces from the lower part of the sediment core section PS51-138 (age about 11 cal. ka, Pl. 4, fig. 5).

Fossil distribution. Pliocene of northern Greenland; Pliocene–Pleistocene of Alaska; Pleistocene of the North Sea; and Holocene of the eastern Laptev Sea.

Modern distribution. The White, Norwegian, Chukchi, Bering, Kara, and Beaufort seas; Norton Sound; and waters off northern Alaska.

Material. Eleven valves of good preservation, Holocene deposits of the eastern Laptev Sea.

Genus *Roundstonia* Neale, 1973

Roundstonia: Neale, 1973a, p. 125.

Type species. *Cythere globulifera* Brady, 1868; Recent; waters off Great Britain; by monotypy.

Diagnosis. Carapace small, subrectangular in lateral view, with flattened anterior and posterior margins, forming narrow rim; valves are equal. Surface reticulate and bears four to five large knobs, their surface punctate, puncta small. Adductor muscle scars are four, they form subvertical row. Large frontal scar and two smaller ones occur in front of them. Hinge gongylodont, in right valve it is represented by two terminal rounded teeth and indented central groove. The frontal tooth is elongated in shape. Left valve complementary.

Taxonomic composition. The author knows of only one species of this genus, *R. globulifera.* Some researchers (Brouwers et al., 2000) attribute *Cytheromorpha macchesneyi* (Brady et Crosskey, 1871) and *Bonnyannella robertsoni* (Brady, 1868) (Athersuch et al., 1989, p. 179, fig. 71) to this genus. In our opinion, this is not correct, since in his description of *Roundstonia* Neale (1973a) indicates the presence of four knobs as a diagnostic feature, while the carapace surface of *C. macchesneyi* and *B. robertsoni* is devoid of them.

Comparison. From genus *Cytheromorpha* Hirschmann, 1909, which is similar in size, carapace shape, and hinge construction, this genus differs in the presence of large knobs.

Stratigraphical range. Neogene–Recent; northern Hemisphere; high latitudes.

Roundstonia globulifera (Brady, 1868)

Plate 4, figs. 7, 8

Cythere globulifera: Brady 1868b, p. 406, pl. 31, fig. 42; Brady et al., 1874, p. 155, pl. 12, figs. 11, 12; Brady and Norman, 1889, p. 144.

Pseudocythere simpsonensis: Swain, 1963, p. 825, pl. 97, fig. 16, non figs. 4, 12, 20, non pl. 98, figs. 12a–12d.

Roundstonia globulifera: Neale and Howe, 1975, pl. 5, fig. 13; Robinson, 1978, pl. 6, fig. 7; Lord, 1980, pl. 3, figs. 15–17; Cronin, 1981, p. 410, pl. 11, figs. 3, 5–7; Lev, 1983, pl. 9, fig. 14; Neale, 1983, fig. 2; McDougall et al., 1986, pl. 10, figs. 3, 5; Whatley and Coles, 1987, pl. 4, fig. 27; Kupriyanova, 1999, pl. 2, fig. 16; Brouwers et al., 2000, p. 134, figs. 5, 6, 12 (E, F); Didié and Bauch, 2001, pl. 4, fig. 29.

Holotype. Hancock Museum in Newcastle, collection of Brady; slide number unknown, male right valve; Great Britain; Pleistocene (Neale, 1973a).

Description. The carapace is small, subrectangular in lateral view. The anterior, posterior, and anteroventral margins are flattened and form a narrow rim. The dorsal margin is straight; it passes into the anterior and posterior margins through obtuse cardinal angles. The ventral margin is not parallel to the dorsal margin, slightly concave in the anterior third. The anterior margin is evenly arcuately rounded. The posterior margin is slightly lower than the anterior margin, it is arcuately rounded. The greatest length is situated at mid-height; the greatest height, at the anterior hinge edge. The surface is evenly reticulate, the fossae are large. Four or five large knobs occur on the lateral surface. The largest knob is located just above the ventral margin approximately at mid-length of the valve, slightly closer to the posterior margin, its extremity is directed posteroventrally. One knob of a smaller size is developed in the lower anterior third of the valve. Above them, the dorsal part of the valve bears two more large knobs of which the anterior is larger and is located slightly lower, and the posterior occurs closer to the dorsal margin and slightly goes beyond the valve's outline. One more knob, the fifth, may occur in the dorsal part of the valve, directly beyond the first largest knob. The whole valve surface is punctate, the puncta are small.

Dimensions in mm:

Specimen, no.	L	H
292/121	0.38	0.22
292/218	0.36	0.18

Variability. The number of knobs varies (from four to five).

Remarks. Describing *Pseudocythere simpsonensis*, Swain (1963) attributed one specimen to this species that in our opinion should be referred to *R. globulifera.*

Fossil distribution. Late Pliocene–Pleistocene of Alaska; Pleistocene of the Pechora Sea, Alaska (Lake Teshekpuk and Canning River), North Atlantic, and Scotland; and Holocene of northeastern North America (St. Lawrence Lowlands, Champlain Sea, Goldthwait Sea in Quebec, Presumpscot Formation in Maine, De Geer Sea, and New Bruinswick), Ireland, and the Kara and Laptev seas.

Modern distribution. Waters off Ireland and Greenland; the White, Barents, Kara, Laptev, Chukchi, and Beaufort seas; Norton Sound; and the Gulf of Alaska.

Material. Forty-five valves of good preservation, Late Pleistocene–Holocene deposits of the Laptev Sea.

Genus *Cytheromorpha* Hirschmann, 1909

Cytheromorpha: Hirschmann, 1909, p. 290; G.O. Sars, 1928, p. 177; Howe and Reyment, 1961, p. 313; Kashevarova et al., 1961, p. 394; Swain, 1963, p. 818; Naidina, 1968, p. 202; Nikolaeva et al., 1989, p. 140.

Type species. *Cythere fuscata* Brady, 1869; Recent; northwestern Europe, designated by G.O. Sars (1925).

Diagnosis. Carapace small, subrectangular in lateral view, with flattened anterior and posterior margins; valves equal. Surface punctate, reticulate, or smooth. Eye tubercule absent. Four adductor muscle scars form subvertical row; frontal scar V-shaped. Hinge gongylodont, in left valve in anterior section hinge is represented by two rounded teeth, located on sides of pit, which is complementary to tooth of anterior section of right valve. Posterior section on left valve has tooth encircled with circular pit, median hinge section is smooth bar. Frontal tooth elongated. Right valve complementary.

Taxonomic composition. About 70 species.

Comparison. From *Palmoconcha* Swain et Gilby, 1974 (Athersuch et al., 1989, p. 188), similar in size, hinge construction, and carapace ornamentation, this genus differs in having subrectangular, not subovate-rhomboidal carapace outline. Comparison with genera *Loxoconcha* and *Roundstonia* are given in their descriptions.

Stratigraphical range. Eocene–Recent; brackish-water basins; worldwide.

Cytheromorpha macchesneyi (Brady et Crosskey, 1871)

Plate 4, figs. 9–11

Cythere macchesneyi: Brady and Crosskey, 1871, p. 4, pl. 2, figs. 1, 2; Brady and Norman, 1889, p. 149, pl. 17, figs. 30, 31.

Cytheromorpha macchesneyi: Neale and Howe, 1975, pl. 3, figs. 5, 6; Cronin, 1977, pl. 3, figs. 1, 2; 1981, p. 410, pl. 9, figs. 5–8; McDougall et al., 1986, pl. 9, figs. 1–3, 6; Siddiqui, 1988, pl. 1, fig. 5; Schoning and Wastegård, 1999, pl. 1, figs. 5, 6.

Pteroloxa cumuloidea: Siddiqui, 1988, pl. 1, fig. 6.

Cytheromorpha sp. A: McDougall et al., 1986, pl. 9, figs. 4, 5, 7.

Leptocythere castanea: Lev, 1983, pl. 18, fig. 10; Kupriyanova, 1999, pl. 2, fig. 13.

Leptocythere macallana: Lev, 1983, pl. 18, fig. 11; Kupriyanova, 1999, pl. 2, fig. 12.

Roundstonia macchesneyi: Brouwers et al., 2000, p. 136, figs. 7–9, 12 (I–L); Stepanova et al., 2003, pl. 1, figs. 7, 8.

Lectotype. Hancock Museum in Newcastle, N1.58.31 from the slide N2.07.07, right and left female valves; northeastern North America, St. Lawrence River valley; Pleistocene; designated by Brouwers et al. (2000).

Description. The carapace is small, elongated-subrectangular in lateral view. The anterior and posterior margins are flattened and form a narrow rim. The dorsal margin is straight, it passes into the anterior margin through an obtuse cardinal angle and into the posterior margin through a slight ledge. The ventral margin is not parallel to the dorsal margin, it is slightly concave at the center. The anterior margin is evenly arcuately rounded. The posterior margin is slightly lower than the anterior margin, arcuately rounded, slightly beveled in the lower half. The greatest length is situated at mid-height; the greatest height, at the anterior hinge edge. The surface is evenly punctate and bears numerous threadlike ribs, parallel to the valve margins, they partly cover the central part of the valve and form a fine reticulate pattern.

Dimensions in mm:

Specimen, no.	L	H
292/191	0.43	0.26
292/192	0.40	0.21

Comparison. From *C. einarssoni* Cronin, 1991, which is similar in carapace outline, size, and punctate valve surface, the species differs in having smaller puncta and threadlike ribs.

Variability. Carapace lateral outline may vary; the ratio of the anterior to posterior margin height varies. On some specimens threadlike ribs are very weakly developed.

Remarks. From the most morphologically similar *Bonnyannella robertsoni* (Brady, 1868) (Athersuch et al., 1989, p. 179, fig. 71, pl. 5, fig. 9) inhabiting waters surrounding the British Isles, *C. macchesneyi* differs in the absence of fine ridges in the posterior part of the carapace.

Siddiqui (1988, pl. 1, fig. 6) figured a valve from the Pliocene–Pleistocene deposits of the Beaufort Sea that he identified as *Pteroloxa cumuloidea* Swain, 1963. We believe that this specimen should be attributed to *C. macchesneyi.*

Lev (1983) illustrated specimens which she identified as *Leptocythere castanea* G.O. Sars, 1866 and *Leptocythere macallana*Brady et Robertson, 1869. We studied her collection in St. Petersburg and revealed that these specimens are identical to those of *C. macchesneyi.* Lev considered specimens with different heights of the anterior margin as two different species, possibly due to intraspecific variability of this species. Kupriyanova for identification of species used publications and collections of Lev, that is why she identified *C. macchesneyi* as *L. castanea* and *L. macallana.*

Fossil distribution. Upper Pliocene–Pleistocene of Alaska and the Beaufort Sea; Pleistocene of the Pechora Sea and the Severnaya Dvina River basin; Upper Pleistocene of northeastern North America (St. Lawrence Lowlands, Champlain Sea, Goldthwait Sea in Quebec, Presumpscot Formation in Maine, De Geer Sea, New Bruinswick, and Boston "blue clays"); and Holocene of Sweden and the Kara and Laptev seas.

Modern distribution. Waters off Greenland and Ireland; the Norwegian, Barents, Kara, Chukchi, Bering, Laptev, and Beaufort seas; waters off northern Alaska; Norton Sound; Hudson Bay; and the straits of the Canadian Arctic Archipelago.

Material. One hundred and six valves and 10 carapaces of good preservation, Holocene and recent surface sediments of the Laptev Sea.

Genus *Pteroloxa* Swain, 1963

Pteroloxa: Swain, 1963, p. 820.

Type species. *P. venipuncta* Swain, 1963; Pliocene–Pleistocene, Gubik Formation; Alaska, original designation (Swain, 1963).

Diagnosis. Carapace small, subrectangular in lateral view, with flattened anterior and posterior margins; valves equal. Surface reticulate or evenly punctate, puncta rounded. Eye tubercule absent. Four adductor muscle scars form subvertical row; frontal scar V-shaped. Hinge gongylodont, in left valve in anterior section it has two rounded teeth, located on sides of pit, which is complementary to tooth of the anterior section of right valve. Posterior section on the left valve has tooth encircled with pit, median hinge section is smooth bar. Right valve complementary.

Taxonomic composition. Three or four species.

Comparison. *Palmoconcha* Swain et Gilby, 1974 (Athersuch et al., 1989, p. 188) resembles *Pteroloxa* in carapace size, hinge construction, and valve ornamentation and is distinguished from it by the subrectangular lateral outline (unlike subovate-rhomboidal outline of *Pteroloxa*).

Stratigraphical range. Pliocene–Recent, brackish-water basins, Arctic.

Pteroloxa cumuloidea Swain, 1963

Plate 4, figs. 12, 13

Pteroloxa cumuloidea: Swain, 1963, p. 821, pl. 97, figs. 6a, 6b, 8; text-fig. 13e.

Holotype. US National Museum (USNM), Department of Microbiology, USNM 647948; Alaska, Fish Creek, shot hole 68, type level 70 feet; Pliocene–Pleistocene, Gubik Formation (Swain, 1963, pl. 97, fig. 8).

Description. The carapace is small, subrectangular in lateral view. The dorsal margin is almost straight, slightly convex, it passes into the anterior margin through an obtuse cardinal angle and into the posterior margin through a slight ledge. The ventral margin is not parallel to the dorsal margin, it is slightly concave at the center. The anterior margin is evenly arcuately rounded. The posterior margin is slightly lower than the anterior margin, arcuately rounded, beveled in the lower half and rounded in the upper half. In the posteroventral part of the valve there is a small ledge. The greatest length is situated at mid-height; the greatest height at the anterior hinge edge. The surface is evenly punctate, the puncta are large, round or irregularly polygonal.

Dimensions in mm:

Specimen, no.	L	H
292/1	0.43	0.24
292/2	0.46	0.25

Comparison. This species is distinguished from *P. venipuncta* Swain, 1963 from Pliocene–Pleistocene deposits of the Gubik Formation (Alaska), which is similar in carapace outline, size, and punctate surface sculpture, by having larger puncta on the valve surface and lacking protruding ridge-like fossae muri.

Variability. The shape of fossae may vary from rounded to irregularly polygonal.

Fossil distribution. Pliocene–Pleistocene of Alaska; and Holocene of the eastern Laptev Sea.

Modern distribution. The Kara and Beaufort seas.

Material. Two valves of good preservation from Holocene deposits of the eastern Laptev Sea.

Family Trachyleberididae Sylvester-Bradley, 1948

Genus *Acanthocythereis* R. C. Howe, 1963

Acanthocythereis: Howe, 1963, p. 34; Hazel, 1967, p. 34; Lev, 1983, p. 123; Athersuch et al., 1989, p. 132; Nikolaeva et al., 1989, p. 150.

Type species. *Acanthocythereis araneosa* Howe, 1963; Eocene; United States (Louisiana); original designation (Howe, 1963).

Diagnosis. Carapace medium, subrectangular to ovate or trapezoidal in lateral view, valves equal. Surface always reticulate and ornamented with spines, arranged in regular rows of variable configuration. Eye tubercule well developed. Four adductor muscle scars in subvertical row. Frontal scar U-, J-, or V-shaped. Hinge holamphidont, four-membered, consists of different elements, and has median bar in left valve. In left valve in anterior section, hinge has rounded pit with conical tooth behind it, median hinge section is notched elongated, and posterior section has deep pit. Right valve complementary.

Taxonomic composition. About 40 species.

Comparison. This genus differs from the genus *Echinocythereis* Puri, 1953, which is similar in carapace shape and hinge construction, in having a more developed sculpture that consists of spines and fossae rather than from nodes and fossae as in *Echinocythereis*.

Stratigraphical range. Upper Cretaceous (Maastrichtian)–Recent; marine deposits worldwide.

***Acanthocythereis dunelmensis* (Norman, 1865)**

Plate 4, figs. 14–18

Cythere dunelmensis: Norman, 1865b, p. 22, pl. 7, figs. 1–4; Brady, 1868b, p. 416, pl. 30, figs. 1–12; Brady et al., 1874, p. 168, pl. 5, figs. 13–20; Brady and Norman, 1889, p. 168; G.O. Sars, 1928, p. 195, pl. 89.

Cythereis dunelmensis: Akatova, 1957, p. 432; Elofson, 1941, p. 296, text-figs. 8–11; 1969, p. 72.

Trachyleberis? *rastromarginata*: Swain, 1961, fig. 2/32.

Actinocythereis sp.: Swain, 1961, fig. 2/36.

Trachyleberis cf. *dunelmensis*: Woszidlo, 1962, p. 81, pl. 4, figs. 8, 9.

Cletocythereis noblissimus: Swain, 1963, p. 824, pl. 98, fig. 5, pl. 99, figs. 15a, 15b, text-fig. 10a.

Cletocythereis dunelmensis minor: Bassiouni, 1965, p. 513, pl. 2, fig. 9.

Cletocythereis dunelmensis dunelmensis: Bassiouni, 1965, p. 513, pl. 2, fig. 8.

Cletocythereis elofsoni elofsoni: Bassiouni, 1965, p. 514, pl. 2, figs. 4, 5.

Cletocythereis elofsoni abbreviata: Bassiouni, 1965, p. 514, pl. 2, figs. 6, 7.

Trachyleberis dunelmensis: Caralp et al., 1967, pl. 13, fig. 1.

Acanthocythereis noblissima: Schmidt, 1967, p. 488, pl. 62, figs. 12–16.

Acanthocythereis agapensis: Lev, 1983, p. 125, pl. 11, figs. 1–6.

Acanthocythereis dunelmensis: Hazel, 1967, p. 34; Neale and Howe, 1975, pl. 1, figs. 11–16; Cronin, 1977, pl. 3, fig. 8; Rosenfeld, 1977, p. 21, pl. 5, figs. 65–68; Lord, 1980, pl. 1, figs. 8–13; Cronin, 1981, p. 400. pl. 8, figs. 1, 2; Lev, 1983, p. 124, pl. 10, figs. 1–7; McDougall et al., 1986, pl. 13, figs. 2–4; Cronin and Ikea, 1987, p. 84, pl. 1, figs. 1, 4; Brouwers, 1988, figs. 5–7; Athersuch et al., 1989, p. 133, fig. 52, pl. 3, fig. 10; Cronin, 1989, pl. 2, fig. 9; Brouwers, 1993, p. 3, pl. 1, figs. 1–5; pl. 2, fig. 1; pl. 16, fig. 1; Lord et al., 1993, pl. 2, figs. 11, 12; Irizuki, 1994, pl. 2, fig. 3; Kupriyanova, 1999, pl. 1, fig. 12; Stepanova et al., 2003, pl. 3, figs. 4, 5.

?*Acanthocythereis dunelmensis*: Ingram, 1998, pl. 1, figs. 9–12.

Holotype. Natural History Museum, London, slide N1911.11.8 female carapace; Seaham, Durham, northeastern England; Recent.

Description. The carapace is of medium size, subrectangular to ovate or trapezoidal in lateral view, moderately inflated laterally, with the maximum inflation in the central part of carapace, the anterior and posterior margins are flattened. The dorsal margin is straight, long, slightly bent towards the posterior margin. The ventral margin is not parallel to the dorsal margin, it is slightly concave in the anterior third. The anterior margin is slightly higher than the posterior margin, it is arcuately rounded. The posterior margin is rounded triangular, gently beveled on the posteroventral part. The greatest length is situated at mid-height; the greatest height, in the anterior third of the valve. The central muscle scar is very distinct, and bears several short vertical spines. The eye tubercule is large, rounded in shape. The valve lateral surface is covered with numerous small spines, grouped in subvertical rows. Spines along the anterior and posterior margins are massive and flattened. A bow-shaped row of rare small spines subvertical to the valve's surface runs on the anterior part of the valve parallel to the anterior margin. This row extends on the ventral side, where spines are located closer to each other, and become larger and more flattened; the row ends at the mid-length of the valve on male carapaces and closer to the posterior margin on female carapaces. Below this row, several small short spines may be observed along the ventral margin. Along the dorsal margin several splintered spines occur. The valve surface between the spines is reticulate, the fossae are large, with low muri. On the anterior and posterior margins the fossae muri become considerably more slender.

Age-related changes. Juvenile valves differ considerably from adult valves, they have a subtriangular lateral outline and a less developed ornamentation represented by spines and fossae.

Sexual dimorphism. Sexual dimorphism is strongly pronounced: female carapaces are shorter than those of males. Besides, the row of spines running parallel to the ventral margin is shorter on male carapaces and longer on female.

Dimensions in mm:

Specimen, no.	L	H
292/108juv.	0.39	0.26
292/109juv.	0.45	0.30
292/107juv.	0.51	0.35
292/104	0.85	0.60
292/105	0.90	0.55

Variability. Surface sculpture of *A. dunelmensis* is highly variable, which is primarily due to the degree of preservation of the material. Very often spines may be partly broken or rows of spines disturbed. Carapaces may vary greatly in length/height ratio. Carapace outline is also variable from rectangular-ovate to trapezoidal.

Comparison. From *A. multispicata* R. Howe et H. Howe, 1973 from Upper Eocene deposits of the United States (Mississippi; Nikolaeva et al., 1989), which is similar in carapace shape and ornamentation, *A. dunelmensis* differs in having spines arranged in regular rows.

Remarks. Many scientists redescribed *A. dunelmensis* or attributed specimens of this species to other species due to its high morphological variability. Swain

(1961) illustrated specimens from the Gubik Formation (Pliocene–Pleistocene of Alaska) that he identified as *Trachyleberis*? *rastromarginata* and *Actinocythereis* sp. We believe that these specimens should be referred to as *A. dunelmensis.* Later, Swain (1963) described a new species, *Cletocythereis noblissimus*, from the same location, which we also consider to be a synonym of *A. dunelmensis* (also Hazel, 1967; Lev, 1983; Brouwers, 1993). Schmidt reconsidered the generic affiliation of the species described by Swain and described *Acanthocythereis noblissima*; thus, we also consider to be a synonym of *A. dunelmensis.*

Bassiouni (1965) in the publication devoted to Pleistocene ostracodes of Denmark described a new species with two subspecies and one new subspecies: *Cletocythereis dunelmensis minor, Cletocythereis dunelmensis dunelmensis, Cletocythereis elofsoni elofsoni*, and *Cletocythereis elofsoni abbreviata.* In our opinion, all specimens illustrated should be attributed to *A. dunelmensis.*

Lev (1983) described a new species, *A. agapensis*, which was distinguished from *A. dunelmensis* by the carapace outline (*A. dunelmensis* has rectangular-ovate carapace, and *A. agapensis* has trapezoidal carapace). We consider these differences as intraspecific variability.

Fossil distribution. Upper Miocene of northern Sakhalin (Okobikaiskaya Formation) and Japan; Neogene–Quaternary marine deposits of the northern Russian Platform and western Siberia (from the Severnaya Dvina River to the Yenisei River), of the Islands Vaigach, Arctic Institute, Isachenko, and Ushakov, Severnaya Zemlya, and Novaya Zemlya, of the Chukchi Sea, of Alaska (Gubik Formation), of the Beaufort Sea, and of Japan; Pleistocene of northern Germany, Denmark, Norway, North Sea, and Great Britain; Pleistocene–Holocene of the North Atlantic, of Greenland, of the Laptev, Chukchi, and Bering seas, of Cook Inlet, of Kodiak shelf, and of the Pribylof Islands; Holocene of northeastern North America (St. Lawrence Lowlands, Champlain Sea, Goldthwait Sea (western Newfoundland), and Presumpscot Formation); and Holocene of the Bay of Biscay and the Kara and Laptev seas.

Modern distribution. Waters off Great Britain and the Hebrides, waters off Ireland, Iceland, and Franz Josef Land; the North Sea; waters off Norway and Greenland; the White, Barents, Kara, Laptev, East Siberian, Chukchi, Beaufort, Bering, and Labrador seas; the Gulf of Alaska; Norton Sound; Hudson Bay; the straits of the Canadian Arctic Archipelago; and the Bay of Biscay.

Material. Four hundred and twenty-one valves and 65 carapaces of good preservation, Holocene and recent surface sediments of the Laptev Sea.

Genus *Rabilimis* Hazel, 1967

Rabilimis: Hazel, 1967, p. 38; Lev, 1983, p. 131; Nikolaeva et al., 1989, p. 165.

Type species. *Cythere mirabilis* Brady, 1868; Arctic seas; original designation (Hazel, 1967).

Diagnosis. Carapace of medium to large size, subtriangular and trapezoidal in lateral view, valves almost equal. Surface reticulate, fossae large; rows of fossae run parallel to valve margins. Eye tubercule present. Four adductor muscle scars form subvertical row, two frontal scars are also present. Hinge holamphidont, four-membered, consists of different elements, and has median bar in left valve. In left valve in anterior section, hinge has rounded deep pit with triangular tooth beyond it that is connected to long smooth median bar, and in posterior section it has bow-shaped pit. Narrow groove in dorsal part of valve stretches parallel to median bar. Right valve complementary.

Taxonomic composition. About ten species.

Comparison. The genus is distinguished from *Echinocythereis* Puri, 1953 (Nikolaeva et al., 1989, p. 163), which is similar in construction of the hinge, by having reticulate ornamentation of the valve surface (unlike tuberculous ornamentation of *Echinocythereis*).

Stratigraphical range. Oligocene–Recent, marine deposits worldwide.

Rabilimis mirabilis (Brady, 1868)

Plate 4, figs. 19, 20

Cythere mirabilis: Brady, 1868b, p. 415, pl. 29, figs. 7, 8; Brady et al., 1874, p. 167, pl. 7, figs. 22–25; Brady and Norman, 1889, p. 168.

Cythereis mirabilis: Akatova, 1946, p. 227, text-figs. 6, 7.

Trachyleberis mirabilis: Kashevarova et al., 1960, text-fig. 1118.

Rabilimis mirabilis: Robinson, 1978, pl. 2, fig. 6, pl. 6, fig. 9; Lord, 1980, pl. 3, figs. 1–4; Siddiqui, 1988, pl. 2, fig. 6; Nikolaeva et al., 1989, text-fig. 297; Hartmann, 1993, p. 241, pl. 1, figs. 5, 6; Lord et al., 1993, pl. 2, fig. 10; Whatley et al., 1998, pl. 3, fig. 17; Kupriyanova, 1999, p. 1, fig. 2; Didié and Bauch, 2001, pl. 4, fig. 8.

Type material. For description of this species, Brady (1868b) originally used material from the Pleistocene–Recent deposits of Errol (Scotland). The current location of the material is unknown. Revision of this species has not been undertaken; holotype and lectotype have not been designated.

Description. The carapace is large, thick-shelled, and subtriangular in lateral view, with a flattened posterior margin. The dorsal margin is straight, bent towards the posterior margin. The ventral margin is gently convex, concave at the center. The anterior margin is arcuately rounded, the posterior margin is considerably lower than the anterior margin and is rounded-triangular to rectangular in shape. The greatest length is situated at mid-height; the greatest height, at the anterior hinge edge. The surface is reticulate, the fossae are large, with thick muri. The fossae are arranged in rows parallel to the valve margins, in the central part of the valve they are arranged concentrically. On the dorsal margin fossae muri project beyond the valve outline and give the dorsal margin denticulated appearance. The lower part of the anterior margin bears several spines. The lower third of the posterior margin also bears several spines.

Dimensions in mm:

Specimen, no.	L	H
292/291	1.01	0.65
292/292	0.98	0.61

Comparison. From *Rabilimis septentrionalis* (Brady, 1866) from bottom surface sediments of the Baffin Bay (Brady and Norman, 1889, p. 149, pl. 16, figs. 13, 14), similar in size and surface ornamentation, the species differs in having subtriangular, not subrectangular, lateral outline. Besides, fossae muri on carapaces of *R. septentrionalis* do not go beyond the carapace outline on the dorsal margin.

Variability. Morphological characteristics on the adult carapaces are quite stable, carapaces may slightly differ in height.

Age-related changes. Juvenile carapaces of genus *Rabilimis* Hazel, 1967, in particular those of *Rabilimis mirabilis* (Brady, 1868) and *Rabilimis septentrionalis* (Brady, 1866), differ considerably from carapaces of adult specimens. Juvenile valves of these species have solely subtriangular outline, flattened anterior and posterior margins, and weakly developed reticulate ornament (Pl. 5, fig. 4). It is apparent that the species *R. mirabilis* and *R. septentrionalis* are closely related, since their juvenile carapaces are practically identical and, thus, difficult to identify.

Fossil distribution. Pliocene–Pleistocene deposits of the Taimyr, Novaya Zemlya, and Severnaya Zemlya; of the lower reaches of the Ob, Pechora, Yenisei, Severnaya Dvina, and Onega rivers; of the Arctic Institute Islands, Isachenko Island, and the New Siberian Islands nearshore area; Pleistocene of Great Britain, Norway, and northern Germany; and Holocene of the eastern Kara and Laptev seas.

Modern distribution. North Atlantic, waters off Great Britain, Ireland, Greenland, Franz Josef Land, Spitsbergen, and Norway and the White, Barents, Kara, Laptev, East Siberian, Chukchi, and Beaufort seas.

Material. Two hundred and sixty-three valves and 2 carapaces of good preservation, Pleistocene–Holocene and recent surface sediments of the Laptev Sea.

Rabilimis septentrionalis (Brady, 1866)

Plate 5, figs. 1–3

Cythere septentrionalis: Brady, 1866, p. 375, pl. 60, figs. 4a–4f; Brady and Norman, 1889, p. 149, pl. 16, figs. 13, 14.

Cythereis septentrionalis: Akatova, 1957, p. 430, text-fig. 3.

Pseudocythereis aff. *septentrionalis*: Swain, 1961, fig. 2.38.

Pseudocythereis simpsonensis: Swain, 1963, p. 825, pl. 97, figs. 4, 12, 20; pl. 98, fig. 12, text-fig. 12a, non pl. 97, fig. 16.

Echinocythereis simpsonensis: Schmidt, 1967, p. 487, pl. 62, figs. 1–11.

Rabilimis paramirabilis: Lev, 1983, p. 132, pl. 12, figs. 2–4.

Rabilimis septentrionalis: Cronin and Ikeya, 1987, pl. 1, fig. 14; Siddiqui, 1988, pl. 2, fig. 2; Kupriyanova, 1999, p. 1, fig. 1; Stepanova et al., 2003, pl. 3, fig. 6.

non *Rabilimis septentrionalis*: Penny, 1990, pl. 1, figs. 11, 12.

Type material. For description of this species Brady and Norman (1889) originally used material from recent sediments of the Baffin Sea. The current location of the type material is unknown. Revision of this species has never been undertaken; holotype and lectotype have not been designated.

Description. The carapace is large, thick-shelled, and subrectangular in lateral view. The dorsal margin is straight or slightly convex, it passes into the anterior and posterior margins through massive hinge protuberances. The ventral margin is straight, slightly concave at the center, almost parallel to the dorsal margin. The anterior margin is arcuately rounded. The posterior margin is slightly lower than the anterior margin, of a rounded-triangular shape. The greatest length is situated at mid-height; the greatest height, at the anterior hinge edge. The surface is reticulate, the fossae are large, with thick muri. The fossae are arranged in rows parallel to the valve margins, in the central part of the valve they are arranged concentrically.

Dimensions in mm:

Specimen, no.	L	H
292/16	0.70	0.41
292/17	0.72	0.40

Comparison. From *R. paramirabilis* Swain, 1963 from Pliocene–Pleistocene deposits of Alaska (Swain, 1963, p. 826, pl. 98, fig. 11, text-fig. 12b), similar in size and valve ornamentation, this species is distinguished by having a subrectangular, not ovate-triangular, elongated lateral outline. Comparison with *R. mirabilis* is given in the description of the latter.

Morphological variability of adult carapaces is insignificant and is expressed in slight variations in the length/height ratio of carapaces.

Remarks. Swain (1963) described *Pseudocythereis simpsonensis*, which was later attributed by Schmidt (1967) to *Echinocythereis* Puri, 1953. In the first description, this species was compared with *R. septentrionalis* and as distinguishing features were pointed out the following characters: more fragile fossae muri forming rows parallel to the valve margins and the absence of spines on the anterior and posterior margins of the carapace. Distinguishing features that were indicated by Swain are typical of *R. mirabilis* and do not characterize *R. septentrionalis.* That is why we, following Hazel (1967), believe that Swain attributed specimens of *R. mirabilis* to *R. septentrionalis* and described *R. septentrionalis* as a new species, *Pseudocythereis simpsonensis.*

Lev (1983) illustrated specimens that were identified as *R. paramirabilis.* However, they have subrectangular lateral outline, typical of *R. septentrionalis*, and not of *R. paramirabilis.*

Plate 5

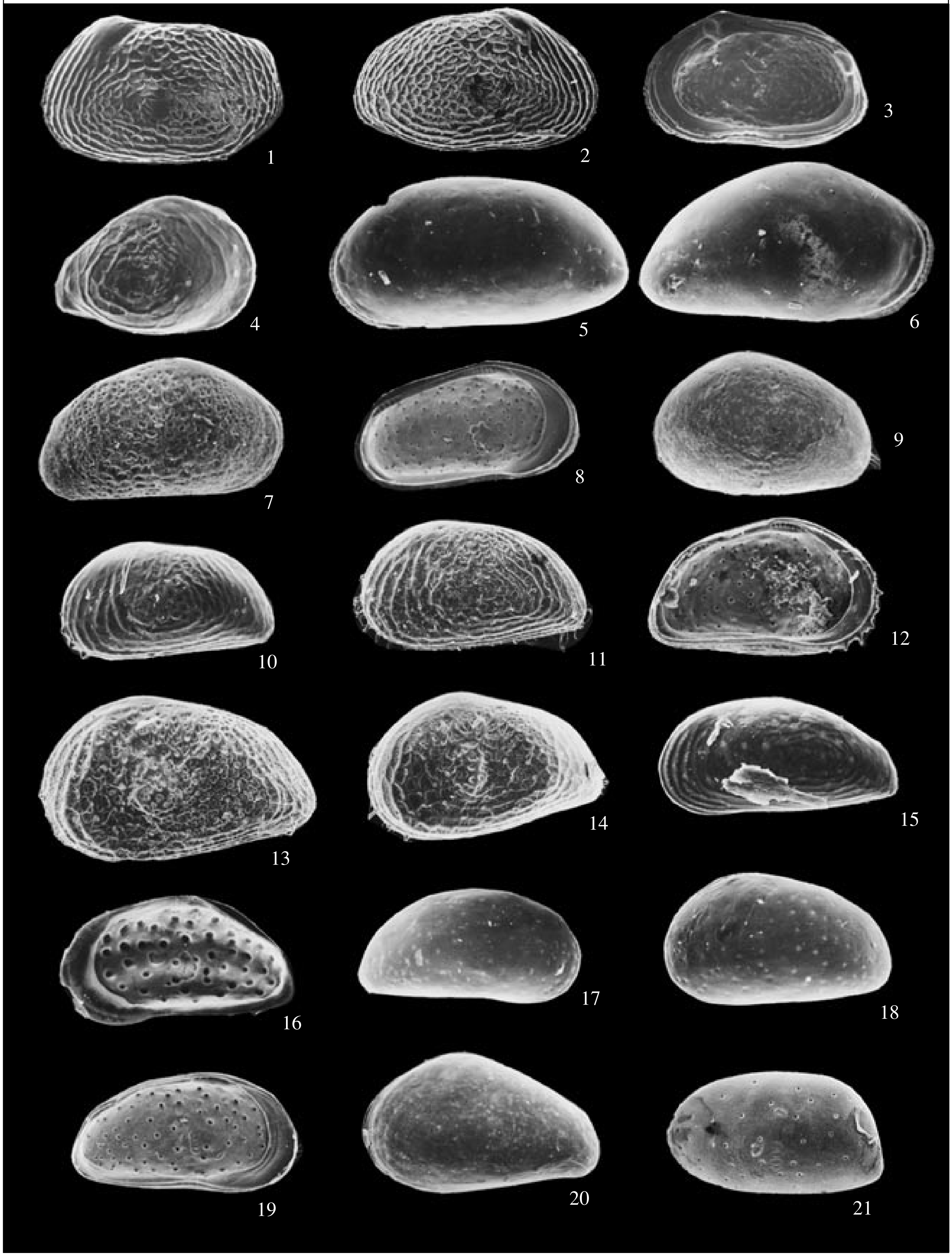

Penny (1990) illustrated valves that he identified as *R. septentrionalis*, but their affiliation to this species is not apparent to us, since carapace outline is typical of *R. paramirabilis.*

Fossil distribution. Neogene–Quaternary deposits of the Bol'shaya Kheta River basin (Varomiyakha and Bol'shoe Khodito rivers), Severnaya Zemlya, Beaufort Sea, Alaska, and Japan; Pleistocene of the lower Severnaya Dvina River and the Pechora Sea; and Holocene of the eastern Kara and Laptev seas.

Modern distribution. Waters off Greenland and Ireland, the White and Norwegian seas, waters off Spitsbergen, and the Barents, Kara, Laptev, Chukchi, and Baffin seas, as well as Norton Sound and the straits of the Canadian Arctic Archipelago.

Material. Three hundred and thirty-three valves and 42 carapaces of good preservation, Holocene and recent surface sediments of the Laptev Sea.

Family Cytherideidae G.O. Sars, 1925

Genus *Sarsicytheridea* Athersuch, 1982

Sarsicytheridea: Athersuch, 1982, p. 240; Athersuch et al., 1989, p. 116; Nikolaeva et al., 1989, p. 181.

Type species. *Cythere bradii* Norman, 1865; nearshore waters of England; Recent; designated by Kollman (1960).

Diagnosis. Carapace medium to large, elongated ovate or subrectangular in lateral view, left valve larger than right valve. Surface smooth or punctate, puncta small to large. Eye tubercule absent. Four adductor muscle scars form subvertical row in anterior third of valve. Hinge antimerodont, with elongated terminal elements and median bar in left valve. In right valve it represents two splintered terminal teeth, located on sides of notched groove. Left valve complementary.

Taxonomic composition. About 15 species.

Comparison. From similar in size and hinge construction *Miocyprideis* Kollman, 1960, the genus differs in lacking marginal spines and reticulation.

Stratigraphical range. Oligocene–Recent, Eurasia.

Sarsicytheridea bradii (Norman, 1865)

Plate 5, figs. 5, 6

Cythere bradii: Norman, 1865a, p. 192.

Cytheridea papillosa: G.O. Sars, 1928, p. 159, pl. 63, 74, fig. 1.

Eucytheridea bradii: Neale and Howe, 1975, pl. 4, fig. 10; Robinson, 1978, pl. 6, fig. 3; Cronin, 1981, p. 395, pl. 3, figs. 1, 2, 4; Lev, 1983, p. 112, pl. 8, figs. 1–6; Nikolaeva et al., 1989, text-fig. 366.

Eucytheridea bairdii: Rosenfeld, 1977, p. 21, pl. 4, figs. 53–56.

Cytheridea punctillata: Benson et al., 1983, pl. 1, figs. 1, 2.

Sarsicytheridea bradii: McDougall et al., 1986, pl. 8, figs. 6–8; Cronin and Ikeya, 1987, p. 76, pl. 1, fig. 12; Siddiqui, 1988, pl. 2, fig. 2; Athersuch et al., 1989, p. 116, fig. 45, pl. 3, fig. 3; Brouwers et al., 1991, pl. 4, fig. 4; Lord et al., 1993, pl. 2, fig. 6; Ingram, 1998, pl. 1, fig. 14; Stepanova, 2002, pl. 1, fig. 6; Stepanova et al., 2003, pl. 3, fig. 14.

Lectotype. Hancock Museum in Newcastle; no. 1.05.21, female left valve; Holy Island, northeastern England; Recent; designated by Van den Bold (1961).

Description. The carapace is of medium size, elongated-ovate in lateral view, with a flattened anterior margin. The dorsal margin is straight or slightly convex, gently beveled towards the anterior and posterior margins. The ventral margin is slightly concave in the anterior third. The anterior margin is arcuately rounded, slightly bent ventrally. The right and left valves differ in outline: the right valves have an almost subtriangular outline, while the left valves' outline is almost subrectangular. The posterior margin is slightly lower than the anterior margin, arcuately rounded, or slightly acuminate, beveled in the upper part and bent ventrally. The greatest length is situated at mid-height; the greatest height, at the anterior hinge edge. The surface is smooth with rare small puncta.

Explanation of Plate 5

Figs. 1–3. *Rabilimis septentrionalis* (Brady, 1866): (1) left valve, external view, no. 292/16, ×60; (2) right valve, external view, no. 292/95, ×57; (3) right valve, internal view, no. 292/17, ×55; Holocene of the eastern Laptev Sea shelf.

Fig. 4. *Rabilimis* sp. juv.: right valve, external view, no. 292/88, ×100; Holocene of the eastern Laptev Sea shelf.

Figs. 5 and 6. *Sarsicytheridea bradii* (Norman, 1864): (5) left valve, external view, no. 292/207, ×67; (6) right valve, external view, no. 292/208, ×65; recent surface sediments of the western Laptev Sea.

Figs. 7–9. *Sarsicytheridea punctillata* (Brady, 1864): (7) right valve, external view, no. 292/171, ×63; (8) left valve, internal view, no. 292/170, ×56; (9) juvenile left valve, external view, no. 292/56, ×100; recent surface sediments of the western Laptev Sea.

Figs. 10–12. *Heterocyprideis sorbyana* (Jones, 1857): (10) left valve, external view, no. 292/3, ×50; (11) left valve, external view, no. 292/173, ×47; (12) left valve, internal view, no. 292/4, ×55; Holocene and recent surface sediments of the Laptev Sea.

Figs. 13 and 14. *Heterocyprideis fascis* (Brady et Norman, 1889): (13) left valve, external view, no. 292/206, ×55; (14) left valve, external view, no. 292/205, ×65; recent surface sediments of the southern Laptev Sea.

Figs. 15 and 16. *Eucythere argus* (Sars, 1866): (15) left valve, external view, no. 292/23, ×100, (16) right valve, internal view, no. 292/24, ×100; Holocene of the eastern Laptev Sea shelf.

Figs. 17–20. *Paracyprideis pseudopunctillata* Swain, 1963: (17) right valve, external view, no. 292/116, ×52; (18) left valve, external view, no. 292/118, ×55; (19) left valve, internal view, no. 292/8, ×52; (20) juvenile left valve, external view, no. 292/132; Holocene and recent surface sediments of the Laptev Sea.

Fig. 21. *Krithe glacialis* Brady, Crosskey et Robertson, 1874: (21) female left valve, external view, no. 292/65, ×57; recent surface sediments of the western Laptev Sea.

Age-related changes. Juvenile valves differ considerably from adult valves, they have a subtriangular lateral outline, and the posterior end of the valve has a rostral outline.

Dimensions in mm:

Specimen, no.	L	H
292/207	0.57	0.32
292/201	0.68	0.36

Comparison. From *S. punctillata* (Brady, 1865), inhabiting nearshore waters of Great Britain and Arctic seas, similar in carapace shape and size, the species differs in having smooth carapace surface with rare puncta, unlike densely punctate surface of *S. punctillata.*

Variability. Carapaces may vary insignificantly in outline: the shape of the posterior margin varies from more acuminate to broadly arcuate.

Remarks. G.O. Sars (1928) illustrated valves identified as *Cytherideа papillosa* Bosquet 1852. In our opinion (also Athersuch et al., 1989), they belong to *S. bradii.* Rosenfeld (1977) published photographs of valves that were identified as *Cytheridea bairdii* Sars, 1866; in our opinion, these specimens belong to *S. bradii.* Benson et al. (1983) identified and illustrated a valve of *Cytheridea punctillata* Brady, 1865. The carapace outline and surface sculpture (smooth surface with rare puncta) of the illustrated specimen are in complete agreement with the characterization of *S. bradii*, and do not agree with that of *S. punctillata*, which has a densely punctate valve surface.

Fossil distribution. Neogene–Quaternary deposits of the lower reaches of the Ob, lower Pechora, lower Yenisei, lower Mezen, and lower Severnaya Dvina rivers; Kola Peninsula; Taimyr; Chukchi Peninsula; and Islands Vaigach, Novaya Zemlya, Arctic Institute, Ushakov, and the Severnaya Zemlya Archipelago; and Alaska; Pliocene of Greenland; Pliocene–Pleistocene of Japan and the Beaufort Sea; Pleistocene of Great Britain, Norway, Canada, northern Germany, Denmark, northeastern North America (St. Lawrence Lowlands, Champlain Sea, Goldthwait Sea (western Newfoundland and Quebec), Presumpscot Formation (in Maine), De Geer Sea, New Bruinswick, and Boston “blue clays”); and Holocene of the eastern Kara Sea and Laptev seas.

Modern distribution. North Atlantic, waters off Great Britain, the Hebrides, Ireland, Greenland, Franz Josef Land, Spitsbergen, Novaya Zemlya, and Norway; the White, Baltic, North, Barents, Kara, Laptev, East Siberian, and Chukchi seas; nearshore waters of northern Aleutian Islands, Anadyr Bay, Bering and Baffin seas, Ungava Bay, Frobisher Bay, Norton Sound, Hudson Bay, nearshore waters of Alaska, straits of the Canadian Arctic Archipelago, Newfoundland, and the Labrador Sea.

Material. Twenty-seven valves of good preservation, Recent surface sediments of the Laptev Sea.

Sarsicytheridea punctillata (Brady, 1865)

Plate 5, figs. 7–9

Cytheridea punctillata: Brady, 1865, p. 189, pl. 9, figs. 9–11; Brady, 1868b, p. 424, pl. 26, figs. 35–38, pl. 28, figs. 17–20; Brady et al., 1874, p. 177, pl. 6, figs. 1–11; G.O. Sars, 1928, p. 160, pl. 74, fig. 2; Elofson, 1941, p. 265; Caralp et al., 1967, pl. 13, fig. 3.

Cytheridea papillosa: Gaevskaya, 1948, p. 180, pl. 41, figs. 2, 3.

Eucytheridea punctillata: Woszidlo, 1962, pl. 4, figs. 3, 4; Bassiouni, 1965, pl. 1, figs. 12, 13; Neale, 1975, pl. 4, figs. 6, 7; Neale and Howe, 1975, pl. 4, figs. 6, 7; Cronin, 1977, pl. 3, fig. 3, 1981, p. 396, pl. 2, figs. 6–8, pl. 3, figs. 7, 9; Rosenfeld, 1977, p. 18, pl. 4, figs. 57–60; Lord, 1980, pl. 3, figs. 9–11; Lev, 1983, p. 114, pl. 8, figs. 7–13.

Sarsicytheridea punctillata: Athersuch et al., 1985, p. 154, pl. 1, figs. 9–11; pl. 2, figs. 9, 10; McDougall et al., 1986, pl. 7, figs. 6, 8; Athersuch et al., 1989, p. 118, fig. 46, pl. 3, fig. 4; Mostafari, 1990, pl. I, fig. 6; Brouwers et al., 1991, pl. 4, fig. 5; Ingram, 1998, pl. 1, figs. 1–8; Kupriyanova, 1999, pl. 1, fig. 7; Stepanova, 2002, pl. 1, figs. 2–5; Stepanova et al., 2003, pl. 3, figs. 11–13.

Type material. The type material from the collection of Brady in the Hancock Museum in Newcastle has not been located and is considered to be lost. It originated from England, Norfolk, Brickearth, Nar valley; Pleistocene (Athersuch et al., 1989).

Description. The carapace is medium to large, elongated-trapezoidal-ovate in lateral view, moderately evenly inflated laterally. The dorsal margin is straight, slightly bent towards the posterior margin and beveled towards the anterior and posterior margins. The ventral margin is slightly concave in the anterior third. The anterior margin is gently arcuately rounded, beveled from the dorsal side. The posterior margin is slightly lower than the anterior margin, evenly arcuately rounded, slightly beveled from the dorsal side. The greatest length is situated at mid-height; the greatest height, at the anterior hinge edge. The surface is punctate, the puncta are small, sometimes two or three puncta are joined in one pit. The valve surface bears numerous pore pits, pore canals are simple.

Sexual dimorphism. Sexual dimorphism is very significant: female carapaces are shorter and higher than those of males.

Age-related changes. Juvenile valves have a rounded-triangular lateral outline.

Dimensions in mm:

Specimen, no.	L	H
292/171	0.7	0.41
292/170	0.7	0.4

Comparison. From *S. macrolaminata* (Elofson, 1939), similar in carapace outline and size, the species differs in having punctate (not smooth) valve surface and in lacking sievelike pores. The comparison with *S. bradii* is given in its description.

Variability. The degree of puncta development on the valve surface may insignificantly vary.

Fossil distribution. Neogene–Quaternary marine deposits of the lower reaches of the Yenisei, Ob, Pechora, Mezen, and Severnaya Dvina rivers; Kola Peninsula; Taimyr; as well as Islands Vaigach, Novaya Zemlya, Arctic Institute, Isachenko, Schmidt, Ushakov, and Severnaya Zemlya; Pliocene of Greenland; Pliocene–Pleistocene of Alaska; and Pleistocene of the North Sea, Great Britain, Norway, Denmark, and northeastern North America (St. Lawrence Lowlands and the Champlain Sea).

Modern distribution. the North Atlantic, waters off the Scandinavian Peninsula, Iceland, Ireland, Greenland, Spitsbergen, and Franz Josef Land; the Norwegian, Baltic, White, Barents, Kara, and western Laptev seas; nearshore waters of New Siberian Islands, East Siberian and Chukchi seas, Fram Strait, Frobisher Bay, Hudson Bay, and the straits of the Canadian Arctic Archipelago.

Material. Two hundred and fifty-eight valves and 32 carapaces of good preservation, Holocene deposits of the western Laptev Sea and recent surface sediments of the entire area of the Laptev Sea.

Genus *Heterocyprideis* Elofson, 1941

Heterocyprideis: Elofson, 1941, p. 258; Howe et al., 1961b, p. 276; Swain, 1963, p. 810; Elofson, 1969, p. 33; Nikolaeva et al., 1989, p. 181.

Type species. *Cytheridea sorbyana* Jones, 1857; England; by monotypy.

Diagnosis. Carapace medium to large, strongly inflated, subtriangular or pear-shaped in lateral view. Surface reticulate or coarsely punctate; fossae muri form ribs and wrinkles, arranged in rows running parallel to valve margins. Anterior margin with marginal spines, on posterior margin they occur only on right valve. Eye tubercule absent. Four adductor muscle scars form subvertical row on mid-length of valve. Hinge antimerodont. In right valve it represents terminal teeth, splintered into six or seven units, and median notched groove. Left valve complementary.

Taxonomic composition. About 15 species.

Comparison. The genus is distinguished from the genus *Cytheridea* Bosquet, 1852, which is similar in carapace outline and size and in surface sculpture, by hinge construction: *Heterocyprideis* Elofson, 1941 has antimerodont hinge, and *Cytheridea* has entomodont hinge.

Stratigraphical range. Pliocene–Recent; Northern Eurasia.

Heterocyprideis sorbyana (Jones, 1857)

Plate 5, figs. 10–12

Cytheridea sorbyana: Jones, 1857, p. 44; Brady, 1868b, p. 428, pl. 29, figs. 1–6; Brady et al., 1874, p. 180, pl. 7, figs. 7–12; Brady and Norman, 1889, p. 178; Hirschmann, 1909, p. 286; G.O. Sars, 1928, p. 157, pl. 72, fig. 2.

Heterocyprideis sorbyanoides: Swain, 1963, p. 810, pl. 95, figs. 7a, 7b, pl. 97, figs. 1a, 1b, text-figs. 6a, 6b; Bassiouni, 1965, pl. 2, figs. 10, 11.

Heterocyprideis sorbyana: Elofson, 1941, p. 258, text-figs. 1–5; Akatova, 1957, p. 428; Howe et al., 1961b, fig. 205.3; Woszidlo, 1962, pl. 4, fig. 5; Caralp et al., 1967, pl. 13, fig. 2; Elofson, 1969, p. 35, figs. 1–5; Neale and Howe, 1975, pl. 4, figs. 3, 8, 9; Cronin, 1977, pl. 3, figs. 11, 12; 1981, p. 395, pl. 2, figs. 1–4; Rosenfeld, 1977, p. 21, pl. 3, figs. 37–41; Robinson, 1978, pl. 2, figs. 3a–3c; Lord, 1980, pl. 1, fig. 5; Lev, 1983, p. 110, pl. 7, figs. 1–8; McDougall, et al., 1986, pl. 6, figs. 1–4; Siddiqui, 1988, pl. 1, fig. 8; Nikolaeva et al., 1989, text-figs. 362, 363; Brouwers et al., 1991, pl. 1, fig. 5; Kupriyanova, 1999, pl. 1, fig. 3; Stepanova et al., 2003, pl. 3, figs. 7, 8.

Type material. Jones (1856) described this species on the basis of the material from Pleistocene deposits of England, Bridlington Crag, Yorkshire. The current location of the material is unknown. Revision of this species has not been undertaken; holotype and lectotype have not been designated.

Description. The carapace is medium to large, thick-shelled, subtriangular to pear-shaped in lateral view. The dorsal margin is straight, or slightly convex, bent towards the posterior margin, and passes into the anterior margin through an obtuse cardinal angle and, very gradually, to the posterior margin. The ventral margin is slightly concave in the anterior third. The anterior margin is broadly arcuately rounded, beveled from the upper part, it bears on average seven marginal spines. The posterior margin is lower than the anterior margin, steeply beveled ventrally and has a rounded-triangular outline, on the right valve there is a marginal spine. The greatest length is situated in the lower third of the valve; the greatest height, at the anterior hinge edge. The surface is reticulate: elongated fossae occur along the valve margins, irregular in the central part of the valve. Fossae muri merge into fine ribs, stretching parallel to the valve margins, they bound the flattened central part of the valve. The valve surface within fossae is covered by small pore pits.

Sexual dimorphism. Carapaces differ in height, the higher, shorter carapaces most probably belong to females.

Dimensions in mm:

Specimen, no.	L	H
292/173	0.85	0.46
292/174	0.62	0.37

Comparison. From *H. fascis* (Brady et Norman, 1889), similar in outline, surface sculpture, and size, the species differs in lacking rounded nodes in the central part of valve.

Variability. The degree of the development of reticulation may vary. In some specimens ribs that are formed by fossae muri form dorsally coarser ribs.

Remarks. In our opinion, this species is indistinguishable from *Heterocyprideis sorbyanoides* from Pliocene–Pleistocene deposits of Alaska and Pleistocene deposits of Denmark (Bassiouni, 1965). As a distinguishing feature Swain pointed to the presence of coarser ribs in the dorsal part of valve, which is in fact due to intraspecific variability (Lev, 1983).

Fossil distribution. Neogene–Quaternary marine deposits of the lower reaches of the Yenisei, Ob, Pechora, Mezen, and Severnaya Dvina rivers; Taimyr; Islands Vaigach, Novaya Zemlya, Arctic Institute, Isachenko, Schmidt, and Severnaya Zemlya; and Anadyr Bay; Pliocene–Pleistocene of the Beaufort Sea, Greenland, and Alaska; Pleistocene of the northern Germany, Great Britain, Norway, Denmark, Sweden, Pechora Sea, northeastern North America (St. Lawrence Lowlands, Champlain Sea, Coastal area of Maine, Boston "blue clays," Goldthwait Sea (Quebec)); and Holocene of the Bay of Biscay, Norton Sound, and the Laptev and Kara seas.

Modern distribution. North Atlantic, waters off northeastern Iceland, Great Britain, Ireland, Finland, and Greenland; the Norwegian Sea; Spitsbergen and Franz Josef Land; the White, Baltic, Barents, Kara, Laptev, East Siberian, and Chukchi seas; Ungava Bay; Norton Sound; nearshore waters of Alaska; Labrador Sea, and Bay of Biscay.

Material. Three hundred and fifty-two valves and 69 carapaces of good preservation, Holocene and recent surface sediments of the Laptev Sea.

Heterocyprideis fascis (Brady et Norman, 1889)

Plate 5, figs. 13, 14

Cytheridea fascis: Brady and Norman, 1889, p. 177, pl. 16, figs. 23, 24. *Heterocyprideis fascis*: Hazel, 1968, text-fig. 2; Lord, 1980, pl. 1, figs. 6, 7; Lev, 1983, p. 111, pl. 7, figs. 9, 10; Cronin and Ikeya, 1987, pl. 1, fig. 15; Cronin, 1989, pl. 2, fig. 3; Brouwers et al., 1991, pl. 1, fig. 6; Kupriyanova, 1999, pl. 1, fig. 4; Schoning and Wastegård, 1999, pl. 1, figs. 9, 10; Stepanova et al., 2003, pl. 3, figs. 9, 10.

Heterocyprideis sorbyana: Benson et al., 1983, pl. 1, figs. 9, 10.

Type material. Brady and Norman (1889) for description of this species used material from recent sediments of the Davis Strait, sample obtained at 64°5′ N, 56°47′ W, depth about 750 m. The current location of the material is unknown. Revision of this species has not been undertaken; holotype and lectotype have not been designated.

Description. The carapace is medium to large, thick-shelled, subtriangular to pear-shaped in lateral view. The dorsal margin is straight, or slightly convex, bent towards the posterior margin, and passes into the anterior margin through an obtuse cardinal angle and, very gradually, to the posterior margin. The ventral margin is slightly concave in the anterior third. The anterior margin is broadly arcuately rounded, slightly beveled from the upper part, bears on average seven marginal spines. The posterior margin is lower than the anterior margin, steeply beveled ventrally, and of rounded-triangular outline, on the right valve there is a marginal spine. The greatest length is situated in the lower third of the valve; the greatest height, at the anterior hinge edge. The surface is reticulate, elongated fossae occur along the valve margins. The central part of the valve is punctate, larger depressions contain two or three puncta in their base. Fossae muri merge into fine ribs stretching parallel to the valve margins, they bound a slightly concave surface of the central part of the valve, in the center of which there is an ovate large knob. The puncta on the node are larger than on the rest part of valve.

Sexual dimorphism. Carapaces differ in height: the higher and shorter ones, most probably, belong to females.

Dimensions in mm:

Specimen, no.	L	H
292/205	0.8	0.5
292/206	0.57	0.37

Comparison. Comparison with *H. sorbyana* is given in its description.

Variability. The degree of the development of reticulation may vary, on some specimens ribs formed of fossae muri form coarser ribs.

Remarks. Benson et al. (1983) illustrated a valve that was identified as *H. sorbyana*, but this specimen has a rounded node in the central part of valve, a feature that does not fit the description of *H. sorbyana* and fits that of *H. fascis.*

Fossil distribution. Pliocene–Pleistocene of Japan, Greenland, Lower Yenisei River, and Malozemelskaya Tundra; and Pleistocene of Taimyr, Pechora Sea, Norway, and northeastern North America.

Modern distribution. The North Atlantic; the Kara, Barents, and western Laptev seas; the Davis Strait; the Beaufort Sea; and Newfoundland.

Material. Sixteen valves of good preservation from recent surface sediments of the western Laptev Sea.

Family Eucytheridae Puri, 1954

Genus *Eucythere* Brady, 1868

Eucythere: Brady, 1868b, p. 429; Brady et al., 1874, p. 182; Kashevarova et al., 1960, p. 379; Howe et al., 1961b, p. 285; Athersuch et al., 1989, p. 85; Nikolaeva et al., 1989, p. 186.

Type species. *Cythere declivis* Norman, 1865, nearshore waters of England; Recent; designated by Brady and Norman (1889).

Diagnosis. Carapace small, subtriangular in lateral view, left valve overlaps right valve. Surface smooth, punctate, rarely reticulate. Eye tubercule absent. Four adductor muscle scars form bow-shaped row on mid-length of valve, frontal scar large, of asymmetrical outline, occasionally split into two. Hinge lophodont, with median bar in left valve. In right valve it has terminal teeth and median smooth groove. Left valve complementary.

Taxonomic composition. About 100 species.

Comparison. This genus is similar in size and carapace outline to the genus *Rotundracythere* Mandelstam, 1958 from Eocene and recent deposits of New

Zeeland (Howe et al., 1961b, p. 288); however, these genera differ in hinge construction: *Rotundracythere* has all elements of the hinge notched, while the genus described here has smooth ones.

Stratigraphical range. Cretaceous–Recent; marine deposits worldwide.

Eucythere argus (G.O. Sars, 1866)

Plate 5, figs. 15, 16

Cytheropsis argus: G.O. Sars, 1866, p. 58.

Eucythere argus: Brady, 1868b, p. 431, pl. 27, figs. 49–51; Brady et al., 1874, p. 183, pl. 10, figs. 12–15; G.O. Sars, 1928, p. 162, pl. 75, fig. 1; Elofson, 1941, p. 268; 1969, p. 45; Rosenfeld, 1977, p. 20, pl. 3, figs. 43–45; Cronin, 1981, p. 396, pl. 4, figs. 3, 4, 6; Athersuch et al., 1989, p. 90, text-fig. 31, pl. 2, fig. 9; Brouwers, 1990, p. 34, pl. 10, figs. 16, 17, pl. 11, fig. 7, pl. 12, figs. 1–6; Didié et al., 1998, pl. 2, fig. 24; Whatley et al., 1998, pl. 2, fig. 22.

Eucythere declivis: Cronin, 1977, pl. 3, figs. 15, 16; McDougall et al., 1986, pl. 9, fig. 8.

Type material. G.O. Sars's (1866) description of this species used material from recent surface sediment of the nearshore waters of Norway, Oslo Fjord, and Oxfjord. The current location of the material is unknown. Revision of this species has not been undertaken; holotype and lectotype have not been designated.

Description. The carapace is small, subtriangular in lateral view. The dorsal margin is convex, it passes into the anterior and posterior margins through obtuse, smoothed cardinal angles. The ventral margin is straight, slightly concave in the anterior third. The anterior margin is evenly arcuately rounded. The posterior margin is considerably lower than the anterior margin, of a rounded-rectangular outline. The greatest length is situated in the lower third of the valve; the greatest height, at the anterior hinge edge. The surface bears fine ribs, stretching parallel to the valve margins. They form elongated fossae due to short ties between them. The central part of the valve is smooth. Pore pits are large, sievelike.

Sexual dimorphism. Brouwers (1990) pointed to pronounced sexual dimorphism: valves differ in height and shape of the two lower adductor muscle scars.

Dimensions in mm:

Specimen, no.	L	H
292/225	0.40	0.22

Comparison. This species is similar in carapace outline to *E. declivis* (Norman, 1865), inhabiting nearshore waters of England and the North and Baltic seas (Athersuch et al., 1989, p. 86, fig. 29, pl. 2, fig. 7); however, it differs in lacking small puncta and having better developed fine ribs.

Variability. Brouwers (1990) pointed to significant intraspecific variability and distinguished between the following zoogeographical morphotypes: (1) specimens found in waters of Great Britain and North and Baltic seas; (2) those that are found in the Pleistocene–Holocene of the North-Western Atlantic (St. Lawrence Lowlands) and the Gulf of Alaska and that are distinct from two other morphotypes in the larger size, outline of adductor scars, and greater development of sexual dimorphism; and (3) specimens from the eastern North Atlantic are distinguished from the rest by their carapace outline and degree of intensity of sexual dimorphism.

Fossil distribution. Pliocene–Pleistocene of Alaska; Pleistocene of Norway, western Canada, and northeastern North America (St. Lawrence Lowlands, Champlain Sea, and Goldthwait Sea (western Newfoundland and Quebec); Pleistocene–Holocene of Great Britain; and Holocene of the Gulf of Alaska, Cook Inlet, Kodiak shelf, Netherlands, Norway, and the Baltic and Laptev seas.

Modern distribution. North Atlantic; nearshore waters of Great Britain, Scandinavia, Ireland, Greenland, northwestern Europe; the Norwegian, North, Baltic, Barents, and Beaufort seas; Gulf of Alaska; and Hudson Bay.

Material. Eighteen valves of good preservation from Pleistocene–Holocene deposits of the Laptev Sea.

Family Cushmanideidae Puri, 1973

Genus *Paracyprideis* Klie, 1929

Paracyprideis: Klie, 1929, p. 272; Triebel, 1941, p. 153; Howe et al., 1961b, p. 290; Swain, 1963, p. 812; Nikolaeva et al., 1989, p. 187.

Type species. *Cytheridea fennica* Hirschmann, 1909; Baltic Sea, Gulf of Finland; Recent; by monotypy.

Diagnosis. Carapace medium-sized, elongated ovate or subrectangular in lateral view, left valve larger than right valve. Surface smooth or punctate, often with spine on posterior margin. Eye tubercule absent. Four adductor muscle scars form subvertical row in anterior third of valve, frontal muscle scar may be split into two. Hinge lophodont, with median bar in left valve. In left valve it has two elongated pits, located on sides of slightly notched bar. Right valve complementary.

Taxonomic composition. About 20 species.

Comparison. This genus is similar to the genus *Pontocythere* Dubowsky, 1939, in size and carapace outline; however, it differs in lacking fossae and ribs on valve surface. Hinge construction is also different: *Pontocythere* has a merodont hinge, and *Paracyprideis* has a lophodont hinge.

Stratigraphical range. Cretaceous–Recent; marine and brackish-water deposits worldwide.

Paracyprideis pseudopunctillata Swain, 1963

Plate 5, figs. 17–20

Paracyprideis sp. nov.: Swain, 1961, fig. 2.12.

Paracyprideis pseudopunctillata: Swain, 1963, p. 812, pl. 95, figs. 9, 13, pl. 96, fig. 12, pl. 97, figs. 14, 17, pl. 98, figs. 4a–4e, text-fig. 7a; McDougall et al., 1986, pl. 8, figs. 1–5; Siddiqui, 1988, pl. 2, fig. 1; Penney, 1990, pl. 1, figs. 7, 8; Kupriyanova, 1999, pl. 1, figs. 5, 6; Stepanova et al., 2003, pl. 4, figs. 5–7.

Holotype. US National Museum (USNM), Department of Microbiology, number of slide not specified, male carapace; Alaska, Simpson, core test no. 1, type

Plate 6

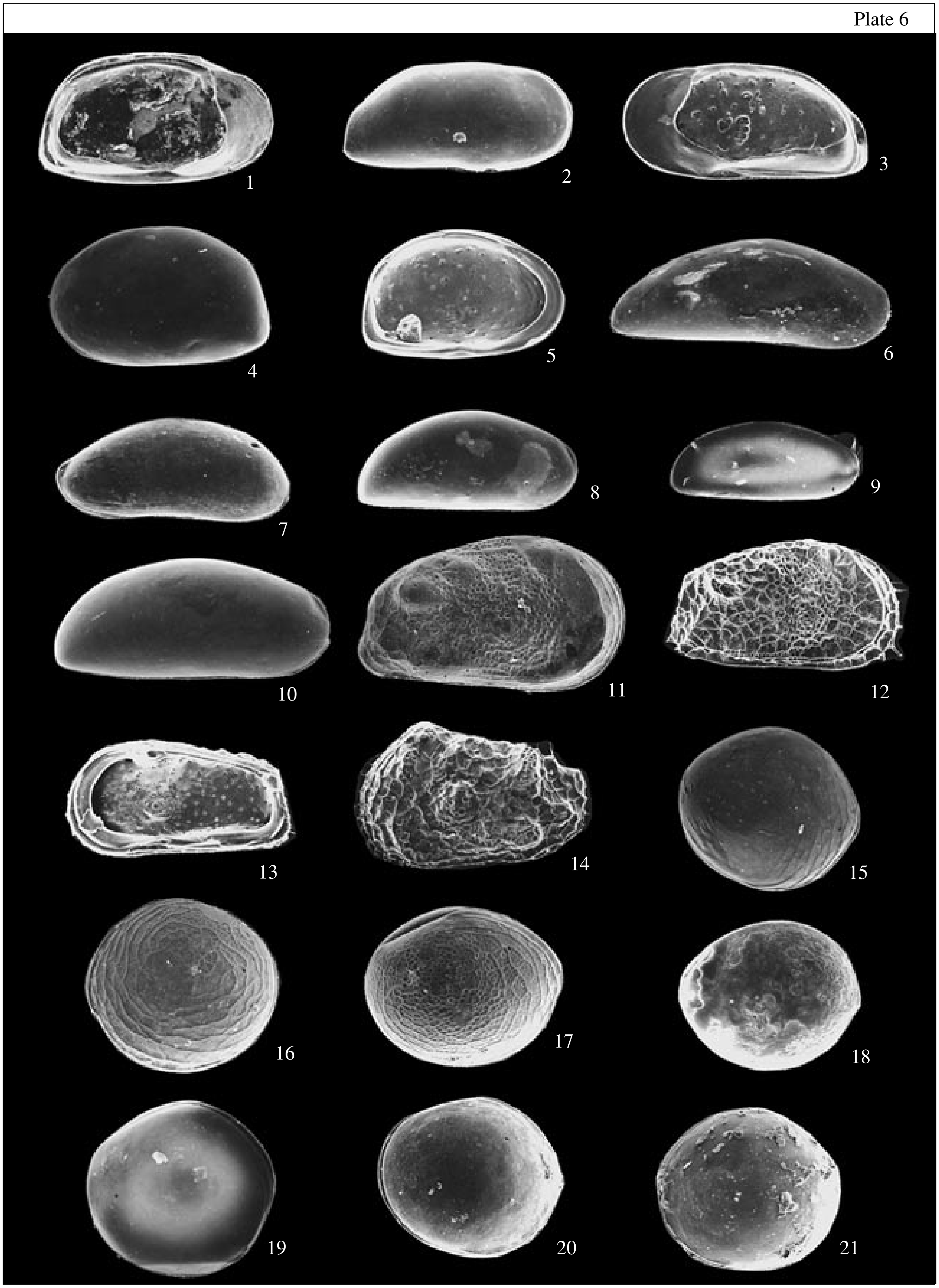

level 40–45 feet; Pliocene–Pleistocene, Gubik Formation (Swain, 1963, pl. 98, figs. 4a, d).

Description. The carapace is of medium size, elongated-ovate in lateral view, with a slightly flattened anterior margin. The dorsal margin is arcuately rounded, very gently beveled towards the anterior and posterior margins. The ventral margin is slightly concave in the anterior third. The anterior margin is arcuately rounded. The posterior margin is lower than the anterior margin, gently beveled ventrally, and of a rounded-triangular outline. The greatest length is situated at mid-height; the greatest height, in the center of the valve. The surface is smooth with rare small puncta. Pores are simple.

Age-related changes. Juvenile valves of this species differ considerably from adult valves, they have very fragile carapaces with a subtriangular lateral outline. The valves are pierced with numerous pore canals, pore puncta form groups consisting of several of them.

Dimensions in mm:

Specimen, no.	L	H
292/118	0.7	0.4
292/116	0.71	0.2
292/8	0.75	0.38

Comparison. From *P. fennica* Hirschmann, 1909, inhabiting the Gulf of Finland and similar in carapace outline and size, the species is distinguished by simple pores, unlike sievelike pores of *P. fennica.*

Variability. Carapaces are variable in the height-to-length ratio (0.7/0.4–0.7/0.2).

Fossil distribution. Pliocene–Pleistocene of the Beaufort Sea and Alaska; Pleistocene of the North and Pechora seas; and Holocene of the eastern Kara and Laptev seas.

Modern distribution. Nearshore waters of Alaska and Greenland; the Norwegian, Kara, East Siberian, Bering, Laptev, and Beaufort seas; and Norton Sound.

Material. Nine hundred and thirty-seven valves and 53 carapaces of good preservation, Late Pleistocene–Holocene and recent deposits of the Laptev Sea.

Family Krithidae Mandelstam, 1958

Genus *Krithe* Brady, Crosskey et Robertson, 1874

Ilyobates: Brady, 1868b, p. 431.

Krithe: Brady et al., 1874, p. 183; Brady, 1880, p. 113; G.O. Sars, 1928, p. 164; Kashevarova et al., 1960, p. 379; Howe et al., 1961b, p. 288; Swain, 1963, p. 814; Athersuch et al., 1989, p. 129; Nikolaeva et al., 1989, p. 189; Coles et al., 1994, p. 71.

Type species. *Ilyobates praetexta* G.O. Sars, 1866; nearshore waters of Norway, Recent; by monotypy.

Diagnosis. Carapace medium to large, subrectangular in lateral view, with subparallel margins, left valve slightly larger than right valve. Surface smooth. Eye tubercule absent. Four adductor muscle scars form vertical row in center of valve. Adductor scars and frontal scar may be split. Hinge adont. In left valve it represents smooth groove, complementary to dorsal margin of right valve. On anterior end of valve pocketlike vestibule, to which marginal pore canals are restricted. On posterior end of valve vestibule is usually not developed.

Taxonomic composition. More than 140 species.

Comparison. This genus is similar to the genus *Thracella* Sonmez, 1963 from Paleogene–Neogene deposits of Eurasia (Nikolaeva et al., 1989, p. 189) in carapace size and outline; however, it differs in having an adont hinge instead of the pseudadont hinge of *Thracella.*

Stratigraphical range. Late Cretaceous–Recent; marine deposits worldwide.

Krithe glacialis Brady, Crosskey et Robertson, 1874

Plate 5, fig. 21; Plate 6, figs. 1–5

Krithe glacialis: Brady, et al., 1874, p. 184, pl. 6, figs. 21–26; Brady and Norman, 1889, p. 182; Akatova, 1946, p. 226, fig. 3; Swain, 1961, fig. 2.39; Swain, 1963, p. 814, pl. 97, fig. 15, pl. 98, figs. 7a–7c, text-figs. 7b, 7c; Robinson, 1978, pl. 6, fig. 8; Lev, 1983,

Explanation of Plate 6

Figs. 1–5. *Krithe glacialis* Brady, Crosskey et Robertson, 1874: (1) female left valve, internal view, no. 292/66, ×62; (2) male right valve, external view, no. 292/82, ×57; (3) male right valve, internal view, no. 292/83, ×62; (4) juvenile left valve, external view, no. 292/62, ×75; (4) juvenile left valve, internal view, no. 292/87, ×65; recent surface sediments of the western Laptev Sea.

Fig. 6. *Argilloecia conoidea* Sars, 1923: right valve, external view, no. 292/249, ×100; Late Pleistocene of the western Laptev Sea.

Fig. 7. *Argilloecia cylindrica* Sars, 1923: right valve, external view, no. 292/100, ×94, recent surface sediments of the western Laptev Sea.

Figs. 8–10. *Argilloecia* sp.: (8) right valve, external view, no. 292/93, ×96; (9) carapace lateral view, no. 292/64, ×72; (9) right valve, external view, no. 292/251, ×100; Holocene and recent surface sediments of the western Laptev Sea.

Figs. 11–14. *Elofsonella concinna* (Jones, 1857): (11) right valve, external view, collection of Lev housed at NIIGA, smooth form, ×70; (12) right valve, external view, no. 292/90, ×49; (13) right valve, internal view, no. 292/91, ×47; (14) left valve, external view, no. 292/111, ×60; recent surface sediments of the western Laptev Sea.

Fig. 15. *Polycope orbicularis* Sars, 1866: carapace, lateral view, no. 292/165, ×92, recent surface sediments of the western Laptev Sea.

Figs. 16 and 17. *Polycope bireticulata* Joy et Clark, 1977: (16) carapace, lateral view, no. 292/166, ×75; (17) carapace, lateral view, no. 292/195, ×90; recent surface sediments of the western Laptev Sea.

Fig. 18. *Polycope punctata* Sars, 1866: carapace, lateral view, no. 292/88, ×120, recent surface sediments of the western Laptev Sea.

Figs. 19–21. *Polycope* sp.: (19) carapace, lateral view, no. 292/175, ×150; (20) carapace lateral view, no. 292/176, ×55; (21) carapace, lateral view, no. 292/182, ×70; recent surface sediments of the western Laptev Sea.

p. 115, pl. 14, figs. 5, 6; McDougall et al., 1986, pl. 7, figs. 3, 5; Siddiqui, 1988, pl. 2, fig. 5; Whatley et al., 1996, pl. 3, figs. 13–16; Didié et al., 1998, pl. 1, figs. 5–8; Whatley et al., 1998, pl. 3, figs. 5, 6, text-figs. 7.1–4; Kupriyanova, 1999, pl. 1, fig. 10; Stepanova et al., 2003, pl. 4, figs. 3, 4.

Krithe minima: Stepanova et al., 2003, pl. 4, figs. 1, 2.

Type material. For description of this species Brady et al. (1874) used material from the Pleistocene deposits of Errol, Scotland. The current location of the material is unknown. Revision of this species has not been undertaken; holotype and lectotype have not been designated.

Description. The carapace is medium to large, subrectangular in lateral view, with slightly flattened anterior margin. The dorsal margin is straight, gradually bent towards the anterior margin and passes into the posterior margin through a rounded almost right angle. The ventral margin is slightly concave in the anterior third or closer to the center. The anterior margin is evenly arcuately rounded. The posterior margin is almost vertically beveled on female carapaces, while on male carapaces it is very gently beveled in the upper part and almost vertically in the lower part. The greatest length is situated at mid-height; the greatest height, in the center of the valve.

Sexual dimorphism. Male carapaces are more elongated and lower than those of females and have a more gently beveled posterior margin in the upper part (Pl. 6, figs. 2, 3).

Dimensions in mm:

Specimen, no.	L	H
292/65 female	0.63	0.36
292/66 female	0.62	0.38
292/82 male	0.66	0.35
292/83 male	0.67	0.33

Comparison. From *K. minima* Coles, Whatley et Moguilevsky, 1994 (Coles et al., 1994, p. 88, pl. 2, figs. 16–18, pl. 3, figs. 1–5, text-fig. 3EE-JJ), found in Late Miocene–Quaternary deposits of the North Atlantic and similar in carapace outline and size, this species differs in having a more steeply beveled posterior margin on both male and female carapaces and a larger and more elongated carapace.

Variability. Depending on preservation, pore puncta on the valve surface may be visible or invisible.

Remarks. The author previously mistakenly identified specimens belonging to males of *K. glacialis*, since the lateral outlines of male and female carapaces differ considerably. The outline of the male carapaces is similar to that of *K. minima*, but more detailed scrutiny of published illustrations of *K. glacialis*, the first description of *K. minima*, a discussion with Carbonel (personal communication, 2004) and Briggs (personal communication, 2004) helped us to broaden our knowledge of the morphology of this species and allowed us to revise our initial point of view.

Fossil distribution. Neogene–Quaternary of the lower reaches of the Ob, Pechora, Izhma, Yenisei, Mezen', and Severnaya Dvina rivers and Novaya Zemlya; Pliocene–Pleistocene of the Beaufort Sea; Pleistocene of Great Britain, Norway, Alaska, and the Pechora Sea; Pleistocene–Holocene of the western Laptev Sea; and Holocene of the eastern Kara Sea.

Modern distribution. North Atlantic, nearshore waters of Great Britain and Ireland, Greenland, and Iceland; the White, Norwegian, Barents, Kara, Laptev, and East Siberian seas; and the straits of the Canadian Arctic Archipelago.

Material. Three hundred and fifty-three valves and 14 carapaces of good preservation, Pleistocene–Holocene and recent surface sediments of the western Laptev Sea.

Family Pontocyprididae G. Müller, 1894

Genus *Argilloecia* G.O. Sars, 1866

Argilloecia: G.O. Sars, 1866, p. 18; Brady et al., 1874, p. 132; Brady, 1880, p. 39; Brady and Norman, 1889, p. 111; G.O. Sars, 1928, p. 53; Lyubimova et al., 1960, p. 349; Swain and van den Bold, 1961, p. 247; Nikolaeva et al., 1989, p. 93.

Type species. *A. cylindrica* G.O. Sars, 1866; nearshore waters of Norway; Recent, by monotypy.

Diagnosis. Carapace small, elongated, laterally compressed, posterior end of carapace usually acuminate, right valve larger than left valve. Surface smooth. Eye tubercule absent. Three to five large adductor muscle scars are grouped in center of valve. Hinge adont. In left valve it represents knifelike edge, complementary to narrow groove of right valve.

Taxonomic composition. About 90 species.

Comparison. This genus differs from the genus *Pontocypris* G.O. Sars, 1966 (Athersuch et al., 1989), which is similar in carapace size and hinge construction, in having a more elongated shape of the carapace.

Stratigraphical range. Upper Cretaceous–Recent; marine deposits worldwide.

Argilloecia conoidea G.O. Sars, 1923

Plate 6, fig. 6

Argilloecia conoidea: G.O. Sars, 1923, p. 56, pl. 25; Elofson, 1941, p. 252; 1969, p. 30; Neale and Howe, 1975, pl. 3, fig. 2; Lord, 1980, pl. 3, fig. 14; Cronin and Ikeya, 1987, p. 76; Whatley et al., 1996, pl. 1, figs. 1–4; Whatley et al., 1998, pl. 1, fig. 1.

?*Argilloecia* sp.: Stepanova et al., 2003, pl. 4, figs. 9, 10.

Type material. For description of this species G.O. Sars (1923) originally used material from the recent surface sediments of the nearshore area of Norway. The current location of the material is unknown. Revision of this species has not been undertaken; holotype and lectotype have not been designated.

Description. The carapace is small, elongated-ovate in lateral view, narrow, the posterior end acuminate, the upper part of the anterior margin is flattened and forms a rim. The dorsal margin is slightly convex, passes into the anterior margin through a small concavity, and is gently beveled towards the posterior margin. The ventral margin is straight, slightly concave in the anterior third. The anterior margin is evenly arcuately rounded. The posterior margin has a subtriangular outline, it is beveled ventrally. The greatest length is situated at mid-height; the greatest height, in the center of the valve.

Sexual dimorphism. Male carapaces are smaller than those of females, narrower and more elongated, with a more convex dorsal margin and more acuminate posterior end.

Dimensions in mm:

Specimen, no.	L	H
292/249	0.51	0.17

Comparison. From *A. cylindrica*, similar in carapace size and outline, the species differs in having an acuminate posterior end of the carapace unlike rounded one of *A. cylindrica.*

Variability. This species is morphologically very stable. Minor variations of the length-to-height ratio may be observed.

Remarks. It is possible that carapaces identified as *Argilloecia* sp. (Pl. 6, figs. 8–10) also belong to *Argilloecia conoidea* G.O. Sars and are its juvenile forms or female specimens. We find it difficult to identify specific affiliation of these specimens and identify them only to generic level.

Fossil distribution. Pliocene–Pleistocene of Japan; Pleistocene of Norway, Scotland, western Laptev Sea, northeastern North America (Goldthwait Sea (Quebec); and Holocene of the Kara Sea.

Modern distribution. Waters off Great Britain, Ireland, Greenland, Norway, and Scandinavia; Skaggerak Strait; the Barents, Kara, Laptev, Beaufort, and Labrador seas; Hudson Bay; Frobisher Bay; and the straits of the Canadian Arctic Archipelago.

Material. Two valves of good preservation from Holocene deposits of the western Laptev Sea identified as *A. conoidea*, and one valve and one carapace identified as *Argilloecia* sp. from Late Pleistocene–Holocene and recent deposits of the western Laptev Sea.

Argilloecia cylindrica G.O. Sars, 1866

Plate 6, fig. 7

Argilloecia cylindrica: G.O. Sars, 1866, p. 18; Brady et al., 1874, p. 132, pl. 16, figs. 29–31; Brady and Norman, 1889, p. 111; G.O. Sars, 1928, p. 54, pl. 24; Elofson, 1941, p. 251; Swain and van den Bold, 1961, fig. 182.1; Elofson, 1969, p. 29; Nikolaeva et al., 1989, text-fig. 49; Whatley et al., 1996, pl. 1, figs. 5, 6; Whatley et al., 1998, pl. 1, figs. 2, 3; Stepanova et al., 2003, pl. 4, fig. 8.

Type material. For description of this species G.O. Sars (1866) originally used material from the recent surface sediments of nearshore area of Norway. Currently, the location of the material is unknown. Revision of this species has not been undertaken; holotype and lectotype have not been designated.

Description. The carapace is small, elongated-ovate in lateral view, narrow, the posterior margin is flattened and forms a narrow rim. The dorsal margin is slightly convex, bent towards the posterior margin, passes into the posterior margin through a small concavity, and is gently beveled towards the anterior margin. The ventral margin is straight, slightly concave in the center. The anterior margin is evenly arcuately rounded, slightly bent ventrally. The posterior margin is subtriangular in outline, arcuately rounded in the lower half, and forms a slight ledge in the intersection with the dorsal margin. The greatest length is situated at mid-height; the greatest height, in the center of the valve.

Sexual dimorphism. Carapaces vary insignificantly in the length-to-height ratio due to sexual dimorphism. Male carapaces are smaller and more elongated than female carapaces.

Dimensions in mm:

Specimen, no.	L	H
292/100	0.42	0.19

Comparison. This species differs from the species *A. acuminata* Müller, 1894, which inhabits the Mediterranean Sea (Nikolaeva et al., 1989, fig. 50) and is similar in carapace size and outline, in having a rounded posterior end of the carapace instead of the acuminate end of *A. acuminata.*

Variability. The outline of the posterior part of the valve varies from gradually rounded to slightly acuminate.

Fossil distribution. Pleistocene of Scotland and Holocene of the Kara and Laptev seas.

Modern distribution. Waters off Great Britain, Skaggerak Strait, Greenland Sea, nearshore waters of Norway, and the Kara and Laptev seas.

Material. Thirteen valves of good preservation from Holocene and recent surface sediments of the Laptev Sea.

Family Hemicytheridae Puri, 1953

Genus *Elofsonella* Pokorny, 1955

Elofsonella: Pokorny, 1955, p. 10; Howe et al., 1961c, p. 303; Swain, 1963, p. 829; Hazel, 1967, p. 15; Lev, 1983, p. 133; Athersuch et al., 1989, p. 162; Nikolaeva, 1989, p. 171.

Type species. *Cythere concinna* Jones, 1857; Great Britain; Pleistocene; by monotypy.

Diagnosis. Carapace massive, of medium to large size, subrectangular in lateral view. Lateral valve surface bears massive marginal rib, stretching along anterior and above ventral margins, subparallel to them. Central part of valve with massive node. Surface densely reticulate and punctate, puncta small. Reticulation primary and secondary. Eye tubercule well developed. Four adductor muscle scars form subvertical row, two median scars are split, in front of them three rounded frontal scars form subvertical row. Hinge merodont in juvenile carapaces and holamphidont in adult carapaces. In right valve, in anterior section, hinge has high triangular tooth and deep rounded socket, median section has long finely denticulate groove; posterior section has massive semilunar tooth, flattened in its upper part. Left valve complementary.

Taxonomic composition. About ten species.

Comparison. From *Hemicythere* G.O. Sars, 1925 (Nikolaeva et al., 1989, p. 170), which is similar in carapace outline, size, and surface sculpture, this genus is distinguished by the presence of three frontal scars instead of two scars in *Hemicythere*. The construction of the hinge is also different: holamphidont in members of *Elofsonella* and hemiamphidont in members of *Hemicythere.*

Stratigraphical range. Miocene–Recent; northern Hemisphere, high latitudes.

Elofsonella concinna (Jones, 1857)

Plate 6, figs. 11–14

Cythere concinna: Jones, 1857, p. 29, pl. 4, figs. 7a–7f; Brady, 1868b, p. 408, pl. 26, figs. 28–33, pl. 38, fig. 7; Brady et al., 1874, p. 160, pl. 4, figs. 1–20; Brady and Norman, 1889, p. 162.

Hemicythere concinna: G.O. Sars, 1928, p. 189, pl. 87, fig. 1.

Cythereis (Paracythereis) concinna: Elofson, 1941, p. 289; 1969, p. 64.

Elofsonella concinna: Pokorny, 1955, p. 12, figs. 3–7; Howe et al., 1961c, fig. 229.1; Swain, 1961, fig. 2.31; 1963, p. 829, pl. 98, figs. 1a, 1b; pl. 99, figs. 11a–11c; text-fig. 12c; Woszidlo, 1962, pl. 4, fig. 11; Hazel, 1967, p. 15, pl. 4, figs. 10, 11, 13; Rosenfeld, 1977, p. 25, pl. 6, figs. 81–83; Robinson, 1978, pl. 2, figs. 1a, 1b; Lord, 1980, pl. 1, fig. 1; Cronin, 1981, p. 396, pl. 4, fig. 5; Lev, 1983, p. 134, pl. 13, fig. 4; Cronin and Ikeya, 1987, p. 77, pl. 1, fig. 13; Athersuch et al., 1989, p. 162, fig. 65, pl. 5, fig. 3; Cronin, 1989, pl. II, figs. 11, 12; 1991, fig. 14.4; Nikolaeva et al., 1989, text-figs. 312–314; Lord et al., 1993, pl. 1, figs. 5–8; Ingram, 1998, pl. 1, fig. 15; Stepanova et al., 2003, pl. 4, figs. 11, 12.

Elofsonella concinna concinna: Bassiouni, 1965, p. 511, pl. 2, figs. 1, 2.

Elofsonella concinna neoconcinna: Bassiouni, 1965, p. 512, pl. 2, figs. 3a–3c.

Baffinicythere pinegensis: Lev, 1983, p. 136, pl. 13, fig. 1.

Thaerocythere crenulata: Lev, 1983, pl. 17, figs. 8, 9.

Elofsonella aff. *concinna*: Stepanova et al., 2003, pl. 4, fig. 13.

Type material. Several valves are housed in the Natural History Museum, London, slide no. I 6380; material derived from Bridlington, West Yorkshire, England; Pleistocene.

Description. The carapace is massive, large, and subrectangular in lateral view. The dorsal margin is straight, slightly bent towards the posterior margin, passes into the anterior margin very gradually and into the posterior margin through an almost right cardinal angle. The ventral margin is straight, concave in the anterior third. The anterior margin is evenly arcuately rounded. The posterior margin has a square outline, it is very steeply beveled and forms an almost right angle in the intersection with the ventral margin. The greatest length is situated at mid-height; the greatest height, at the anterior hinge edge. The surface is reticulate, fossae are large with thick muri. Fossae are arranged in rows parallel to the valve margins, in the central part of the valve they are arranged concentrically. On the dorsal margin fossae muri project beyond the valve outline and give the dorsal margin denticulated appearance. The lower part of the anterior margin bears several spines. The lower third of the posterior margin also bears several spines. Along the anterior and ventral margins a ridge-like rib is found, it starts at the anterior hinge edge and stops short of the posterior margin. The central part of the valve bears a massive muscle node. A well-developed eye tubercule is situated in the anterodorsal part of the valve. Two more nodes occur in the dorsal part of the valve: the first one is located in the posterodorsal part of the valve, it is especially well developed on juvenile carapaces, where it goes beyond the carapace outline; the second small node is located at the mid-length of the dorsal margin, it is, on the contrary, only pronounced on adult carapaces. In the posteroventral part of the valve one more node is located, it is more distinct on juvenile carapaces, it merges with the node located in the posterodorsal part of the valve. The valve surface is densely punctate (puncta are small) and reticulate; fossae are of two orders: large and small. On the anterior margin there is a rim.

Dimensions in mm:

Specimen, no.	L	H
292/90	0.77	0.44
292/91	0.78	0.43

Comparison. From *E. amberii* Carbonnel, 1969, (Carbonnel, 1969, p. 85, pl. 1, figs. 1–10) from Tortonian marine deposits of the Rhone River valley, similar in carapace size and outline, this species differs in lacking oblique ridgelike ribs on the lateral valve surface.

Variability. Carapaces vary significantly in the degree of development of surface sculpture: from smoothed surface with predominantly punctate sculpture to strongly ornamented with massive ridges, fossae, and nodes.

Age-related changes. Juvenile valves differ considerably from adult ones in carapace outline and ornamentation: they have subtriangular lateral outline, and nodes in the posterior part of valve are developed to a greater degree than those on adult valves. Juvenile specimens have merodont hinge, and adult specimens possess holamphidont hinge.

Remarks. There are two morphotypes of *E. concinna* (Jones, 1857): (1) with smoothed valve surface and (2) with pronounced massive sculpture (Fig. 19). Brady et al. (1874) described the species *Cythere concinna* and both its morphotypes, pointing to the fact that they could not find any correlation between the morphology of carapace and the geological distribution of this species, since both morphotypes occur both together and separately. Based on morphological differences, Bassiouni (1965) described two subspecies, smooth specimens as *E. concinna concinna* and strongly ornamented specimens as *E. concinna neoconcinna.*

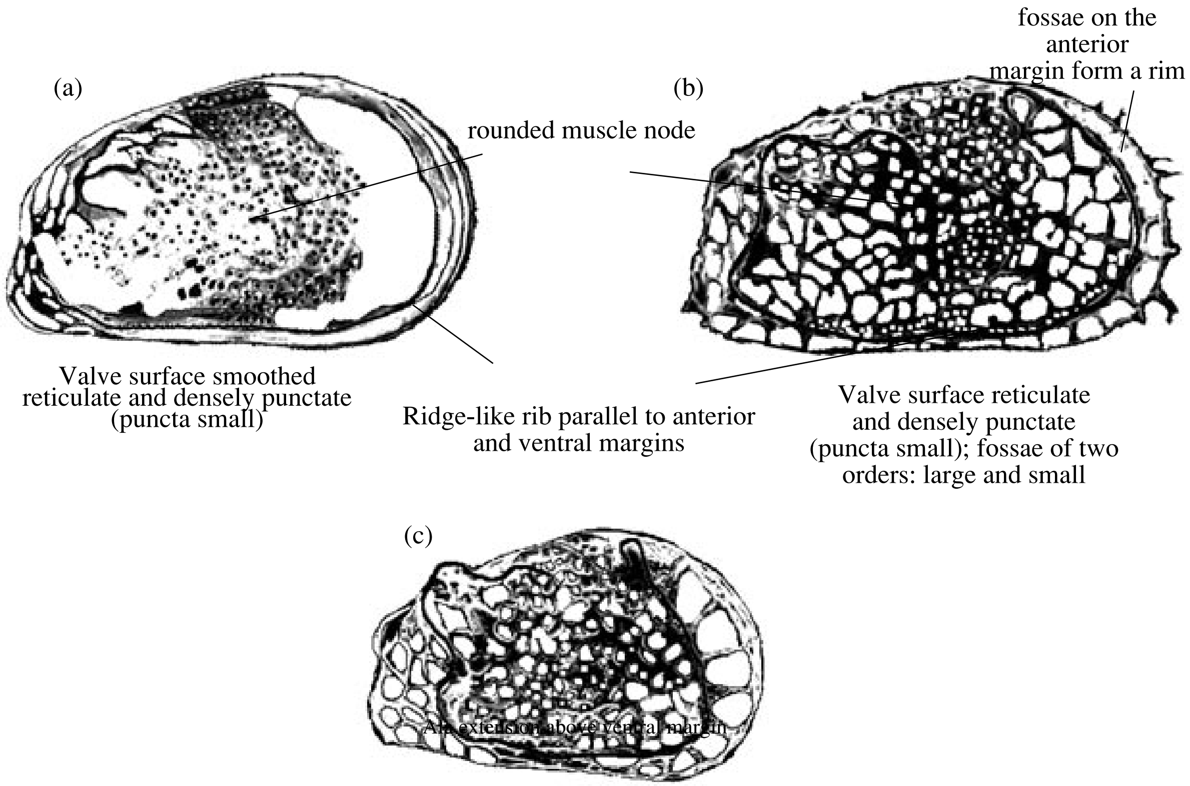

Fig. 19. Intraspecific variability and age-related changes on carapaces of *Elofsonella concinna* (Jones, 1857): (a) smooth form; (b) strongly ornamented form; (c) juvenile valve.

He believed that *E. concinna concinna* is restricted to Pleistocene deposits, while *E. concinna neoconcinna* is a modern subspecies. Later, Hazel (1967) and Athersuch et al. (1989) cast doubt on the expediency of establishment of these species, since both morphotypes most often occur together both in Pleistocene–Holocene and in recent surface sediments. We follow the latter point of view and believe that there is no necessity to designate these subspecies. However, it is noteworthy that in the Laptev Sea only ornamented morphotype with well-developed sculptural elements have been recorded. However, some scientists consider the difference between the two subspecies to be significant enough to establish two distinct species (Schornikov, 2001; Briggs, personal communication, 2004).

Lev (1983) described a new species, *Baffinicythere pinegensis*, from Pleistocene deposits of the lower reaches of the Severnaya Dvina and Yenisei rivers and the Kola Peninsula. Based on the hinge construction, she attributed the species to *Baffinicythere*; however, she remarked that the surface ornamentation does not fit the description of this genus. In Lev's collection we found specimens of both morphotypes of *Elofsonella concinna*, specimens with smooth valve surface she attributed to *E. concinna*; and specimens with strong ornamentation, to the new species *Baffinicythere pinegensis.* That is why we consider *B. pinegensis* to be a synonym of *E. concinna.*

Significant morphological differences between adult and juvenile carapaces made some scientists attribute juvenile specimens to a separate species (Fig. 19c). Lev (1983) illustrated specimens that she identified as *Thaerocythere crenulata* G.O. Sars. We studied these specimens described by Lev and concluded that they do not differ from the juvenile forms of *E. concinna* from the Laptev Sea. We were not sure of the affiliation of these specimens to *E. concinna* either, since the juvenile valves are quite thick, although considerably more fragile than those of adults, and we cannot be sure that they do not belong to adults of the other species.

Fossil distribution. Neogene–Quaternary deposits of the lower reaches of the Yenisei, Pechora, Ob, and Severnaya Dvina rivers and of the Kola Peninsula, Isachenko Island, North and South Islands of the Novaya Zemlya Archipelago, Chukchi Sea, Anadyr Bay, and Malozemelskaya Tundra; Miocene of Sakhalin; Pliocene–Pleistocene of Japan and Alaska; Pleistocene of the North Sea, Great Britain, Norway, Denmark, northern Germany, and northeastern North America (St. Lawrence Lowlands, Champlain Sea, and Goldthwait Sea (western Newfoundland)); and Holocene of the Kara and Laptev seas.

Modern distribution. North Atlantic, waters off Great Britain, the Hebrides, Ireland, Greenland, Atlantic coast of North America, North Sea, Skaggerak

Strait, Norwegian Sea, Baltic Sea, Barents Sea, nearshore waters of Spitsbergen, Kara Sea, Laptev Sea, East Siberian Sea, Chukchi Sea, nearshore waters of Aleutian Islands, Davis Strait, Beaufort and Labrador seas, Ungava and Frobisher bays, Norton Sound, Hudson Bay, and the straits of the Canadian Arctic Archipelago.

Material. Thirty-five valves and 15 carapaces of good preservation, Holocene and recent surface sediments of the Laptev Sea.

Order Halocyprida Dana, 1853

Suborder Cladocopina G.O. Sars, 1866

Family Polycopidae G.O. Sars, 1866

Genus *Polycope* G.O. Sars, 1866

Polycope: G.O. Sars, 1866, p. 122; Brady, 1868a, p. 470; Brady et al, 1874, p. 219; Brady, 1880, p. 168; Brady and Norman, 1896, p. 705; G.O. Sars, 1928, p. 29; Zanina and Polenova, 1960, p. 330; Sylvester-Bradley, 1961, p. 405; Joy and Clark, 1977, p. 143; Chavtur, 1983, p. 96; Nikolaeva, 1989a, p. 86.

Type species. *P. orbicularis* G.O. Sars, 1866; Recent; nearshore waters of Norway; by monotypy.

Diagnosis. Carapace small, thin-shelled, lenticular, rounded in lateral view, valves almost equal. Surface smooth, reticulate or punctate, may bear ribs and marginal spines. Eye tubercule absent. Three to four adductor muscle scars are grouped in center of valve. Hinge adont, terminal elements on left valve are represented by short ridges above and protruding ridges below with grooves in between; on right valve, by ridge above groove.

Taxonomic composition. More than 100 species.

Comparison. From *Polycopsis* G.W. Müller, 1894 (Sylvester-Bradley, 1961, p. 405), similar in carapace outline and size, this genus differs in having a less laterally compressed carapace and in lacking the crenation on the anterior margin.

Stratigraphical range. Jurassic–Recent; worldwide.

Polycope orbicularis G.O. Sars, 1866

Plate 6, fig. 15

Polycope orbicularis: G.O. Sars, 1866, p. 122; Brady and Norman, 1896, p. 706, pl. 54, figs. 9, 10, pl. 55, figs. 12–16; pl. 68, figs. 1–3; G.O. Sars, 1928, p. 31, pl. 14, pl. 15, fig. 1; Elofson, 1941, p. 244; Sylvester-Bradley, 1961, figs. 330.2a–c; Elofson, 1969, p. 22; Chavtur, 1983, p. 97; Nikolaeva, 1989a, text-fig. 27; Whatley et al., 1996, pl. 4, fig. 13; Whatley et al., 1998, pl. 3, fig. 24; Stepanova et al., 2003, pl. 4, fig. 16.

?*Polycope orbicularis*: Brady, 1868a, p. 471, pl. 35, figs. 53–57.

Non *Polycope orbicularis*: Brady et al., 1874, p. 219, pl. 12, figs. 22, 23; Brady, 1880, p. 169.

Type material. For the description of this species G.O. Sars (1866) used the material from recent surface sediments of the nearshore waters of Norway. Currently, the location of the material is unknown. Revision of this species has not been undertaken; holotype and lectotype have not been designated.

Description. The carapace is small, lenticular, rounded in lateral view. The dorsal margin is evenly arcuately rounded. The ventral margin is also evenly arcuately rounded. The anterior margin is evenly arcuately rounded. The posterior margin is evenly arcuately rounded. The greatest length is situated slightly above the mid-height; the greatest height, at the center of the valve. Fine ribs run along the valve margins, merge and form elongated fossae, the central part of the valve is smooth.

Dimensions in mm:

Specimen, no.	L	H
292/165	0.35	0.29

Comparison. From *P. bireticulata* Joy et Clark, 1977, inhabiting the Greenland Sea and Central Arctic Ocean and similar in carapace outline and ornamentation, this species differs in having sculptural elements only along carapace margins, not on the entire surface.

Variability. The degree of development of ribs and fossae may slightly vary.

Remarks. G.O. Sars (1928) pointed out that specimens illustrated by Brady (1868a) and identified as *P. orbicularis*, probably, do not belong to this species, that is why we also doubt that they belong to the described here species.

In his work devoted to recent Sweden ostracodes, Elofson (1941) holds that specimens illustrated by Brady et al. (1874) and described by Brady (1880) cannot be attributed to this species. Thus, we also put in doubt the relevance of this identification.

Fossil distribution. Holocene of the western Laptev Sea.

Modern distribution. Waters off Great Britain, Greenland Sea, nearshore waters of Norway and Sweden, Shetland Islands, and the Laptev Sea.

Material. Scarce carapaces and valves of good preservation from recent surface sediments of the western Laptev Sea.

Polycope bireticulata Joy et Clark, 1977

Plate 6, figs. 16, 17

Polycope bireticulata: Joy and Clark, 1977, p. 144, pl. 1, figs. 21, 22; Chavtur, 1983, p. 101; Whatley et al., 1996, pl. 4, fig. 12; Stepanova et al, 2003, pl. 4, figs. 14, 15.

Polycope sp.: Hartmann, 1993, pl. 1, figs. 1a and 1b.

Holotype. University of Wisconsin, UW 1597-16c, adult right valve; Central Arctic Ocean, upper 3 cm of sediment, core FL 423, 16-1; Chukchi Rise and Alpha Cordillera; Recent.

Description. The carapace small, lenticular, rounded in lateral view. The dorsal margin is evenly arcuately rounded. The ventral margin is also evenly arcuately rounded. The anterior margin is evenly arcuately rounded. The posterior margin is evenly arcuately rounded. The greatest length is slightly above mid-height; the greatest height is in the center of the valve. The entire surface is reticulate and punctate, puncta are small. Fine ribs along the valve margins merge and form a secondary reticulation.

Dimensions in mm:

Specimen, no.	L	H
292/166	0.28	0.26
292/195	0.35	0.31

Comparison. From *P. punctata* G.O. Sars, 1866, inhabiting nearshore waters of Norway and the Central Arctic Ocean (Joy and Clark, 1977) and similar in carapace outline, this species differs in lacking the spine on the anterior margin and in having reticulate ornamentation, unlike punctate ornamentation of *P. punctata.*

Variability. The degree of development of ribs and fossae may vary insignificantly.

Fossil distribution. Holocene of the western Laptev Sea.

Modern distribution. Greenland Sea, nearshore waters of Spitsbergen, Laptev Sea, central part of the Central Arctic Ocean, and Canada Basin.

Material. Single carapaces and valves of good preservation from recent surface sediments of the western Laptev Sea.

Polycope punctata G.O. Sars, 1870

Plate 6, fig. 18

Polycope punctata: G.O. Sars, 1870, p. 171; Brady and Norman, 1896, p. 708, pl. 68, fig. 9; G.O. Sars, 1928, p. 32, pl. 15, fig. 2; Elofson, 1969, p. 23; Chavtur, 1983, p. 97; Athersuch et al., 1989, fig. 21c; Whatley et al., 1996, pl. 4, fig. 14.

?*Polycope punctata*: Brady and Norman, 1896, p. 708, pl. 68, figs. 10–12; Elofson, 1941, p. 246.

Type material. For the description of this species G.O. Sars (1870) used material from recent surface sediments of the nearshore waters of Norway. Currently, the location of the material is unknown. Revision of this species has not been undertaken; holotype and lectotype have not been designated.

Description. The carapace is small, lenticular, rounded in lateral view. The dorsal margin is evenly arcuately rounded. The ventral margin is also evenly arcuately rounded. The anterior margin is evenly arcuately rounded and has a spine in the mid-length. The posterior margin is evenly arcuately rounded. The greatest length is slightly above mid-height; the greatest height is in the center of the valve. The entire valve surface is densely punctate, puncta are small.

Dimensions in mm:

Specimen, no.	L	H
292/88	0.28	0.22

Comparison. From *P. orbicularis*, similar in carapace size and outline, this species differs in lacking reticulation.

Variability. Carapaces differ strongly in size, Arctic specimens are considerably smaller. The spine located on the mid-length of the anterior margin is often not preserved.

Remarks. Joy and Clark (1977) noted that *P. punctata* is the largest species of Arctic Polycopidae. However, our specimen is about half the size of the specimens described by G.O. Sars (1928) and Joy and Clark (1977). It is possible that the specimen described is a juvenile carapace. It has no spine on the mid-length of the anterior margin, a feature typical of the Arctic representatives of this species, due to the fact that it is usually broken (Joy and Clark, 1977).

Joy and Clark have cast doubt on the affiliation of specimens described by Elofson (1941) to *P. punctata*, since Elofson pointed to the presence of reticulation, which is in conflict with the original description of this species. Elofson (1941) and G.O. Sars (1928) questioned the affiliation of specimens described by Brady and Norman (1896) to *P. punctata*, although one of these specimens is likely to belong to this species, since it was collected by Sars himself (Brady and Norman, 1896, p. 708, pl. 68, fig. 9). That is why we are not sure that the above illustrations belong to the species described.

Modern distribution. Waters off Great Britain, Greenland Sea, nearshore waters of Norway, Sweden, Laptev Sea, and the central part of the Arctic Ocean.

Material. One well-preserved carapace from recent surface sediments of the western Laptev Sea.

Polycope sp. 1

Plate 6, figs. 19–21

Polycope sp.: Stepanova et al., 2003, pl. 4, fig. 17.

Description. The carapace is small, lenticular, rounded in lateral view. The dorsal margin is evenly arcuately rounded. The ventral margin is also evenly arcuately rounded. The anterior margin is evenly arcuately rounded. The posterior margin is evenly arcuately rounded. The greatest length is situated slightly above mid-height; the greatest height, in the center of the valve. The surface is smooth.

Dimensions in mm:

Specimen, no.	L	H
292/182	0.45	0.42
292/175	0.22	0.14

Comparison. From *P. orbicularis*, similar in carapace size and outline, this species differs in lacking reticulation.

Remarks. Specimens of this species are most similar to *P. pseudoinornata* Chavtur 1983, inhabiting the Kara and Barents seas, Chukchi Rise, and the Canadian Basin. However, studied specimens are about half the size of those described by Chavtur (1983) and, since we have very poor material of this species, we identify this form only to generic level.

Modern distribution. Laptev and Kara seas.

Material. Single carapaces and valves of good preservation from recent surface sediments of the western Laptev Sea.

Remarks

It is noteworthy that all the species of the Polycopidae G.O. Sars, 1866 (except for *P. bireticulata* Joy et Clark, 1977) described here, differ significantly in their carapace sizes from members of these species inhabiting nearshore waters of Norway and the central part of the Arctic Ocean; this is, probably, because of unfavorable environmental conditions in the Laptev Sea, this supposition is additionally proved by the low abundance of these species.

CONCLUSIONS

Our investigation established three different ecological assemblages of ostracodes in surface sediments of the Laptev Sea. Comparison of fossil assemblages from AMS^{14}C-dated sediment cores obtained from the shelf and upper continental slope areas with their modern analogues allowed us to reconstruct paleoenvironmental changes that occurred during the postglacial transgression and considerably supplement previously obtained data.

The following conclusions were made:

(1) In total 35 species were identified in coretop samples, all of them are modern inhabitants of this region. Significant variability was observed in their distribution, reflecting varying water depth and salinity. Recent ostracodes of the Laptev Sea are combined into three different assemblages, corresponding to the three regions of the sea: (1) the taxonomically diverse assemblage of the continental slope of the western-central Laptev Sea (depth range 62–276 m) that is characterized by deepwater species; (2) the assemblage of the middle shelf of the eastern Laptev Sea that is represented by shallow-water normal-marine species; and (3) the assemblage of the southern Laptev Sea dominated by euryhaline and brackish-water species. In the western-central Laptev Sea at several stations, unusually large numbers of valves of shallow-water species were recorded, which is supposed to be due to ice-rafting.

(2) Comparison of the recent ostracode association of the Laptev Sea with those from other Arctic areas revealed that it is most similar to the assemblage of the Kara and Beaufort seas, a result of similar environmental conditions in these seas.

(3) Morphological analysis of ostracode assemblages revealed that in the Laptev Sea only one correlation is observed: a considerable increase of smooth and slightly ornamented forms in regions with lowest salinity. The size of carapace does not reflect different environmental parameters.

(4) Analysis of fossil assemblages from AMS^{14}C-dated sediment cores and comparison of established assemblages with modern analogues allowed us to reconstruct the development of the postglacial transgression in different parts of the sea. Three phases of transgression were established on the central part of the shelf of the eastern part of the Sea. During the first phase (11.3–11.1 cal. ka BP in the Yana paleovalley and 11.2–10.8 cal. ka BP in the Lena paleovalley) nearshore brackish-water environment existed with depths less than 10 m, reduced (on average 18–20‰) and seasonally variable bottom salinity. During the second phase (11.1–10.3 cal. ka BP in the Yana paleovalley and 10.8–8.2 cal. ka BP in the Lena paleovalley) shallow-water environment existed that was affected by fluvial runoff, with water depths around 20–25 m and average bottom salinity around 26–28‰. Since 10.3 cal. ka BP in the Yana paleovalley and 8.2 cal. ka BP in the Lena paleovalley the third phase has started: a transition to the onset of present marine environment with bottom salinity around 30–32‰.

In the inner shelf zone, starting from 6.4 cal. ka BP nearshore brackish-water environment with considerable fluvial influence and relatively low sedimentation rates (30 cm/kyr) existed. Around 2.7 cal. ka BP it was replaced by the modernlike environment. We assumed that the river runoff increased or changed its direction around 1.5 cal. ka BP.

In the Late Pleistocene, on the western continental slope, most probably, the environment was characterized by cold, low nutrient conditions, high sedimentation rates, and plant debris influx. Continuous influence of the Atlantic waters on the continental slope is supposed to have started from 15.8 cal. ka BP. During 15.8–13.8 cal. ka BP, a polynya was probably formed on the core site location due to the proximity of the paleocoast and off-land winds. This supposition is proved by a high percentage of planktonic foraminifers in samples. Deposits that accumulated during 13.8–11.6 cal. ka BP contain different ecological groups of ostracodes; even shallow brackish-water species are present, which points to great influence of river runoff and ice-rafting. Around 11.1 cal. ka BP sedimentation rates dramatically decreased due to the beginning of shelf inundation. Deposits dated back to 11.6–6.5 cal. ka BP (assemblage 4) contain only normal marine species with predominance of species of the Atlantic origin. This fact, most probably, evidences the increasing influence of the North Atlantic water inflow during this time. Around 6.5 cal. ka BP onset of modernlike environments occurs, the assemblage is dominated by shallow-water taxa, this predominance is probably due to ice-rafting and, maybe, points to the increase in the ice coverage of the Laptev Sea during this time.

APPENDIX

Description of Studied Core Sections

Sediment core PS-51/138-12 was obtained from the eastern part of the Lena valley, 75°07′04″ N, 130°52′ 09″ E, it exposes deposits 538 cm thick.

538–436 cm: the sediment is clayey silt of a blackish gray color, it is homogenous and finely mottled, with spots of organic matter.

In the interval 538–436 cm the following mollusks were found: *Cyrtodaria kurriana, Portlandia arctica,* and *Portlandia arctica* cf. *aestuariorum.*

At 525 cm core depth a date of 11339 cal. yr. BP was obtained (here and forth AMS^{14}C dates were converted to calendar years BP using the CALIB 4.3).

436–337 cm: the sediment is silt of a dark gray color, it is slightly bioturbated. Strong bioturbation is observed between 366–373 cm and 399–406 cm.

In the interval 436–337 cm the following mollusks were found: *Portlandia arctica, Portlandia arctica* cf. *aestuariorum, Cyrtodaria kurriana, Lora* sp., *Cylichna* sp., and *Cylichna* cf. *alba.*

337–225 cm: the sediment is clayey silt of a gray blackish color, it is bioturbated.

In the interval 337–225 cm the following mollusks were found: *Portlandia arctica, Portlandia arctica* cf. *aestuariorum, Cylichna* sp., *Tridonta borealis*, and *Cylichna* cf. *scalpta.*

At 298 cm core depth a date of 10333 cal. yr. BP was obtained.

225–136 cm: the sediment is silty clay of a homogeneously gray color. Ikaite crystals were found at core depths of 148, 195, 214, and 220 cm.

In the interval 225–136 cm the following mollusks were found: *Portlandia arctica, Cylichna* sp., *Ciliatocardium ciliatum, Oenopota* sp., *Leionucula bellotii, Lyonsia arenosa, Nuculana* sp., and *Macoma* sp.

At 197 cm core depth a date of 10274 cal. yr. BP was obtained.

136–54 cm: the sediment is clayey silt of a blackish to dark grayish color. Slight bioturbation is observed.

In the interval 136–54 cm the following mollusks were found: *Portlandia arctica, Cylichna* sp., *Leionucula bellotii, Lyonsia arenosa, Ciliatocardium ciliatum, Hiatella arctica, Liocyma* sp., *Macoma calcarea, Macoma* sp., *Yoldia* sp., *Thyasira* sp., and *Buccinum* sp.

85–79 cm: a fine erosive contact is observed. Silt becomes finer upwards.

54–33 cm: the sediment is clayey silt of a gray color, it is bioturbated.

In the interval 54–33 cm the following mollusks were found: *Portlandia arctica, Cylichna* sp., *Leionucula bellotii, Macoma* sp., and *Nuculana* sp.

At 53 cm core depth a date of 2374 cal. yr. BP was obtained.

Box core PS51/138-10

39–25 cm: the sediment is silt of a gray color with sandy clasts up to several centimeters in diameter and black spots and streaks of organic matter. Deposits are bioturbated.

In the interval 39–25 cm the following mollusks were found: *Cryptonatica clausa, Nuculana* sp., *Macoma calcarea*, and *Leionucula bellotii.*

25–2 cm: the sediment is sandy-silty clay of a gray color with black spots and streaks of organic matter and scattered fragments of shells. Deposits are bioturbated.

In the interval 25–2 cm the following mollusks were found: *Pandora glacialis, Portlandia arctica, Yoldia* sp., *Macoma calcarea, Leionucula bellotii*, and *Ciliatocardium ciliatum.*

2–0 cm: the sediment is sandy silt of an olive-gray color with smooth surface. Live brittle stars, holothurians, and crustaceans were found.

Sediment core PS51/135-4 was obtained from the Yana valley, 76°09′ 92″ N, 133°14′ 68″ E, it exposes deposits 514 cm thick.

562–514 cm: the sediment is silty clay of a gray color.

In the interval 562–514 cm the following mollusks were found: *Portlandia arctica, Portlandia arctica* cf. *aestuariorum*, and *Acrybia islandica.*

At 562 cm core depth a date of 11339 cal. yr. BP was obtained.

514–415 cm: the sediment is silty clay of a gray to dark gray color. Strong mottling, black spots of organic matter, and shell debris are observed. Black inclusions of sulfides and sandy clasts are found. At 467 cm a sandy-silty lens a few millimeters thick occurs.

In the interval 514–415 cm the following mollusks were found: *Portlandia arctica.*

At 456 cm core depth a date a 11142 cal. yr. BP was obtained.

415–330 cm: the sediment is silty clay of a gray color with black spots and streaks of organic matter (less than in the underlying section). Thin sandy layers and black inclusions of sulfides are observed; sediment is bioturbated. The lower contact is gradual and is marked by a sandy-silty lens a few millimeters thick.

In the interval 415–330 cm the following mollusks were found: *Cylichna* sp., *Macoma* sp., *Leionucula bellotii*, and *Portlandia arctica.*

At 403 cm core depth a date of 10306 cal. yr. BP was obtained.

330–210 cm: the sediment is sandy-silty clay of a dark gray color with abundant black spots of organic matter and sulfides. Thin sandy layers and shell debris are observed; the sediment is bioturbated. The lower contact is gradual and is marked by a black layer.

In the interval 330–210 cm the following mollusks were found: *Cylichna* sp., *Macoma* sp., *Macoma calcarea, Leionucula bellotii*, and *Portlandia arctica.*

At 266 cm core depth a date of 9613 cal. yr. BP was obtained.

210–47 cm: the sediment is sandy-silty clay of a very dark gray color. It becomes darker downwards due to precipitation of Fe and Mn. Black spots and streaks of organic matter, as well as thin sandy layers and dark inclusions of sulfides are observed. The sediment contains shell debris and complete valves of bivalves, strong bioturbation is observed. At 58 cm core depth a fragment of wood was found. The lower contact is gradual and is marked by a black layer (arranged obliquely from 209 to 211 cm).

In the interval 210–47 cm the following mollusks were found: *Lyonsia arenosa, Cylichna* sp., *Buccinum* sp., *Macoma* sp., *Macoma calcarea, Macoma* cf. *moesta, Musculus niger, Nuculana* sp., *Leionucula bellotii,* and *Portlandia arctica.*

At 147 cm core depth a date of 8956 cal. yr. BP was obtained.

At 80 cm core depth a date of 7610 cal. yr. BP was obtained.

47–0 cm: the sediment is sandy-silty clay of a dark gray color, with thin sandy layers, shell debris, complete valves of bivalves and black spots of organic matter; it is bioturbated. At 24 cm core depth a fragment of wood was found.

In the interval 47–0 cm the following mollusks were found: *Yoldia amygdalea hyperborea, Cylichna* sp., *Macoma* sp., *Macoma* cf. *calcarea, Nuculana* sp., *Leionucula bellotii,* and *Portlandia arctica.*

At 40 cm core depth a date of 7017 cal. yr. BP was obtained.

At 4 cm core depth a date of 5301 cal. yr. BP was obtained.

Sediment core PS51/92-12 was obtained from the eastern part of the Lena valley, 73°35′59″ N, 130°08′33″ E, it exposes deposits 589 cm thick.

589–561 cm: silty clay, gray.

561–488 cm: the sediment is silty clay of a gray to dark gray color with weak striation and dark spots of organic matter. Sediment contains mollusk shell fragments and is bioturbated.

At 500 cm core depth a date of 8408 cal. yr. BP was obtained.

488–403 cm: the sediment is silty clay of a dark gray color, enriched in organic matter. Black spots of sulfides, silty clasts, rare sandy clasts and mollusk shell fragments were found. Small gray spots (0.5–1.5 cm) and black lenses (0.5 cm thick) are observed. The sediment is strongly bioturbated. In the interval 425–430 cm there is a gap in the core; deposits are destroyed. The contacts with the overlying and underlying deposits are gradual. The contact with the overlying layer is marked by a black lens enriched in organic matter. In the interval 488–403 cm the following mollusks were found: *Cylichna* sp., *Macoma* sp., *Macoma* cf. *moesta*, and *Leionucula bellotii.*

403–379 cm: the sediment is clay of a gray color, mottled, with black dots of sulfides. Strong bioturbation is observed.

In the interval 403–379 cm the following mollusks were found: *Leionucula bellotii* and *Portlandia arctica.*

At 402 cm core depth a date of 7754 cal. yr. BP was obtained.

379–352 cm: the sediment is clay of a dark gray color with black inclusions of sulfides and organic matter, silty clasts, and mollusk shell fragments. Strong bioturbation is observed.

In the interval 379–352 cm the following mollusks were found: *Leionucula bellotii* and *Portlandia arctica.*

352–188 cm: the sediment is clay of a gray color with inclusions and lenses of dark gray and light gray clay (0.5–2.5 cm) and small scattered sandy-silty clasts, (up to 0.5–1 cm in diameter). Sediment contains mollusk shell fragments. Strong mottling and bioturbation are observed. There is a gap between 270 and 280 cm in the core, deposits are destroyed.

In the interval 352–188 cm the following mollusks were found: *Leionucula bellotii, Macoma* sp., *Macoma calcarea, Yoldia* sp., *Yoldia amygdalea hyperborea, Nuculana minuta*, and *Cylichna* sp.

At 300 cm core depth a date of 7270 cal. yr. BP was obtained.

188–160 cm: the sediment is clay with a thin interbedding of a dark gray and light gray color (0.2–1 cm) and small white sandy-silty clasts (up to 0.5 cm in diameter). Shell debris has low abundance; the sediment is bioturbated.

In the interval 188–160 cm the following mollusks were found: *Nuculana* sp. and *Macoma* cf. *moesta*.

160–99 cm: the sediment is silty clay of a gray color. Mottling, small black spots enriched in organic matter and sulfides (less than 1 cm in diameter) are observed. Deposits are striate, interbedding of dark gray and light gray colored sediment (2–9 cm) occurs. Small sandy-silty clasts and mollusk shell fragments are found. At 137 cm core depth thin layer of black clay with minor amounts of organic matter is located.

In the interval 160–99 cm the following mollusks were found: *Leionucula bellotii, Yoldia amygdalea hyperborea, Macoma calcarea, Macoma* cf. *moesta,* and *Macoma* sp.

At 160 cm core depth a of date 1267 cal. yr. BP was obtained.

99–48 cm: the sediment is silty clay of a gray color. Mottling, spots of dark gray clay (up to 1 cm in diameter) and sandy-silty clasts are observed. The sediment contains mollusk shell fragments; it is bioturbated.

In the interval 99–48 cm the following mollusks were found: *Leionucula bellotii, Macoma calcarea*, and *Cylichna* sp.

48–0 cm: the sediment is silty clay of a dark gray color with tiny spots of sulfides, black spots of organic matter, and mollusk shell fragments. Strong bioturbation is observed.

In the interval 48–0 cm the following mollusks were found: *Leionucula bellotii* and *Portlandia arctica.*

At 6.4 cm core depth a date of 1078 cal. yr. BP was obtained.

At 2 cm core depth a date of 273 cal. yr. BP was obtained.

The core was sampled in 2-cm intervals; most of samples were barren of ostracodes.

Box core PS51/092-11

41–4 cm: the sediment is silty clay of a dark gray color, with tiny inclusions of sulfides and black spots of organic matter and mollusk shell fragments, their abundance increases upwards. Bioturbation is observed.

In the interval 41–4 cm the following mollusks were found: *Leionucula bellotii, Ciliatocardium ciliatum, Montacuta spitsbergensis, Portlandia arctica, Margarites groenlandicus, Pandora glacialis, Nuculana* sp., *Nuculana lamellosa, Macoma* sp., and *Cylichna* sp.

4–0 cm: the sediment is sandy-silty clay of an olive brown color, it is homogenous. Contact with underlying layer is distinct, it is marked by a sharp transition to another color and density of the sediment; density decreases upwards. Bioturbation is observed.

In the interval 4–0 cm the following mollusks were found: *Leionucula bellotii, Ciliatocardium ciliatum, Portlandia arctica, Nuculana* sp., *Macoma calcarea, Macoma* sp., *Cyrtodaria kurriana, Nicania montagui*, and *Cylichna* sp.

Sediment core PS51/080-13 was obtained from the eastern part of the Lena River valley, 73°27′56″ N, 131°38′30″ E, it exposes deposits 206 cm thick.

206–187 cm: silty clay, dark gray.

At 202 cm core depth a date of 6393 cal. yr. BP was obtained.

187–152 cm: the sediment is silty clay of a dark gray color. It is mottled; with light gray lenses and spots, black inclusions of organic matter, and mollusk shell fragments are found.

In the interval 187–152 cm the following mollusks were found: *Portlandia arctica.*

152–120 cm: the sediment is silty clay with low sand content of a dark gray color. It is mottled, light gray spots and mollusk shell fragments are found.

In the interval 152–120 cm the following mollusks were found: *Portlandia arctica, Lyonsia arenosa*, and *Macoma* sp.

At 142 cm core depth a date of 5097 cal. yr. BP was obtained.

120–118 cm: the sediment is silty clay of a gray color, it is more homogenous than in the underlying layers.

118–60 cm: the sediment is silty clay of a blackish-gray color with high content of organic matter in lenses and spots. Sediment color changes wavelike on the lower border of the interval. Bioturbation is observed. At 70 cm core depth two fragments of wood are found (1.5 × 2.5 × 0.5 cm). At the 75–77 cm core depth a thin layer of black clay occurs.

At 71.5 cm core depth a date of 1522 cal. yr. BP was obtained.

In the interval 118–60 cm the following mollusks were found: *Portlandia arctica, Thyasira gouldi, Cylichna* sp., *Leionucula bellotii, Macoma* sp., *Yoldiella* sp. 2, and *Lyonsia arenosa.*

60–30 cm: the sediment is silty clay of a dark gray color with inclusions of sulfides and spots of organic matter up to 1 cm in diameter. Bioturbation is observed.

In the interval 60–30 cm the following mollusks were found: *Ciliatocardium ciliatum, Axinopsida orbiculata, Portlandia arctica, Thyasira gouldi, Leionucula bellotii*, and *Lyonsia arenosa.*

At 41.5 cm core depth a date of 1503 cal. yr. BP was obtained.

The upper part of the section was destroyed during drilling.

Box core PS51/080-11

42–19 cm: the sediment is silty clay of a gray color, with a minor content of sulfide inclusions. Bioturbation is observed. At 35 cm core depth ice crystals are found.

In the interval 42–19 cm the following mollusks were found: *Portlandia arctica, Leionucula bellotii*, and *Macoma* sp.

19–9 cm: the sediment is silty clay of a dark gray color, with numerous sulfide inclusions and mollusk fragments. Bioturbation is observed.

In the interval 19–9 cm the following mollusks were found: *Onoba aculeus, Cylichna* sp., and *Portlandia arctica.*

9–1 cm: the sediment is silty clay of a light gray color with inclusions of sulfides and mollusk shell fragments. Bioturbation is observed.

In the interval 9–1 cm the following mollusks were found: *Onoba aculeus, Cylichna* sp., *Portlandia arctica, Tridonta borealis, Tridonta* sp., *Macoma* sp., *Axinopsida orbiculata,* and *Leionucula bellotii.*

1–0 cm: the sediment is silty clay of an olive brown color with mollusk shell fragments.

Sediment core PS51/154-11 was obtained from the western part of the Laptev Sea 77°16′56″ N, 120°36′5″ E, it exposes deposits 708 cm thick.

708–630 cm: the sediment is sandy-silty clay of a gray color with spots of organic matter and shell debris.

In the interval 708–630 cm the following mollusks were found: *Yoldiella* cf. *lenticula*.

630–627 cm: the sediment is silty sand of a dark gray color; it is enriched in organic material.

627–571 cm: the sediment is sandy-silty homogenous clay with dim layers of compacted clays of light and olive colors. Sediment contains scattered shell debris.

571–532 cm: the sediment is sandy-silty clay of a gray color with tiny black spots of organic matter and sulfides.

In the interval 571–532 cm the following mollusks were found: *Portlandia arctica* and *Axinopsida orbiculata.*

At 569 cm core depth a date of 15776 cal. yr. BP was obtained.

At 567 cm core depth a date of 15741 cal. yr. BP was obtained.

532–524 (540) cm: cross bedding in the contact with the overlying layer is observed. The sediment is sand of a dark gray color, enriched in coal-like organic matter, scattered shell debris.

524–506 cm: the sediment is silty clay of a gray color with rare black spots of organic matter and shell debris. Deposits are similar to those from the interval 433–504 cm. At 520 cm core depth a shell of bivalve was found.

In the interval 524–506 cm the following mollusks were found: *Portlandia arctica.*

At 518 cm core depth a date of 15293 cal. yr. BP was obtained.

504–433 cm: the sediment is silty clay of a gray color; it is homogenous with rare black spots of organic material and tiny spots of sulfides. The sediment contains shell debris. Deposits are similar to those from interval 388–429 cm.

In the interval 504–433 cm the following mollusks were found: *Portlandia arctica, Axinopsida orbiculata, Yoldiella intermedia, Yoldiella fraternal, Dacrydium vitreum, Nuculana pernula*, and *Leionucula bellotii.*

At 440 cm core depth a date of 14086 cal. yr. BP was obtained.

506–504 cm: the sediment is sand of a blackish-gray to black color with a very high content of organic matter and scattered shell debris.

433–429 cm: the sediment is silty clay of a black color with blackish-gray colored interlayers of sandy-silty clay enriched in organic matter and thin lenses of sand and sandy clasts.

In the interval 433–429 cm the following mollusks were found: *Nuculana* sp.

429–388 cm: the sediment is silty clay of a gray to dark gray color with black spots and lenses of organic matter (more abundant in the upper part), tiny spots of sulfides and shell debris.

In the interval 429–388 cm the following mollusks were found: *Nuculana* sp., *Leionucula bellotii*, and *Cryptonatica* sp.

388–383 cm: the sediment is sandy silt of a black color with a high content of organic matter and thin lenses of sand (2–5 mm). Deposits are stratified.

383–295 cm: the sediment is silty clay of a gray to dark gray color; it is very similar to the deposits from interval 41–286 cm. At 305 cm core depth a coal-like fragment of wood was found. At 365–375 cm core depth several crystals of ikait were found.

In the interval 383–295 cm the following mollusks were found: *Nuculana* sp., *Yoldiella lenticula, Yoldiella* cf. *lenticula, Yoldiella* sp., *Portlandia arctica*, and *Leionucula bellotii.*

At 375 cm core depth a date of 13680 cal. yr. BP was obtained.

At 300 cm core depth a date of 12022 cal. yr. BP was obtained.

295–286 cm: the sediment is silty clay of a black color with high content of organic matter and shell debris. Bioturbation is observed.

286–41 cm: the sediment is sandy-silty clay of a dark gray color. It is soft and contains abundant sandy clasts, black spots, shell debris, and lenses of organic matter, which in a number of cases lead to pseudostratification. Bioturbation is observed. At 240 cm core depth a big spot of organic matter (3 cm in diameter) is found. The sediment color becomes darker downwards due to precipitation of Fe and Mn.

In the interval 286–41 cm the following mollusks were found: *Nuculana* sp., *Yoldiella lenticula, Yoldiella* cf. *lenticula, Portlandia arctica, Leionucula bellotii, Yoldiella* sp., *Yoldia* sp., *Thyasira gouldi, Macoma* sp., *Macoma calcarea, Cryptonatica clausa*, and *Cuspidaria glacialis.*

At 204 cm core depth a date of 11151 cal. yr. BP was obtained.

At 138 cm core depth a date of 11143 cal. yr. BP was obtained.

41–10 cm: the sediment is sandy-silty clay, it is homogenous and very soft, contains shell debris and sandy clasts.

In the interval 41–10 cm the following mollusks were found: *Yoldiella* cf. *intermedia, Yoldiella intermedia, Thyasira* sp., and *Macoma* cf. *calcarea*.

At 31 cm core depth a date of 1136 cal. yr. BP was obtained.

10–0 cm: the sediment is sandy-clayey silt of an olive black color, it is very soft and bioturbated. The upper part of the section was destroyed during drilling.

In the interval 10–1 cm the following mollusks were found: *Cuspidaria* sp., *Yoldiella intermedia, Lyonsia arenosa*, and *Yoldiella intermedia.*

ACKNOWLEDGMENTS

I gratefully acknowledge the assistance and supervision of E.M. Tesakova, E.E. Taldenkova, and A.S. Alekseev, who cooperated closely throughout most of this work. I am also grateful to collaborators of the Russian-German Otto Schmidt Laboratory for Polar and Marine Research, located in the Arctic and Antarctic Research Institute (St. Petersburg), and to my colleagues from GEOMAR (Kiel, Germany), especially to H.A. Bauch. I am grateful to my colleagues-ostracodologists for their help with literature selection and valuable discussions: T.M. Cronin (US Geological Survey, Reston, the United States), W. Briggs (NAMPO, Colorado, the United States), P. Frenzel (University of Rostok, Germany), C. Didié (AWI Bremerhaven, Germany), R. Whatley (University of Aberystwyth, Great Britain), I. Boomer (University of New-Castle, Great Britain), E.I. Schornikov (Far East Division of the Russian Academy of Sciences, Vladivostok), and N.V. Kupriyanova (VNIIOkeangeologiya, St. Petersburg). This study was supported by the BMBF and the Russian Ministry for Education and Science (Otto Schmidt Laboratory for Polar and Marine Sciences, project no. OSL-05-31), the Russian Ministry for Industry, Science, and Technology, Russian Foundation for Basic Research, project no. 05-05-64823, and INTAS, project no. 03-51-6682.

REFERENCES

1. A. E. Aitken and R. Gilbert, "Marine Mollusca from Expedition Fiord, Western Axel Heiberg Island, Northwest Territories, Canada," Arctic **49** (1), 29–43 (1996).
2. N. A. Akatova, "A Contribution to the Fauna of Ostracodes from the Shallow Waters of the New Siberian Islands," in *Proceedings of the Glavsevmorput' Drifting Expeditions on the Icebreaker Sedov, 1937–1940* (Biologiya, Moscow-Leningrad, 1946), Vol. 3, pp. 224–230 [in Russian].
3. N. A. Akatova, "Ostracodes of the Onega Bay in the White Sea," in *Materials for the Integrated Study of the White Sea* (Akad. Nauk SSSR, Moscow–Leningrad, 1957), Issue 1, pp. 428–433 [in Russian].
4. N. V. Aladin, "Adaptations to Salinity and Osmoregulatory Abilities of Ostracoda (Crustacea) from the Barents and White Seas: Evolution of the Osmoregulatory Function within the Subclass Ostracoda," Zool. Zh. **64**, 368–376 (1985).
5. M. N. Alekseev, *Stratigraphy of the Neogene–Quaternary Continental Deposits of the Vilyui Rift and Lower Lena River Valley* (Akad. Nauk SSSR, Moscow, 1961) [in Russian].
6. M. N. Alekseev, *Anthropogene of Eastern Asia: Stratigraphy and Correlation* (Nauka, Moscow, 1978) [in Russian].
7. M. N. Alekseev, "Stratigraphy of the Quaternary Deposits of the New Siberian Islands," in *Quaternary Period: Stratigraphy* (Nauka, Moscow, 1989), pp. 159–168 [in Russian].
8. S. M. Andreeva, B. I. Kim, V. Kosheleva, et al., "Lithology of the Upper Quaternary Veneer and Late Cenozoic Paleogeography of the Laptev Sea Margin," Polarforschung **69**, 185–193 (2001).
9. S. M. Andreeva, "The North Siberian Lowland in the Karginskoe Time: Paleogeography, Radiocarbon Chronology," in *Geochronology of the Quaternary Period* (Nauka, Moscow, 1980), pp. 183–191 [in Russian].
10. S. M. Andreeva, "The Development of the Ideas on the Stratigraphy and Paleogeography of the Late Quaternary Time in Northern Siberia," in *The Anthropogene of the Taimyr Peninsula*, Ed. by N. V. Kind and B. N. Leonov (Nauka, Moscow, 1982), pp. 7–10 [in Russian].
11. S. M. Andreeva, L. L. Isaeva, N. V. Kind, and M. V. Nikol'skaya, "Glaciation, Marine Transgressions, and Climate in the Late Pleistocene and Holocene," in *The Anthropogene of the Taimyr Peninsula*, Ed. by N. V. Kind and B. N. Leonov (Nauka, Moscow, 1982), pp. 157–165 [in Russian].
12. F. Are, "About Relative Sea-Level Changes in the Laptev and East Siberian Seas in the Postglacial Period," in *Fluctuations of the Level of Seas and Oceans during the Last 15000 Years* (Nauka, Moscow, 1982), pp. 168–174 [in Russian].
13. S. A. Arkhipov, *The Quaternary Period in Western Siberia* (Nauka, Novosibirsk, 1971) [in Russian].
14. J. Athersuch, "Some Ostracod Genera Formerly of the Family Cytherideidae Sars," in *Fossil and Recent Ostracods*, Ed. by Bate R. H., E. Robinson, and L. M. Sheppard (Ellis Horwood, Chichester, 1982), pp. 231–275.
15. J. Athersuch, D. J. Horne, and J. E. Whittaker, "Some Species of the Ostracod Genus *Bythocythere* Sars from British Waters," J. Micropalaentol., No. 2, 71–81 (1983).
16. J. Athersuch, D. J. Horne, and J. E. Whittaker, "G.S. Brady's Pleistocene Ostracods from the Brickearth of the Nar Valley, Norfolk, U.K.," J. Micropalaentol. **4** (2), 153–158 (1985).
17. J. Athersuch, D. J. Horne, and J. E. Whittaker, *Marine and Brackish Water Ostracods*, Ed. by J. Athersuch, D. J. Horne, and J. E. Whittaker (Linn. Soc. London, Leiden, 1989).
18. M. A. Bardeeva and L. L. Isaeva, "On the Recognition of the Muruktinskii Horizon in the Upper Pleistocene Deposits in Central Siberia," Dokl. Akad. Nauk SSSR **251** (1), 169–173 (1980).
19. M. A. A. Bassiouni, "Über einige Ostracoden aus dem Interglazial von Esbjerg," Bull. Geol. Soc. Denmark **15** (4), 507–519 (1965).
20. H. A. Bauch, M. Kubisch-Popp, T. M. Cronin, and B. Rossak, "Scientific TRANSDRIFT I Shipboard Party, 1995: A Study of the Calcareous Microfauna from Laptev Sea Sediments," Ber. Polarforsch. **176**, 334–339 (1995).
21. H. A. Bauch, H. Kassens, H. Erlenkeuser, et al., "Depositional Environment of the Laptev Sea (Arctic Siberia) during the Holocene," Boreas **28** (1), 201–204 (1999).
22. H. A. Bauch, H. Kassens, O. D. Naidina, M. Kunz-Pirrung, and J. Thiede, "Composition and Flux of Holocene Sediments on the Eastern Laptev Sea Shelf, Arctic Siberia," Quatern. Res. **55**, 341–351 (2001a).
23. H. A. Bauch, T. Mueller-Lupp, E. Taldenkova, et al., "Chronology of the Holocene Transgression at the North Siberian Margin," Global and Planetary Change **31**, 125–139 (2001b).
24. R. H. Benson, "Morphologic Stability in Ostracoda," Bull. Am. Paleontol. **65**, 13–45 (1975).
25. R. H. Benson, R. M. DelGrosso, and P. L. Steinbeck, "Ostracode Distribution and Biofacies, Newfoundland

Continental Slope and Rise," Micropaleontol. **29** (4), 430–453 (1983).

26. N. A. Bogdanov, V. E. Khain, O. M. Rozen, et al., *Explanatory Notes to the Tectonic Map of the Kara and Laptev Seas and Northern Siberia (Scale 1 : 2500000)* (Inst. Litosfery Ross. Akad. Nauk, Moscow, 1998), pp. 87–94 [in Russian].
27. W. A. van den Bold, "Contributions to the Study of Ostracoda with Special Reference to the Tertiary and Cretaceous Microfauna of the Caribbean Region," Dissertation (Univ. of Utrecht, Utrecht, 1946).
28. W. A. van den Bold, "The genus *Eucytheridea* Bronstein (Crustacea: Ostracoda) with a Redescription of the Type Species," Ann. Mag. Nat. Hist., Ser. 13, No. 4, 283–303 (1961).
29. B. Boucsein, K. Fahl, and R. Stein, "Variability of River Discharge and Atlantic-Water Inflow at the Laptev Sea Continental Margin during the Past 15000 Years: Implications from Maceral and Biomarker Records," Int. J. Earth Sci. **89**, 578–591 (2000).
30. G. S. Brady, "On Undescribed Fossil Entomostraca from the Brickearth of the Nar," Ann. Mag. Nat. Hist., Ser. 3, No. 16, 189–191 (1865).
31. G. S. Brady, "On New or Imperfectly Known Species of Marine Ostracoda," Trans. Linn. Soc. London **26**, 353–496 (1866).
32. G. S. Brady, "Contribution to the Study of the Entomostraca," Ann. Mag. Nat. Hist., Ser. 4, No. 2, 30–35 (1868a).
33. G. S. Brady, "A Monograph of the Recent British Ostracoda," Transact. Linn. Soc. London **26** (2), 353–495 (1868b).
34. G. S. Brady, "Report on the Ostracoda Dredged by H.M.S. *Challenger*: Scientific Results of the Voyages of H.M.S. *Challenger* 1873–1876," in *Zoology* (1880).
35. G. S. Brady and H. W. Crosskey, "Notes on Fossil Ostracoda from the Post-Tertiary Deposits of Canada and New England," Geol. Mag. **8**, 60–65 (1871).
36. G. S. Brady and A. M. Norman, "A Monograph of the Marine and Freshwater Ostracoda of the North Atlantic and of North-Western Europe: Sect. 1. Podocopa," Sci. Transact. R. Dublin Soc., Ser. 2 **4**, 61–270 (1889).
37. G. S. Brady and A. M. Norman, "A Monograph of the Marine and Freshwater Ostracoda of the North Atlantic and of North-Western Europe: Part 2. Sections 2–4: Myodocopa, Cladocopa, and Platycopa," Sci. Transact. R. Dublin Soc., Ser. 2 **5**, 621–743 (1896).
38. G. S. Brady, H. W. Crosskey, and D. Robertson, "A Monograph of the Post-Tertiary Entomostraca of Scotland, Including Species from England and Ireland," Paleontograph. Soc. London **28**, 1–232 (1874).
39. E. M. Brouwers, "Palaeobathymetry on the Continental Shelf Based on Examples Using Ostracods from the Gulf of Alaska," in *Ostracoda in the Earth Sciences* (Elsevier, Amsterdam, 1988), pp. 55–77.
40. E. M. Brouwers, "Systematic Paleontology of Quaternary Ostracode Assemblages from the Gulf of Alaska: Part 1. Families Cytherellidae, Bairdiidae, Cytheridae, Leptocytheridae, Limnocytheridae, Eucytheridae, Krithidae, Cushmanideidae," U.S. Geol. Surv. Prof. Pap., No. 1510, 1–40 (1990).
41. E. M. Brouwers, "Systematic Paleontology of Quaternary Ostracode Assemblages from the Gulf of Alaska: Part 2. Families Trachyleberididae, Hemicytheridae, Loxoconchidae, Paracytheridae," U.S. Geol. Surv. Prof. Pap., No. 1531, 1–49 (1993).
42. E. M. Brouwers, "Systematic Paleontology of Quaternary Ostracode Assemblages from the Gulf of Alaska: Part 3. Family Cytheruridae," U.S. Geol. Surv. Prof. Pap., No. 1544, 1–43 (1994).
43. E. M. Brouwers, N. O. Jorgensen, and T. Cronin, "Climatic Significance of the Ostracode Fauna from the Pliocene Kap Kobenhavn Formation, North Greenland," Micropaleontol. **37** (3), 245–267 (1991).
44. E. M. Brouwers, T. M. Cronin, D. J. Horne, and A. R. Lord, "Recent Shallow Marine Ostracods from High Latitudes: Implications for Late Pliocene and Quaternary Palaeoclimatology," Boreas **29**, 127–142 (2000).
45. M. Caralp, J. Moyes, and M. Vigneaux, "La microfaune actuelle et subrécente d'une carotte Atlantique (Golfe De Gascogne): observations écologiques et climatiques," Bull. Soc. Géol. France, Sér. 7, **9**, 418–425 (1967).
46. G. Carbonnel, "Variations phénotypiques chez une espèce tortonienne du genre *Elofsonella* Pokorny," in *The Taxonomy, Morphology, and Ecology of Recent Ostracoda* (Oliver and Boyd, Edinburgh, 1969), pp. 85–93.
47. V. G. Chavtur, *Ostracodes Myodocopina and Cladocopina of Cool and Cold Waters in the Northern Hemisphere* (Dal'nevost. Nauchn. Tsentr Akad. Nauk SSSR, Vladivostok, 1983) [in Russian].
48. V. G. Chavtur, "Class Ostracoda, Orders Myodocopida and Halocyprida," in *Investigations of the Fauna of Seas*, Vol. 51 (59): *The List of Free-Living Invertebrate Species of the Eurasian Seas and Adjacent Deepwater Areas of the Arctic Ocean*, Ed. by B. I. Sirenko (Zool. Inst. Ross. Akad. Nauk, St. Petersburg, 2001), pp. 98–99 [in Russian].
49. G. P. Coles and R. C. Whatley, "Paleocene to Miocene Genera and Species of Ostracoda from DSDP Sites in the North Atlantic," Rev. Esp. Micropaleontol. **21** (1), 81–124 (1987).
50. G. P. Coles, R. C. Whatley, and A. Moguilevsky, "The Ostracod Genus *Krithe* from the Tertiary and Quaternary of the North Atlantic," Palaeontology **37** (1), 71–120 (1994).
51. T. Correge, "On *Jonesia marecorallinensis* Correge sp. nov.," Stereo-Atlas of Ostracod Shells **19** (2), 103–106 (1992).
52. T. M. Cronin, "Champlanian Sea Foraminifera and Ostracoda: A Systematic and Paleontological Synthesis," Geogr. Phys. Quat. **31** (1–2), 107–122 (1977).
53. T. M. Cronin, "Paleoclimatic Implications of Late Pleistocene Marine Ostracods from the St. Lawrence Lowlands," Micropaleontol. **27** (4), 384–418 (1981).
54. T. M. Cronin, "Paleozoogeography of Postglacial Ostracoda from Northeastern North America: The Late Quaternary Development of the Champlanian Sea Basin," Geol. Assoc. Can. Spec. Pap., No. 35, 125–144 (1989).
55. T. M. Cronin, "Late Neogen Marine Ostracoda from Tjornes, Iceland," J. Paleontol. **65** (5), 767–794 (1991).

56. T. M. Cronin, "Distribution of Deep-Sea Ostracoda in the Arctic Ocean," Ber. Polarforsch. **212**, 269–284 (1996).
57. T. M. Cronin and N. Ikeya, "The Omma-Manganji Ostracod Fauna (Plio-Pleistocene) of Japan and the Zoogeography of Circumpolar Species," J. Micropalaentol. **6** (2), 65–88 (1987).
58. T. M. Cronin, W. M. Briggs, Jr., E. M. Brouwers, et al., "Modern Arctic Podocopid Database," in *USGS Open-File Report* (1991), pp. 91–385.
59. T. M. Cronin, T. R. Holtz, and R. C. Whatley, "Quaternary Paleoceanography of the Deep Arctic Ocean Based on Quantitative Analysis of Ostracoda," Marine Geology, No. 119, 305–332 (1994).
60. T. M. Cronin, T. R. Holtz, R. Stein, et al., "Late Quaternary Paleoceanography of the Eurasian Basin, Arctic Ocean," Paleoceanography, No. 10, 259–281 (1995).
61. C. Didié and H. A. Bauch, "Species Composition and Glacial–Interglacial Variations in the Ostracode Fauna of the Northeast Atlantic during the Past 200000 Years," Marine Micropaleontol. **40**, 105–129 (2000).
62. C. Didié and H. A. Bauch, "Species Composition and Glacial–Interglacial Variations in the Ostracode Fauna of the Northeast Atlantic during the Past 200000 Years," Marine Micropaleontol. **41**, 103–108 (2001).
63. C. Didié, H. A. Bauch, H. Erlenkeuser, and J.-M. Wolfsdorf, "Verteilung und Artenzusammensetzung benthischer Ostracoden der Islandsee im Spätquartär," Zbl. Geol. Paläontol. **1** (5–6), 353–365 (1998).
64. I. A. Dmitrenko, J. Hoelemann, S. A. Kirillov, et al., "The Role of Barotropic Changes in Sea Level in the Formation of the Circulation Pattern of Currents in the Western Part of the Laptev Sea," Dokl. Ross. Akad. Nauk **377** (1), 1–8 (2001a).
65. I. A. Dmitrenko, J. Hoelemann, S. A. Kirillov, et al., "The Bottom Layer of the Laptev Sea: The Thermal Regime and the Processes Controlling Its Development," Kriosfera Zemli **5** (3), 40–55 (2001b).
66. S. S. Drachev, L. A. Savostin, and I. E. Bruni, "Structural Pattern and Tectonic History of the Laptev Sea Region," Ber. Polarforsch., No. 175, 348–366 (1995).
67. S. S. Drachev, G. L. Johnson, S. W. Laxon, et al., "Main Structural Elements of Eastern Russian Arctic Continental Margin Derived from Satellite Gravity and Multichannel Seismic Reflection Data," in *Land–Ocean Systems in the Siberian Arctic: Dynamics and History*, Ed. by H. Kassens, H. A. Bauch, I. A. Dmitrenko, et al. (Springer-Verlag, Berlin, 1999), pp. 667–682.
68. J.-C. Duplessy, E. Ivanova, I. Murdmaa, et al., "Holocene Palaeoceanography of the Northern Barents Sea and Variations of the Northward Heat Transport by the Atlantic Ocean," Boreas **30**, 2–16 (2001).
69. A. S. Dyke, J. E. Dale, and R. N. McNeely, "Marine Molluscs as Indicators of Environmental Change in Glaciated North America and Greenland during the Last 18000 Years," Géogr. Phys. et Quaternaire **50** (2), 125–184 (1996).
70. O. Elofson, "Neue und wenig bekannte Cytheriden von der Schwedischen Westküste," Aktiv Zool. **30A** (21), 1–21 (1938).
71. O. Elofson, "Zur Kenntnis der marinen Ostracoden Schwedens mit besonderer Berücksichtigung der Skageraks," Zool. Bidr. Upps., No. 19, 217–534 (1941).
72. O. Elofson, *Marine Ostracoda of Sweden with Special Consideration of the Skagerrak* (Israel Program for Sci. Translations, Jerusalem, 1969).
73. H. Erlenkeuser and U. von Grafenstein, "Stable Oxygen Isotope Ratios in Benthic Carbonate Shells of Ostracoda, Foraminifera, and Bivalvia from Surface Sediments of the Laptev Sea, Summer 1993 and 1994," in *Land–Ocean Systems in the Siberian Arctic: Dynamics and History,* Ed. by H. Kassens, H. A. Bauch, I. A. Dmitrenko, et al. (Springer-Verlag, Berlin, 1999), pp. 503–514.
74. P. Frenzel and I. Boomer, "The Use of Ostracods from Marginal-Marine, Brackish Waters as Bioindicators of Modern and Quaternary Environmental Change," Palaeogeogr. Palaeoclimatol., Palaeoecol. **225** (104), 68–92 (2005).
75. N. S. Gaevskaya, *The Atlas of the Fauna of Northern Seas* (Sovetskaya Nauka, Moscow, 1948), pp. 176–183 [in Russian].
76. P. Golovin, I. Dmitrenko, H. Kassens, and J. Hoelemann, "Frazil Ice Formation during the Spring Flood and Its Role in Transport of Sediments to the Ice Cover," in *Land–Ocean Systems in the Siberian Arctic: Dynamics and History*, Ed. by H. Kassens, H. A. Bauch, I. A. Dmitrenko, et al. (Springer-Verlag, Berlin, 1999), pp. 125–142.
77. G. P. Gorbunov, "The Benthic Population of the Shallow Offshore Waters around the New Siberian Islands and in the Central Part of the Arctic Ocean," in *Proceedings of the Drifting Expeditions of Glavsevmorput' on the Icebreaker* Sedov, 1937–1940 (Biologiya, Moscow-Leningrad, 1946), Vol. 3, pp. 30–138 [in Russian].
78. S. Gordillo and A. E. Aitken, "Postglacial Succession and Palaeoecology of Late Quaternary Macrofaunal Assemblages from the Canadian Arctic Archipelago," Boreas **30**, 61–72 (2001).
79. A. Yu. Gukov, *The Ecosystem of Siberian Polynya* (Nauchnyi Mir, Moscow, 1999) [in Russian].
80. A. Yu. Gukov, *The Estuarine Area of the Lena River: Hydrobiology* (Nauchnyi Mir, Moscow, 2001) [in Russian].
81. Y. C. Hao, "Systematic Description of Microfossils: 2. Ostracoda," in *Quaternary Microbiotas in the Okinawa Trough and Their Geological Significance,* Ed. by P. H. Ruan and Y. C. Hao (Geol. Publishing House, Beijing, 1988), pp. 227–395.
82. G. Hartmann, "Zur Kenntnis der rezenten und subfossilen Ostracoden des Liefdefjords (Nordspitzbergen, Svålbard)," Mitt. Hamb. Zool. Mus. Inst. **90**, 239–250 (1993).
83. J. E. Hazel, "Classification and Distribution of the Recent Hemicytheridae and Trachyleberididae (Ostracoda) off Northeastern North America," U.S. Geol. Surv. Prof. Pap., No. 564, 1–49 (1967).
84. J. E. Hazel, "Pleistocene Ostracode Zoogeography in Atlantic Coast Submarine Canyons," J. Paleontol. **42** (5), 1264–1271 (1968).

85. N. Hirschmann, "Beitrag zur Kenntnis der Ostracoden Fauna des Finnischen Meerbesens," Meddn. Soc. Fauna Flora Fenn. **35**, 282–296 (1909).

86. N. Hirschmann, "Ostracodenfauna des Finnischen Meerbusens," Acta Soc. pro Fauna et Flora Fennica **36** (2), 1–68 (1912).

87. N. Hirschmann, "Baltic Sea Ostracoda Collected by N.M. Knipovich and S.A. Pavlovich in Summer 1908," Ezhegodn. Zool. Muzeya **20** (4), 567–597 (1916).

88. M. L. Holmes and J. S. Creager, "Holocene History of the Laptev Sea Continental Shelf," in *Marine Geology and Oceanography of the Arctic Seas*, Ed. by Y. B. Herman (Springer-Verlag, Berlin, 1974), pp. 211–229.

89. J. Horne, A. Cohen, and K. Martens, "Taxonomy, Morphology, and Biology of Quaternary and Living Ostracoda: The Ostracoda: Application in Quaternary Research, Ed. by J. A. Holmes and A. R. Chivas," Geophys. Monograph, No. 131, 5–37 (2002).

90. H. V. Howe, "Family Psammocytheridae Klie, 1938," in *Treatise on Invertebrate Paleontology, Parts P and Q, Arthropoda 3: Crustacea, Ostracoda* (Univ. Kansas Press, Lawrence, 1961), pp. 330–331.

91. H. V. Howe and R. A. Reyment, "Family Loxoconchidae Sars, 1925," in *Treatise on Invertebrate Paleontology, Parts P and Q, Arthropoda 3: Crustacea, Ostracoda* (Univ. Kansas Press, Lawrence, 1961), pp. 312–315.

92. H. V. Howe, P. C. Sylvester-Bradley, and R. A. Reyment, "Family Schizocytheridae Howe, 1961," in *Treatise on Invertebrate Paleontology, Parts P and Q, Arthropoda 3: Crustacea, Ostracoda* (Univ. Kansas Press, Lawrence, 1961a), p. 331.

93. H. V. Howe, W. A. van den Bold, and R. A. Reyment, "Family Cytherideidae Sars, 1925," in *Treatise on Invertebrate Paleontology, Parts P and Q, Arthropoda 3: Crustacea, Ostracoda* (Univ. Kansas Press, Lawrence, 1961b), pp. 272–290.

94. H. V. Howe, W. A. van den Bold, and R. A. Reyment, "Family Hemicytheridae Puri, 1953," in *Treatise on Invertebrate Paleontology, Parts P and Q, Arthropoda 3: Crustacea, Ostracoda* (Univ. Kansas Press, Lawrence, 1961c), pp. 300–306.

95. H. C. Howe, "Type Saline Bayou Ostracoda of Louisiana," Louisiana Geol. Surv. Bull., No. 40, 1–62 (1963).

96. C. Ingram, "Palaeoecology and Geochemistry of Shallow Marine Ostracoda from the Sand Hole Formation, Inner Silver Pit, Southern North Sea," Quatern. Sci. Rev. **17**, 913–929 (1998).

97. T. Irizuki, "Late Miocene Ostracods from the Fujikotogawa Formation, Northern Japan, with Reference to Cold Water Species Involved with Trans-Arctic Interchange," J. Micropaleontol., No. 13, 3–15 (1994).

98. L. L. Isaeva, "The Undivided Sartanian–Holocene Deposits of the North Siberian Lowland," in *The Anthropogene of the Taimyr Peninsula*, Ed. by N. V. Kind and B. N. Leonov (Nauka, Moscow, 1982a), pp. 136–138 [in Russian].

99. L. L. Isaeva, "The Sartanian Deposits of the North Siberian Lowland," in *The Anthropogene of the Taimyr Peninsula*, Ed. by N. V. Kind and B. N. Leonov (Nauka, Moscow, 1982b), pp. 114–136 [in Russian].

100. L. L. Isaeva, "The Holocene Deposits of the North Siberian Lowland," in *The Anthropogene of the Taimyr Peninsula*, Ed. by N. V. Kind and B. N. Leonov (Nauka, Moscow, 1982c), pp. 138–142 [in Russian].

101. L. L. Isaeva and N. V. Kind, "On Contradictions in the Interpretation of the Scale of the Latest Late Pleistocene Glaciation," in *The Anthropogene of the Taimyr Peninsula*, Ed. by N. V. Kind and B. N. Leonov (Nauka, Moscow, 1982), pp. 165–168 [in Russian].

102. L. L. Isaeva, N. V. Kind, M. A. Kraush, and L. D. Sulerzhitskii, "On the Age and Structure of the Marginal Glacier Complexes at the Northern Foot of the Putoran Plateau," Byull. Komm. po Izuchen. Chetvertich. Perioda, No. 45, 117–123 (1976).

103. L. L. Isaeva, N. V. Kind, S. M. Andreeva, and M. A. Bardeeva, "Quaternary Glaciation of North-Central Siberia," Tr. Novosibirsk. Inst. Geol. Geofiz., Issue 494, 98–105 (1981).

104. P. Jaccard, "The Distribution of the Flora in the Alpine Zone," New Phytol. **11**, 37–50 (1912).

105. R. Jones, R. C. Whatley, and T. Cronin, "The Zoogeographical Distribution of Deep Water Ostracoda in the Arctic Ocean," in *What about Ostracoda!—3rd European Ostracodologists Meeting, Paris-Bierville, France, 8–12 July, 1996* (Elf Exploration Production-Editions, CEDEX, Pau, 1998), pp. 83–90.

106. R. L. Jones, R. C. Whatley, T. M. Cronin, and H. J. Dowsett, "Reconstructing Late Quaternary Deep-Water Masses in the Eastern Arctic Ocean Using Benthonic Ostracoda," Marine Micropaleontol. **37**, 251–272 (1999).

107. T. R. Jones, *A Monograph of the Tertiary Entomostraca of England* (Paleontograph. Soc., London, 1857), pp. 1–68.

108. J. A. Joy and D. L. Clark, "The Distribution, Ecology, and Systematics of the Benthic Ostracoda of the Central Arctic Ocean," Micropaleontol. **23** (2), 129–154 (1977).

109. N. P. Kashevarova, M. I. Mandel'shtam, and G. F. Schneider, "Superfamily Cytheracea," in *Fundamentals of Paleontology: Arthropoda, Trilobita, and Crustacea* (Gos. Nauchno-Tekhn. Izd. Liter. po Geol. Okhrane Nedr, Moscow, 1960), Vol. 8, pp. 365–411 [in Russian].

110. D. Keyser and R. Walter, "Calcification in Ostracods," Rev. Españ. Micropaleontol. **36** (1), 1–11 (2004).

111. B. Kim, G. Grikurov, and V. Soloviev, "High Resolution Seismic Studies in the Laptev Sea Shelf: First Results and Future Needs," in *Land–Ocean Systems in the Siberian Arctic: Dynamics and History*, Ed. by H. Kassens, H. A. Bauch, I. Dmitrenko, et al. (Springer-Verlag, Berlin, 1999), pp. 683–692.

112. V. I. Kim and V. V. Verba, "The Geological Structure of the Laptev Shelf and Adjacent Parts of the Eurasian Subbasin (in the Context of Planned Drilling)," Ber. Polarforsch. **176**, 383–387 (1995).

113. H. P. Kleiber and F. Niessen, "Late Pleistocene Paleoriver Channels on the Laptev Sea Shelf—Implications from Subbottom Profiling," in *Land–Ocean Systems in the Siberian Arctic: Dynamics and History* (Springer-Verlag, Berlin, 1999), pp. 657–666.

114. H. P. Kleiber and F. Niessen, "Variations of Continental Discharge Patterns in Space and Time: Implications from the Laptev Sea Continental Margin, Arctic Siberia," Int. J. Earth Sci. **89**, 605–616 (2000).

115. H. P. Kleiber, F. Niessen, and D. Weiel, "The Late Quaternary Evolution of the Western Laptev Sea Continental Margin, Arctic Siberia—Implications from Sub-Bottom Profiling," Global and Planetary Change **31**, 105–124 (2001).
116. W. Klie, "Beitrag zur Kenntnis der Ostracoden der südlichen und westlichen Ostsee, der festländischen Nordseeküste und der Insel Helgoland," Z. Wiss. Zool., No. 134, 270–306 (1929).
117. W. Klie, "Die von Römer und Schaudinn 1898 bei Spitzbergen gesammelten Ostracoden," Zool. Anz., No. 137, 1–10 (1942).
118. K. Kollman, "Cytherideinae und Schulerideinae n. subfam. (Ostracoda) aus dem Neogene des Östl. Oesterreich," Mitt. Geol. Ges. Wien., No. 51, 89–195 (1960).
119. V. Kosheleva, D. Yashin, and E. Musatov, "On the Volume of Terrigenous Sedimentation in the Laptev Sea," Polarforschung, No. 69, 207–211 (2001).
120. N. V. Kupriyanova, "Biostratigraphy of Upper Cenozoic Sediment of the Pechora Sea by Ostracods," Ber. Polarforsch. **306**, 62–79 (1999).
121. V. M. Kuptsov and A. P. Lisitsin, "Radiocarbon of Quaternary along Shore and Bottom Deposits of the Lena and the Laptev Sea Sediments," Mar. Chem. **52**, 301–311 (1996).
122. O. M. Lev, "Ostracode Assemblages from the Late Cenozoic Marine Deposits of the North European Part of the USSR and Western Siberia and Their Significance for Paleogeography," in *The Arctic Ocean and Its Coastal Zone in the Cenozoic* (Gidrometeoizdat, Leningrad, 1970), pp. 352–355 [in Russian].
123. O. M. Lev, "Bionomic and Paleogeographic Conditions in the Neogene–Quaternary Marine Basins in the Northern Part of the USSR Based on the Ostracode Fauna: The Modern Tectonics and Paleogeography of the Soviet Arctic in the Context of the Estimation of Mineral Resources," Tr. Nauchno-Issled. Inst. Geol. Arktiki, 15–21 (1972).
124. O. M. Lev, "Neogene–Quaternary Ostracode Assemblages," in *The Main Problems of the Late Cenozoic of the Arctic* (Nedra, St. Petersburg, 1983), pp. 104–143 [in Russian].
125. A. Lord, "Weichselian (Late Quaternary) Ostracods from the Sandnes Clay, Norway," Geol. Mag. **117** (3), 227–242 (1980).
126. A. Lord, J. E. Robinson, and S. G. Moutzourides, "Ostracoda from Holstenian Deposits in the Hamburg Area," Geol. J. **138**, 127–145 (1993).
127. D. J. Lubinski, L. A. Polyak, and S. L. Forman, "Freshwater and Atlantic Water Inflows to the Deep Northern Barents and Kara Seas since ca 13 ^{14}C ka: Foraminifera and Stable Isotopes," Quatern. Sci. Rev. **20**, 1851–1879 (2001).
128. P. S. Lyubimova, M. I. Mandel'shtam, and G. F. Shneider, "Superfamily Cypracea," in *Fundamentals of Paleontology. Arthropoda, Trilobita, and Crustacea* (Gos. Nauchno-Tekhn. Izd. Liter. po Geol. Okhr. Nedr, Moscow, 1960), Vol. 8, pp. 347–365 [in Russian].
129. K. McDougall, E. M. Brouwers, and P. Smith, "Micropaleontology and Sedimentology of the PB Borehole Series, Prudhoe Bay, Alaska," U.S. Geol. Surv. Bull., No. 1598, 1–62 (1986).
130. N. Mostafawi, "Ostracods in Late Pleistocene and Holocene Sediments from the Fram Strait, Eastern Arctic," in *Ostracoda and Global Events* (London, Chapman and Hall, 1990), pp. 489–494.
131. J. Moyes and J. Peypouquet, "Évolution de l'environnement marin au Tertiaire supérior en Aquitain méridionale," Bull. Soc. Géol. France **19** (2), 289–298 (1977).
132. T. Mueller-Lupp, H. A. Bauch, H. Erlenkeuser, J. Hefter, H. Kassens, and J. Thiede, "Changes in the Deposition of Terrestrial Organic Matter on the Laptev Sea Shelf during the Holocene: Evidence from Stable Carbon Isotopes," Int. J. Earth Sci. **89**, 563–568 (2000).
133. G. W. Müller, "Die Ostracoden des arktischen Gebietes," Fauna Arctica **6**, 23–32 (1931).
134. N. N. Naidina, "Phylum Arthropoda: Order Ostracoda," in *Atlas of Invertebrates of the Caspian Sea* (Pishchev. Prom-st, Moscow, 1968), pp. 187–213.
135. J. W. Neale, "An Ostracod Fauna from Halley Bay, Coats Land, British Antarctic Territory," Sci. Rep. Publ. British Antarctic Surv., No. 58, 1–50 (1967).
136. J. W. Neale, "*Roundstonia globulifera* (Brady) 1868 n. gen. (Crustacea, Ostracoda). Une espèce caractéristique du Pléistocène et (?) de l'actuele," Rev. Micropaleontol., No. 2, 125–131 (1973a).
137. J. W. Neale, "*Cluthia* (Crustacea, Ostracoda), a New Pleistocene and Recent Leptocytherid Genus," J. Paleontol. **47** (4), 683–688 (1973b).
138. J. W. Neale, "The Ostracoda and Uniformitarianism: I. The Later Record: Recent Pleistocene and Tertiary (Presidential Address, 1981)," Proc. Yorkshire Geol. Soc. **44** (3/21), 305–326 (1983).
139. J. W. Neale and H. V. Howe, "New Cold Water Recent and Pleistocene Species of the Ostracod Genus *Cytheropteron*," Crustaceana **25** (3), 237–245 (1973).
140. J. W. Neale and H. V. Howe, "The Marine Ostracoda of Russian Harbour, Novaya Zemlya, and Other High Latitude Faunas," Bull. Am. Paleontol. **65** (282), 381–431 (1975).
141. I. A. Nikolaeva, "Order Cladocopida Sars, 1865," in *Practical Handbook of the Microfauna of the USSR: Cenozoic Ostracodes* (St. Petersburg, Nedra, 1989a), pp. 85–86 [in Russian].
142. I. A. Nikolaeva, "Paleoecology and Its Association with Facies," in *Practical Handbook of the Microfauna of the USSR: Cenozoic Ostracodes* (Nedra, St. Petersburg, 1989b), pp. 204–207 [in Russian].
143. I. A. Nikolaeva, V. I. Pavlovskaya, G. I. Karmishina, and A. L. Kovalenko, "Order Podocopida Sars, 1865," in *Practical Handbook of the Microfauna of the USSR: Cenozoic Ostracodes* (Nedra, St. Petersburg, 1989). pp. 88–193 [in Russian].
144. N. Norgaard-Pedersen, R. F. Spielhagen, J. Thiede, and H. Kassens, "Central Arctic Surface Ocean Environment during the Past 80000 Years," Paleoceanography **13**, 193–204 (1998).
145. A. M. Norman, "Deepsea Dredging on the Coasts of Northumberland and Durham, in 1864," in *Rep. Br. Ass. Advmt. Sci. (34 Meeting, Bath, 1864)*, Ed. by G. S. Brady (1865a), pp. 189–193.
146. A. M. Norman, "Report on the Crustacea," in G. S. Brady (ed.) "Reports of Deepsea Dredging on the Coasts of

Northumberland and Durham, 1862–64," Nat. Hist. Trans. Northumb. **1** (1), 12–29 (1865b).

147. T. S. Novichkova, Ye. I. Polyakova, and H. A. Bauch, "Detailed Reconstructions of Depositional Environments and Water Salinity Fluctuations on the Eastern Laptev Sea Shelf during the Early to Middle Holocene," in *Abstracts of the "Climate Drivers of the North" Conference, Kiel, May 8–11, 2002* (Terra Nostra, GeoForschungs Zentrum, Potsdam, 2002).
148. Yu. A. Pavlidis, A. S. Ionin, F. A. Shcherbakov, et al., *Arctic Shelf: Its Late Quaternary History as a Basis for the Forecast of Its Further Development* (Geos, Moscow, 1998) [in Russian].
149. D. N. Penney, "Quaternary Ostracod Chronology of the Central North Sea: The Record from BH 81/29," Cour. Forsch.-Inst. Senckenberg **123**, 97–109 (1990).
150. V. Pokorny, "Contribution to the Morphology and Taxonomy of the Subfamily Hemicytherinae Puri," Geologica **3**, 1–35 (1955).
151. L. Polyak, M. Levitan, V. Gataullin, T. Khusid, V. Mikhailov, and V. Mukhina, "The Impact of Glaciation, River-Discharge, and Sea-Level Change on Late Quaternary Environments in the Southwestern Kara Sea," Int. J. Earth Sci. **89** (3), 550–562 (2000).
152. L. Polyak, S. Korsun, L. Febo, V. Stanovoy, T. Khusid, M. Hald, B. E. Paulsen, and D. A. Lubinski, "Benthic Foraminiferal Assemblages from the Southern Kara Sea, a River-Influenced Arctic Marine Environment," J. Foraminiferal Res. **32** (3), 252–273 (2002).
153. E. I. Polyakova, *The Arctic Seas of Eurasia in the Late Cenozoic* (Nauchnyi Mir, Moscow, 1997) [in Russian].
154. Ye. I. Polyakova and H. A. Bauch, "Holocene Changes of Riverine Discharge and Surface Water Salinity in the Laptev Sea Inferred from Diatom Assemblages," in *Abstracts of the "Climate Drivers of the North" Conference, Kiel, May 8–11, 2002* (2002), pp. 87–88.
155. Ye. I. Polyakova, H. A. Bauch, and T. S. Novichkova, "Past Changes in Laptev Sea Water Masses Deduced from Diatom and Aquatic Palynomorph Assemblages," Global and Planetary Change (in press).
156. *Practical Handbook of the Microfauna of the USSR: Cenozoic Ostracodes* (Nedra, St. Petersburg, 1989) [in Russian].
157. T. M. Puckett, "Ecologic Atlas of Upper Cretaceous Ostracodes of Alabama," Geol. Surv. Alabama Monograph, No. 14, 1–176 (1996).
158. M. E. Raymo, "The Timing of Major Climate Terminations," Paleoceanography **12** (4), 577–585 (1997).
159. E. Reimnitz, L. Marincovich, Jr., M. McCormick, and W. M. Briggs, "Suspension Freezing of Bottom Sediment and Biota in the Northwest Passage and Implications for Arctic Ocean Sedimentation," Can. J. Earth Sci. **29**, 693–703 (1992).
160. E. Reimnitz, M. McCormick, K. McDougall, and E. M. Brouwers, "Sediment Export by Ice Rafting from a Coastal Polynya, Arctic Alaska, U.S.A.," Arctic and Alpine Res. **25** (2), 83–98 (1993).
161. P. V. Rekant, "The Geological Structure and Sedimentation Environment during Accumulation of Pliocene–Quaternary Formations of the Laptev Sea Continental Margin," Extended Abstract of Candidate's Dissertation in Geology and Mineralogy (VNIIOkeangeologiya, St. Petersburg, 2002).
162. C. A. Repenning, E. M. Brouwers, L. D. Carter, L. Marincovich, Jr., and T. A. Ager, "The Beringian Ancestry of *Phenacomys* (Rodentia: Cricetidae) and the Beginning of the Modern Arctic Borderland Biota," U.S. Geol. Surv. Bull., No. 1687, 1–31 (1987).
163. R. A. Reyment, H. V. Howe, and T. Hanai, "Family Cytheruridae G.W. Müller, 1894," in *Treatise on Invertebrate Paleontology, Parts P and Q, Arthropoda 3: Crustacea, Ostracoda* (Univ. Kansas Press, Lawrence, 1961), pp. 291–300.
164. E. Robinson, "The Pleistocene," Geol. J. Spec. Issue, No. 8, 451–472 (1978).
165. N. N. Romanovskii, A. V. Gavrilov, V. E. Tumskoy, A. L. Kholodov, C. Siegert, H.-W. Hubberten, and A. V. Sher, "Environmental Evolution in the Laptev Sea Region during Late Pleistocene and Holocene," Polarforschung, No. 68, 237–245 (2000).
166. N. N. Romanovskii, H.-W. Hubberten, A. V. Gavrilov, et al., "Permafrost of the East Siberian Arctic Shelf and Coastal Lowlands," Quatern. Sci. Rev., No. 23, 1359–1369 (2004).
167. A. Rosenfeld, "Die Ostracoden-Arten in der Ostee," Meyniana **29**, 11–49 (1977).
168. Yu. A. Rudyakov, "Ostracoda in the Shallow Waters of the Kandalaksha Bay in the White Sea," in *Biology of the White Sea* (Mosk. Gos. Univ., Moscow, 1962), pp. 130–142 [in Russian].
169. G. O. Sars, "Oversigt af Norges marine Ostracoder," in *Forh. Vidensk.-Selsk. Krist., 1864–65* (1866), pp. 1–130.
170. G. O. Sars, "Nye dybans crustaceer fra Lofoten," in *Forh. Vidensk.-Selsk. Krist., 1869* (1870), pp. 147–174.
171. G. O. Sars, *An Account of the Crustacea of Norway Published by Bergen Museum, 1922–1923–1925a–1925b–1926–1928* (Bergen Museum, Bergen, 1928), Vol. 9, pp. 1–277.
172. L. Schirrmeister, C. Siegert, T. Kuznetsova, S. Kuzmina, A. Andreev, F. Kienast, H. Meyer, and A. Bobrov, "Paleoenvironmental and Paleoclimatic Records from Permafrost Deposits in the Arctic Region of Northern Siberia," Quatern. Int. **89**, 97–118 (2002).
173. R. A. M. Schmidt, "New Generic Assignment for Some Pleistocene Ostracoda from Alaska," J. Paleontol. **41** (2), 487–488 (1967).
174. K. Schoning and S. Wastegård, "Ostracod Assemblages in Late Quaternary Varved Glaciomarine Clay of the Baltic Sea Yoldia Stage in Eastern Middle Sweden," Marine Micropalaeontol. **37**, 313–325 (1999).
175. G. Schwamborn, V. Rachold, and M. Grigoriev, "Late Quaternary Sedimentation History of the Lena Delta," Quatern. Int. **89** (1), 119–134 (2002).
176. H. W. Scott, "Shell Morphology of Ostracoda," in *Treatise on Invertebrate Paleontology, Parts P and Q, Arthropoda 3: Crustacea, Ostracoda* (Univ. Kansas Press, Lawrence, 1961), pp. 21–37.
177. T. Scott, "Report on the Marine and Freshwater Crustacea from Franz Josef Land Collected by Mr. William S. Bruce of the Jackson–Harmsworth Expedition," J. Linn. Soc. London, No. 27, 60–126 (1899).

178. Yu. P. Semenov and E. P. Shkatov, "Geomorphology of the Laptev Sea Bottom," Tr. Nauchno-Issled. Inst. Geol. Arktiki **1**, 42–47 (1971).

179. G. F. Shneider, "Ostracodes of the Arctic Basin," in *The Arctic Basin Sediments: Data of the Drift of the Icebreaker* Sedov (Akad. Nauk SSSR, Moscow, 1962), pp. 103–104 [in Russian].

180. E. I. Schornikov, "Ostracodes of the Genus *Jonesia* Brady, 1866 from the White and Barents Seas," Zool. Zh. **59** (8), 1123–1129 (1980).

181. E. I. Schornikov, *Ostracodes Bythocytheridae of the Far Eastern Seas* (Nauka, Moscow, 1981) [in Russian].

182. E. I. Schornikov, "Class Ostracoda, Orders Platycopida and Podocopida," in *Investigations of the Fauna of Seas*, Vol. 51 (59): *The List of Free-Living Invertebrate Species of the Eurasian Seas and Adjacent Deepwater Areas of the Arctic Ocean*, Ed. by B. I. Sirenko (Zool. Inst. Ross. Akad. Nauk, St. Petersburg, 2001), pp. 99–103 [in Russian].

183. E. I. Schornikov, "The Fauna of Benthic Ostracodes (Crustacea, Ostracoda) of the Laptev Sea," in *Investigations of the Fauna of Seas* (Zool. Inst. Ross. Akad. Nauk, St. Petersburg, 2004), Vol. 54 (62), pp. 58–70 [in Russian].

184. E. I. Schornikov and O. A. Tsareva, "Heterochronies in the Development of the Sculpture of Carapaces of the Ostracode Genus *Hemicythere*," Biol. Morya **28** (1), 19–29 (2002).

185. Q. A. Siddiqui, "The Iperk Sequence (Plio-Pleistocene) and Its Ostracod Assemblages in the Eastern Beaufort Sea," in *Evolutionary Biology of Ostracoda* (Elsevier, Tokyo, 1988), pp. 533–540.

186. R. Stein and K. Fahl, "Holocene Accumulation of Organic Carbon at the Laptev Sea Continental Margin (Arctic Siberia): Sources, Pathways, and Sinks," Geo-Marine Lett. **20**, 27–36 (2000).

187. A. Yu. Stepanova, "Recent Ostracodes of the Kandalaksha Bay, White Sea, and Their Distribution according to Water Depth," Tr. Nauchno-Issled. Inst. Geol. Saratov Gos. Univ., Nov. Ser. **11**, 123–134 (2002).

188. A. Stepanova, E. Taldenkova, and H. A. Bauch, "Recent Ostracoda from the Laptev Sea (Arctic Siberia): Species Assemblages and Some Environmental Applications," Marine Micropaleontol. **48** (1–2), 23–48 (2003).

189. A. Stepanova, E. Taldenkova, and H. A. Bauch, "Ostracod Species of the Genus *Cytheropteron* from Late Pleistocene, Holocene, and Recent Sediments of the Laptev Sea (Arctic Siberia)," Rev. Esp. Micropaleontol. **36** (1), 83–108 (2004).

190. M. Stuiver, P. J. Reimer, E. Bard, et al., "INTCAL 98 Radiocarbon Age Calibration, 24,000–0 cal BP," Radiocarbon, No. 40, 1041–1083 (1998).

191. J. I. Svendsen, V. I. Astakhov, D. Yu. Bolshiyanov, et al., "Maximum Extent of the Eurasian Ice Sheets in the Barents and Kara Sea Region during the Weichselian," Boreas **28** (1), 234–242 (1999).

192. J. I. Svendsen, H. Alexanderson, V. I. Astakhov, et al., "Late Quaternary Ice Sheet History of Northern Eurasia," Quatern. Sci. Rev., No. 23, 1229–1271 (2004).

193. F. Swain, "Ostracoda from the Gubik Formation, Arctic Coastal Plain, Alaska," in *Geology of the Arctic* (Univ. Toronto Press, Toronto, 1961), pp. 600–606.

194. F. Swain, "Pleistocene Ostracoda from the Gubik Formation, Arctic Coastal Plain, Alaska," J. Paleontol. **37** (4), 798–834 (1963).

195. F. Swain and W. A. van den Bold, "Family Pontocyprididae G.W. Müller, 1894," in *Treatise on Invertebrate Paleontology, Parts P and Q, Arthropoda 3: Crustacea, Ostracoda* (Univ. Kansas Press, Lawrence, 1961), p. 247.

196. K. M. Swanson and A. Ayress, "*Cytheropteron testudo* and Related Species from SW Pacific with Analyses of Their Soft Anatomies, Relationship, and Distribution," Senckenbergiana Biol. **79** (2), 151–193 (1999).

197. P. C. Sylvester-Bradley, "Family Polycopidae Sars, 1866," in *Treatise on Invertebrate Paleontology, Parts P and Q, Arthropoda 3: Crustacea, Ostracoda* (Univ. Kansas Press, Lawrence, 1961), p. 405.

198. P. C. Sylvester-Bradley and H. V. Howe, "Family Paradoxostomatidae Brady and Norman, 1889," in *Treatise on Invertebrate Paleontology, Parts P and Q, Arthropoda 3: Crustacea, Ostracoda* (Univ. Kansas Press, Lawrence, 1961), p. 407.

199. P. C. Sylvester-Bradley and R. V. Kesling, "Family Bythocytheridae Sars, 1926," in *Treatise on Invertebrate Paleontology, Parts P and Q, Arthropoda 3: Crustacea, Ostracoda* (Univ. Kansas Press, Lawrence, 1961), pp. 267–268.

200. J. P. M. Syvitski, G. E. Farrow, R. J. A. Atkinson, et al., "Baffin Island Fjord Macrobenthos: Bottom Communities and Environmental Significance," Arctic **42** (3), 232–247.

201. E. Taldenkova, H. A. Bauch, A. Stepanova, et al., "Last Postglacial Environmental Evolution of the Laptev Sea Shelf as Reflected in Molluscan, Ostracodal, and Foraminiferal Faunas," Global and Planetary Change **48** (1–3), 223–251 (2005).

202. S. V. Tamanova, "Foraminifers of the Laptev Sea," Tr. Nauchno-Issled. Inst. Geol. Arktiki **1**, 54–63 (1971).

203. Erich von Triebel, "Fossile Arten der Ostracoden-Gattung *Paracyprideis* Klie," Senckenbergiana **23** (1/3), 153–164 (1941).

204. Erich von Triebel, "Mikropaläontologische Kennzeichnung der Ostracoden-Gattungen *Xenocythere* und *Palmenella*," Senckenbergiana **30** (4/6), 185–192 (1949).

205. Erich von Triebel, "Neu Ostracoden aus dem Pleistozän von Kalifornien," Senckenbergiana **38** (5/6), 291–309 (1957).

206. S. L. Troitskii, *The Marine Pleistocene of Siberian Plains* (Nauka, Novosibirsk, 1979) [in Russian].

207. V. A. Vinogradov and S. S. Drachev, "A Contribution to the Tectonic Nature of the Basement of the Southwestern Part of the Laptev Sea Shelf," Dokl. Ross. Akad. Nauk **372** (1), 72–74 (2000).

208. C. W. Wagner, "Sur les Ostracodes du Quaternaire Récent de Pays-Bas et leur utilization dans l'étude géologique des dépôts Holocènes," Thèse (Université de Paris, Paris, 1957).

209. C. Wegner, "Sediment Transport on Arctic Shelves—Seasonal Variations in Suspended Particulate Matter Dynamics on the Laptev Sea Shelf (Siberian Arctic)," PhD Thesis (Kiel Univ., Kiel, 2002).

210. C. Wegner, "Sediment Transport on Arctic Shelves—Seasonal Variations in Suspended Particulate Matter

Dynamics on the Laptev Sea Shelf (Siberian Arctic)," Ber. Polar and Meeresforsch., No. 455, 87 (2004).

211. R. C. Whatley and M. Ayress, "Pandemic and Endemic Distribution Patterns in Quaternary Deep-Sea Ostracoda," in *Evolutionary Biology of Ostracoda* (Elsevier, Tokyo, 1988), pp. 739–755.

212. R. C. Whatley and G. Coles, "The Late Miocene to Quaternary Ostracoda of Leg 94, Deep Sea Drilling Project," Rev. Esp. Micropaleontol. **19** (1), 33–97 (1987).

213. R. C. Whatley and D. G. Masson, "The Ostracod Genus *Cytheropteron* from the Quaternary and Recent of Great Britain," Rev. Esp. Micropaleontol. **11** (2), 223–277 (1979).

214. R. C. Whatley and Q. Zhau, "The *Krithe* Problem: A Case History of the Distribution of *Krithe* and *Parakrithe* (Crustacea, Ostracoda) in the South China Sea," Palaeogeogr., Palaeoclimatol., Palaeoecol., No. 103, 281–297 (1993).

215. R. C. Whatley, M. Eynon, and A. Moguilevsky, "Recent Ostracoda of the Scoresby Sund Fjord System, East Greenland," Rev. Esp. Micropaleontol. **28** (2), 5–23 (1996).

216. R. C. Whatley, M. Eynon, and A. Moguilevsky, "The Depth Distribution of Ostracoda from the Greenland Sea," J. Micropaleontol. **17**, 15–32 (1998).

217. H. Woszidlo, "Foraminiferen und Ostracoden aus dem marin Elster-Saale-Interglazial in Schleswig-Holstein," Meyniana **12**, 65–96 (1962).

218. B. S. Zalogin and A. D. Dobrovol'skii, *The Seas of the USSR* (Mosk. Gos. Univ., Moscow, 1982) [in Russian].

219. I. E. Zanina and E. N. Polenova, "Suborder Cladocopa," in *Fundamentals of Paleontology: Arthropoda, Trilobita, and Crustacea* (Gos. Nauchno-Tekhn. Izd. Liter. po Geol. Okhrane Nedr, Moscow, 1960), Vol. 8, pp. 330–332 [in Russian].